OPTIMISATION OF PROCESS PARAMETERS AND ASSESSMENT OF MECHANICAL PROPERTIES OF IN-SITU AA6082-TiB$_2$ PARTICLE REINFORCED COMPOSITES

Thesis

Submitted in partial fulfillment of the requirements for the degree of

DOCTOR OF PHILOSOPHY

by

HEMANTHKUMAR V.

DEPARTMENT OF METALLURGICAL AND MATERIALS ENGINEERING

NATIONAL INSTITUTE OF TECHNOLOGY KARNATAKA,

SURATHKAL, MANGALORE - 575025

June, 2017

D E C L A R A T I O N

by the

Ph. D. RESEARCH SCHOLAR

I hereby *declare* that the Research thesis entitled **"Optimisation of Process Parameters and Assessment of Mechanical Properties of In-Situ AA6082-TiB$_2$ Particle Reinforced Composites"** which is being submitted to the **National Institute of Technology Karnataka, Surathkal** in partial fulfillment of the requirements for the award of the Degree of **Doctor of Philosophy** in Metallurgical and Materials Engineering is a *bonafide report of the research work carried out by me*. The material contained in this **Research Thesis** has not been submitted to any University or Institution for the award of any degree.

HEMANTHKUMAR V.

Register No. MT09F02

Department of Metallurgical and Materials Engineering

National Institute of Technology Karnataka, Surathkal

Place: NITK-Surathkal

Date: 02-06-2017

C E R T I F I C A T E

This is to *certify* that the Research Thesis entitled **"Optimisation of Process Parameters and Assessment of Mechanical Properties of In-Situ AA6082-TiB$_2$ Particle Reinforced Composites"** submitted by **Hemanthkumar V.** (Register Number: **MT09F02**) as the record of the research work carried out by him, *is accepted as the Research Thesis submission* in partial fulfillment of the requirements for the award of degree of **Doctor of Philosophy**.

Research Guide

Dr. Ravishankar K.S.

(Signature with Date and Seal)

Chairman – DRPC

(Signature with Date and Seal)

Dedicated to my beloved family members and well wishers…

ACKNOWLEDGEMENTS

all technical and non-technical staff of the Department of Metallurgical and Materials Engineering for their whole hearted help during the course of my work.

I thank Mr.Senchudar, Mr.Nirmal and Mr.Munuswamy and Serval Engineers for their support in prepration of Die.

I take this opportunity to thank my all friends from NITK for their love and affection, Mr.Gopinath K., Mr.Shyam Prasad, Mr.Kamal Babu P.,Dr.Rajashekeran, Dr.Gibin George, Dr.Senthil, Dr.Ramesh, Dr.Rijesh, Dr.Selvakumar, Dr. Pramodh, Mr.Kumaran, Mr.Palak Shaw, Mr. Manojkumar N, Mrs. Jayalakshami, Mr. Arun Augustin,, and Mr. Prashanth Huilgol, Mr.Suresh are only a few among them.

I thank the Director and administration of National Institute of Technology Karnataka, Surathkal for permitting me to pursue my research work at the Institute.

I also thank all of my friends of NITK for their support and cooperation during my stay in the NITK campus.

I render my deepest gratitude to my parents, my brother and my sister for the love, affection and support.

Finally, I thank all those who directly / indirectly helped me to complete the research work.

<div align="right">HEMANTHKUMAR V.</div>

ABSTRACT

The specific properties exhibited by aluminium matrix composites make them attractive for different applications, especially in the automotive and aerospace industries. The main objective of this research work was to produce *in-situ* AA6082-TiB_2 particle reinforced composite using flux assisted synthesis technique. The in-situ TiB_2 ceramic reinforcements were prepared by adding K_2TiF_6 and KBF_4 fluoride salts to the AA6082 alloy melt. Addition of salts caused severe exothermic reaction in the melt, where Ti and B are reduced from their respective salts leading to the formation of TiB_2 particles in the melt. However, incomplete reaction will always lead to the formation of unwanted Al_3Ti and AlB_2 intermediate intermetallic particles along with TiB_2. Hence, in order to supress the formation of intermetallic particles and to result in the complete formation of TiB_2 particles, several preliminary experiments were carried out. Initially, the AA6082-TiB_2 composites with 5wt.% of TiB_2 particles were prepared by optimising the process parameters such as melt holding time, melt holding temperature, stoichiometry of the added fluoride salts and intermittent melt stirring interval. For the optimisation of composites, characterisation techniques such as XRD, SEM, EDS, Optical microscopy and chemical analysis using ICP-OES were used. The mechanical properties were assessed using hardness and tensile tests. Experiments on melt holding time and temperature indicated that, melt holding time of 60 minutes and a temperature of 850°C is essential during the processing of AA6082-5wt.%TiB_2 composite. The experimental results showed that the addition of stoichiometric mixture of K_2TiF_6 and KBF_4 resulted in the formation of Al_3Ti and AlB_2 intermetallic particle along with TiB_2 particles in the matrix alloy. Studies carried out by varying the percentage of KBF_4 salts in the stoichiometric mixture confirmed that 10% of excess addition of KBF_4 salts to the stoichiometric mixture is necessary to eliminate the formation of intermetallic particles. The excess addition of KBF_4 salts to the stoichiometric mixture compensated the loss of B which occurred during the addition of fluoride salts to the aluminium melt thereby forming only TiB_2 particles in the matrix alloy. Investigations on the intermittent stirring interval time

revealed that an interval of 8 minutes intermittent stirring time for 20 seconds is essential for the homogeneous distribution of TiB_2 particles in the composite.

In spite of adding TiB_2 reinforcements, the composites processed during the melt holding time showed deterioration in hardness and tensile properties, when compared with the unreinforced alloy. Hence to understand this peculiar behavior observed among the processed composite, studies were focused to understand the influence of matrix alloy. Hence a thorough investigation on the influence of major alloying elements (Mg, Mn and Si) present in AA6082 matrix alloy during the processing of composites was carried out. Chemical compositional analysis on the processed composites using ICP-OES confirmed the complete loss of Mg in the matrix alloy of the processed composites. Investigations confirmed that the loss of Mg has occurred due to the reaction of Mg with $KAlF_4$ and AlF_3 fluxes which were formed in the melt by the dissociation of K_2TiF_6 and KBF_4 salts. The loss of Mg in the matrix melt was compensated by adding the required amount of Mg to the matrix melt, soon after the removal of slag, thereby restoring the overall properties of composite. Influence of Mg in the AA6082-5wt.%TiB_2 composite was investigated by varying the Mg percent in the matrix alloy. Compared to the unreinforced alloy, composite with the addition of Mg showed 13% increase in hardness and the Y.S and U.T.S were found to increase by 26.5 and 19.2%. However, addition of Mn showed minor improvement in hardness and tensile properties. Presence of Mn in some of the TiB_2 particles indicates the diffusion of Mn atoms into the TiB_2 lattice. During the investigation on the influence of Si, no excess or varying of Si was done. The influence of Si on AlTiSi particles formed during processing of composites was studied with respect to time. Considerable amount of Si from the matrix alloy is seen to diffuse into the Al_3Ti lattice forming AlTiSi particles. However, during the dissolution of AlTiSi particles with increase in melt holding time, Si tends to diffuse out thereby leaving fine Al_3Ti particles in the matrix.

AA6082-TiB_2 particles with different weight percent (2.5, 5, 7.5 and 10wt.%), with and without the addition of Mg was prepared and analysed. Composites processed with the addition of Mg showed better properties, than the composites processed without the addition of Mg.

Ageing treatment on unreinforced AA6082 alloy and AA6082-TiB$_2$ composites at 180ºC after solution treatment at 560ºC show significant reduction in the time for peak ageing and increase in peak age hardness for the as cast composites with respect to those of as cast unreinforced alloy. Ageing kinetics is enhanced with increase in density of particles in the composites. The faster kinetics of ageing is attributed to the higher density of dislocations formed due to the presence of TiB$_2$ particles and fine precipitates formed during ageing treatment.

CONTENTS

LIST OF FIGURES

iv

LIST OF TABLES

NOMENCLATURE

Symbol

T   temperature, °C

μm   micrometre

°C   Degree Celsius

ρ density, kg/m^3

ρ_{th} Theoretical density, kg/m^3

ρ_{Ex} Experimental density, kg/m^3

KeV   Kilo electron volt

Kgf   Kilogram force

KN   Kilo Newton

MPa   Mega Pascal

θ Bragg Angle

m   mass, kg

CHAPTER 1

INTRODUCTION

1.1 General background

The growing demand for lighter and stronger materials has initiated the development of metal matrix composites (MMCs). MMCs are developed by combining the desirable attributes of metals (matrix) and ceramics (reinforcements), leading to superior strength to weight and strength to cost ratio, compared to monolithic alloys. The uniqueness of MMCs is that the desired properties for particular application can be tailored by suitable selection of proper matrix, reinforcements and processing methods. Depending on the type of reinforcements added to the matrix, the MMCs can be categorized into continuous fiber reinforced MMCs and discontinuously reinforced MMCs. The discontinuously reinforced MMCs are further categorized into whisker, short fiber and particulate reinforced MMCs. Although the continuous fiber reinforced composites provide the most effective strengthening capabilities among MMCs, complex fabrication routes, anisotropic and the enormous cost of continuous fibers has limited its applications. High cost, health hazards posed by whiskers and dispersion problems observed in short fibers among the discontinuously reinforced MMCs has led to the development of particulate reinforced MMCs. Moreover the availability of wide range of matrix materials, inexpensive reinforcements and easy fabrication methods has made particulate reinforced MMCs find its applications among the automobile, aerospace, defense and space industries.

With the development of particulate reinforced MMCs, several processing methods were also established in order to overcome the discrepancies observed among one or the other processing methods so as to prepare particulate reinforced MMCs with superior properties. Based on the processing techniques, particulate reinforced MMCs were divided into *ex-situ* and *in-situ* composites. Composites prepared by from processing techniques such as spray deposition, powder metallurgy, mechanical alloying and several other casting methods, namely rheocasting, compocasting and squeeze casting were normally referred to as *ex-situ* composites. In all the above

mentioned *ex-situ* processing techniques, composites were prepared by the addition of prior prepared ceramic reinforcements to the matrix alloy present either in the molten state or in the powder form. The intention of adding reinforcements to the alloy matrix is to improve its strength. Upon the addition of reinforcements to the alloy matrix, contributions from both the matrix alloy and reinforcements aids in improving the overall strength of the composites. The most common strengthening mechanism observed among the particulate reinforced MMCs were found to arise due to the load transfer and generation of high dislocation density. Differences in coefficient of thermal expansion (CTE) between matrix and reinforcements generate high dislocation density in the matrix alloy thereby improving the strength of composites. During loading of composites, the load is transferred from the ductile matrix to the hard ceramic phase which in turn increases the load bearing ability of the composites.

For the load transfer mechanism to be effective the interfacial bonding between the matrix and reinforcements has to be strong. Investigations have revealed that the *ex-situ* processed composites had a poor interfacial bonding strength [Shorowordi et al., 2003]. Moreover complications such as poor wettability, formation of unwanted interfacial products between the matrix and reinforcements, constraints in the size of the reinforcements observed among the ex-situ processed composites led to the development of *in-situ* composites. *In-situ* particulate reinforce MMCs composites are prepared by adding suitable chemical salts to the matrix alloy, where the reinforcements are formed in the matrix alloy by the reaction between the salts and the alloy matrix. Since the reinforcements are nucleated inside the matrix alloy through nucleation and growth mechanisms, homogeneously dispersed, thermodynamically stable, submicron size reinforcements with clean interface leading to better mechanical properties were developed. With the realised potential of *in-situ* metal matrix composites, host of processing techniques was developed. The processing techniques were broadly categorized into liquid-liquid, solid-solid, solid-liquid and vapour-liquid solid (VLS) reaction process [Tjong and Ma, 2000]. Among the available processing methods, solid-liquid based flux assisted synthesis (FAS) technique using liquid metallurgy is found to be a superior and economically viable method for preparing aluminium and its alloy based particle reinforced *in-situ* composites. The main motive of the investigators in the field of MMCs was to

develop light composite material with higher strength, so that when applied in the aerospace, automobile and defense sectors would result in fuel consumption and help in energy conservation. The specific mechanical properties of light metals based composites were found to have significant advantage over the traditional iron based materials. Among the light metals (aluminium, magnesium and titanium), aluminium and its alloys have been much preferred as matrix material for their excellent properties such as low density, high specific strength, good castability, higher thermal stability, good weldability and high corrosion resistance. On comparing with other metals such as Mg and Ti, aluminium alloys are cheaper. Commonly used ceramic reinforcements in aluminium based *in-situ* composites include borides, carbides, oxides and nitrides.

Amongst the available *in-situ* processed reinforcements, titanium diboride (TiB_2) has been attractive for its unique properties like high hardness (34.8 GPa), high melting point (2900ºC), good toughness, good corrosion resistance and its ability to refine the aluminium matrix by acting as a heterogeneous nucleating sites[Munro, 2000]. Addition of TiB_2 particles not only improves the strength of the matrix alloy but also aids in the modification of the matrix microstructure by acting as heterogeneous nucleating sites thereby improving its properties. Although there are several *in-situ* processing techniques available, the flux assisted synthesis (FAS) technique, has been found to be an easy and a reliable method for the processing of *in-situ* Al-TiB₂ composites. This FAS technique was developed from a well-established method for the production of Al-Ti-B master alloys, which were used for the grain refinement of aluminum and its alloys [Murty et al., 1999]. In-situ Al-TiB₂ composites by FAS technique is commonly produced by the adding Ti and B bearing fluoride salts like potassium hexafluortitanate (K_2TiF_6) and potassium tetrafluroborate (KBF_4) into the aluminium melt, where TiB_2 reinforcements are formed by the dissociation Ti and B present in fluoride salts by a strong exothermic reaction which occurs between the melt and the added salts [Davies et al., 1992]. Thus formed TiB_2 reinforcements were found to be fine in size, homogeneously distributed and has good bonding with the matrix alloy.

1.2 Scope of the present investigation

Formation of TiB_2 particles in the melt is a strong function of exothermic reaction, which in turn is dependent on the processing conditions like holding time and temperature of the matrix melt. Inadequate knowledge on the processing conditions will lead to incomplete reaction of the salts with the matrix which results in the formation of intermediate intermetallic phases like Al_3Ti and AlB_2 in the composite. The presences of intermediate phases were found to be detrimental to the properties of the composite. Since the development of *in-situ* Al-TiB_2 composites by FAS, people have been trying to produce this composite without the formation of intermediate reaction products and very few have been successful [Lu et al., 1997, Mandal et al., 2004].

The primary challenge was to find an optimum processing parameter (holding time, holding temperature, salt stoichiometry and stirring time) so as to completely avoid the formation of Al_3Ti and AlB_2 phases in the AA6082-5TiB_2 composites. Composite properties are not only influenced by the reinforcements, but also by the matrix alloy. Minor variation in alloy chemistry of matrix can completely change the overall properties of the composite. Experience gained from the grain refinement studies using Al-Ti-B master alloy indicates that certain solute elements like Mg, Mn, Si, Cu present in the alloy system has considerable influence on the refinement process. Unlike the grain refinement method, in FAS technique there is a direct interaction of the fluoride salts with aluminium alloy which might equally have an influence on the solute elements present in the alloy.

Addition of K_2TiF_6 and KBF_4 flux to the aluminium alloy melt not only forms TiB_2 particulates but can also have a huge influence on the alloying elements present in the matrix alloy. Literatures indicate that in most of the investigations carried out to prepare *in-situ* Al-TiB_2 composites, the matrix alloy used were of either pure aluminium or binary aluminium alloys and very few were on ternary alloy systems. In this study an attempt has been made to understand the influence of Mg and Mn solutes on the microstructure and mechanical properties of AA6082-5TiB_2 composite. Depending on the weight percent of reinforcement particles added to the composite the properties of the composites can be improved. Hence the AA6082 alloy was

reinforced with different weight fraction (2.5, 5, 7.5 and 10) of TiB_2 reinforcements and its effect on the microstructural and mechanical properties has been investigated. Finally ageing studies were carried out on the as cast AA6082-TiB_2 composites in order to understand the ageing kinetics of composite.

1.3 Objectives of the research work

The objectives for the present research work are:

1. To elucidated and optimize the holding time, holding temperature, fluoride salt stoichiometry and stirring time to synthesis AA6082-$5TiB_2$ composites.
2. To study the influence of Mg and Mn solutes on the microstructure and mechanical properties of AA6082-$5TiB_2$ composites.
3. To synthesis AA6082-$xTiB_2$ composites with different weight percent (x-2.5, 5, 7.5, 10wt.%) with and without the addition of solute elements and to understand its properties.
4. To study and compare the ageing kinetics and behavior of the as cast unreinforced AA6082 alloy and AA6082-$xTiB_2$ composites with different weigh percent of TiB_2 reinforcements.

1.4 Organization of the thesis

The thesis is divided into six chapters.

Chapter 1 presents the scope and objectives of the present work.

Chapter 2 presents a through and critical review of the existing literatures in the field of Al-TiB_2 composites.

Chapter 3 deals with the selection and characterization of raw materials, and a detailed description of the experimental procedure.

Chapter 4 deals with the results and discussion of the microstructural characterization and mechanical property evaluation of the alloy and *in-situ* AA6082-$5TiB_2$ composites synthesized with various processing parameters.

Chapter 5 deals with results and discussion on the influence of Mg and Mn solutes on the microstructural and mechanical properties during the processing of AA6082-5wt%TiB_2 composites. With the optimized conditions, AA6082-TiB_2 composites with different weight fractions were processed with and without the addition of Mg was processed and its microstructural and mechanical property changes that occur during the incorporation of different wt.% of TiB_2 particles in the AA6082 alloy matrix was studied. The aging kinetics of as cast unreinforced AA6082 alloy and AA6082-TiB_2 composites was studied. The time for peak ageing and hardness of the alloys and composites have been compared. The effect of ageing behaviour has been discussed.

Chapter 6 presents the summary and major conclusions drawn from the present work.

CHAPTER 2
LITERATURE REVIEW

2.1 Introduction

The increase in demand for stronger, stiffer and lighter materials, in the field of automobile, aerospace and defense sectors has led to the development of particulate reinforced MMCs. Since the development of particulate reinforced MMCs, the scientific investigations by materials scientist have been continuously directed towards improving the properties and performance of these materials. Poor interfacial bonding, formation of unwanted interfacial reaction products between the matrix and reinforcements has led to the reduction in strength of the particulate reinforced MMCs synthesized by traditional (*ex-situ*) techniques. The recently developed *in-situ* processing techniques to prepare these composites provide an alternative to the conventional processing techniques, which results in better improvements in properties. Since the development of *in-situ* method, several processing techniques to prepare in-situ composites were developed. Among the available *in-situ* techniques, the FAS technique has been a much reliable, easy and cost effective method for preparing composites with superior properties. The present work deals with the in-situ synthesis of Al alloy based composites reinforced with TiB_2 particles as reinforcements.

In this chapter, a through and critical review of the existing literature in the field of *in-situ* techniques of Al and its alloy based composites, especially the *in-situ* TiB_2 reinforced Aluminium matrix composites (AMCs) has been carried out and presented. The review is divided into the following broad sections:

❖ Selection of Matrix material for *in-situ* composites

❖ Reinforcements

❖ TiB_2 as reinforcements in aluminium alloy matrix

❖ TiB_2 as grain refiners in aluminium alloy matrix

❖ Fabrication methods for the processing of *in-situ* MMCs

❖ Synthesis of Al and its alloy composites with *in-situ* MMCs

- ❖ Thermodynamics of *in-situ* Al-TiB$_2$ composites
- ❖ Influence of processing parameters
- ❖ Influence of alloying elements
- ❖ Mechanical properties
- ❖ Age hardening behavior
- ❖ Application of TiB$_2$ reinforced AMCs
- ❖ Summary

2.2 Selection of matrix material for *in-situ* composites

Over the centuries metals have been found to be extremely flexible engineering materials. The desired properties in metallic materials can be achieved by suitable selection of alloy composition and thermo-mechanical processing methods. The strength and toughness along with a wide range of manufacturing processes has been the cause behind the abundant usage of metallic materials in engineering application. The need for materials with superior properties compared with the monolithic metals has propelled the materials scientist to develop MMCs. The uniqueness of MMCs is that, its properties can be tailored to meet specific demand with the proper selection of matrix material and reinforcements.

As the name suggests (MMCs) the matrix phase is metallic in nature. The purpose of matrix phase in MMCs is to hold the reinforcements thereby aid in transfer and distribution of the applied load to the hard ceramic reinforcement phase. The bonding strength between the matrix and reinforcements decides the load transfer efficiency of the composite. However the bonding strength depends on factors like the type of matrix alloy, reinforcement and fabrication methods used to process the composite. Both matrix and reinforcements have equal role in the transfer of load. Along with the strong ceramic reinforcements, a strong matrix material is essential for an efficient load transfer mechanism. It is well known that alloys are stronger and are superior in properties compared with the pure metals; therefore higher composite strength can be achieved by use of alloys as matrix materials rather than pure metals. Depending on the fabrication methods the matrix material is used in different forms. The matrix alloy is used in the powder form in composites processed through powder metallurgy

whereas in composites processed thorough liquid metallurgy, the matrix alloy is used in the form of melt.

In *in-situ* composites, the reinforcements are formed in the matrix alloy by a suitable chemical reaction which occurs between the matrix and the added salts. For the reaction to occur between the matrix and salts, suitable matrix alloy has to be selected. Hence for the processing of *in-situ* composites, there is a narrow choice for the investigator in the selection of matrix material. However the conventionally used light metals alloy such as Al, Ti and Mg are very much suitable to be used as matrix material for the processing of *in-situ* composites. Low density, good thermal conductivities and the possible reactive nature of these materials with certain chemicals, makes them the most appropriate matrix material for the processing of *in-situ* composites.

Aluminium and its alloys are found to be the second most extensively used metallic materials next to steels, because of its unique properties like low density, high corrosion resistance, and good formability. Moreover the aluminium alloys are inexpensive compared to Mg and Ti. Pure aluminium has poor strength (tensile strength of 90 MPa) and is soft and ductile. The strength of pure aluminium is improved by the addition of alloying elements like Mg, Si, Mn, Cu, Zn and Li. The aluminium alloys are basically classified as cast and wrought alloys. The cast alloys are used for different casting processes where they can be easily casted into complex shapes because of their high fluidity. The wrought alloys are designed to have low percent of alloying elements with superior mechanical properties than cast alloys. Depending on the addition of alloying elements, the wrought alloys are classified into different alloy systems.

The wrought alloys are generally designated with a four-digit numerical designation system. Pure aluminium systems are denoted by AA1XXX. The 2XXX system belongs to the aluminium alloy where copper is the major alloying elements. Similarly aluminium alloys with manganese is designated as 3XXX, with silicon as 4XXX, with magnesium as 5XXX, with both magnesium and silicon as 6XXX and with zinc as 7XXX. The 8XXX group is used to designate the alloy system with other alloying elements [Grard, 1921]. The 6XXX series alloys are known for their higher

strength, high extrudability, and ease of joining, high formability, weldability and good corrosion resistance. For the above mentioned characteristics the AA6XXX series alloy are used in most of the automobile, aerospace and defense applications [Mukhopadhyay, 2012]. Among the AA6XXX (Al-Mg-Si) alloys, AA6061 and AA6082 possess higher strength values. With the higher amount of Si and Mg the strength AA6082 is slightly higher than AA6061 alloy. The Si present in the alloy improves its age hardening response and the Mn aids in the control of grain size [Birol, 2006].

Titanium (Ti) and its alloys have been known for their high temperature applications. With the melting point of 1750ºC, Ti tends to maintain it the oxidation resistance and structural properties even at 315ºC. Density of Ti alloys (4317 Kg/m^3) is 60% higher than aluminium alloys and 40% lower than alloy steels. The excellent strength to weight ratio, stiffness to weight ratio and good corrosion resistance of Ti alloys make them ideal for aerospace applications. The Ti based MMCs were developed to improve the specific strength of the material. Ti-MMCs were basically developed to be used in the turbine engines, and were subsequently extended for other components. Several processing methods were developed for the processing of Ti-MMCs, which includes powder metallurgy and *in-situ* reaction techniques. The foremost problem associated with the development of Ti-MMCs is the reactive nature of the Ti matrix with the reinforcements at high temperatures. This problem was overcome by the use or coated reinforcements. This limited the use of particulate reinforcements to be used in Ti-MMCs. Moreover complex processing routes, high production cost, and need of vacuum environments for rapid solidification process with the high cost of Ti-MMCs has limited its use in wide range of applications [Naka, 1996, Polmear, 1995].

Magnesium (Mg) and its alloys also belong to the group of light metals, and it is 35% lighter than aluminium alloys. Mg has higher specific strength than Al. However the difference between the two metals seems to be small. Although Mg alloys have good castability, damping capacity and superior machinability, complications such as limited workability at room temperatures, low toughness, low elastic modulus, poor creep resistance and poor corrosion resistance has reduced its usage when compared with Al [Mordike and Ebert, 2001, Xiuqing et al., 2005]. Moreover further

improvement of mechanical properties among Mg alloys has been hindered because of the limited solubility of alloying elements in Mg. Hence further improvements in properties of Mg alloys were obtained by the addition of reinforcements to the Mg alloy matrix. The magnesium matrix composites possessed higher specific strength, higher stiffness, good wear resistance and good high temperature creep properties than aluminium [Zhang et al., 2006]. However the poor workability and highly corrosive nature of Mg-MMCs has affected its development.

2.3 Reinforcements

The intention of adding reinforcements to the metallic matrix is to improve the overall properties of the matrix alloy. The high strength and stiffness of ceramics at ambient and high temperatures makes it a suitable material to be added as reinforcements in aluminium alloy matrix. The reinforcements are added to the matrix alloy either in the form of fibers, whiskers of particulates. Addition of reinforcements not only improves the properties of the matrix alloy it is also equally responsible for the reduction in fracture toughness and ductility. Hence careful and correct selection of reinforcements is very much essential for the processing of MMCs. Lower cost, finer size, cable of exhibiting isotropic property and the availability of conventional fabrication methods to process particulate composites had made material scientist to look for particulate reinforcements rather than the expensive fiber reinforcements. In the selection of reinforcements certain factors like density, particle size, aspect ratio, wettability and its chemical compatibility with the matrix alloy used should be considered. Moreover during processing, the distribution of the reinforcements in the matrix, interfacial bonding strength between the matrix and reinforcement and the composite manufacturing technique also has an equal role in deciding the properties of the composite.

In liquid metal processing of composites reinforcements with equaling density values as that of the matrix alloy is chosen so as to avoid problems like particle sinking and floating. The reinforcements with size ranging between 10-20 μm are used in the *ex-situ* processing of composites. Further decrease in size of reinforcements generally lead to problems segregation and agglomeration [Hashim et al., 2002]. Particles with sharp edges are generally avoided because the sharp edges acts as stress raisers which

subsequently lead to the early failure of MMCs. Spherical shaped reinforcements tend to shown better ductility than angular shaped particles [Romanova et al., 2009]. The ceramic particle reinforcements used among aluminium based MMCs include graphite, carbides (SiC, TiC, TaC, WC, VC, B_4C, Mo_2C, etc.), oxides (Al_2O_3, BeO, CeO_2, SiO_2, MgO, ZrO_2, etc.), nitrides (BN, Si_3N_4, TiN, AlN, TaN, ZrN, etc.) and borides (TaB_2, ZrB_2, TiB_2, WB, etc.). Although the use of these reinforcements seemed to be satisfactory in the beginning, critical problems such as poor bonding and formation of intermediate phases leading to serious interfacial problems between the matrix and reinforcements began to surface. It is well known that strong bonding between the matrix and reinforcements decides the final strength of aluminium matrix composites (AMCs).

Certain well proven reinforcements like SiC, B_4C, TiC, Al_2O_3 tends to react with aluminium alloy matrix leading to the formation of intermediate phases [Rahul and Mahajan, 1993]. Formation of strong intermediate intermetallic phases will lead to better bonding strength whereas formation of brittle intermetallic phases can be extremely detrimental to the properties of the composites. Unfortunately most of the intermetallic phases formed have been found to be detrimental to the properties of the composites. For example the formation of Al_3C_4 intermetallic phase among the carbide (SiC, B_4C, TiC) reinforced AMCs. The formation of Al_3C_4 during the reaction of SiC with Al alloy can be represented as [Lloyd and Jin, 1988].

$$4Al + 3SiC \rightarrow 3Si + Al_4C_3$$
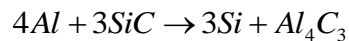
Similarly the reaction with TiC with Al is represented as [Mitra et al., 1993, Satyaprasad et al., 1992].

$$7Al + 3TiC \rightarrow Al_3Ti + Al_4C_3$$
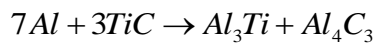
This Al_3C_4 formed is a brittle and unstable phase; moreover the hydrophilic nature of this intermetallic phase could be very sensitive to corrosion environments [Gonzalez et al., 1995, Lloyd et al., 1989, Wang. and Zhang, 1994]. The intermetallic phases formed are brittle and partially ceramic in nature and this leads to weaker ceramic-ceramic bond at the reinforcement/intermetallic phase. On the application of load, cracks are initiated at the interface between the intermetallic phase and matrix leading

to early failure of the AMCs [Clough. et al., 1990]. Over the years several methods were developed for supressing the formation of Al_4C_3. Some of the methods include coating of reinforcements, passive oxidation and addition of Si to the matrix. Coating of metallic materials on reinforcements has been found to be satisfactory in supressing the interfacial reaction and in improving wetting characteristics of the reinforcements with the matrix. But the reaction of the coating with matrix alloy causing unintended matrix composition at elevated temperatures leading to structural instabilies and the overall increase in cost of composites production process has hindered this reinforcement coating method.

Compared to the other methods addition of Si to supress Al_4C_3 has been found to be successful. However addition of Si to the AMCs partially suppressed the formation of Al_4C_3, other problems like increase in viscosity of the melt, high amount of Si in the matrix alloy, reduction in ductility of the composites were encountered. The literatures and experience gained from the composite processing methods using *ex-situ* techniques reveals that addition of prior prepared reinforcements to the matrix alloy has been the main cause for most of the problems encountered among *ex-situ* composites. Hence to overcome the problems encountered among *ex-situ* composites, a new type of MMCs called *in-situ* composites were developed.

In *in-situ* processing methods, very fine, homogeneously distributed and thermodynamically stable reinforcements are nucleated and grown inside the matrix alloy by a suitable chemical reaction between the matrix and added chemicals salts. Other advantages of *in-situ* process reinforcements include: Thermodynamically stable with the matrix alloy even at high temperatures and strong interfacial bonding with the matrix alloy which results from the clean particle matrix interface. Using the *in-situ* processing routes different types of reinforcements based on borides, nitrides, carbides, oxides and their mixtures were formed in matrix like Al, Cu, Ni, Mg and Fe. Among the available reinforcements, TiB_2 with its excellent properties is one of the most preferred reinforcements amongst aluminium alloy based MMCs. Addition of TiB_2 particles not only improves the strength of aluminium alloys matrix by acting as reinforcements, they also contribute to the grain refinement of the matrix alloy.

2.4 TiB$_2$ as reinforcements in aluminium alloy matrix

TiB$_2$ is a ceramic material belonging to the family of transition metal diborides. It is well known that next to diamond, the condensed boron compounds are the hardest materials. TiB$_2$ also belongs to this condensed boron compounds making it one of the hardest material. High excellent properties such as, chemical inertness, high melting point, high strength to density ratio, modulus, hardness, combined with high corrosion resistance, has made TiB$_2$ as a potential candidate in the field of erosive, abrasive and high temperature applications.

TiB$_2$ does not occur in nature, they are artificially made. Fused-salt electrolysis [Gu et al., 2003], mechanical alloying [Hwanga. and Lee., 2002], carbothermal reduction [Kang and Kim, 2007] and mechano-chemical synthesis [Calka and Oleszak, 2007] are some of the methods currently employed to prepare TiB$_2$ powders. Even at high temperatures of TiB$_2$ tends to retain its stability and hardness. The hardness of the TiB$_2$ has been found to be extremely isotropic and the electrical conductivity is high and isotropic. Some of the properties of TiB$_2$ are shown in table 2.1.

TiB$_2$ exhibits hexagonal crystal structure with a space group of P6/mmm and a lattice parameters of a = 3.0236 Å, c = 3.2204 Å, where a=b≠c, α=β=90º, γ=120º. TiB$_2$ belongs to the AlB$_2$ structure related to C32 type, where titanium and boron atoms get stacked in an alternating hexagonal layer. The Ti atoms are located at the origin of the unit cell, whereas the two boron atoms are at the (1/3, 2/3, 1/2) and (2/3, 1/3, 1/2) sites, the crystal structure of TiB$_2$ is shown in Fig.2.1 [Milman and Warren, 2001, Munro, 2000].
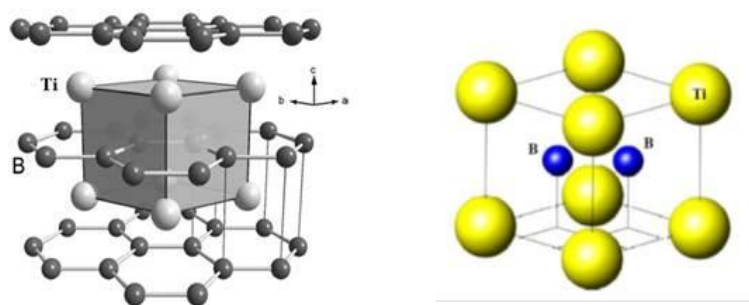
Fig. 2.1 (a) Crystal structure of TiB$_2$, (b) the unit cell of single TiB$_2$ crystal.

The high wettability, formation of clean interface between TiB_2 and aluminium matrix and possession of above mentioned excellent properties and characteristics of TiB_2 makes it the best alternative for the presently available reinforcements. Moreover the Hamaker constant of TiB_2 is very close to molten aluminium, it can be easily captured by liquid aluminium [Karbalaei Akbari et al., 2015].

Table 2.1 Typical properties of TiB_2 [Munro, 2000].

Properties	Values
Density (g/cm^3)	4.5
Melting point	3225°C
CTE, 10-6/K	6.4
Specific Heat, J/Kg. K	617
Thermal Conductivity, W/m. K	96 at RT and 78.1 at 1000ºC
Poisson' Ratio	0.108
Elastic Modulus, GPa	565 at RT
Shear Modulus, GPa	255
Compressive Strength, MPa	1800
Flexural Strength, 4-point bending, MPa	500
Microhardness (VH), 50g Ceramic , kg/mm2	3400

2.5 TiB_2 as grain refiners in aluminium alloy matrix

Grain refinement is generally defined as the deliberate suppression of columnar grain growth in the ingot and castings and formation of fine equiaxed solidification structure throughout the material [McCartney, 1989].

Metals and alloys usually solidify with coarse columnar grain structure under normal casting conditions, unless the mode of solidification is carefully controlled. In order to achieve fine grains several methods such as including addition of heterogeneous

15

nucleants, rapid cooling, ultrasonic vibration, solute addition, mechanical agitation are used [Greer et al., 2000, Zhang et al., 2005]. Of these methods the grain refinement by addition of heterogeneous nucleants (inoculants) is been widely followed because of ease of use and the ductility and toughness of the material is retained even after grain refinement [Pattnaik et al., 2015].

During casting addition of solutes reduces the grain structure to some extent, whereas noticeable refinement was observed during inoculation. Inoculation is the word coined by material scientist for the process in which the equiaxed grains are formed in the cast structure by the addition of solid particles to metallic melt prior to casting. When the solid particles are added to the melt, upon solidification they act as nucleating sites for the grain growth and restricts the formation of columnar grain structure. Grain refinement in metals leads to good surface quality, improved machining, reduced hot tearing tendency, strength, reduced porosity [Kori et al., 2000]. In principle the mechanism of grain refinement is very simple. First numerous effective heterogeneous nucleating sites are introduced into the melt and second, constitutional and heat flow conditions must be such that a large number of these added nucleating sites becomes active enough to nucleate the grain. During this process stable clusters of α-aluminium grains (nucleus) are first formed on the nucleating particles.

With the favourable conditions such as undercooling the growth of grains takes place. The nucleation process is controlled by rate of undercooling. For the nucleate particle to behave as heterogeneous nucleating sites the undercooling must be lower. Moreover equiaxed grains are formed at lower undercooling condition. The process of grain refinement by inoculation has been carried out in the aluminium industry for more than 50 years. The effectiveness of Ti and Ti+B in grain refining of aluminium was first identified by cibula in 1949 [Davis et al., 1970]. Since then several studies related to grain refinement using various refiners is being carried out. Of the available grain refiners, use of Al-Ti-B master alloys has been proven to be efficient. Addition of Al-Ti-B master alloys to the melt introduces heterogeneous particles like Al_3Ti, AlB_2 and TiB_2. Al_3Ti has proved itself to be an effective grain refiner [Jonas et al.,

1999] and AlB_2 has poor grain refining ability compared to Al_3Ti. The grain refining efficiency of TiB_2 is still under debate.

In recent times TiB_2 has been one of the most preferred reinforcements in the *in-situ* processed AMCs for its high strength and other unique properties. The Al-TiB$_2$ *in-situ* processing technique was developed from the technique used to develop Al-Ti-B master alloy. Before being used as reinforcements the TiB_2 particles were added to the melt as inoculants for improving the grain refinement efficiency.

It was Cibula in 1951 who proposed the "boride/carbide" theory [Cibula, 1951], suggested that TiB_2 particles as an efficient heterogeneous nucleant, during the inoculation of melts with Al-Ti-B master alloy. In 1972 Cibula again suggest that although the dispersed TiB_2 particles were acting as nucleating centres for aluminium, it does not have a good match with any of crystallographic planes of aluminium [Cibula, 1972]. The suggestion made by Cibula was further supported by Jones and Pearson in1976 [Jones and Pearson, 1976]. With the observation of TiB_2 particles on the grain boundaries of Al-Ti-B master alloy, Sigworth et al. in 1987 argued that TiB_2 particles were poor nucleants [Guzowski et al., 1987]. Later in 1993, Sigworth et al. in 1993, accepted that TiB_2 as a most active nucleant [Johnsson. et al., 1993]. P. S. Mohanty and J. E. Gruzleski came up with "Duplex theory" where they suggest that solute segregation on the substrate/melt interface was responsible for the nucleation mechanism. They concluded that TiB_2 as poor nucleants when added to pure aluminium, whereas they were found to effective when added to alloys [Mohanty and Gruzleski, 1995]. Since then till now, the investigations have revealed that TiB_2 as an effective nucleant in the presence of solutes.

2.6 Fabrication methods for the processing of *in-situ* MMCs

A variety of MMCs fabrication techniques has been developed in order to improve the structure and properties of particulate reinforced MMCs. The fabrication methods were developed by considering certain important factors like decrease of reinforcement damage, preservation of reinforcement's strength and the improvement related to wetting and bonding of reinforcements. In the last four decades several fabrication methods based on liquid metallurgy, powder metallurgy, vapour phase

infiltration etc., were developed for the synthesis of MMCs. These fabrication methods were basically developed for the synthesis of *ex-situ* composites. However the inevitable shortcomings such as interfacial reaction between the reinforcements and matrix, particle segregation, agglomeration and coarse grain structure in particulate reinforced MMCs observed among *ex-situ* process methods has made materials scientist device a new processing technique called *in-situ* composites. In the *in-situ* fabrication methods the reinforcements are produced inside the matrix alloy rather than adding prior prepared particles. The common *in-situ* based MMCs were fabricated by using techniques based on liquid metallurgy, powder metallurgy etc. Although the terminology (liquid metallurgy, powder metallurgy) used for both *in-situ* and *ex-situ* processing methods were seem to be same, the mechanism and processing techniques were entirely different.

Since the development of *in-situ* composites, several fabrication methods were developed for the processing of *in-situ* MMCs. It was Kozak and Premkumar [Koczak and Premkumar, 1993] who first categorised the *in-situ* processing methods as gas-liquid, liquid-solid, liquid-liquid, etc., based on the starting phases. At latter stage S.C. Tjong and Z.Y. Ma categorised the *in-situ* MMC fabrication methods based on the metallic matrix temperature and reactants as (a) solid-solid, (b) solid-liquid, (c) vapour-liquid-solid and (d) liquid-liquid reaction process [Koczak and Premkumar, 1993]. Of these fabrication methods the solid-solid and solid-liquid based techniques are widely used for the development of *in-situ* Al-TiB$_2$ composites. As the present investigation is related to the development of *in-situ* TiB$_2$ reinforced AMCs, in this section we will discuss some of the advancements that has occurred during the past few years in the development of Al-TiB$_2$ *in-situ* composites.

2.7 Solid-Solid processing

Solid-solid processing commonly refers to the methods involving the processing of *in-situ* Al-TiB$_2$ composites from a solid phase, i.e. the starting material for the processing of *in-situ* composites (matrix and reactants) are taken in the solid form. It is to be noted that the powder metallurgy has been the base for all the available solid-solid based techniques. Reactive hot pressing (RHP), mechanical alloying (MA), and isothermal heat treatment are some of the established solid-solid processing

techniques for the preparation of Al-TiB$_2$ *in-situ* composites. Among the available solid-solid based processing methods the mechanical alloying has been used widely.

Mechanical alloying is a powder processing technique, where the elemental powder mixtures are blended and with a suitable heat treatment a homogeneous material is produced. In this technique the elemental powder mixtures are repeatedly fractured, welded and re-welded by using a high energy ball mill. Processing of Al based *in-situ* MMCs using MA started around 1990s. In 1993 M.A Zongyi et al. synthesised 15Vol% of TiB$_2$ in Aluminium matrix using Al, Ti and B powders as starting material. The powders were milled for 10hrs and hot pressed in vacuum and extruded into rods at 450ºC. The composites showed good tensile properties and poor ductility. The reduction in ductility was related to the presence of Ti aluminides [Zongyi et al., 1993].

Later Z.Y.Ma et al. fabricated Al$_2$O$_3$ and TiB$_2$ reinforced *in-situ* AMCs using Al, B and TiO$_2$ powders as starting material. The powders were cold compacted, heated to 800ºC in vacuum, hot pressed and extruded at 420ºC after 8hrs of milling. They concluded that elimination of Al$_3$Ti phase would certainly improve the properties of the composites [Ma et al., 1994]. In an attempt to prepare 40vol% of TIB$_2$ reinforced AMCs using Al, Ti and amorphous B as starting material H.J.Brinkman et al. identified the formation of AlB$_2$ and Al$_3$Ti phases [Brinkman et al., 1997]. During the development of *in-situ* Al$_2$O$_3$ and TiB$_2$ reinforced AMCs using Al, TiO$_2$ and B as starting material C.F. Feng and L. Froyen confirmed that minor amount of TiB$_2$, Al$_2$O$_3$ and Al$_3$Ti is always formed [Feng and Froyen, 1998].

On investigating the TiB$_2$ formation using Ti and B powders via MA, Lu et al. reported that extensive period of milling (>40 hrs.) time is required even for a low volume fraction. Presence of only TiB$_2$ phase (absence of Al$_3$Ti) in the matrix alloy was due to the fact that at room temperature the enthalpy of formation of TiB$_2$ (-323.6 KJ/mol) is lower that than of Al$_3$Ti (-75.3 KJ/mol). The Al$_3$Ti phases were found to form, when the powders were annealed at 450ºC, but when annealed at high temperature of 600ºC decrease of Al$_3$Ti phases and increase of TiB$_2$ phases was observed. From the observations they suggested three stages in the formation of *in-situ* particles by solid reaction. In the first stage, small amount of TiB$_2$ is formed, and

the other unreacted Ti and B were homogeneously distributed in the solid solution of Al matrix. When annealed at higher temperatures of 450ºC Al_3Ti precipitates out on reacting with the Al matrix in the second stage and in the third stage at higher annealing temperatures Al_3Ti decomposes into Al and Ti where the decomposed Ti reacts with B and form TiB_2 [Lu et al., 1998] Lu et al. prepared *in-situ* Al-TiB_2 composites using Al, TiO_2 and B_2O_3 powders as starting material ball milled at 150 rpm for 4 hrs. From the thermodynamic assessments they suggested that two steps in the formation of TiB_2 particles. First Al_2O_3 tend to form and later Al_3Ti, AlB_2 and TiB_2 were formed [Lu et al., 2001]. Recently Toufic Tayeh et al. produced nano particle TiB_2 reinforced Al matrix composites using Ti and B elemental powders in a planetary ball mill at a constant rotational speed of 250 rpm. Al-TiB_2 composites with three volume fractions (5%, 10%, and 15%) with three grain size of (30, 100 and 450 nm) were prepared. Agglomeration of TiB_2 particles was observed and were separated using ultrasound [Tayeh et al., 2014].

2.8 Solid-Liquid processing

In this solid-liquid processing methods *in-situ* reinforcements are formed by the reaction of solid phase (chemical salts) with the liquid phase. During the reaction process of the solid phase reactants with the matrix alloy (liquid) the reinforcements are formed by nucleation and growth or by diffusion. Compared to the other processing methods the solid-liquid processing methods are being widely used for the processing of *in-situ* Al-TiB_2 composites. Several solid-liquid based processing methods have been established which includes self-propagating high temperature synthesis (SHS), exothermic dispersion (XD), reactive hot pressing (RHP), and flux assisted synthesis (FAS).

2.8.1 Self-propagating high temperature synthesis (SHS)

SHS process was developed by Borovinskaya et al. in 1967 at the institute of chemical physics, USSR academy of sciences [Munir. and Holt, 1989]. SHS or combustion synthesis is a process in which materials with high heat of formation are prepared by from a dynamic combustion wave, which after ignition propagates through the reactants and transforms them into products. SHS reaction takes by the

self-sustaining front. For the reaction from to be self-sustaining three conditions must be met. First the nature of the reaction must be highly exothermic, secondly to enhance the transport of the reaction front one of the reactant must be in liquid or vapour form and thirdly the rate of heat dissipation should be less than the rate of heat generation, thereby ensuring that the reaction is not hindered by heat losses. To develop the material through SHS process, the reactant materials taken in powder form are mixed together and compacted in the green state. On initiating the combustion wave using external sources, the wave propagates through the compact with high velocity thereby converting the reactants into products. The advantage of this process includes high speed of processing and purification because of the volatilization of impurities and effective use of the reaction energy.

The major drawback of this technique is presence of high porosity in the final product [Munir, 1988, Munir, 1992, Munir. and Holt, 1989]. Using this method, variety of ceramics [Holt and Munir, 1986] and intermetallic composite [Philpot et al., 1987] can be prepared. However reports related to SHS processing of *in-situ* MMCs is very less. This is because during *in-situ* MMCs processing the matrix is inert, which at times results in the damping of combustion wave. The formation of *in-situ* TiB_2 and TiC reinforcements in the aluminium matrix was feasible through SHS because of the high exothermic reaction nature of the reactants with the Al matrix.

In 1990 Gotman et al. synthesized 30vol% of *in-situ* TiB_2, TiC and TiB_2+TiC reinforced AMCs using SHS from Al, B, carbon black and B_4C powders. In order to active the combustion process they used very small amount of halogenide-based gas transport agents and the mixture was ignited by passing electric current through tungsten wire. Although they were able to successfully prepare TiB_2 and TiC reinforcements, a small amount of unreacted carbon black was observed in the final component. This was due to the agglomeration of carbon black powder. Moreover they also suggested that this could be overcome by using attrition milling [Gotman and Koczak, 1994].

2.8.2 Exothermic dispersion (XD)

This XD technique was developed during 1980s by Martin and Marietta Laboratories, Baltimore, MD, USA [Mitra et al., 1991]. In this technique the ceramic

21

reinforcements are precipitated in the matrix alloy, when the elemental reactant powders are heated by the matrix alloy. The ability to precipitate the reinforcements inside the matrix by an accelerated chemical reaction makes this method more attractive. For example to develop *in-situ* TiB_2 reinforced AMCs, the elemental powders such as Al-Ti and Al-B are mixed and heated, during which the elements diffuse and precipitate as TiB_2 in the aluminium melt. The reinforcements formed in this method are very fine (0.1- 0.3 µm). Since the interface between the matrix alloy and reinforcements are clean among XD processed materials, the toughness and modulus gets improved.

Using XD technique kurivilla et al. prepared *in-situ* Al-20vol%TiB_2 composites using Al, Ti and B as starting material. First the powders were cold-isostatically pressed with a pressure of 200 MPa with further degassing in vacuum for 1 hr. At 800ºC the Al-Ti-B compacts were heated in the argon atmosphere for 15 min. [Kuruvilla et al., 1990]. ZHU He-guo et al. investigated the exothermic dispersion reaction during the fabrication of aluminium matrix composite in Al-TiO_2-B_2O system. The results obtained from thermal analysis revealed that the reaction process was spontaneous. Among the combustion products, Al_3Ti phases were found to be higher, followed by TiB_2 and α-Al_2O_3 in composites prepared with B_2O_3/TiO_2 with mole ratio lower than 1. The disappearance of Al_3Ti phase was observed when the mole ratio of B_2O_3/TiO_2 increased to 1[Zhu et al., 2007].

2.8.3 Reactive hot pressing (RHP)

RHP processing method was developed from XD technique by Ma et al. for the fabrication of *in-situ* TiB_2 reinforced AMCs. In this processing method *in-situ* Al-TiB_2 composites are prepared by first converting the reactants to the required product by exothermic reaction and then they were further subjected to hot compaction. Al, Ti and B powders with the required stoichiometry are fist cold compacted after through blending. The compacted billet is heated above 800ºC in vacuum for 10 min, and then subjected to hot pressing after cooling down to 600ºC. Ma et al detected the presence of Al_3Ti blocks in the composite[Ma et al., 1993]. In order to eliminated the Al_3Ti phase, Al-TiO_2-B powders were used by Ma et al. rather than the Ti and B powders [Ma and Tjong, 1997]. Addition of B reduced the presence of Al_3Ti and increased the

TiB$_2$ phase in the system. Complete disappearance of Al$_3$Ti phase was observed, when the molecular ratio of B/TiO$_2$ was 2/1. They concluded that *in-situ* AMCs with fine TiB$_2$ and Al$_2$O$_3$ particulates can be produced from Al-TiO$_2$-B powders using RHP technique.

2.8.4 Flux assisted synthesis (FAS)

The FAS or the mixed salt reaction method was developed in 1992 by London Scandinavian Metallurgical Company (LSM) to prepare *in-situ* particulate reinforced composites [Davies et al., 1992]. In this processing method elements bearing chemical salts which can produce exothermic reaction when added with aluminium are mixed and added to aluminium matrix kept in the molten form. Further the added salts react exothermically with the aluminium melt and required elements are dissociated. With further reaction of these elements with aluminium melt the required reinforcements are generated in the aluminium melt. This method was basically developed for preparing *in-situ* TiB$_2$ reinforced AMCs, which was further implemented in the development of *in-situ* AlN, AlB$_2$, ZrB$_2$ and TiB reinforced AMCs [Chen. and Chung, 1996, Mathan Kumar et al., 2016]. Yuyong chen and D.D.L chun prepared 10Vol% of *in-situ* TiB reinforced Al2024 AMCs using TiO$_2$, Na$_3$AlF$_6$ and KBF$_4$ salts [Chen. and Chung, 1996].

Along with TiB reinforcements they observed the presence of Al$_3$Ti phase in the matrix alloy. Recently Narendra Kumar et al produced *in-situ* ZrB$_2$ particles in AA5052 aluminium matrix in different volume fractions using K$_2$ZrF$_6$–KBF$_4$ salts[Kumar et al., 2015]. Y.S and U.T.S values were seen to increase up to 9Vol%, beyond this the strength depleted. Ductility of the matrix alloy improved with the addition of ZrB$_2$ particles. Although people have been trying to prepare various reinforcements using FAS, the development of *in-situ* TiB$_2$ reinforced AMCs has been well established. However doubts on the nature of particle matrix interface in *in-situ* Al-TiB$_2$ composites was raised by Davies et al and Koczak and Premkumar [Davies et al., 1992, Koczak and Premkumar, 1993]. They suggest that some undesirable reaction products are formed on the TiB$_2$ particles. Although several studies relating to this problem has been carried out, the topic is still unclear. Since our investigation is on the development of *in-situ* Al-TiB$_2$ composites a brief

understanding on the literatures based on the processing of *in-situ* Al-TiB$_2$ composites is necessary and it has been discussed briefly in the next topic.

2.9 Synthesis of in-situ Al-TiB$_2$ reinforced composites using FAS technique

Processing of *in-situ* Al-TiB$_2$ composites by FAS technique has been developed from a well-established method for producing Al-Ti-B master alloys used in grain refinement [Mayes et al., 1993]. In-situ Al-TiB$_2$ composites by FAS technique is prepared by the adding Ti and B bearing fluoride salts like potassium hexafluortitanate (K$_2$TiF$_6$) and potassium tetrafluroborate (KBF$_4$) into the aluminium melt, where TiB$_2$ reinforcements are formed by the dissociation Ti and B present in salts by a strong exothermic reaction between the melt and the added salts. The common reaction sequence of the K$_2$TIF$_6$ and KBF$_4$ salts with aluminium melt is as follows [Kellie and Wood, 1995].

$$K_2TiF_6 + 13Al \rightarrow 3Al_3Ti + 3KAlF_4 + K_3AlF_6$$
$$2KBF_4 + 3Al \rightarrow AlB_2 + 2KAlF_4$$
$$AlB_2 + Al_3Ti \rightarrow TiB_2 + 4Al$$
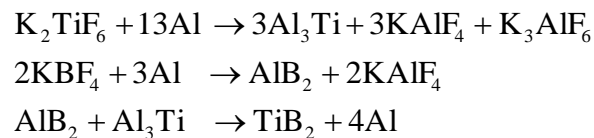
The KAlF$_4$ and K$_3$AlF$_6$ slag which are formed during the reaction tends to float on the surface of the melt. Once the reaction between the salts and melt ceases the slag is decanted and composite melt is cast into a mold of required shape. Since the development of *in-situ* TiB$_2$ composites using FAS technique, people have been trying to improve the properties of the composites by using different raw materials in different aluminium matrix systems. In this topic a through and critical review of the existing literatures in the field of FAS method for the development of *in-situ* TiB$_2$ AMCs has been carried out.

The first literature on the processing of *in-situ* TiB$_2$ reinforced composites using FAS technique was published by P.Davis et al. in 1992 [Davies et al., 1992]. They synthesis *in-situ* TiB$_2$ reinforced composites using A356 cast alloy and Al2014 alloy. The A356 alloy was reinforced with 8wt% TiB$_2$ particles and the Al2014 alloy was reinforced with 9wt% TiB$_2$ particles. They did not reveal the processing temperature and time. The Al2014-9wt%TiB$_2$ composites were further extruded. The tensile property of the matrix alloy was seen to improve over the addition of TiB$_2$ particles in

24

both as cast condition as well as during heat treatment. Later L.Lu et al. [Lu et al., 1997] prepared *in-situ* TiB_2 reinforced composite using Al-4wt.%Cu alloy at 850ºC with a holding time of 35 min. Presence of Al_3Ti was observed along with TiB_2 particles, this shows that the reaction is not complete. Grain size of the composites was found to depend on the duration of the chemical reaction. Moreover they found that the grain refinement was due to the peritectic reaction of Al_3Ti.

In an attempt to incorporate Al into TiB_2 in Al matrix composites and Al-Ti-B master alloys, C.F. Feng and L. Froyen prepared 5 samples via different processes with varying starting material. Sample 1 was prepared by PM route using Al, TiO_2 and B powder mixtures. The samples were heated up to 1400ºC at 10°C/min for 20 min. in a protective atmosphere. TiB_2 and Al_2O_3 particles with size of 1-2 μm were observed. The second and third sample was prepared by FAS route using K_2TiF_6 and KBF_4 salts at 810ºC with a holding time of 35 and 300 min. The fourth sample was prepared by adding AlB_2 and TiB_2 powders to the pure Al melt held 1550ºC for a holding time of 15min along with stirring by rotating the crucible. The fifth sample was prepared with the same condition as followed in sample 4, except that rather than rotating the crucible stirring of the melt was carried out using argon gas. From the observation they concluded that, irrespective of the starting material and processing method, some amount of Al gets incorporated into the TiB_2 phase.

When the melt was held at 810ºC, they observed the reduction of $(Al,Ti)B_2$ to pure TiB_2. Moreover slight change in composition of starting material or stirring did not have any effect on Al in the $(Al,Ti)B_2$ phase [Feng and Froyen, 1997].Lakshmi et al. fabricated *in-situ* TiB_2 reinforcement up to 14.5wt.% in pure aluminium matrix using FAS technique at 850ºC for a reaction time of 45 min. the effect of reaction time and temperature was also analysed during the processing of composites. From the experiments they suggested that there is a specific relationship between the volume of cryolite slag and the rate of formation of TiB_2 particles. Increase in reaction time led to increase in volume of the cryolite slag [Lakshmi and Gupta, 1998]. Jonas Fjellstedt et al. studied the phases such as AlB_2, AlB_{12} and TiB_2 in the Al rich Al-B and Al-Ti-B master alloys prepared by different processing techniques including FAS. They found that there is no mutual solubility between AlB_2 and TiB_2 in samples having Ti/B ratio

1/2. Solubility of Ti was found to very low in AlB_{12} [Jonas et al., 1999]. Nahed El-Mahallawya et al. analysed the reaction between molten Al, K_2TiF_6 and KBF_4 by adding the two salts separately, simultaneously and consecutively at temperature of 800 and 1000ºC. Upon adding K_2TiF_6 salts to aluminium melt emulsification of salts tends to occur and the Al_3Ti particles formed were globular. KBF_4 did not emulsify upon addition to the melt and the AlB_2 formed were in the form of thin plates. Addition of both the salts together resulted in formation of larger dispersed particles at both 800ºC and 1000ºC [El-Mahallawy. et al., 1999]. Z.Y. Chen et al. synthesized *in-situ* TiB_2 reinforcements in Al-4wt.%Cu alloy using TiO_2, H_3BO_3, and Na_3AlF_6 as raw materials at 900ºC.

TiB_2 particles formed were of the average size of 0.93 µm and during low volume percentages (<5Vol%) the particles tends to agglomerate. Needles of Al_3Ti were seen to form besides TiB_2 when the Na_3AlF_6 was added lesser than the stoichiometry [Chen et al., 2000]. C. F. Feng and L. Froyen on investigating the microstructural changes during the preparation said that the FAS reaction using K_2TiF_6 and KBF_4 salts can only be carried in aluminium and its alloy melts. They found that the dispersion was seen to improve when the composites was synthesized using Al-Si alloys as matrix rather than pure aluminium. The Al-Si alloys with low Si did not yield good results in dispersion of the TiB_2 particles [Feng and Froyen, 2000]. B.S.Murthy et al. compared *in-situ* TiB_2 reinforced AMCs, developed using K_2TiF_6 and KBF_4 fluxes as well by Al-Ti-B master alloys in pure aluminium matrix. They observed the presence of Al_3Ti particles along with TiB_2 in composite prepared using fluoride salts.

The composites prepared using Al-Ti and Al-B showed the presence of both Al_3Ti and AlB_2 particles. They found that the reaction between Al-Ti and Al-B master alloys was almost complete at 1000ºC for 60 min and the TiB_2 particles formed were of the size ranging between 4-30 µm with an average size of 10 µm [Murthy et al., 2001]. Yanfeng Han et al. synthesized *in-situ* TiB_2 reinforcements in Al-Si alloy matrix. TiB_2 particles less than 1 µm were found to be within the coralline like eutectic Si and very few were observed in α-Al. Tensile strength was found to increase while high elongation values were retained [Han et al., 2002].

26

Degang Zhao et al. prepared *in-situ* TiB_2 and ZrB_2 reinforcements in pure aluminium matrix using K_2TiF_6, KBF_4 and K_2ZrF_6. The average size of TiB_2 particles were about the 1μm and ZrB_2 was 0.30 μm. The particles were found to be agglomerated and were distributed uniformly in the Al matrix [Zhao et al., 2005]. During the study on precipitation of TiB_2 reinforcements in aluminium melts on reacting with K_2TiF_6 and KBF_4 salts, Jonas Fjellstedt and Anders E.W. Jarfors observed that AlB_2 and AlB_{12} particles were formed on adding KBF_4 salts and the TiB_2 and Al_3Ti were formed from the emulsified slag. Strong evolution of heat was observed during the addition of K_2TiF_6 salts whereas KBF_4 addition resulted in the low rate of heat evolution [Fjellstedt and Jarfors, 2005].

M. Emamy et al. studied the formation of *in-situ* TiB_2 particles in Al matrix using Al-8Ti and Al-4B master alloys at various holding temperatures of 850, 950 and 1050ºC for a constant time of 30 min. They observed that TiB_2 nucleated by the diffusion of boron atoms into the Al_3Ti particles [Emamy et al., 2006]. Hongzhan Yi et al. fabricate sub-micron TiB_2 particles in Al-12Si- Si–1.2% Cu–1% Ni–1% Mg (ZL109) matrix using fluoride salts and evaluated its high temperature tensile properties. The results showed that the U.T.S of composites was higher than base alloy over the temperature range of 25 to 400ºC.

The composite continued show excellent strength, even when the strength of base alloy and composites seems to descent over the temperature of 260ºC [Yi et al., 2006]. T.V. Christy et al. fabricated 12wt.% TiB_2 reinforcements in Al6061 matrix alloy at 840°C using fluoride salts and compared the prepared composite with the base alloy. The composite exhibited increase in tensile strength and decrease in ductility [Christy et al., 2010]. Junping Yao et al. fabricated 0, 5 and 10wt.% of TiB_2 particles in Al-8Si alloy using fluoride salts at a temperature of 780ºC for 60 min. Significant increment in strength was observed due to the addition of TiB_2 particles. Moreover addition of TiB_2 particles not only refined the grains of base alloy, it also modified the Si present in the alloy [Yao et al., 2010]. V.M. Nimbalkar et al. developed *in-situ* 10wt% TiB_2 reinforcement in A356 alloy for a reaction time of 15 min using fluoride fluxes. TiB_2 particles clusters with particle size ranging from 100 to 200 nm were observed on the

inter-dendritic eutectic regions. TiB_2 reinforced composites showed better tensile properties when compared to SiC reinforced composites [Nimbalkar et al., 2011].

N.R. Rajasekaran and V. Sampath prepared 5wt.% and 10wt.% TiB_2 reinforcements in AA2219 alloy matrix at 800°C for 60 min and mechanical properties were evaluated. As the weight percent of TiB_2 particles was increased improvements in mechanical properties was also observed with respect to the wt.%. of TiB_2 [Rajesekaran and Sampath, 2011]. During the development of *in-situ* TiB_2 reinforced Al2014 AMCs processed at 850°C for 45 min., Mallikarjuna et al. concluded that the number of TiB_2 particles decreased at longer melt holding time. Significant decrease in grain size was observed for a holding time of 30 min and at longer holding times fading was observed [Mallikarjuna et al., 2011]. Haimin Ding et al. studied the preparation of TiB_2 particles by TiC in aluminium melts by re-melting the Al-3Ti-0.75C master alloys and adding them with 0.8% and 0.4%B using Al-3B master alloys for a holding time to 10 min. The particles were extracted from the cast by dissolving in HCl and were further anlysed using XRD and FESEM. They found that due to the addition of B, TiC particles became unstable and transformed into TiB_2 and Al_4C_3.

The diameter of TiB_2 particles were found to be in the range of 200 nm to 1 μm and the height was from 100 to 300 nm [Ding et al., 2012]. H.B. Michael Rajan et al. prepared synthesized and characterized the *in-situ* TiB_2 reinforcements with varying wt. % (3, 6 and 9) in AA7075 aluminium alloy matrix at 850°C for 40 min. An excess of 20%KBF_4 salts were added to the stoichiometry mixture of K_2TiF_6 and KBF_4 salts. Due to this excess addition of KBF_4 salts they were able to eliminate the intermediate Al_3Ti and AlB_2 phases. TiB_2 particles with cubic, spherical and hexagonal shapes were present [Michael Rajan et al., 2013]. Zongning Chen et al. developed 5wt.% TiB_2 reinforcement in pure aluminium matrix at different temperatures ranging from 750 to 950°C for different hold time (15, 30, 60, 90 min.) by an improved halide salt route.

During processing of the composites no intermittent stirring was employed. They suggest that high speeds of stirring helps in homogeneous dispersion of TiB_2 particles whereas results in low Ti and B recoveries in the final casting [Chen et al., 2014].

With the successful development of 5wt.%TiB$_2$ reinforcement in pure aluminium matrix by Zongning Chen et al., Tongmin Wang et al. extended it to different aluminium alloys matrix systems (AlSi7Mg0.3, AlCu4.5Si1.1 and AlZn6Mg0.5). In this method the master composites prepared by using Zongning chen et al. were weighed and melted in electric furnace to make a series of AlSi7Mg0.3, AlCu4.5Si1.1 and AlZn6Mg0.5 alloy matrix reinforced with 1, 2, 3 and 4wt.%TiB$_2$ reinforcements. Although the TiB$_2$ particles were seen to be homogeneously distributed, on the microscopic scale the distribution was dependent on the alloy systems.

Depending on the agglomeration observed in different alloy systems the strength of composites varied. Different alloy systems exhibited different strengthening mechanisms. Drawbacks encountered during processing of composites using halide salts can be overcome by this remelting and diluting process. Easy control of alloy composition and TiB$_2$ content with improved melt quality and high strengthening efficiency was achieved by this processing technique [Wang, Tongmin et al., 2014]. Tongmin Wang extended his previous work of preparing *in-situ* TiB$_2$ composites by remelting and diluting and determined the effect of Sr in 3wt.%TiB$_2$ reinforced A356 matrix alloy. Sr with four different weight percent (0, 0.01, 0.03, 0.1) using Al-10wt.% Sr master alloy was added to the remelted A356-3wt.%TiB$_2$ composite melt at 750ºC for 30 min.

For evaluating the re-melting approach a reference A356 alloy reinforced with 3wt.%TiB$_2$ composite was prepared using FAS technique and was directly modified with 0.03wt.% Sr. Comparison showed that complete modification was achieved when Sr was added to composite prepared by re-melting whereas modification was less when Sr was added to composite prepared from FAS. To achieve full modification 0.03wt%Sr was enough, addition of 0.1wt%Sr resulted in over modification of A356-3wt.%TiB$_2$ composite and this over modification was found to determinant to the strength and ductility of the composite [Wang, Tongmin et al., 2014]. Zhiwei Liu et al. fabricated *in-situ* 5wt.%TiB$_2$ particles in pure aluminium matrix using fluoride salts and ultrasound at 700ºC for 10 min.

By using ultrasound 90.4% yield of TiB$_2$ was achieved rather than the 28% achieved in normal FAS technique. Moreover the average size of the *in-situ* TiB$_2$ particles

formed in this technique was around 300 nm [Liu et al., 2015]. S.L. Zhang et al. fabricated *in-situ* TiB_2 reinforced 6063Al composites by using both ball milling and FAS techniques. Al-TiO_2-B_2O_3 powders were used as starting material and were first milled using high energy ball milling for different range of milling time (6-10 hrs.). The milled powders were added to Al6063 alloy melt held at 740ºC with mechanical stirring. After a holding time of 10-20 min the melt was degassed and cast. The TiB_2 particle formed were irregular and circular in shape with size ranging from 0.2 to 1.2 µm with a clean interface between particle matrix reinforcements. The milling time had a profound effect on formation of TiB_2 reinforcements. Longer milling times (10 hrs.) led to the formation of unnecessary brittle phase due to the contamination of Fe with Al and Si. Excellent mechanical properties were obtained in composite prepared from powders added to the alloy melt kept at 740ºC for 15 min added after 8hrs of milling [Zhang et al., 2015].

Jing Sun et al. investigated the effect of alloying elements on the morphology of *in-situ* TiB_2 particles developed using FAS technique at 850ºC for 60 min in Al-7Si, Al-4.5Cu and Al-12Si-4.5Cu alloy systems. Significant changes in morphology transformation of TiB_2 particles were observed due to Si and Cu. TiB_2 particles prepared in pure aluminium matrix exhibited hexagonal plate morphology with smooth surface and clear corners. In Al-7Si and Al-12Si-4.5Cu alloys the TiB_2 particles were of polyhedron morphology with chamfered planes due to the adsorption of Si on the high-index planes. The Cu was found to be adsorbed on the side prismatic planes in Al-4.5Cu alloy. The size and aspect ratio of TiB_2 particles in Al-12Si-4.5Cu and Al-7Si indicates that the evolution of particle morphology is dominated by Si during the coexistence of Si and Cu [Sun et al., 2015].

S.L. Pramod et al. invested the effect of Sc addition on the microstructure and wear properties of *in-situ* 10wt.%TiB_2 reinforced A356 alloy matrix processed at 800°C for 60min. 0.2 and 0.4wt.% of Sc was added to the composite melt using Al-2wt.%Sc master alloy. Fading characteristics of Sc on A356 alloy was determined from the casting obtained at different time intervals (2, 30, 60 and 120 min) held at 730ºC. The observations revealed the modification of eutectic Si and reduction of α-Al SDAS in both A356 and A356-10wt.% TiB_2 composites.

Different Holding time did not have any effect on Si morphology and SDAS. Compared to A356 alloy, addition of 0.4wt.%Sc to A356 alloy and A356-10wt.%TiB$_2$ composite exhibited 20% and 45% increase in hardness. Wear resistance of the alloy was improved by the addition of Sc, whereas decrease in wear resistance of composite was found [Pramod et al., 2015]. Gang Han et al. investigated the high temperature mechanical properties and fracture mechanisms of 4wt.%TiB$_2$ particles in Al-Si piston alloy prepared at 850ºC. Tensile and fracture behavior of the prepared composites was investigated in the temperature range of 25 to 350ºC. Equiaxed shaped TiB$_2$ particles with size of 50-400 nm were formed and were locally agglomerated. Addition of TiB$_2$ particles altered the morphology of needle like eutectic Si to short pole. At room temperature the composites showed high tensile strength, whereas beyond 200ºC the composites and unreinforced alloy exhibited similar tensile strength [Han et al., 2015].

Fei Chen et al. synthesized different wt.% (1, 4 and 7wt.%) of *in-situ* TiB$_2$ reinforcements in pure aluminium matrix by using stir casting in FAS technique. The composites were prepared by adding the stoichiometric fluoride salts to the aluminium melt kept at 860ºC for 60 min. After the addition of salts to the melt, the melt was intermittently stirred at 5, 15, 30 and 60 min with different stirring speeds of 60, 180 and 300rpm using impeller with four straight blades. In the first 15 min of processing the morphology of the TiB$_2$ particles is determined whereas the distribution of the particles is decided by the whole holding process. On stirring the composite melt for first 15 min and last 15 min improves the distribution of TiB$_2$ particles in the melt [Chen et al., 2015]. N.V. Rengasamy et al. developed *in-situ* TiB$_2$ and ZrB$_2$ reinforcements in Al4043 with different wt.% (0, 2, 4, 6 and 8) using K$_2$ZrF$_6$, K$_2$TiF$_6$ and KBF$_4$ salts at 850ºC. The melt was continuously stirred using mild steel stirring coated with zirconia. No detail of the stirring conditions is given. In the final cast the particles were homogeneously distributed.

With the addition of 2wt.% reinforcements the grain size of matrix alloy was found to increase and for the rest of the reinforcements wt.% the grain size decreased [Rengasamy et al., 2016]. Jayakrishnan Nampoothiri et al. prepared *in-situ* 2wt.% TiB$_2$ particles reinforced in Al-4.4wt.%Cu alloy matrix by using FAS and ultrasonic

technique. The composites were first prepared using FAS technique by adding fluoride salts to the alloy melt held at 800ºC for 60 min. Intermittent stirring of the melt at regular intervals was carried out. The composite melt was cast after the removal of slag. The as cast composite was re-melted again at 750ºC and was subjected to ultrasonic treatment using 1.25 and 1.75 kW. The ultrasonic treatment on the composite melt effectively reduced the particle size from micro meter to nano rage. Dissolution and re-precipitation mechanism induced by ultrasonic cavitation was found to responsible for the reduction in size of TiB_2 particles.

Clean particle/matrix interface and nano size of TiB_2 particles was responsible for the drastic improvements in strength of prepared composite [Nampoothiri et al., 2016]. Qi Gao et al. developed *in-situ* 5Vol.%TiB_2 particle reinforced Al-4.5wt.%Cu aluminium alloy composites adding K_2TiF_6 an KBF_4 fluoride flux at 830ºC for 30 min. They added a small amount of MgF_2 and Na_3AlF_6 fluxes to the fluoride mixture in order to accelerate the reaction process. The melt was continuously stirred using mechanical stirring at different speeds of 0, 180, 360 and 540 rpm. Fine TiB_2 particles with size of 0.4 µm were formed. With increase in stirring speeds the homogeneous distribution of particles was observed and large agglomerations are reduced and eliminated when the melt was stirred at speed of 540 rpm. Moreover the tensile properties of the composites improved with increase in stirring speed [Gao et al., 2016].

2.10 Thermodynamics of *in-situ* Al-TiB₂ composites

During the development of *in-situ* TiB_2 reinforcements in aluminium melt by FAS technique using K_2TiF_6 and KBF_4 salts, vigorous exothermic reaction between the melt and added salts takes place resulting in particle phases like Al_3Ti, AlB_2, AlB_{12} and TiB_2 in the casting. Although different particles phases form during the reaction, our intention lies in the production of composite with only TiB_2 particles. Hence a thorough understanding on the kinetics and thermodynamics of the reaction process is a must. In common during this composite processing K_2TiF_6 and KBF_4 salts are added with a Ti/B stoichiometric ratio of 0.5 to the aluminium melt held at temperature range of 750 to 1000ºC.

This technique of preparing *in-situ* TiB$_2$ reinforced AMCs FAS technique was developed from the well-established method used to prepare Al-Ti-B master alloys. Long before the development of *in-situ* Al-TiB$_2$ composites, investigators have been trying to understand the thermodynamics and kinetics of the reaction sequence of fluoride salts with aluminium melt. It was Maxwell and Hellawell [Maxwell and Hellawell, 1972] suggested a ternary peritectic reaction ($L(liquid) + Al_3Ti + TiB_2$) occurred above 665ºC and a ternary eutectic reaction which tends to occurred below 659ºC ($L(liquid) \rightarrow Al_3Ti + TiB_2 + Al$). Later Abdel Hamid and Durand [Abdel Hamid and Durand, 1985] proposed that at temperature ranges of 659 to 665ºC two transition reaction occurred, in the first reaction $L + Al_3Ti \rightarrow TiB_2 + Al$, and in the second reaction $L + TiB_2 \rightarrow AlB_2 + Ti$. Thermodynamic calculations has shown that during the reaction of Ti and B with Al, Al$_3$Ti, AlB$_2$, TiB$_2$ and (Al,Ti)B$_2$ phases were formed [Murray et al., 1986].

In 1999 N.L. Yue et al. established a thermo-dynamical model on the formation of *in-situ* TiB$_2$ particles in Al matrix and compared it with the experimental results obtained from the Al-TiB$_2$ composite made from K$_2$TiF$_6$ and KBF$_4$ salts at melt temperatures of 750 and 850ºC for a holding time of 25 min. Gibbs free energies of formation of Al$_3$Ti, AlB$_2$ and TiB$_2$ at different temperatures was evaluated from the available thermodynamic data and is shown in Fig.2.2 [Yue et al., 1999]
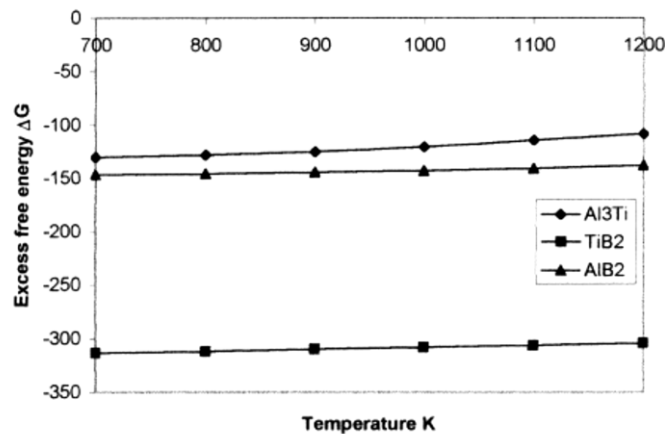
Fig. 2.2 Relation between excess free energy and temperature [Yue et al., 1999].

It can be observed that at temperature ranges of 427 to 927ºC, Gibbs free energy of TiB$_2$ (ΔG_{TiB_2}) was negative than the Gibbs free energy of Al$_3$Ti (ΔG_{Al_3Ti}) and AlB$_2$(ΔG_{AlB_2}). This result confirms that the formation of TiB$_2$ is easier compared to Al$_3$Ti and AlB$_2$. Moreover with increase in temperature, Gibbs free energy of Al$_3$Ti becomes small, whereas for Al$_3$Ti and AlB$_2$ it was almost constant. This shows that at higher temperatures Al$_3$Ti is unstable. Tongxian Fan et al. evaluated the effect of alloying elements during the processing of *in-situ* TiB$_2$ reinforced AMCs using Wilson equation and Miedema model. They suggested that formation of Al$_3$Ti and TiB$_2$ phases can be promoted by certain alloying elements like Mg, Cu, Zr, Ni, Fe, V and La on the other hand these elements can also hinder the formation of AlB$_2$ to a some extent. Presence of Si in matrix alloy has no effect on TiB$_2$ whereas they can hinder the formation of Al$_3$Ti to some extent [Fan, Tongxiang et al., 2005].

2.11 Formation mechanism of *in-situ* TiB$_2$ particles

It is well known that the addition of K$_2$TiF$_6$ and KBF$_4$ salts to the aluminium melt maintained at specific temperature results in the formation of particles like Al$_3$Ti, AlB$_2$, AlB$_{12}$ and TiB$_2$ in the cast. Over the last four decades people have been successfully using this method for preparing Al-Ti, Al-B and Al-Ti-B master alloys, which are commonly used for the grain refinement of aluminium alloys. Since then several theoretical prediction and experimental results have been proposed by investigators on the mechanism related to the formation of particles in the aluminium melt. Recently, based on the master alloy processing technique, the *in-situ* TiB$_2$ reinforced aluminium matrix composites have been developed [Wood et al., 1993].

Two methods are used to prepare the *in-situ* TiB$_2$ reinforced composites. One of the methods involves the synthesizing of *in-situ* TiB$_2$ particles by direct addition of stoichiometrically weighed K$_2$TiF$_6$ and KBF$_4$ salts to the aluminium melt, and the other method involves the addition of prior prepared Al-Ti and Al-B master alloys to the melt. In both of these methods, Ti and B atoms dissolves in the melt and precipitates as Al$_3$Ti and AlB$_2$ particles, which on further dissolution forms into TiB$_2$ particles. M. Emamy et al. suggested the formation mechanism of TiB$_2$ particles during the development of *in-situ* TiB$_2$ reinforced AMCs using Al–8Ti and Al–4B master alloys with a Ti:B weight ratio of 5:2. They observed that TiB$_2$ particles were

34

formed by diffusion of boron atoms on the Al_3Ti particle. They also proposed that five steps were involved during the formation of TiB_2 particles.

In the first step boron atoms moved towards Al_3Ti particles, in the second step the atoms of B reacted with Ti present on the surface of Al_3Ti particles leading to the formation of TiB_2 particles at the melt/Al_3Ti particle interface. Small atomic size of boron was responsible for its diffusion into the Ti lattice thereby forming TiB_2 particles in the third step. In the fourth step the dissolution of Al_3Ti particles seem to occur by the diffusion of boron and with the fragmentation of Al_3Ti particles further diffusion of boron was easy thereby forming more TiB_2 particles and in the fifty stage agglomeration of TiB_2 particles leading to ring structure were present because of the formation of TiB_2 particles at the Al_3Ti particle matrix interface. They also established a schematic representation of TiB_2 formation during the dissolution of Al_3Ti particles and it is shown in Fig.2.3. [Emamy et al., 2006].

LI Peng-ting et al. observed that the processing technique had a commendable impact on the growth and morphology of the TiB_2 particles. They prepared *in-situ* TiB_2 particles by using both Al-Ti-B master alloy and using (K_2TiF_6 and KBF_4) halide salt routes at two different temperatures of 850 and 1200ºC.
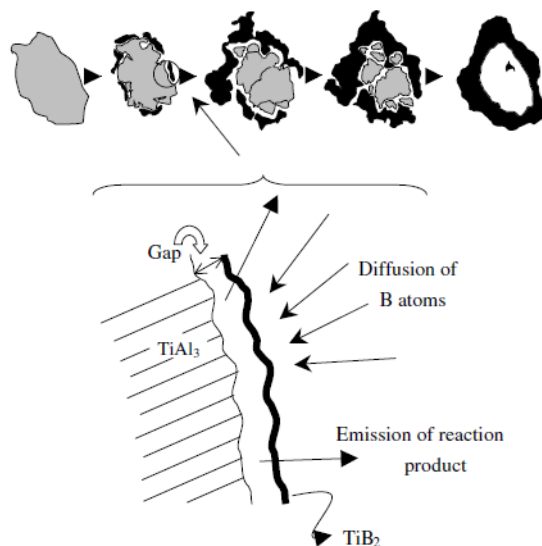
Fig.2.3 Schematic illustrations showing the formation of TiB_2 particle [Emamy et al., 2006].

35

The morphology of TiB$_2$ particles prepared using halide salt routes were mostly of hexagonal platelet and the morphology of the particles did not change with temperature. However TiB$_2$ particles with different morphology were seen in composite prepared using master alloy technique.
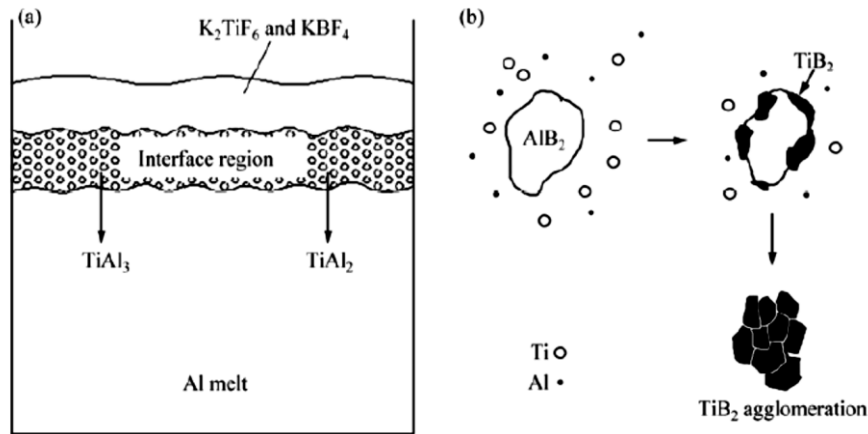
Fig.2.4 Schematic illustrations showing the TiB$_2$ particle (a) Halide salt route, (b) Master alloy route

Agglomeration of TiB$_2$ particles with sizes larger 5 μm was observed in composite prepared at 850ºC and as the processing temperature was increased to 1200ºC the morphology of TiB$_2$ particles changed to layer stacking morphology and even to a dendritic morphology. They suggested that TiB$_2$ particles were formed at the slag/melt interface in composite processed through halide route, whereas in the master alloy route the TiB$_2$ particles were formed by the diffusion of Ti atoms into the AlB$_2$ particles [Li et al., 2012]. They also schematically showed the formation mechanisms and it is shown in Fig.2.4

2.12 Influence of process parameters

2.12.1 Melt holding time (reaction time)

Meld holding time or reaction time of the salts with the melt plays an important role in deciding the formation of the TiB$_2$ reinforcements, during the processing of *in-situ* TiB$_2$ reinforced AMCs. L. Lu et al. investigated the influence of fluoride salts with melt to understand the relationship between the degree of reaction, growth behavior of TiB$_2$ particles and the microstructural and mechanical properties at a temperature of

850ºC by varying the holding time from 5 to 15 min. in pure aluminium and 15 to 35 min in Al-4Cu. They found that the exothermic reaction became complete with increase in holding time and the size of TiB_2 particles formed were independent of reaction time. The formations of more Al_3Ti particles were observed at small holding time, whereas with increase in holding time it became lesser leading to the formation of more TiB_2 particles [Lu et al., 1997].

C.F. Feng and L. Froyen found that with prolonged holding time the duplex (Al,Ti) transformed into TiB_2 [Feng and Froyen, 1997]. Similarly Lakshmi et al. observed that the weight percent of TiB_2 particles increased for a holding time of 20 min and subsequently decreased. Presence of only TiB_2 particles, even for a smaller holding time of 10 min at 850ºC indicates that all the A_3Ti particles have transformed into TiB_2 even at smaller holding times [Lakshmi and Gupta, 1998]. In an attempt to understand reaction between the fluoride salts and aluminium for a maximum time of 60 sec at 800 and 1000ºC, Nahed El-Mahallawya et al. observed the presence of Al_3Ti, AlB_2, AlB_{12} and TiB_2 phases [El-Mahallawy. et al., 1999]. I.G. Watson et al. on investigating the clustering behavior as a function of hold time at 700ºC, suggested that the clustering of TiB_2 particles seems to reduce from 50 to 10 μm for a melt holding time of 73 hrs. [Watson et al., 2005]. Prapas Kunnam and Chaowalit Limmaneevichitr on investigating the different holding times of 1, 30, and 60 min. at 800ºC found that the morphology of Al_3Ti and TiB_2 became too large when the holding time were beyond 30 min.

Composite processed at 30 min. showed higher grain refinement efficiency. Even at longer holding time of 60 min. they observed the presence of Al_3Ti particles along with TiB_2 [Kunnam and Limmaneevichitr, 2008]. Whereas C. Mallikarjuna et al. on processing of *in-situ* TiB_2 reinforced Al2014 composites at different holding time of 15 to 45min at 850ºC, found that the grain size gradually decreased with increase in holding time [Mallikarjuna et al., 2011]. Recently Zongning Chen et al. during the development of *in-situ* TiB_2 reinforced AMCs, investigated the influence of holding time (15, 30, 60 and 90 min) at constant temperature of 850ºC. Presence of AlB_2 particles and agglomeration of TiB_2 particles has occurred at lower holding time of 15 and 30 min. Further holding the melt till 60 min. showed the presence of only TiB_2

particles with lesser agglomerations. Whereas with longer holding time of 90 min. homogeneous distribution of TiB_2 particles were observed [Chen et al., 2014].

2.12.2 Melt holding temperature (reaction temperature)

In FAS technique of preparing *in-situ* TiB_2 reinforced AMCs, melt holding temperature of reaction temperature of the melt decides kinetics of the reaction of salts with aluminium. Several investigators have tried to process and understand the influence of holding temperature during the processing of *in-situ* TiB_2 composites using K_2TiF_6 and KBF_4 salts. KVS Prasad et al. observed that, KBF_4 salts were able to react with solid aluminium, whereas K_2TiF_6 reacted with aluminium only above its melting point (728ºC) [Prasad, K. V. S. et al., 1996]. They also found that samples prepared at 750ºC had Al_3Ti particles present along with TiB_2. Al-TiB_2 composite fabricated at 850ºC by varying the holding time did not yield Al_3Ti or AlB_2 particulates even for 10 min. of holding [Lakshmi and Gupta, 1998]. Whereas N.L.Yue et al. and Jonas Fjellstedt observed the presence of Al_3Ti, AlB_2 and TiB_2 phases composite processed at 750ºC as well as at 850ºC for a reaction time of 25 min. [Jonas et al., 1999, Yue et al., 1999] . No change in the size, morphology and microstructure was observed among the composites processed at various holding temperatures (810, 910 and 1010ºC) for a prolonged holding time of 10 to 300 min[Feng and Froyen, 2000]. Murty et al. observed more number of Al_3Ti particles along with TiB_2 in the composite processed at 800ºC for 60 min. [Murthy et al., 2001]. More recently Zongning Chen et al. [Chen et al., 2014] observed that no significant change in the grain size among the composites prepared at different holding temperatures of 750, 850 and 950ºC for a constant holding time of 60 min.

2.12.3 Salt stoichiometry

It is well known that *in-situ* TiB_2 reinforcements are formed in the matrix melt by the addition of K_2TiF_6 and KBF_4 salts to the melt maintained at a suitable temperature and time. Upon addition of the salts to the melt Ti and B dissociate from the salts and form Al_3Ti, AlB_2, AlB_{12} and TiB_2 particles. Although several factors are involved in deciding the TiB_2 particle formation, the stoichiometry of the salts added (Ti/B ratio) plays an important role in deciding the formation of final particle. If the excess of Ti is added compared to B, it results in the formation of large amount of Al_3Ti particles

in the melt, on the other hand if B is added in excess it leads to the formation of AlB_2 particle in the melt along with TiB_2.

Presence of these Al_3Ti and AlB_2 particles in the composite will deteriorate the composites properties. Hence the ratio of Ti to B should be so precise that it should lead to the formation of only TiB_2 particles in the melt rather than Al_3Ti and AlB_2. Since the development of Al-Ti-B master alloy to the development of *in-situ* TiB_2 reinforced composites, several investigations related to the understanding of Ti:B ratio in the melt has been carried out. A.J.Cornish et al. and L.Bacaerud found that, a rim Al_3Ti phase tends to form on the TiB_2 particles when the Ti/B ratio was > ½. They explained that $(Al,Ti)B_2$ phase is formed first by the diffusion of Al into the TiB_2 particles. Thus the Ti in $(Al,Ti)B_2$ diffuses out of the particles forming a rim of Al_3Ti phase. But when $(Al,Ti)B_2$ is most thermodynamically stable phase its composition should be on the Ti rich end when Ti/B>1/2. Hence the explanation given by L.Bacaerud et al. has been found to be incorrect. Moreover Al_3Ti should be unstable when Ti/B<1/2, and hence the stability of Al_3Ti changes at the surface of TiB_2 and this explains that Ti reacts with Al forming Al_3Ti [Backerud, 1971, Cornish, 1975].

During the growth of TiB_2 particle in aluminium melt with a Ti/B>1/2, Higashi and Atoda and Higashi et al. found that Al found in the TiB_2 crystal was less than 0.0001wt.% [Higashi and Atoda, 1970, Higashi et al., 1976]. H.Li et al showed that when the Ti:B ratio is equal to 1 or slightly less than 1, Ti is completely consumed in the formation of TiB_2 particles in the melt, because TiB_2 has larger enthalpy of formation (326.41 kJ mol $^{-1}$) [Li et al., 1997]. Jonas Fjellstedt et al. showed that mutual solubility between AlB_2 and TiB_2 is impossible, and hence they were found to coexist in samples having Ti/B ratio of <1/2 [Jonas et al., 1999].

2.12.4 Melt stirring

During the processing of *in-situ* composites, sever exothermic reaction between the salts and fluoride flux along with intermittent stirring caused the homogeneous dispersion of the reinforcements. Since the development of in-situ composites by FAS technique several people have been preparing the composites by employing the standard intermittent stirring of the melt by manual stirring at regular interval of time

[Murthy et al., 2001]. More recently Fei Chen et al. investigated the influence mechanical stirring on the microstructural and mechanical properties at various stirring speed, stirring duration and stirring start time. The investigations revealed that more uniform microstructure can be achieved when stirred at a 180rpm in both the first and last 15 min. of the total 60 min. processing time. Most of investigation reported so far on the microstructural development on in situ processes composites using FAS techniques were on manual intermittent melt stirring, other possibilities such as without stirring and mechanical stirring at high rpm has not been elaborately reported [Chen et al., 2015].

2.13 Influence of alloying elements

2.13.1 Influence of Mg

It is well known that the microstructural and mechanical properties of aluminium alloys are dictated by the alloying elements present in them. Among the principal alloying elements added to the aluminium alloys, magnesium (Mg) addition has been found to enhance the strength and corrosion resistance of the alloys. Mg when added as a sole element to aluminium, the strength of alloy is improved by solid solution strengthening [Iwahashi et al., 1998, Wen et al., 2005] whereas when added with other alloying elements especially with silicon the alloy is strengthened by precipitation hardening [Salleh et al., 2015, Tao et al., 2015]. Apart from the aluminium alloy systems, Mg additions was found to have greater impact on the properties of *ex-situ* processed aluminium based Metal matrix composites [Pai et al., 1995]. The presence of Mg in the recently developed *in-situ* TiB_2 particle reinforced AMCs has enhanced the properties of the composites. Addition of Mg and Li to the composite melt favoured the low surface energy conditions in the melt which promoted the formation of fine TiB_2 particles by high nucleation and low growth rate. Moreover addition of Mg and Li was found to be the reason behind clustering of TiB_2 particles [Jha and Dometakis, 1997].

DSC and dilatometery studies by H.J. Brinkman et al. showed that addition of Cu increased the reaction rate to form TiB_2 reinforcements during the processing of 2124-TiB_2 MMCs. The observations also showed that Mg present in the alloy did not

volatize during exothermic reaction [Brinkman et al., 1997]. However the theory behind the process has not been explained. Murty et al. showed that Mg addition reduced the poisoning effect due to Si and in improved the grain refining efficiency during the manufacturing of Al-7Si master alloys [Murty et al., 1999]. C.F.Feng and Froyen observed no improvements in grain refinement or dispersion of TiB_2 particles over the addition of Mg during the processing of Al-TiB_2 MMCs [Feng and Froyen, 2000]. Besides understanding the reaction of aluminium with fluoride salts, the first insight on the feasibility of Mg to react with fluoride salts was given by M.A.Martin et al. By both theoretical prediction and experimental results they confirmed the reaction between Mg melt and the fluoride salts is chemically and thermodynamically feasible.

The results also confirmed that the formation of titanium boride particles due to the exothermic reaction between Mg and fluoride salts is a strong function of time and temperature[Matin et al., 2001]. The theoretical evaluation on the thermodynamic effect of alloying elements on the precipitated phases in *in-situ* reinforced Al/TiB_2 composites using Wilson equation and by extended Miedema model prophesied the formation of Al_3Ti and TiB_2 phases can be promoted by the Mg present in the alloy. The evaluated results also showed that Mg has higher affinity to react with the salts to form TiB_2 than aluminium [Fan, Tongxiang et al., 2005]. The insitu processed as cast A356-TiB_2 composites showed a reduction in hardness up to 5wt% of TiB_2 reinforcements was observed compared to the monolithic alloy. They predicted that the loss of hardness in the as-cast composite was due the depletion of Mg in the matrix alloy. Although the predictions were found to be valid no concrete evidence was given.

2.13.2 Influence of Mn

The intention of adding alloying elements to the pure aluminium or aluminium alloys is to improve the alloy properties. Elements like Si, Mn, Mg, Cr and Li are the most preferred alloying elements used in the development of different aluminium alloy systems. Although these elements are added externally to improve its properties, certain elements like Fe which are present in the aluminium as impurities tends to form harmful intermetallics (AlFeSi) because of its low solubility in aluminium

41

alloys. Hence manganese is added to the aluminium alloys in order to neutralize the harmful effects of Fe by modifying the morphology of intermetallic phases[Seifeddine and Svensson, 2009, Shebestari et al., 2002]. Along with the correction the embrittling effect of iron, manganese addition to Al-Mg-Si alloys forms high melting intermetallic compounds such as $Al_{15}(FeMn)_3Si_2$ or $Al_{15}(FeMnCr)_3Si_2$ thereby resulting in high temperature strength and creep resistance of the alloys [Nam and Lee, 2000]. Addition of manganese also helps in control of grain size.

He Yongdong et al. suggested that Mn when added with Cr in minor quantities acts as for the nucleation of Al_3Ti particles. The combined addition of Mn with Cr, Ti, Zr and B can result in intensive grain refinement. The Mn and Cr tends to form atomic clusters, which are responsible for the nucleation of $Al_3(Ti_x,Zr_{1-x})$ particles [Yongdong et al., 2010]. Investigation on the effect of alloying elements like Mg, Sb, Mn, Cu, Zn, Fe, Cr and Si in the formation of microstructures during the development of *in-situ* $Al-TiB_2$ AMCs, C. F. Feng and L. Froyen observed that none of these elements aided in the distribution of TiB_2 particles. Moreover they did not have any effect on the grain refinement of the Al matrix [Feng and Froyen, 2000].

2.13.3 Influence of Si

Among the Al alloy based castings the presence of impurity and alloying elements complicates the microstructure by forming a wide range of intermetallic phases. Two major classes of impurities can be distinguished in molten aluminum as dissolved elements and suspended particles, which may be non-metallic or intermetallic in character. Elements such as Fe and Si may be referred to as non-reactive because they are very difficult to remove from aluminium by ordinary fluxing processes. The application of grain refiners and/or Ti containing master alloys for improving mechanical properties may result in formation of Al–Ti based intermetallics. Although the grain refinement produces many desirable qualities in aluminum castings such as improved castability and mechanical properties, the addition of Ti to Al–Si foundry alloys may lead to the formation of some undesirable intermetallic particles and operational problems. Birol Y. [Birol, Y. 2013] reported that when Ti containing Al–Si hypoeutectic melts are held over a long period of time, AlTiSi crystals could segregate out of the melt to form ''sludge'' at the bottom of melting or

holding furnace. Sokolowski et al. [Sokolowski et al., 2001] showed that an excess Ti promoted the formation of insoluble AlTiSi crystals, either within the cast structure or within the liquid metal processing line. These crystals are detrimental to the mechanical properties of the as-cast components and their continuous growth, depending on the particles morphology, could disturb the flow of molten metal during filtration and feeding. Therefore, it is of great technical and technological importance to control the formation and morphology of AlTiSi intermetallics in Al–Si foundry alloys in order to eliminate the above-mentioned problems. In the presence of Na_3AlF_6 and $K_{1-3}AlF_6$ fluxes, Peijie Li et al. [Peijie Li et al., 2003] observed that the diffusion of Si into the AlTi lattice did not take place. Investigations carried out Tang Gao et al. [Tang Gao et al., 2011] on the influence of Si and Ti contents on the influence of Si and Ti contents on the microstructure, microhardness and morphology of TiAlSi intermetallics in ternary Al–Si–Ti alloys indicated that The increase of Si addition in Al–xSi–2Ti alloys leads to an increase of Si content in TiAlSi phase as well as an increase of microhardness.

2.14 Mechanical properties

Westwood and Winzer were the first people who reported that the *in-situ* Al-TiB$_2$ reinforced composites prepared by XD technique showed an increase in moduli of 40% higher than that of the base matrix alloy [Westwood, 1988]. Kurivilla et al. compared the tensile properties of the *in-situ* Al-TiB$_2$ composites with that of the *ex-situ* Al-TiB$_2$ composites prepared by using the XD technique. The results confirmed that the properties of *in-situ* Al-TiB$_2$ composites were twice as large as the *ex-situ* processed composites. They suggested that an improvement in properties was due to the well bonded and finely dispersed TiB$_2$ particles [Kuruvilla et al., 1990].

During the development of *in-situ* TiB$_2$ reinforcements in AA2014 alloy using FAS technique, Davis et al. observed that, composites showed better tensile strength and decrease in ductility than base alloy [Davies et al., 1992]. Since then people have tried to develop *in-situ* TiB$_2$ reinforced AMCs using different alloy system with different wt.%. Some of the available data from the literatures about mechanical properties of

43

in-situ Al-TiB$_2$ composites using FAS technique (as-cast condition) are listed in Table 2.2.

Table.2.2 Tensile properties of various TiB$_2$ reinforced AMCs prepared using FAS technique.

System	TiB$_2$ Wt.%	Time (Min.)	Temp. (ºC)	0.2% Y.S (MPa)	UTS (MPa)	% Elong.	Ref.
Al-4Cu	5	0	850	51	119	17.4	[Lu et al., 1997]
		15		111	243	9.6	
		25		179	277	3.1	
		35		156	282	7.9	
Al-4Cu	0	60	800	108	117	11	[Mandal et al., 2004]
	2.5			171	196	23	
	5			208	232	20	
	7.5			220	260	18	
	10			230	290	15	
A356	0	60	800	110	184	9	[Mandal et al., 2008]
	2.5			135	206	7	
	5			151	215	6	
	7.5			196	231	5	
	10			200	256	4	
Al6061	0	60	840	80	135	8	[Christy et al., 2010]
	12			94	174	7	
Al-8Si	0	60	780	71	152	11	[Yao et al., 2010]
	5			132	184	8	
	10			160	219	5.3	

AA2219	0	60	800	144	211	11	[Rajesekaran and Sampath, 2011]
	5			165	219	7	
	10			205	234	6	
A356	0	60	850	80	139	4.2	[Wang, Tongmin et al., 2014]
	3			106	166	3.6	
A356	0	30	850	200	232	11	[Wang, Mingliang et al., 2014]
	2.12 Vol			209	235	8	
	4.66 Vol			213	252	7	
	8.37 Vol			218	258	2.3	
Al-12Si	0	30	850	221	287	3.3	[Han et al., 2015]
	4			240	298	1.5	
Al-Cu-Li	0		780	331	397	4.8	[Shen et al., 2016]
	7			389	469	3.0	

2.15 Age-hardening behaviour

It was Alfred Wilm in 1906, who first accidentally discovered that after being quenched from 450ºC, the soft AlCuMgMn alloy became harder by ageing treatment. In 1919, Paul Merica an American metallurgist on investigating the effect of ageing in Al-4%Cu alloys, suggested that during ageing, more or less coherent clusters or precipitates of Cu atoms are formed first due to the segregation of Cu atoms. Later the age-hardening was explained by the interactions of local defects and dislocations. Hence studies on zones or coherent precipitates have become more important in understanding the age-hardening behavior of aluminium alloys [Guinier, 1996]. During quenching an excessive amount of vacancies and dislocations are introduced in the aluminium alloys and this accelerates the precipitation in the aluminium alloys thereby leading to increase in strength. Improvements in strength attained during age-hardening of aluminium alloy have motivated the researchers to explore new possibilities in attaining age-hardening effect in new alloy systems. With the

development of AMCs using age-hardenable alloys as matrix, the strength of the matrix alloy was drastically improved by the strengthening attained from both reinforcements and age-hardening. Upon the addition of ceramic reinforcements to the matrix alloy, residual stresses are developed in the matrix surrounding the reinforcements because of the difference in coefficient of thermal expansion (CTE) between matrix and reinforcements.

These residual stress fields are formed depending on the difference in magnitude of CTE between the matrix and reinforcements. Furthermore the stress fields generated are relieved by the generation of dislocations at the particles/matrix interface [Rohatgi et al., 2001]. Arsenault et al. suggested that the high dislocation density formed was responsible for the strengthening in composites [Arsenault, 1984]. During the ageing studies in the *ex-situ* Al/SiC (Particulate/whiskers) composites Z.Y.Ma et al. observed improvements in tensile strength after quench treatments and the strength were seen to increase with further increase in quench temperatures. They also suggested that, increase in strength was attributed to the formation of high dislocation density. The formation of Al_4C_3 phase due to the interfacial reaction between SiC and Al, at the interface between the Al matrix and SiC reinforcements was also observed [Ma et al., 1993]. With the presence of reinforcements, the matrix alloys exhibited an accelerated kinetics in ageing, compared to that of unreinforced alloys.

Ageing studies on A356 alloy reinforced with SiC reinforcements showed a decrease in ageing kinetics. This decrease was attributed to the formation of spinel, $MgAlO_4$ leading to the depletion of Mg in the matrix alloy [Wang et al., 1992]. During the development of *in-situ* TiB_2 reinforced composites, P.Davis et al. studied the ageing behaviour of AA2014 and A356 matrix alloy, they reported that the tensile properties of AA2014 alloy improved whereas in A356 alloy depletion of tensile properties was observed [Davies et al., 1992]. Over-ageing was found to be the reason behind the decrease in tensile properties of A356 alloys. Heat treatment studies on *in-situ* 6wt.% TiB_2 particles reinforced Al-11Si-0.5Mg composites not only showed an increase in tensile strength but also transformed the eutectic Si morphology from coralline to particle[Han et al., 2002]. Mandal et al. showed that on increasing the amount of TiB_2 particles from 0 to 10wt.% in Al-4Cu alloy matrix, at ageing temperature of 170ºC,

the time to peak ageing and ageing kinetics came down from 40 to 6hrs. [Mandal et al., 2004]. Similarly Mandal et al. also have shown that at the ageing temperature of 155ºC, compared to the base alloy, the ageing time of 10t.%/A356 composites came down from 12 to 4 hrs. [Mandal et al., 2008].

Studies on precipitation kinetics of *in-situ* Al-Si-Mg-TiB$_2$ composites using DSC and TEM, Sree Harsha Nandam et al. found that with increase in TiB$_2$ content decreases the activation energies of GP zones [Nandam, Sree Harsha et al., 2011]. Tianaran Hong et al. discussed the ageing process in composites by combining its precipitation mechanism with the effect of reinforcements. During the ageing studies on *in-situ* TiB$_2$/Al–Cu–Mg composites, they observed two hardness peak behaviors as a function of ageing time in composites aged at 180°C. They also suggested that a two-step process which occurred during precipitation of composites[Hong et al., 2015]. The literature survey reveals that apart from the numerous age-hardening studies available on the *ex-situ* processed composites, the ageing behavior of *in-situ* composites has been less studied.

2.16 Applications of TiB$_2$ reinforced AMCs

Aluminium matrix composites have been considered to be a best replacement for traditional materials used in several automotive, aerospace and military applications. Although the in-situ TiB$_2$ reinforced components are newly developed, a variety of components like car pistons, motorcycle pistons, train brake discs, clutch discs etc., have been produced. Depending on the component, the production technique and precise specification of the material, the alloy and percentage of reinforcements are varied. Prior to the application the selected materials were characterized in terms of microstructure, mechanical properties and wear resistance. Typical applications of these MMCs include connecting rod made of AA2618-TiB$_2$ composites. In aerospace industries AA7075 reinforced with TiB$_2$ particles are used in helicopter blade sleeves. These composites are also used in seat track application. In the automotive sector A356 alloy reinforced with TiB$_2$ particles produced from high pressure die casting are used as cylinder liners. The use of TiB$_2$ reinforced composites in various components clearly indicate that this type of composite material has promising applications in different applications.

2.17 Summary

In the present literature review, the status of knowledge concerning current developments in synthesis, mechanism, microstructure, mechanical properties and ageing of *in-situ* TiB$_2$ reinforced AMCs has been addressed. Although varieties of *in-situ* processing techniques have been developed, the review confirms that liquid-solid based FAS methods have been an easy method for synthesizing *in-situ* Al-TiB$_2$ composites. The thermodynamics and mechanism responsible for *in-situ* formation of TiB$_2$ reinforcements in aluminium matrix has also been explained. The mechanical properties and ageing studies of *in-situ* Al-TiB$_2$ composites carried out by various investigators have also been discussed.

Reviews on the available literatures shows that either pure aluminium or binary aluminium alloys and very less of ternary based alloys have been used in the development of *in-situ* TiB$_2$ reinforced composites. The existing studies suggest that there is a lack of understanding on reaction mechanisms and optimization of processing parameters. Hence in the present work an effort has been carried out to optimize the process parameters like holding time, holding temperature, melt stirring speed and salt stoichiometry during the development of *in-situ* AA6082-5wt.%TiB$_2$ composites. Little information is available on the influence of alloying elements during the processing of *in-situ* AA6082-5wt.%TiB$_2$ composites by FAS technique. Hence an attempt is made in order to understand the influence of alloying elements like Mg and Mn. With the above understanding AA6082-TiB$_2$ *in-situ* composites with different wt.% of TiB$_2$ particles were developed and its mechanical properties and ageing studies were carried out.

CHAPTER 3
EXPERIMENTAL DETAILS

In-situ processing of Metal Matrix Composites (MMCs) by liquid metallurgy is a relatively new, cheap and promising technique for the processing of TiB_2 particulate reinforced aluminium based MMCs. Literature survey reveals that either pure aluminium or aluminium alloy having very less alloying elements were used as matrix in most of the investigation on processing of *in-situ* TiB_2 composites. Processing of *in-situ* TiB_2 particulates reinforced aluminium MMCs involves nucleation of fine TiB_2 particulates in the melt by exothermic reactions of the salts with aluminium melt. Careful control on the processing parameters like reaction time, reaction temperature, chemical composition of fluoride salts and stirring of the melt dictates the formation of TiB_2 particulate phase in the matrix.

Negligence in controlling the processing parameters will lead to incomplete chemical reaction between the fluoride salts and melt forming unwanted intermediate particulate phase in the final as-cast composite. Interaction of alloying elements present in melt with the fluoride salts should also be understood. Weak matrix may lead to the deterioration in properties of the composites, therefore interaction of alloying elements present in the matrix with the fluoride salts should be understood to produce composite with superior properties. Increasing the percentage of TiB_2 particulates in the matrix normally leads to improvement in properties of the composites.

Ageing treatment on composites tends to improve the properties by the formation of fine precipitates depending on the matrix system. Therefore for successful processing of in situ TiB_2 reinforced aluminium alloy composites, through understanding of mechanism and thermodynamics of the reactions should be well understood. The present work is an attempt to study the influence of processing parameters, alloying elements, varying the wt.% of TiB_2 particulates, ageing and mechanical properties of the processed AA6082-xTiB_2 composites where x (x = 2.5, 5, 7.5, 10) wt. %. Investigations on influence of processing parameters and alloying elements were

carried out in AA6082-5 wt.% TiB_2. Composites with different weight fractions were prepared, upon the successful preparation of AA6082-5TiB_2 composite.

The experimental part of this work can be divided into four sections. As a first, systematic experiments were performed to understand influence of process parameters (holding time, reaction temperature, flux composition and stirring time) during the *in situ* formation of 5 wt. % TiB_2 composites in AA6082 alloy. The relevant factors in the processing parameters variables were varied systematically. Microstructure and mechanical property results were analyzed in order to identify optimal conditions for the processing of AA6082-5TiB_2 composite.

Second part of the experimental study was carried out to understand the influence of fluoride fluxes on the major alloying elements (Mg, Mn and Si) present in the molten matrix in order to improve the properties of AA6082-5TiB_2 composite.

Third part of experimentation was performed to understand the influence of TiB_2 particulates on AA6082 matrix by varying the weight percent of TiB_2 particulates. Weight percent of TiB_2 in the AA6082 matrix was varied from 2.5% to 10% in steps of 2.5%. Fourth part of the experimental study was focused on the ageing studies of the processed AA6082-xTiB_2 (x = 2.5, 5, 7.5, 10 wt. %) composites.

DTA (Differential thermal analysis) and TGA (Thermo Gravimetric Analysis) analysis were carried out to understand the reaction behavior between the fluoride salts and aluminium alloy. ICP-OES analysis was performed on the processed composite casting to determine the elemental composition. The percentage of porosity present in the casting were found using Archimedes method. The weight percent of the particulates present in the processed composites were found by acid dissolution method. The processed composites were further analysed by subjecting it to different microstructural analysis and mechanical testing methods. The work begins with the selection of raw materials followed by planning of the experiments. Detailed explanation on experimental procedure is given in the following sections. Overview of the experimental procedure is shown by means of flow chart in Fig.3.1.
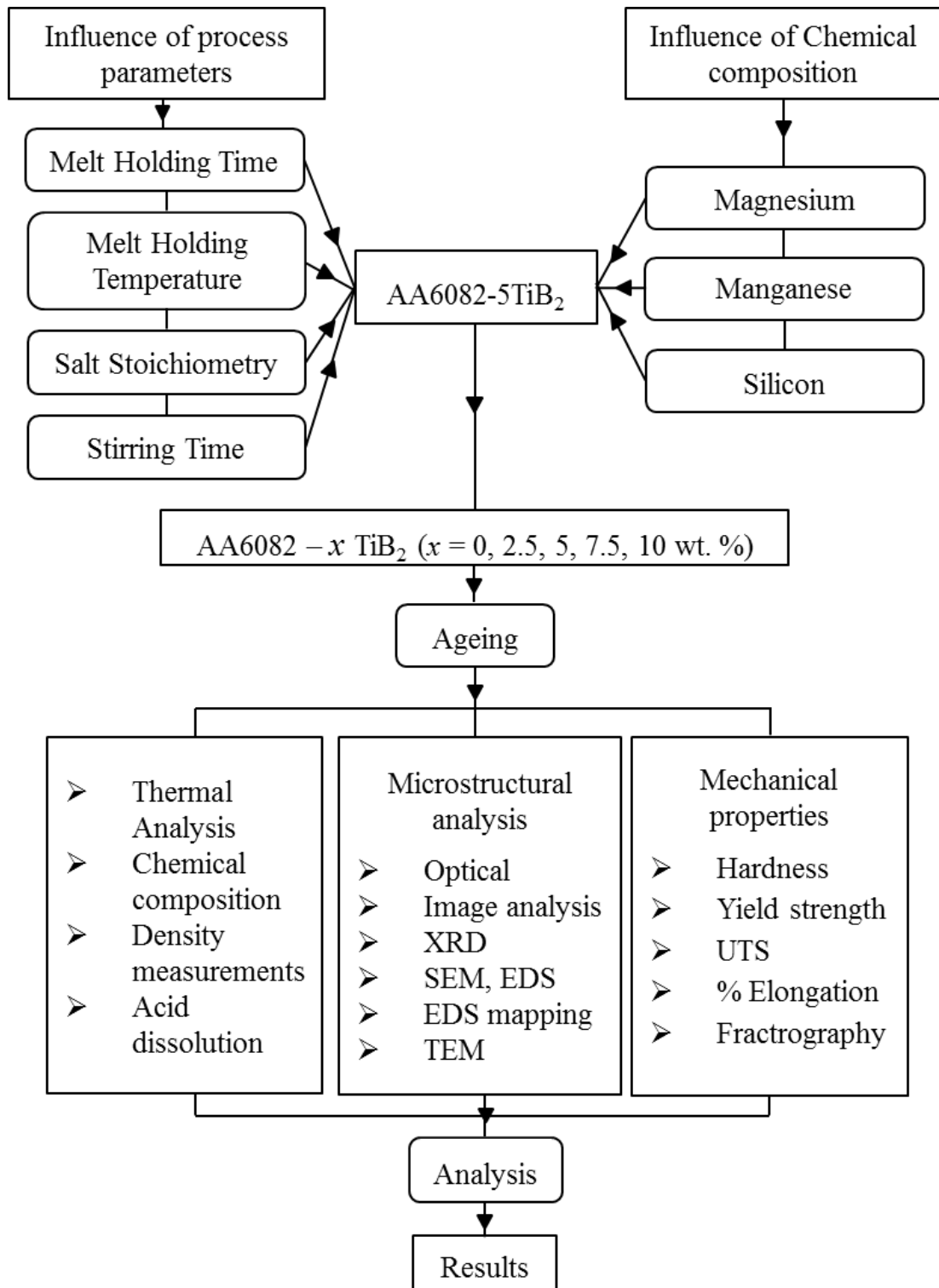
Fig 3.1 Schematic representation of experimental work.

3.1 Selection of raw materials

The raw materials used in the present work are, AA6082 aluminium alloy, potassium titanium fluoride (K_2TiF_6), potassium borofluoride (KBF_4), Coverall 11 and hexachloroethane (C_2Cl_6) tablets for the preparation of composites. AA6082 aluminium alloy is an alloy in the wrought aluminium-magnesium-silicon family (6000 or 6xxx series). It is one of the more popular alloys in its series (alongside alloys 6005, 6061, and 6063), although it is not strongly featured in ASTM (North American) standards. It is typically formed by extrusion and rolling, but as a wrought alloy it is not used in casting. It can also be forged and clad, but that is not common practice with this alloy. It cannot be work hardened, but is commonly heat treated to produce tempers with a higher strength but lower ductility. AA6082 aluminium alloy (HINDALCO, INDIA) chosen and used as the matrix material was procured from Hi-Tech, Mangalore. The composition of the alloy was analysed by an Optical Emission Spectrometer (OES) (Model LMS 04 of spectromax, Germany). The elemental composition of the procured alloy is presented in Table 4.1. Halide salts used in the present work were commercial grade K_2TiF_6 and KBF_4 in the powder form ($\leq$ 74 μm) purchased from Madras Fluorine Pvt. Ltd. Chennai. The Halide fluxes, K_2TiF_6 and KBF_4 were analysed by XRD. Coverall 11 and hexachloroethane (C_2Cl_6) tablets were procured from Servel Engineers, Mangalore.

3.2. Melting and casting of *in-situ* AA6082-5TiB$_2$ composites

Preliminary experiments were performed in order to identify optimal conditions for the processing of AA6082-5TiB$_2$ composites. Upon the successful preparation of AA6082-5TiB$_2$ composite, same conditions were followed to prepare composite with varying TiB$_2$ particles (2.5, 7.5, 10 wt. %). Although the processing parameters (holding time, reaction temperature, flux composition and stirring time) and chemical composition (Mn, Mg and Si) was varied systematically during AA6082-5TiB$_2$ composite preparation, standard melting and casting procedures were followed for the processing of composites. The procedure for processing of the composite was followed from a patented process for preparing Al-TiB$_2$ composites by mixed salt route or flux assisted synthesis [Davies et al., 1992]. In order to accommodate AA6082 ingots into the graphite crucible, the ingots were cut to suitable size using

power saw. The small cut pieces were pickled by using dilute HCl and were thoroughly cleaned with acetone to remove unwanted grease or any other oily contaminants. The requisite amount of K_2TiF_6 and KBF_4 salts were mixed thoroughly to get homogeneous mixture. The mixed salts were wrapped in Al foils into number of small batches to form packets of convenient size. The wrapped salt packets were dried in an oven at 250 ºC for 1 hr. in order to remove the moisture present in salts.

Aluminium alloy AA6082 was melted in the graphite crucible in an electrical resistance furnace, which was set to a temperature of 850 °C. Temperature of the melt was carefully observed by using K-Type thermocouple. During the melting process of alloy, coverall 11 was used to protect the melt from any contamination.

Once the melt reached 850ºC, degassing of the melt was carried out by plunging hexachloroethane (C_2Cl_6) tablets using a graphite plunger. The degassing was accompanied by a slight drop in temperature. Once the melt attained the set temperature again, the dried salt packets were added to the melt in batches and the melt was stirred with a zirconia coated mild steel rod for uniform mixing. In order to ensure complete reaction between the salts and melt, the entire mixture was held at the reaction temperature for one hour from the time of addition of salts. To ensure uniform distribution the precipitated particulates and to kindle the reaction between the salts and melt, the melt was stirred intermittently every 8 min. In situ TiB_2 particulates were formed by the reduction of K_2TiF_6 and KBF_4 in the aluminium alloy melt.

Once the reaction was complete, the dross was decanted from the melt. As soon as the dross was removed the melt was poured (top pouring) into a mild steel mould, 30 mm diameter and 170 mm high which was preheated to about 250°C. The overall reaction between the salts and the aluminium alloy melt is given as

$$K_2TiF_6 + 13Al \rightarrow 3Al_3Ti + 3KAlF_4 + K_3AlF_6 \qquad (3.1)$$
$$2KBF_4 + 3Al \rightarrow AlB_2 + 2KAlF_4 \qquad (3.2)$$
$$AlB_2 + Al_3Ti \rightarrow TiB_2 + 4Al \qquad (3.3)$$
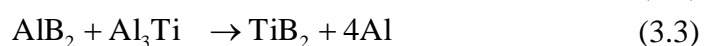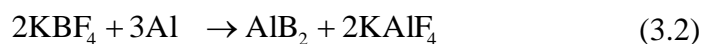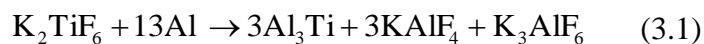
3.3. Influence of process parameters

Process parameters like melt holding time, melt holding temperature, stoichiometry of added fluoride salts and interval of intermittent stirring time were analyzed to identify the optimal conditions necessary for the development of *in-situ* AA6082-5TiB$_2$ composites.

3.3.1. Influence of melt holding time

3.3.1.1 Influence of melt holding time without the addition Mg - Part I

The experiments were carried out to understand the influence of melt holding time in synthesizing AA6082-5wt.%TiB$_2$ composite. The AA6082 ingots were melted in a graphite crucible using resistance furnace. A constant melt temperature of 800°C was maintained throughout experiment. Preheated stoichiometrically weighed K$_2$TiF$_6$ and KBF$_4$ salts corresponding to the Ti:B ratio of 2.2:1 were added to the aluminium melt. To catalyze the reaction the between the salts and melt intermittent stirred at regular intervals of 8 min. As the predetermined melt holding time was reached the slag which was floating on the top of melt was removed and the composite melt was casted in the preheated mild steel die. The composite castings were prepared at different holding times of 15, 30, 45, 60 and 90 min.

3.3.1.2 Influence of melt holding time without the addition of Mg - Part II

In order to understand the influence of melt holding time, during the preparation of AA6082-5wt.%TiB$_2$ composite the second set of experiments were carried out. During the experimentation, the composites were prepared at different melt holding time of 15, 30, 45 and 60 min., by following the same procedures carried out in section 3.3.1.2. Although the procedures for preparing the composites in this section were similar to the composite prepared in section 3.3.1.2, certain important changes were made during experimentation. Firstly, the temperature of the alloy melt was raised and held at 850°C, i.e, the whole experiments were carried out at the melt temperature of 850°C. Secondly, an excess of 10%KBF$_4$ salts were added to the stoichimetrically weighed K$_2$TiF$_6$ and KBF$_4$ salts, and were added to the aluminium melt to form TiB$_2$ reinforcements in the final composite. These experiments were

carried out with an intention of form only TiB_2 reinforcements in the prepared as cast composites.

3.3.1.3 Influence of melt holding time with the addition of Mg

From the knowledge obtained from experiments carried out in section 3.3.1.1 and 3.3.1.2, the third set of experiments on the influence of melt holding time was carried out to overcome the discrepancies observed in the previous sections. The same experimental procedure followed in section 3.3.1.2 were carried out for the synthesis of AA6082-5wt.%TiB_2 composite. In the experiments carried out K_2TiF_6 and KBF_4 salts with 10% excess KBF_4 salt than the stoichiometry was added to the melt held at a temperature of 850ºC. As the predetermined melt holding time was reached, the slag was decanted from the melt and the required amount of Mg (Strips) was added to the composite melt using a plunger. Upon the addition of alloying element the melt was casted in the preheated mild steel. Using the above mentioned experimental procedure the composite castings were prepared at different holding times of 15 to 60 min. in step of 15 min.

3.3.2 Influence of melt holding temperature

The experiments were carried out to understand and to optimize the melt holding temperature suitable for the synthesis of *in-situ* AA6082-5wt.%TiB_2 composite. Four castings were made at different melt holding temperatures. To maintain accuracy the temperature of the melt was monitored using a K-Type thermocouple. The reaction temperature of K_2TiF_6 and KBF_4 salts with aluminium melt was varied from 750 to 900 ºC in steps of 50 ºC. After the constant holding time of 60 min, the slag was skimmed out of the melt with subsequent Mg was added to the melt in order to compensate for its loss. Upon addition of the Mg the composite melt was poured into the preheated mild steel die after a dwell time of 2 minutes.

3.3.3 Influence of salt stoichiometry

In order to prepare AA6082-5wt.% *in-situ* composites, without the presence of Al_3Ti and AlB_2 composites, it is very much necessary to understand and control the different parameters involved in the processing of the composite. Of the various parameters, the stoichiometry of the salts added to the melt dictates the formation of

reinforcements. If more Ti is added than B, then the presence of Al_3Ti particles will be more in the matrix. If excess of B is added then it will result in the formation of more AlB_2 particles in the matrix. Hence, in order to prepare a composite with only TiB_2 reinforcements the stoichiometry of Ti and B has to be balanced. Moreover, literatures and our previous experiments indicate that there is huge loss of B. Therefore, the following experiments were carried out by adding excess of KBF_4 salts to the stoichiometric mixture of K_2TiF_6 and KBF_4 salts. Five composite casting were obtained, The first casting was obtained by keeping K_2TiF_6 and KBF_4 ratio according to the stoichiometry ratio between Ti:B as 2.2:1, i.e. no excess of KBF_4 was added to the melt. In the second casting 10% excess KBF_4 was added to the melt. During the third casting 20% of excess KBF_4 was added, and in the fourth and fifth casting, the excess amount of KBF_4 added to the melt was increased by 10% in every casting. Intermittent stirring of the composite melt at regular intervals of 8 min was carried out. After the constant holding time of 60 min, the slag was skimmed out of the melt and Mg was added to composite melt in order to compensate its loss. Upon addition of the alloying elements, the melt was poured into a preheated mild steel die.

3.3.4 Influence of intermittent stirring time

Investigation on the influence of intermittent stirring time during the development of in-situ AA6082-5wt.%TiB_2 composites was carried out. An excess of 10% KBF_4 salt to the stoichiometry ratio of K_2TiF_6 and KBF_4 salt mixture was added, which was further added to the melt. A constant melt temperature of 850ºC was maintained during the processing of composites. Intermittent stirring at regular intervals was carried out in the composite melt. Four composite casting were prepared by different intervals of intermittent stirring time. The first casting was prepared by stirring the melt at regular interval of every 5 min for 20 sec. The second casting was prepared with a melt stirring interval of 8 min. 10 min of stirring interval was employed for the casting three and 15 min. for the fourth casting. It should be noted that, though the interval of intermittent stirring was carried out at different time intervals, a constant stirring time of 20 sec. was employed during the intermittent stirring of all the castings.

3.4 Influence of alloying elements

The chemical composition of AA6082 aluminium matrix was varied systematically in order to understand the effect of the alloying elements during processing of composite. The major elements that were varied in the matrix alloy are Mn and Mg whereas the Si present in the alloy was not varied but the influence of Si during the reaction process was understood with respect to the holding time.

3.4.1 Addition of Mg

To understand the influence of Mg in AA6082-5wt.% composites four composite casting were made. Prior to the addition of magnesium, the AA6082-5TiB$_2$ composites were prepared by following the same procedure as in section 3.3.1.2. Upon the completion of the melt holding time of 60 min., the slag was removed from the melt and the required Mg was added to the composite melt. The Mg in AA6082-5TiB$_2$ composite casting was varied from 0.6 to 1.2% in steps of 0.2%. The Mg was added to the melt in the form of fine chips. The weighed Mg chips were added with chips of aluminium and then it was plunged in the melt by using a graphite plunger. By doing so the quick oxidation of Mg was stopped. Extreme care was taken during the addition of Mg. The composite melt was poured as soon as the Mg was added to the composite melt. The results of composites processed with the addition of Mg was compared with the composite processed with 60 min. (section 4.5) processed without the addition of Mg. This was done to standardize the chemical composition in matrix alloy so that its chemical composition is well between the standard compositions of AA6082. It should be noted that the Mg in the matrix alloy was varied in the matrix alloy melt without changing the composition of the other alloying elements.

3.4.2 Addition of Mn

The influence of Mn on the AA6082-5TiB$_2$ composite was investigated by varying the weight percent of Mn to the matrix alloy melt. Since the investigation on the influence of Mg in AA6082-5TiB$_2$ composites revealed that addition of 0.8% would be the sufficient enough to produce AA6082-5TiB$_2$ with good properties. Hence during the present investigation the loss of Mg was compensated with the addition of 0.8wt.% of Mg and the composition of the matrix alloy was kept constant in all the

casting except Mn. Four casting were made by adding excess of Mn to the composite melt in order to understand the influence of Mn in AA6082-5TiB$_2$.

The first casting was prepared with the intention producing AA6082-5TiB$_2$ composite with 0.4% of Mn in the matrix. Since 0.4% of Mn was present in the AA6082-5TiB$_2$ matrix alloy, during the investigation of Mg, the same casting was considered for comparison in the present investigation. The second casting was processed with the addition of Mn to the AA6082-5TiB$_2$ such that the final composition of Mn in the matrix alloy was 0.6%. Similarly, the third and fourth casting with 0.8 and 1% of Mn in AA6082-5TiB$_2$ composite was processed with the addition of required amount of Mn to the AA6082-5TiB$_2$ composite melt. The addition of excess Mn to the composite melt was done by using a Al-10%Mn master alloy. It should be noted that the calculated amount of Al-Mn master alloy was added to the composite melt immediately after skimming of slag from the melt.

3.4.3 Influence of Si

The influence of Si during the processing of AA6082-5TiB$_2$ composite was investigated in the present section. Since no change in composition of Si in matrix alloy was observed during the processing of AA6082-5TiB$_2$ composite in the previous sections, no change in composition of Si in the matrix alloy was made. To be precise the influence of Si on the formation of AlTiSi particles during the processing of AA6082-5TiB$_2$ composite was investigated in the present section. The AA6082-5TiB$_2$ composite were prepared at 850ºC with a melt holding time of 60 min. During the processing of composite the slag was slightly skimmed out and some portion of the composite melt was removed from the crucible and casted at every 15 min. of interval. The microstructural investigation was carried out on these castings.

3.5 Synthesis of AA6082-TiB$_2$ composites with different weight percent of TiB$_2$

As the optimum processing parameter for the processing of AA6082 composite was found from the results obtained from the experiments in chapter 1 and 2, composite castings with varying TiB$_2$ wt.% in AA6082 alloy was prepared. Two set of composites castings with four different wt.% of TiB$_2$ varying from 2.5% to 10% in steps of 2.5% was prepared. The composites were prepared with constant holding

time of 60 min by adding 10% excess KBF$_4$ salts to the melt maintained at a temperature of 850 ºC. Intermittent stirring of composite melt was done at regular intervals of 8 min. The same procedure for melting and casting was followed as mentioned in section 3.4. The first set of casting was prepared without the addition of Mg and the second set of castings were processed with the addition of Mg. The mechanical properties of both the composites were compared.

3.6 Solutionizing and ageing studies on AA6082 aluminium alloy and AA6082-TiB$_2$ composites

As cast unreinforced AA6082 alloy and AA6082-TiB$_2$ composites were subjected to age hardening heat treatment. The cycle of heat treatment comprises solutionizing at 560ºC, and aging at 180 ºC for a total time of 22 hrs with an interval of 2 hrs . The solutionising temperature was chosen from the Al-Mg-Si ternary diagram. The chosen AA6082 alloy is in single phase region at 560°C according to Al-Mg and Al-Si binary phase diagram. A ternary isothermal section of Al-Mg-Si alloy at 550°C [Feufel, 1997] shown in Fig. 3.2 shows a single phase region. Hence this temperature of 560°C has been chosen as the solutionising temperature.
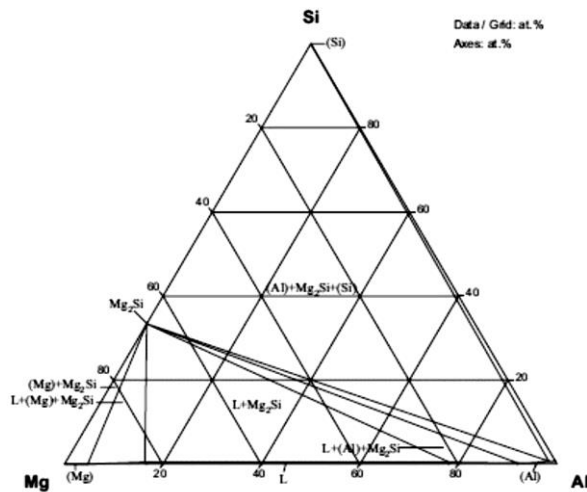
Fig.3.2 Al-Mg-Si isothermal section at 550°C [Feufel, 1997].

Heat treatment was carried out in muffle furnace with an accuracy of ± 3 ºC. For heat treatment studies, 10 mm thick sized samples were cut from the as cast unreinforced alloy and composites. The cut samples were polished with different grades of SiC

papers up to 1000 grit then carefully cleaned with soap solution and finally washed with alcohol and finally dried.

The dried samples were loaded into the furnace, once it attained the solutionizing temperature; the time for solutionizing was recorded. The samples were soaked for 4 hrs. After the completion of soaking for solutionizing time, the samples were quenched in water kept at room temperature. The quenched samples were immediately subjected to ageing treatment. Ageing of the samples was carried out at 180 ℃. At certain fixed interval of ageing time, the samples were removed time to time from the furnace, air cooled and tested for their hardness using Vickers hardness tester. The obtained hardness values were plotted and the curve showing kinetics of ageing for the as cast and the prepared composites with different wt.% of TiB_2.

3.7 Thermal Analysis (Differential thermal analysis (DTA) and Thermo Gravimetric Analysis (TGA))

DTA and TGA analysis were carried out to understand the reaction process between the salts and the aluminium. High temperature DTA and TGA analysis was carried out using a (EXSTAR 6000 TG/DTA 6300-Japan) thermofisher instrument. The procured K_2TiF_6 and KBF_4 salt and aluminium alloy powder was mixed in the required proportions. The salts and the aluminium alloy powder were mixed thoroughly in order to get a homogeneous mixture. The mixture was loaded in a platinum vial and then subjected to DTA and TGA studies over the temperature ranging from 30 to 950 ℃.

3.8 Analysis of chemical composition in alloy and composites

3.8.1 Inductive coupled plasma optical emission spectrometry (ICP-OES)

The prepared castings were subjected to chemical analysis in order to determine the elemental percentage. The chemical analysis of casted alloy and composites was carried out using Inductive coupled plasma optical emission spectrometry (ICP-OES) (model GBC 932 plus). Fine drillings of 10 grams metal was taken from the obtained castings. 10 ml of HCl and 2 ml of Nitric acid was added to 10 ml of distilled water. 10 ml of the fine drillings of the metal was dissolved by adding it to the prepared

solution. Intermittent stirring of the solution was performed for the complete dissolution of the metal drillings. Once the drilling got dissolved in the solution, the solution was filtered using (No.42) Whatman Ashless filter paper. The filtrate was made up to 100 ml solution. The prepared solution was used for the chemical analysis.

3.9 Archimedes method to calculate the porosity percentage

This technique is based on the well-known Archimedes' principle. Percentage of porosity is determined by measuring the density of the samples. Ten specimens were cut from casted composite and ultrasonically cleaned with acetone. A very sensitive balance of 0.1 mg was used to measure the weight of the samples. The samples were first weighed in air and then weighed by suspended in xylene of known density. Since the density of the liquid (ρ_L) is known the displaced volume was calculated using the formula $\left(\frac{W-Ws}{\rho_L}\right)$.

The density of the sample was found by dividing weight of the sample in air, W, by volume of liquid displaced. The density of the sample which is called experimental density was determined from equation

$$\rho_{Ex} = \left(\frac{W\rho_L}{W-Ws}\right) \tag{3.4}$$

Where, Ws is the suspended weight of the sample. The theoretical densities were obtained from the expression

$$\rho_{Th} = \frac{1}{\left(\frac{W_p}{\rho_p}\right)+\left(\frac{W_m}{\rho_m}\right)} \tag{3.5}$$

Where, W is the weight fraction, ρ is the density, p particulate, M is matrix.

From the obtained theoretical density and experimental density the percentage of porosity was calculated from the expression

$$\% \text{ Porosity} = \left(\frac{\rho_{Th}-\rho_{Ex}}{\rho_{Th}}\right) \times 100 \tag{3.6}$$

Where, ρ_{Th} = Theoretical Density (g/cm3), ρ_{Ex} = Experimental Density (g/cm3).

3.10 Dissolution of matrix alloy

The weight percent of TiB_2 particulates present in the matrix was estimated by acid dissolution method. In in situ processing the particulates are precipitated in the melt by exothermic chemical reaction between the salts and melt. During the chemical reaction there is always a possibility of formation of other intermediate phases like AlB_2 and Al_3Ti as shown in equation 3.1 and 3.2. Estimating the weight percent of particulates in casting with the intermediate phases will give error in results. The weight percent of particulates in the matrix was estimated in composites which had only TiB_2 particulates.

Ten samples were cut from the prepared composite. The samples were ultrasonically rinsed with acetone and dried. The dried samples were weighed by using a sensitive balance of 0.1 mg. The weighed samples were separately dissolved in sodium hydroxide solution in a clean beaker. Once the matrix was dissolved in the solution, the solution was diluted by adding excess amount distilled water. The particulates were separated from the solution by filtering using (No.42) Whatman Ashless filter paper. The filtered particulates were carefully removed, dried and weighed. The weight percent of particulates was calculated by comparing the values obtained from before and after the dissolution.

3.11 Metallographic sample preparation

Samples were prepared from the as cast alloy and composites for microstructural observations using Optical microscope and SEM. The samples for microstructural analysis were sectioned at a height of 20 mm from the base of the castings. The sectioned samples were prepared for the microstructure study by belt polishing and then by using different grades of emery sheets such as 400, 800, 1000, 1200, 1500 and 2000. The samples were then polished on lapping clothes attached to a rotating disc, and smeared with 1 and 0.25 μm diamond pastes until a scratch free mirror finish was obtained. The samples were thoroughly cleaned carefully with soap solution and in running water followed by drying. The polished samples were then etched with Keller's reagent (2.5% HNO_3, 1.5% HCl, 1% HF amd 95% H_2O) for a period of 5-10 seconds. The samples for grain structural analysis were prepared by following the

same procedure mentioned above except the etchant. Poultons reagent (60% HCl, 30% HNO_3, 5% HF,5% H_2O) was used for etching the samples intended for grain analysis. The etched samples were carefully cleaned in acetone bath using an ultrasonic cleaner and finally the sample were dried using hot air blower.

3.12 Preparation of fracture surfaces for fractography

The fracture behaviour on the tensile samples was understood by studying the fracture surface in SEM. To clearly understand the fracture behaviour it is very important to have a clean and un-oxidized fracture surface. As soon as the tensile testing was performed, the samples were cut at a sufficient distance from the fracture surface and SEM analysis was carried out. The cutting distance of the fractured sample was chosen such that, the size of the sample should fit in the SEM stage and the heat generated during cutting should not affect the fracture surface.

3.13 Characterisation of the prepared composites

3.13.1 X – ray diffraction analysis (XRD)

To identify the phases present in the prepared composite, samples were cut from the prepared from alloy and composite, and subjected to X – ray diffraction studies. The samples were characterised by using a X-ray diffractometer (Model: JPX8, JEOL, Japan) operated with Cu-Kα radiation at 30 KV and 20 mA. The 2θ range selected was between 30 to 90 degree, this range was selected because all the major intense peaks of the phases expected in the sample were present in this region. The diffracted data of the samples was analysed with the help of JCPDF data files to identify the peaks corresponding to different constituent phases.

3.13.2 Optical microscopy and Image analysis

Optical microscopy and grain size analysis on the polished samples were carried out using Union microscope interfaced image analysis software. The samples for analysis were prepared by following the procedures as explained in the section 3.11. All the optical photomicrographs were obtained at 100X magnification. Optical photomicrographs of prepared alloy and composite etched with Kellers reagent was used to anlayse the second phase particle present in the matrix. For the grain size

analysis the samples were etched with poulants reagent. The grain size was measured on the optical photomicrographs using linear intercept method by following the procedure in ASTM E112-10 using BIOVIS image analysis software. Minimum of two fields were calculated for each measurements with the intercept points obtained on the optical photomicrograph in each field depending on the grain size.

3.13.3 Scanning electron microscopy (SEM)–Energy dispersive spectroscopy (EDS)

The microstructure were also examined by using SEM (Model: JSM 6380, JEOL, Japan) using secondary electron (SE) and backscattered electron (BSE) imaging modes accompanied by use of EDS (Oxford Instruments Limited, U.K). The SEM microphotographs were obtained with an operating voltage of 20 KV. The SEM instrument is interfaced with Link JED 2300 analysis station software for Energy Dispersive X-ray mapping. The samples used for optical studies were used in SEM/EDS analysis.

The microstructures were examined in SEM in order to analyse the morphology, size, shape and distribution of the particulate present in the matrix. The EDS analysis on the processed samples was also carried out for the elemental analysis in the particulate as well as matrix. In order to have a complete understanding on the microstructural features a number of regions were examined in each sample. The fractured surface of alloy and composite were also investigated using SEM to determine the characteristics of fracture surface and mode of failure. Both SE and BSE imaging modes were used to analyse the fracture surface.

3.13.4 Transmission electron microscopy (TEM)

To understand the formation of TiB_2 particles and its ageing behaviour, samples from both as-cast and aged composites were examined using the transmission electron microscope (TEM). For observation on the TEM, slices of 200-250 μm were sectioned from the composite castings, using a lubricated low speed diamond saw disk cutter. This ensures the preservation of microstructural details, which could be lost by conventional abrasive cutter. Part of the slices was further thinned carefully by mechanical polishing on a 600 mesh silicon carbide paper until the thickness was

reduced below 80μm. After cleaning the sample with acetone and methanol to remove contaminants such as oil, external particles ad grease, a sample was punched using a Gatan punch into 3mm discs. The 3 mm is discs sample were dimpled using dimple grinder. After dimpling the sample were loaded into ion milling unit (Gatan model-pips), and milled with 5 KeV gun set at 6º top and bottom.

The microstructure of specimen was studied on a JEM 2100 (JEOL Japan) high resolution transmission electron microscope operated at an accelerating voltage of 200 KV to observe the presence of particle morphology and the precipitates. The images were recorded in bright and dark field modes. The electron diffraction studies were also carried out to identify the phases.

3.14 Assessment of mechanical properties of as cast AA6082 alloy and AA6082-xTiB$_2$ composites

3.14.1 Vickers hardness

The hardness of the as cast alloy and composite was measured with the help of Zwick (Model: 3212) Vickers hardness tester. The sample preparation procedure was similar to that of the sample prepared for microstructural analysis as explained in section 3.11, except that the samples were not etched. A load of 5 Kg was applied for a dwell time of 15 seconds using a diamond indenter. After the indentation the diagonal lengths of indentations was carefully measured and the Vickers hardness number was calculated by using the expression:

$$HV = 1.854 \left(\frac{P}{d^2} \right)$$
(3.7)

Where P is the applied indentation load (kgf) and d is the mean diagonal length (mm). The distance between one indentation and the other was kept at least five times from the diagonal of the previous indentation. At least five indentations were taken for each specimen, and the average value was reported as the hardness of the composite.

3.14.2 Tensile testing of alloy and composites

The Tensile properties of as cast alloy and composites were studied. Tensile testing of dog bone shaped specimens was carried out on a Shimadzu Testing Machine (Model: AGX plus) with 100 KN capacity. Special fixtures were made to hold the

samples. A constant strain rate of 0.5 mm/min was applied during the tensile test of the specimens. The Tensile specimens were prepared according to the ASTM E8 standards. The specimen dimensions are shown in Fig.3.3. The fractured surface of the tensile specimens was carefully examined using SEM in order to understand the influence of microstructural features on the fracture behaviour of alloy and composites.
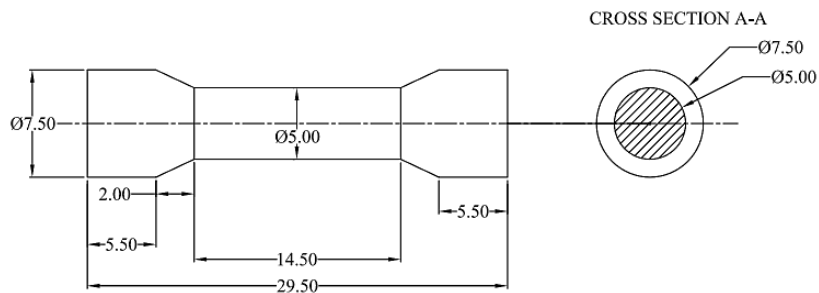
All dimensions are in mm

Fig. 3.3 Tensile test specimen (ASTM E8).

CHAPTER 4

Influence of Process Parameters on the Evolution of Microstructural and Mechanical properties of the AA6082-5TiB$_2$ *in-situ* composites

4.1 Introduction

The present chapter deals with the characterization of the as cast AA6082-5TiB$_2$ *in-situ* composites synthesized using various processing parameters. From the literatures it is evident that uncontrolled reaction between the salts and melt leads to unwanted intermediate particles like Al$_3$Ti and AlB$_2$ along with TiB$_2$ particles. Hence it is very much necessary to optimize the processing parameters in order to synthesis a sound *in-situ* TiB$_2$ reinforced composite. Melt holding time, melt holding temperature, stoichiometry of the fluoride salts added and melt stirring time were the processing parameters which were analysed during the synthesis of AA6082-5TiB$_2$ *in-situ* composites. The as-cast AA6082-5TiB$_2$ *in-situ* composite synthesized at different processing parameters were systematically characterized using, Archimedes method, XRD, optical microscopy, SEM/EDS microanalysis and fractography analysis. Vickers hardness measurements and tensile studies were carried out and the results were interpreted with the obtained microstructure of the synthesized composite. For convenience AA6082-5TiB$_2$ *in-situ* composites will be represented as AA6082-5TiB$_2$ *in-situ* composites in all the following sections.

4.2 As-cast AA6082 alloy

The process followed in the synthesis of AA6082 aluminium alloy has been explained in section 3.2 in chapter 3.

4.2.1 Chemical composition of the AA6082 alloy

The chemical composition of AA6082 alloy is presented in table 4.1. It can be seen that the chemical composition of the procured alloy and its composition after casting (as cast) were almost similar. Although the composition of the as cast alloy were found to be similar, a minor depletion of Mg is evident. Depletion of Mg in the as-cast alloy has occurred due to the high melt temperature. Apart from Mg, no change is

observed among the other alloy elements present in the alloy compared to the procured alloy. Although a marginal depletion of Mg was observed in the as-cast alloy compared to the procured alloy the analysis confirms that the as cast composition of the alloy is in good agreement with the standard composition of alloy.

Table 4.1 Chemical composition of AA6082 alloy used in the present investigation

Samples	Process Cond.		Chemical Composition (Wt. %)					
	Time (min)	Temp. (ºC)	Mg	Si	Mn	Cr	Fe	Al
Standard	-	-	0.6-1.2	0.7-1.3	0.4-1	0.25	0.5	Bal.
Procured	-	-	1.131	1.300	0.475	0.147	0.183	Bal.
As cast	60	850	1.026	1.297	0.471	0.146	0.174	Bal.

4.2.2 X-ray diffraction analysis

Fig. 4.1 shows the XRD pattern obtained from the as-cast AA6082 alloy. On indexing it with JCPDS data it was found that all the peaks obtained corresponds to α-Al and were in good agreement with JCPDS card number 04-0787. Other than α-Al no other peaks corresponding to intermetallic were found. This might be due to presence of low volume percent of intermetallics, which were well below the detection limit by XRD.
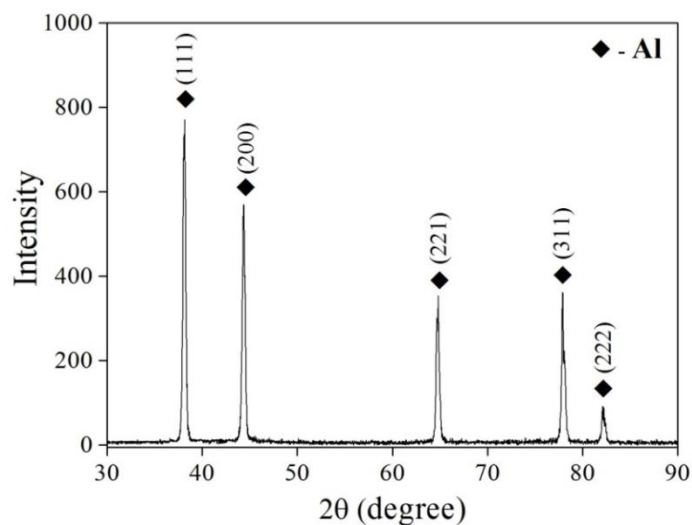
Fig. 4.1 XRD pattern showing the peaks of α-Al in as cast AA6082 alloy

4.2.3 Optical microscopy

Fig. 4.2 shows the optical micrograph of as cast AA6082 alloy, exhibiting a typical dendritic structure. The dendrites of primary α-Al in the as cast alloy seems to be coarser, elongated with high aspect ratios. The size of the grains was found to 211μm, and the aspect ratio of the dendrites was found to be 2.4. The intermetallics which gets formed during solidification is not evident in the microstructure. This may be due to loss of intermetallic constituent due to pull out from alloy during polishing. Moreover, at this lower magnification it is difficult to identify the constituents.
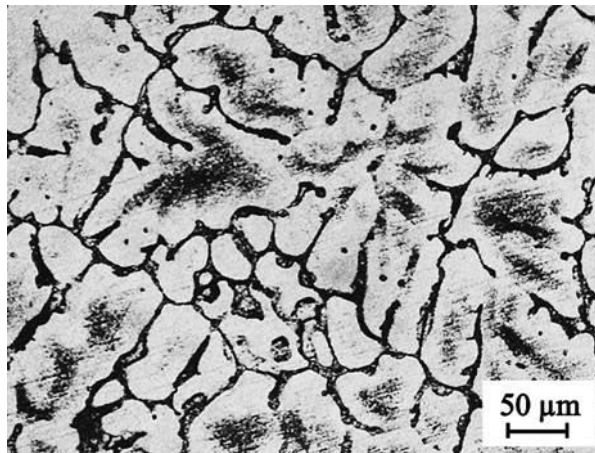
Fig. 4.2 Optical micrographs of as cast AA6082 aluminium alloy showing a dendritic structure.

4.2.4 Scanning electron microscopy

Fig 4.3(a) shows the secondary electron SEM image of the as cast AA6082 alloy and the corresponding EDS spectrum obtained from the bright region on the SEM image are shown in Fig.4.3(b) respectively. The EDS spectrum obtain from the particles present in the interdendritic regions confirm that they belong to α-$Al_{12}(FeMn)_3Si$ phase. The dark region hollow region present near to the α-$Al_{12}(FeMn)_3Si$ particles represents the particle pullout which has occurred during polishing. The Mn and Si present in the alloy will bind with Fe which has low solubility in the Al matrix. Upon solidification these constituent particles are formed at the interdendritic regions. The α-$Al_{12}(FeMn)_3Si$ intermetallics formed in the present investigation belongs to cubic structure [Mrówka-Nowotnik et al., 2007].
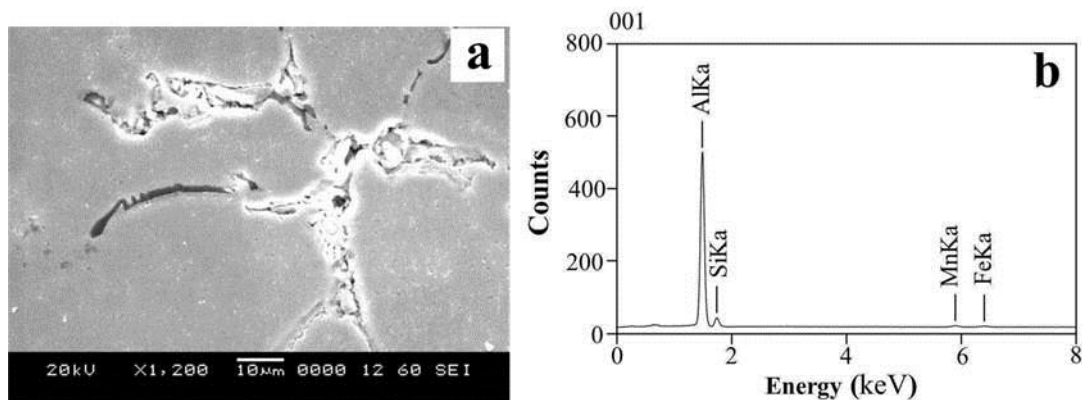
Fig. 4.3 As cast AA6082 alloy: (a) SEM micrographs showing intermetallic phase, (b) EDS spectrum showing the presence of Si, Mn and Fe peaks along with Al obtained from the bright interdendritic area

4.2.5 Mechanical properties

The mechanical property of as-cast alloy is shown in Table.4.2. The values of Yield Strength (Y.S) and Ultimate Tensile Strength (U.T.S) of the as cast alloy, shown in Table 4.2, are much higher than that of as cast pure Al, implying that strengthening occurs due to present of solutes. The alloy showed an average hardness of 55 VHN (Vickers Hardness Number). The yield strength and ultimate tensile strength were found to be 128 and 172 MPa respectively. The alloy showed an average ductility of 8%.The fractured surface of AA6082 alloy shown in Fig.4.3 indicates that the fracture has initiated in the dendrites and were moving across the dendrites. Mixed mode of ductile and more of brittle nature of fracture is evident.

Table 4.2 Mechanical properties of as-cast AA6082 alloy

Sample	Hardness (HV$_5$)	0.2% Y.S (MPa)	U.T.S (MPa)	% Elong.
AA6082	55	128	172	8
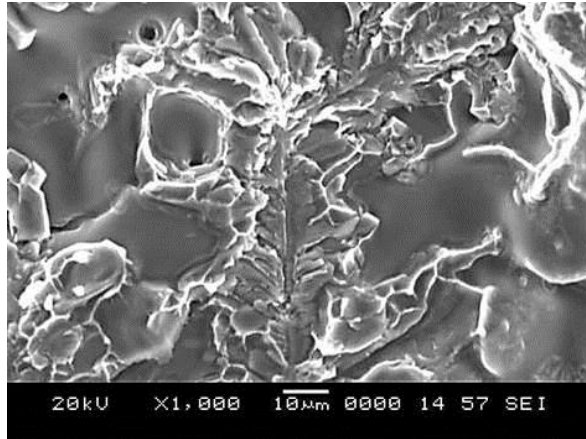
Fig. 4.4 SEM photomicorgraph showing the tensile fracture surface of as-cast AA6082

4.3 Fluoride fluxes
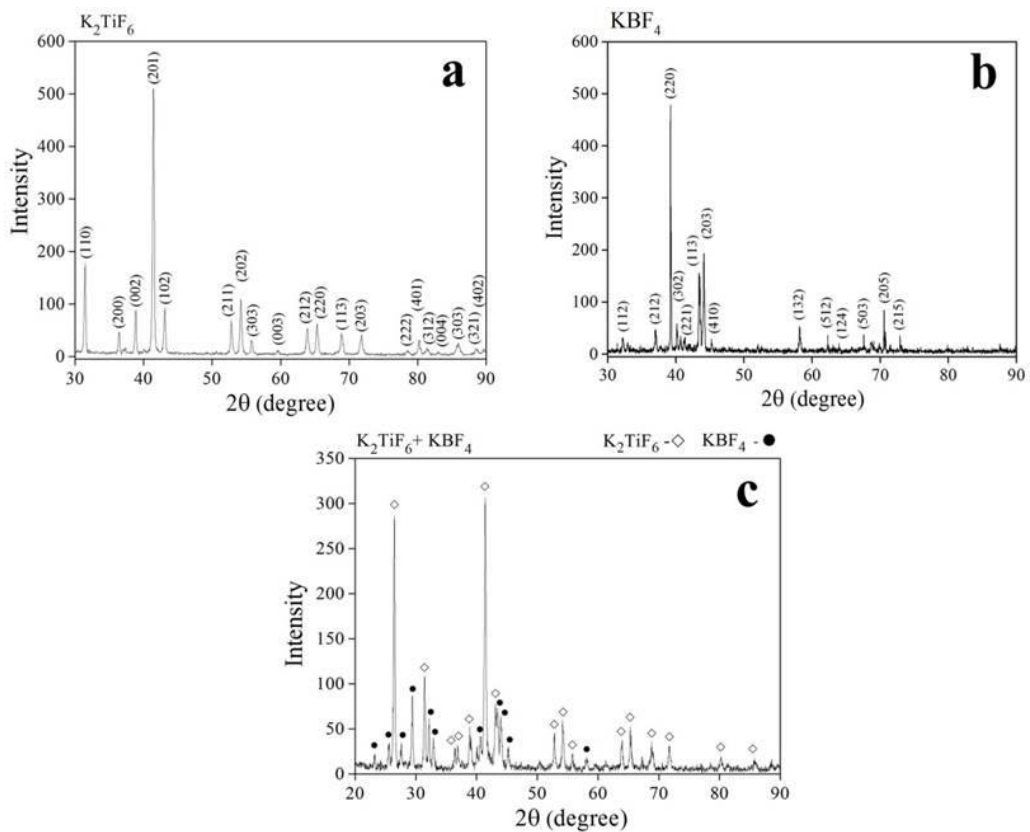
Fig. 4.5 X-ray diffraction pattern showing the peaks of procured fluoride salts (a) peaks obtained from K_2TiF_6 fluoride salt; (b) peaks obtained from KBF_4 fluoride salt; (c) peaks obtained from the mixture of K_2TiF_6 and KBF_4 fluoride salts

Fig 4.5(a) and (b) shows the XRD pattern acquired from the individual K_2TiF_6 and KBF_4 salts used in the development of TiB_2 reinforcements in the aluminium alloy melt. The indexed X-ray diffractograms obtained from K_2TiF_6 salts were in good agreement with the standard JCPDS 08-0488 file. Similarly the diffractograms obtained from KBF_4 slats were in good agreement with JCPDS No.71-1185 file. Absence of additional peaks in both the K_2TiF_6 and KBF_4 salts confirm that the salts were of pure without much contamination. Fig 4.5 (c) shows the XRD pattern acquired from the mixture of K_2TiF_6 and KBF_4 fluoride salts. Presence of all the peaks corresponding to the K_2TiF_6 and KBF_4 salts confirms that the salts have blended well.

4.4 Influence of melt holding time without the addition Mg - Part I

4.4.1 X-ray diffraction analysis

X-ray diffractograms acquired from the as cast unreinforced alloy and the AA6082-$5TiB_2$ composites synthesized at different holding time is shown in Fig.4.6 (a-f). The XRD pattern obtained from the composite synthesised with a holding time of 15 min is shown in Fig.4.6 (b). Analysis on the acquired pattern from composite confirmed the coexistence of Al_3Ti, AlB_2, TiB_2 particles along with Al. The difference in intensities observed among the phases from the XRD pattern suggests that the composite consisted of particles with different weight fractions. From the acquired XRD peak intensity it evident that more of Al_3Ti and AlB_2 particles are present in the composite than TiB_2. With the addition of K_2TiF_6 and KBF_4 salts to the aluminium alloy melt, Ti and B are spontaneously released into the melt because of the strong exothermic reaction, which occurs between the melt and the salts.

As the solubility limit of Ti and B exceeds in the melt, precipitation of Al_3Ti and AlB_2 particles occurs. These particles dissociate further to form TiB_2 particles. Compared to the TiB_2 peaks, the higher peak intensities exhibited by Al_3Ti and AlB_2 peaks suggest that the melt holding time of 15 min was insufficient for the synthesis for the *in-situ* TiB_2 reinforced composites. As the melt, holding time was further increased to 30 min. the composite showed a similar XRD pattern as that of composite processed at 15 min comprising of the same phases (Fig 4.6(c)). Although the diffraction peaks

72

of composite processed at 30 min. shows the presence of Al_3Ti, AlB_2 and TiB_2 phases similar to that of composite processed at 15 min, there seems to be a significant variation in the peak intensities of phases.
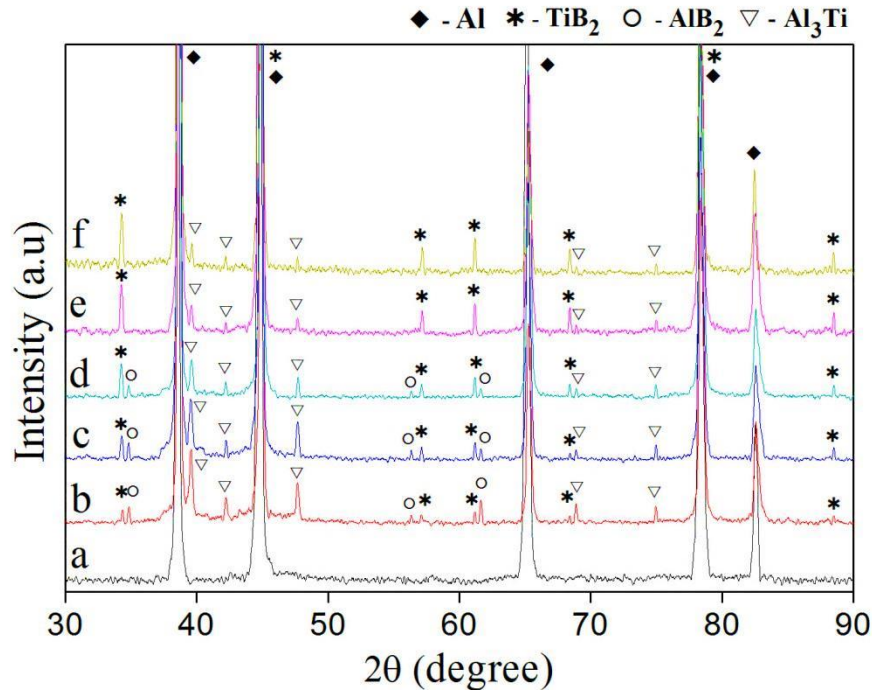
Fig. 4.6 X-ray diffraction pattern showing the peaks of Al, Al_3Ti, AlB_2 and TiB_2 from the processed composites with different holding time at a constant temperature of 800°C without the addition of alloying elements; (a) AA6082 alloy, (b) 15, (c) 30, (d) 45, (e) 60 and (f) 90 min.

With increase in holding time, decrease in intensity of Al_3Ti and AlB_2 peaks and the increase in intensity of TiB_2 peak indicates that at longer holding durations more of the AlB_2 and Al_3Ti particles have dissociated thereby transforming into TiB_2 particles. Fig. 4.6(d) shows the diffraction pattern obtained from composite processed with 45 min of holding time. The intensity of AlB_2 peaks have almost reduced compared to the Al_3Ti peaks. This suggests that the dissolution rate of AlB_2 is faster than Al_3Ti particles. The diffraction pattern obtained from the composite processed with a holding time of 60 min shows the presence of Al_3Ti and TiB_2 particles (Fig.4.6(e)). The relative peak intensities of TiB_2 and Al_3Ti particles indicate that more of TiB_2 particles are present in the matrix than the Al_3Ti particle. The disappearance of AlB_2

peaks in composites further confirm that complete dissociation of AlB_2 particles seem to occur at a holding time of 60 min. Fig. 4.6(f) shows the diffraction pattern obtained from the composite processed with a holding time of 90 min. On comparing the XRD pattern of composite processed at 90 min with that of the pattern obtained from the composite processed at 60 min, it is evident that there is no significant change the peak intensity or phases in composite processed with a holding time of 90 min. As the holding time was increased beyond 60 min decomposition of Al_3Ti particles was expected, whereas in the present case no change peak intensity of Al_3Ti particles confirms that there is no further dissociation of Al_3Ti particles. This inability of Al_3Ti particles to dissociate further is attributed to the absence B in the melt. This indicates that there is no sufficient amount of B is present in the melt for the formation of TiB_2 particles.

4.4.2 Scanning electron microscopy

Fig. 4.7 (a-e) shows the scanning electron micrographs acquired from composite processed at different melt holding time with a constant temperature of 800°C, during an attempt to synthesis *in-situ* AA6082-5TiB_2 composite. The micrograph of composite processed at a minimum holding time of 15 min, shows the presence of blocky and flaky particles with different sizes. Along with these particles, fine bright particles with the size ranging from 1-2 µm are also evident. The EDS spectrum obtained from the particles present in are shown in Fig.4.8 (a-e). Quantitative analysis on the flaky particles reveals that, along with Al and Ti small amount of Si is also present (Fig 4.8 (b)). Since the composition of Si present in the Al_3Ti particle changed from particle to particle, the particles were commonly designated as AlTiSi. Moreover literature indicates that, due to the presence of Si, no significant change in the lattice parameters of Al_3Ti particles was observed [Mohanty and Gurezleski, 1996]. Hence the reflections obtained from these particles in X-ray diffraction pattern, matched well with the standard Al_3Ti reflections indicated in the JCPDS data (Fig.4.6 (a-e)). The influence of Si during the synthesis of *in-situ* AA6082-5TiB_2 composites has been briefly discussed in chapter 5. EDS analysis on the darker blocky particles were identified to be AlB_2 particles (Fig 4.8 (c)). The EDS spectrum shown in Fig.4.8 (d) confirms that the fine bright particles belong to TiB_2 phase. As the melt holding time

74

was further increased to 30 min, average size of AlB_2 particles present in composite was found to reduce to sizes lesser than 10 μm (Fig.4.7(b)). Large cracks on Al_3Ti particles seem to occur at this melt holding time. At longer holding time, reduction in size of AlB_2 particles and larger cracks on the Al_3Ti particles is attributed to the dissolution of particles present in composite melt.
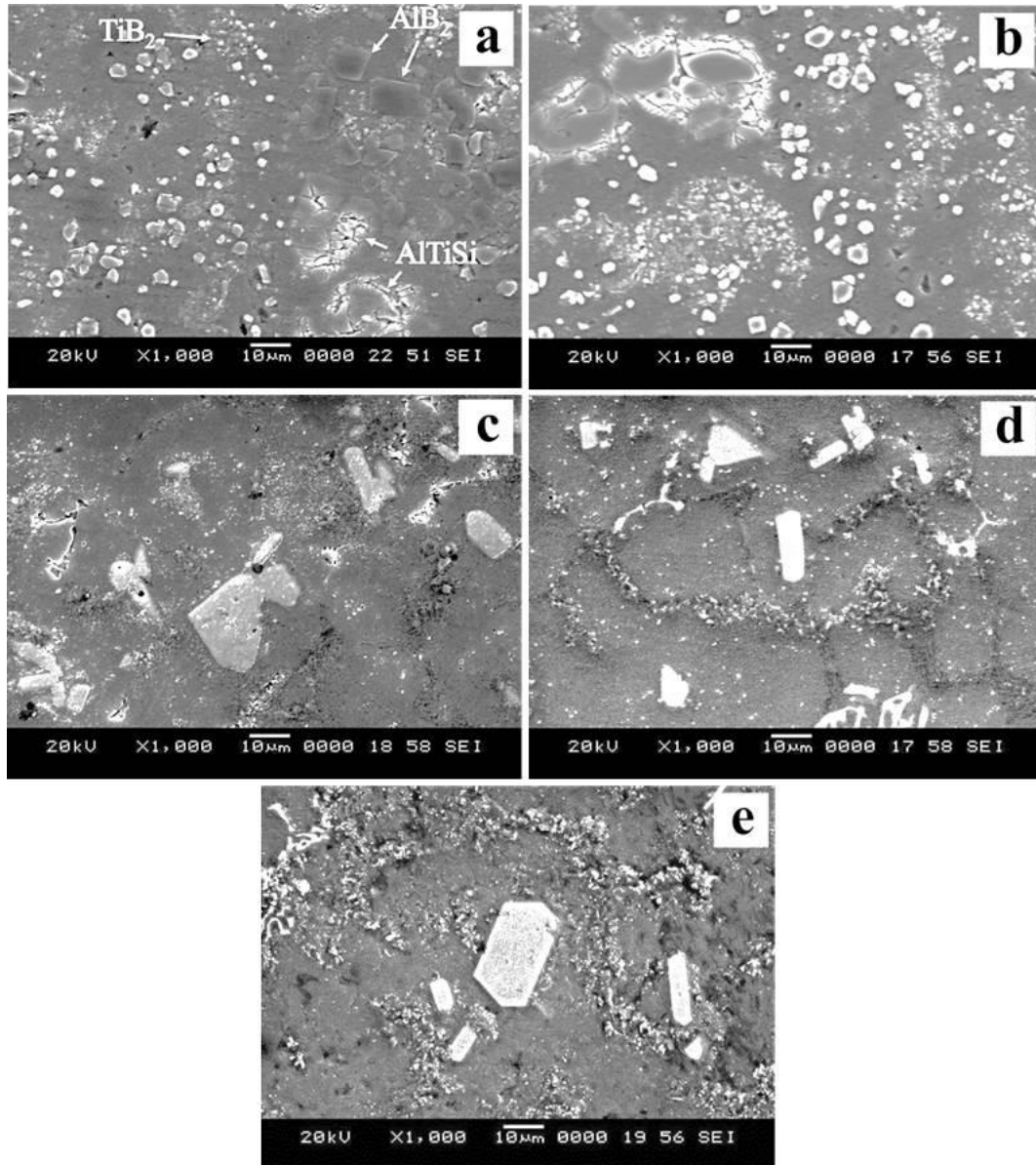
Fig. 4.7 (a-e) SEM photomicrographs showing the composite processed at different melt holding times; (a) 15, (b) 30, (c) 45, (d) 60 and (e) 90 min.

With the dissolution of AlB_2 particles, more of boron is release into the melt, which subsequently diffuses into the Al_3Ti lattice, thereby transforming into TiB_2 particles

[Emamy et al., 2006]. The bright contrasted regions, which are seen on the edges of Al_3Ti particles indicates that the diffusion of boron into the Al_3Ti particles has occurred.
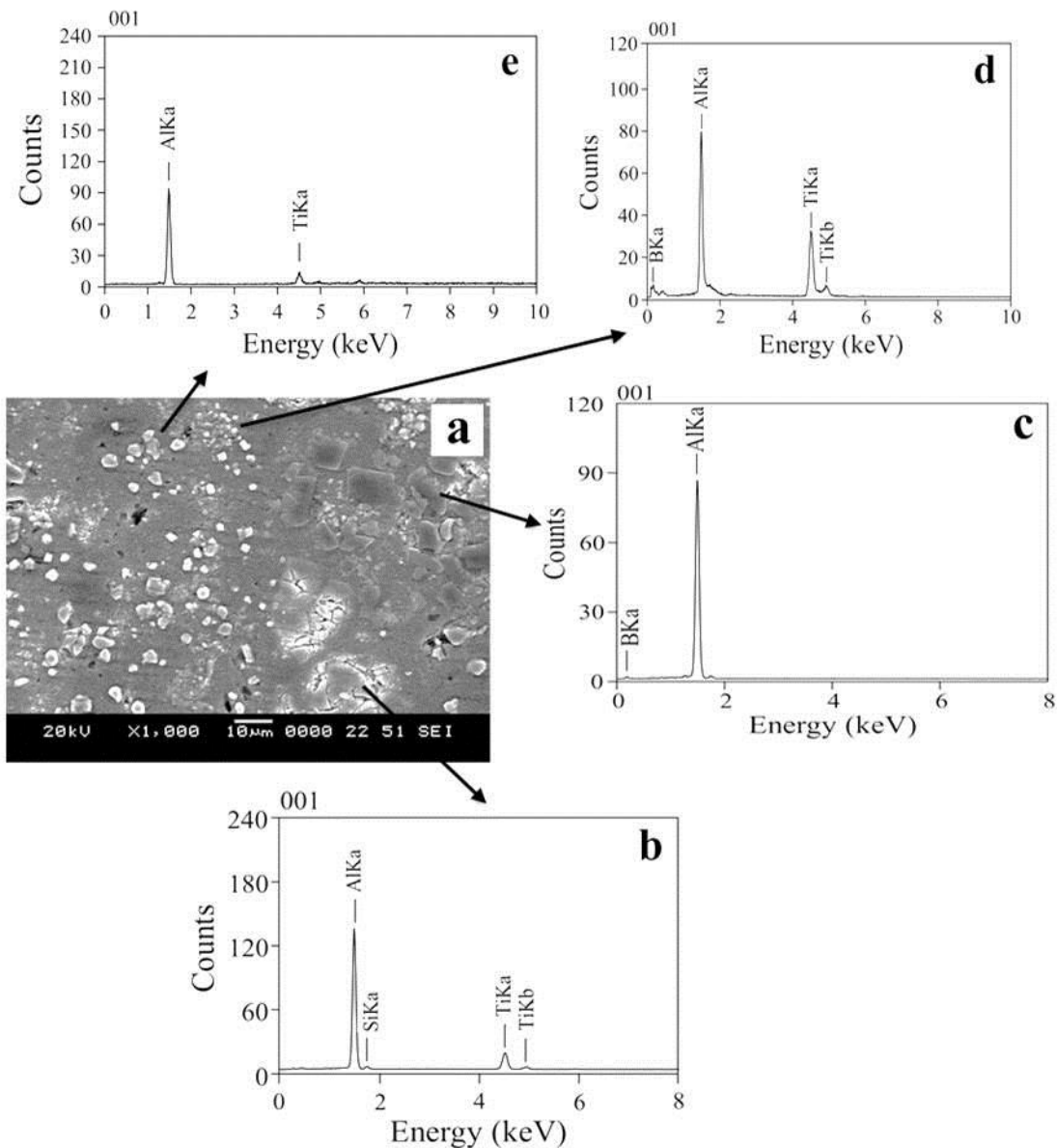
Fig. 4.8 SEM photomicrograph and EDS spectrum acquired from particles present in the as cast composites (a) SEM photomicrograph of composite 15 min, EDS spectrum of (b) AlTiSi, (c) AlB_2, (d) TiB_2, and (e) Al_3Ti particles

The SEM micrograph obtained from the composite processed at a melt holding time of 45 min shows the presence of blocky Al_3Ti particles and fine TiB_2 particles in the matrix (Fig.4.7 (c)). No boron-based particles other than TiB_2 particles is present in

the matrix alloy, this suggest that at a holding time of 45 min, all the available boron has transformed into TiB_2 particles. Although the size and density of Al_3Ti particles have reduced in composite processed at 45 min, compared to composite processed at 15 and 30 min, complete dissolution of Al_3Ti particles did not occur.

The absence of cracks on Al_3Ti particles in composite processed at 45 min further indicates that there is no sufficient boron left in the composite melt, for further transformation of Al_3Ti particles into TiB_2. These observations conclude that in the aluminium melt dissolution of boron is quicker that Ti [Guzowski et al., 1987]. The micrographs obtained from composite processed at a melt holding time of 60 and 90 min were almost similar, except that more of TiB_2 particles are pushed to the grain boundaries with increase in melt holding time.

It can be seen that even after longer holding time of 90 min, the Al_3Ti (AlTiSi) particles present in the composite were of blocky morphology, and similar results were observed before by Reza Ghomashchi [Ghomashchi, 2012]. Presence of blocky Al_3Ti particles in the matrix indicates its inability to dissolve or transform into TiB_2 particles due to the absence of boron. From the micrographs of processed composite, it is very much evident that there is no significant change in size of TiB_2 particles even at longer melt holding time.

4.4.3 Optical microscopy

The optical micrograph showing the grain sturcture obtained from as-cast composites processed at different melt holding times is shown in Fig.4.9(a-e). During *in-situ* composite synthesis, addition of secondary particles to the alloy system brings a significant change in size and shape of grains. Fig.4.9 shows the bar diagram representing the mean and standard deviation of the grains as measured from the composites. The as cast unreinforced AA6082 alloy shows large and coarsed dendritic structure with dendritic arms with large aspect ratio (Fig.4.2). The composite processed with a hoding time of 15 min showed fine exquiaxed grain structure with an average grain size of 41.67±13.75 µm.   The drastic change in grain size and morphology of composite processed at 15 min compared with the unreinforced alloy is attributed to the combined effect of Al_3Ti, AlB_2 and TiB_2 particles present in the alloy. It has been well established that the presence of Al_3Ti particles in the melt acts

as a potent nucleant for aluminium during solidification [Schumacher et al., 2013]. At this melt holding time, complete dissolution of Al_3Ti (AlTiSi) and AlB_2 particles did not occurred, hence the density of these intermetallic particles is higher, which inturn enhances the grain refinement in the composite alloy matrix.

When these particles are present in the melt, during solidification they act as potent nucleation sites, thereby inducing high nucleation rate in aluminium which results in fine equiaxed grain structure. Hence in our case the formation of fine equiaxed grain structure is due to the presence of these numerous potent nucleating particles. The grain structure of composite processed with a holding time of 30 min is shown in Fig.4.9(b). Although the grain morphology seems to remain equiaxed, insignificant increase in size of grains (52.86±9.12 μm) can be observed. As the melt holding time was increased more of Al_3Ti and AlB_2 began to tranform into TiB_2 particles, thereby reducing the number of potent nucleating particles. The reduction in the number of nucleating particles has resulted in the negligible growth of grains.

However the potent nucleating particles in the melt were sufficient enough to cause formation of equiaxed grains during solidification in the composite processed at 30 min. Composite processed with melt holding time of 45 min (Fig.4.9(c)) showed no change in morphology, whereas a slight increse in grain size (52.86±9.12 to 57.40±13.20 μm) can be observed when compared to compostie processed at 30 min. Although this change in grain size is insignificant, the observations reveals that more of active nucleating particles is present even at a melt holding time of 45 min. The grain structure of composite processed with a melt holding time of 60 min is shown in Fig. 4.9d.

The size of the grains were found to be 70.98±14.67 μm and they exhibited equiaxed morphology. Significant growth of grains in composite processed at 60 min suggests that more of Al_3Ti particles have dissolved thereby transmorming into TiB_2 particles. This observations further proves that more the Al_3Ti dissolution has occurred between 45 to 60 min of holding time. However, the presence of Al_3Ti particles in the composite matrix, indicates that complete transformation of did not occur even at this longer melt holding time. Fig.4.8(e) shows the micrograph obtained from composite processed with melt holding time 90 min. Although there seems to be a minor change

in the grain morphology absence of dendritic enclosure on the grain boundaries suggests that still the morphology remains equiaxed.
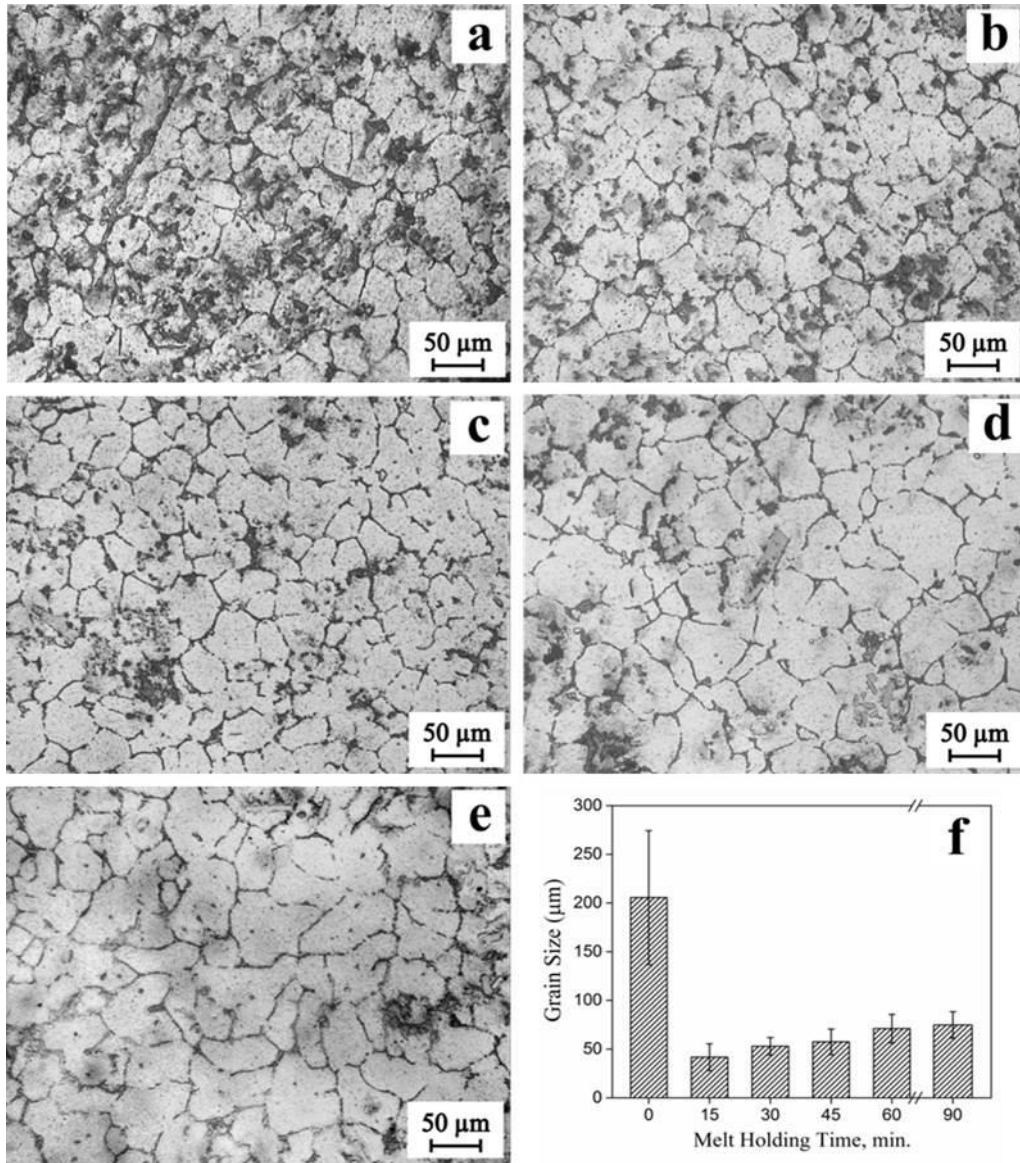
Fig. 4.9 (a-e) Optical micrographs and bar diagram of as-cast composite processed at different melt hold time:(a) 15, (b) 30, (c) 45, (d) 60, (d) 90 min, and (f) Bar diagrams showing the mean grain size and standard deviation for the unreinforced alloy and the composite processed at different holding time

The grains size measurments shows there no significant chage in the size of grain is observed in composite processed at 90 min (70.98±14.67 to 74.83±13.56 μm) when compared to composite processed at 60 min.

The presence of Al$_3$Ti particles in composite processed at 90 min confirmes that even at a holding time of 90 min the dissolution of Al$_3$Ti particles has not occurred. Moreover the XRD (Fig4.6) and SEM (Fig.4.7) analysis further confirms the presence of Al$_3$Ti and TiB$_2$ particles and the absence of AlB$_2$ or other boron base particles at the melt holding time of 60 and 90 min. Hence the unavailability of boron based intermetallics has hindered the dissolution of Al$_3$Ti particles. Therefore even at longer melt holding time the existance of Al$_3$Ti particles has catalysed the grain refinement of the composite alloy matrix during solidification.

4.4.4 Mechanical properties

The results of hardness, 0.2% proof stress (0.2%Y.S), tensile stress and % elongation of as-cast unreinforced alloy and AA6082-5TiB$_2$ composites are shown in Table 4.3. The bulk hardness measurments obtained using Vickers hardness testing is shown in Table 4.3. When compared with the unreiforced alloy , the prepared composites showed a reduction in hardness values. Moreover from the results it is evident that there is a significant reduction in the composite hardness as the melt hoding time was increased from 15 to 90 min. Composite processed at 90 min of melt holding time showed a 25% decrease in hardness. Generally in the as cast alloys factors such as porosity, blow holes contribute to the reduction of hardness. However 2-3% of porosity obeseved in the present composites would not have affected the hardness of the composites.

Earlier investigations reveal that the presence of Al$_3$Ti intermetallic particle would probably bring down the strength of the composites [Ma et al., 1994]. Hence during the processing of Al-TiB$_2$ composites utmost care should be taken to avoid the presence of Al$_3$Ti particle in the final composite matrix. It should be noted that in the present investigation AlTiSi particles were formed rather that Al$_3$Ti intermetallics. Literatures indicated that the presence of AlTiSi phase would subtancially improve the micro hardness of the composite and no literature on the bulk hardness of alloys with AlTiSi is available. In Al-Ti-Si alloys Tong Gao et. al. [Gao et al., 2011] observed that AlTiSi particles with 6.77 at.%Si showed a 3% increase in hardness. However, observations from quantitative EDS analysis from the present investigation indicated that only a maximum of 1.50 at.% Si was present in the AlTiSi

intermetallic, which probably would not have contributed to the hardness of composite. Moreover, the hardness estimations by other investigators were based on micro hardness, whereas in the present cast bulk hardness has been reported.

Table 4.3 Results of hardness and tensile properties of as cast unreinforced alloy and AA6082-5TiB$_2$ composites

Melt holding Time (Min.)	Hardness (HV$_5$)	(0.2%) Y.S (MPa)	U.T.S (MPa)	% Elong.
0	55	128	172	8
15	48	134	179	16
30	46	130	173	17
45	45	127	159	19
60	42	120	144	20
90	41	117	141	20

Apart from Al$_3$Ti, presence of AlB$_2$ and TiB$_2$ particles in the matrix alloy should have increased of hardness of the composite. Whereas a reduction in composite hardness when compared with unreinforced alloy hardness is very peculiar. Hence, further investigation on the hardness of composite has to be carried out in order to understand its reduction in hardness behavior, besides the presence of secondary particles.

Tensile properties of composites is generally decided by several factors such as type of reinforcements, volume fraction of reinforcements, matrix material, size and shape of reinforcements and the compatibility between matrix and reinforcements. The tensile property values obtained from the unreinforced alloy and composites are shown in Table 4.3. It can be seen that the composite processed at 15 min shows a 4.68 and 4.06% of increase in yield stress and ultimate tensile strength when compared to the unreinforced alloy. The composite exhibits a 100% elongation.
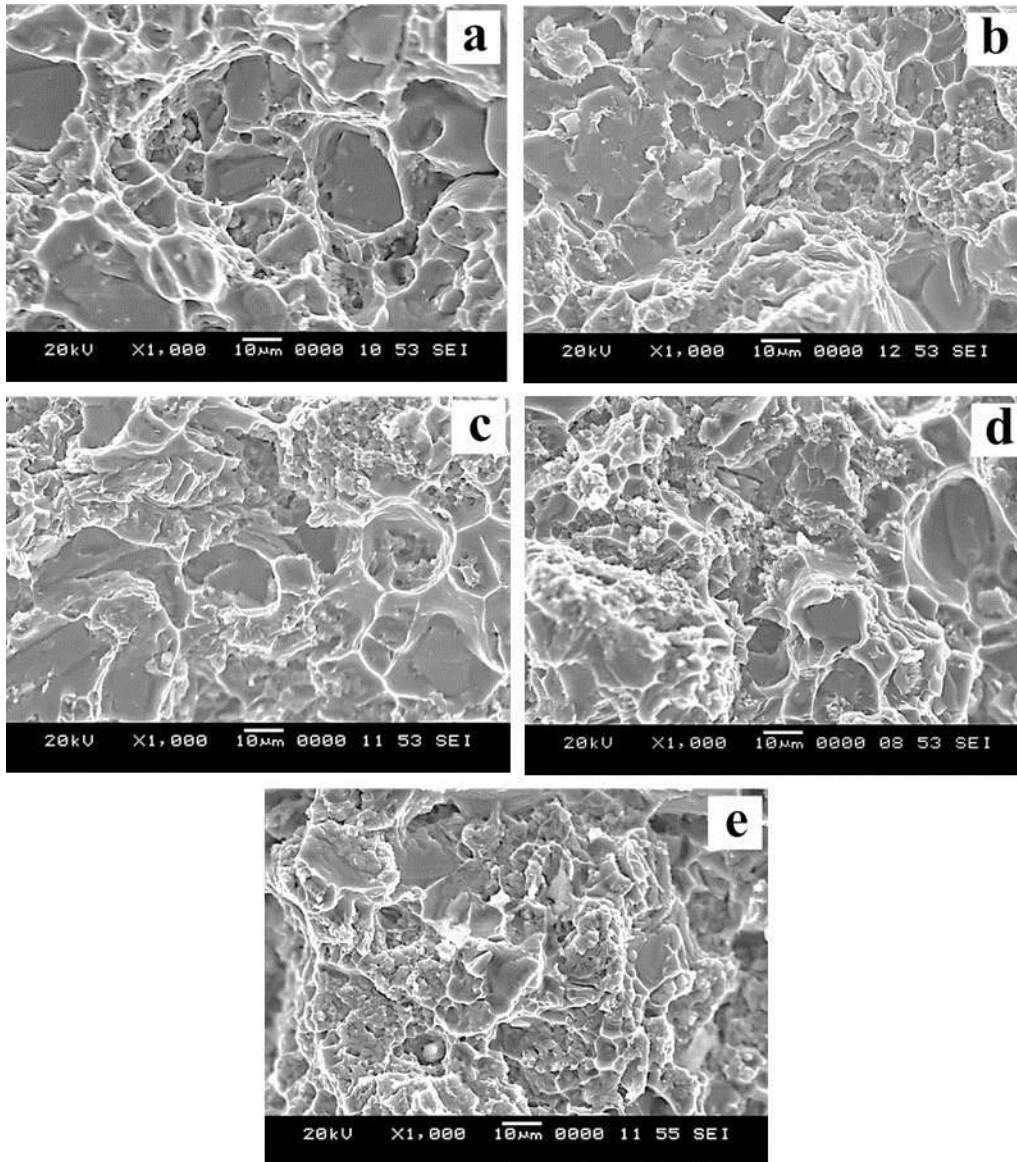
Fig. 4.10 SEM fractographs showing the tensile fracture surface of AA6082-5TiB$_2$ composites (a) 15, (b) 30, (c) 45, (d) 60 and (e) 90 min.

The composite processed at 30 min showed a 1.56% and 0.58% of increase in tensile strength compared to unreinforced alloy. Compared to the unreinforced alloy, the small increase in yield and tensile strength observed in the composite processed at 15 and 30 min could be due to the presence of higher weight fraction of reinforcement particles in the matrix alloy. In other words, the presence of AlTiSi, AlB$_2$ and TiB$_2$ particles would have contributed for the improvement of the strength in composite. Moreover, along with high weight fraction of particles, the decrease in grain size (Fig.4.9a&b) should have also contributed to the strengthening of the composite

82

processed at 15 and 30 min. Composite processed at 30, 45 and 60 min showed a drastic decrease in tensile strength as the melt holding time was increased from 45 to 90 min. Composite processed at 90 min shows an 8.59% and 18.02% decrease in yield stress and U.T.S., whereas the percentage of elongation is seems to increase by 150%. Presence of high weight fraction of fine TiB_2 particles have contributed to the high ductility of the composites.

Fig 4.10 (a-e) shows the SEM fractographs acquired from the tensile fracture surface of unreinforced alloy and composites processed at different holding times. Larger and deeper sized dimples with large unbroken AlTiSi particles seen in (Fig.4.10a) the fracture surface of composite processed at 15 min of holding time, this shows that the particles AlTiSi particles were strong enough to withstand the applied load. As the holding time increased the size of the AlTiSi particles present in the fracture surface decreases. Moreover, increase in the area of fine dimples in the fracture surface of composite prepared at longer holding time also confirms the increase in density of TiB_2 particles. The presence of AlTiSi particles even at holding time of 90 min is also confirmed from the fractographic studies. The fractographic studies correlates well with results obtained from the tensile results.

4.4.5 Inference

An overall observation reveals that the processed composites exhibit poor mechanical properties than the unreinforced alloy. The reduction in properties of the composites can be attributed to several factors: (i) The presence of large number of AlTiSi particles rather than TiB_2 particles (ii) reduction in matrix alloy strengthening and (iii) presence of unwanted slag, which is entrapped during solidification. The characterization of the composites confirms that no slag is present the matrix alloy. Hence, the reduction in the properties of the composites could be from the above-mentioned first two factors. From the experience gained from the present observation, it was concluded to eliminate the presence of AlTiSi particles in the matrix alloy so as to understand and improve the overall properties of the composites.

4.5 Influence of melt holding time without the addition of Mg - Part II

4.5.1 X-ray diffraction analysis

Fig. 4.11 (a-e) shows the normalized XRD patterns obtained from the composite processed at different holding time of 15, 30, 45 and 60 min at constant temperature of 850ºC. Fig.4.11b shows the XRD peaks obtained from composites processed at 15 min of holding time.
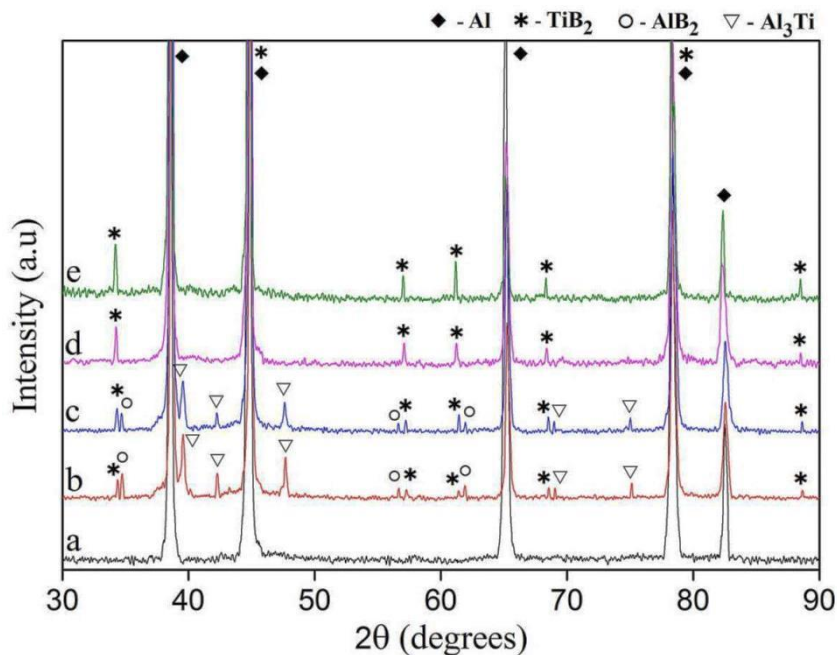
Fig. 4.11 X-ray diffraction pattern showing the peaks of Al, Al_3Ti, AlB_2 and TiB_2 from the processed composites with different holding time at a constant temperature of 850°C without the addition of alloying elements: (a) AA6082 alloy, (b) 15, (c) 30, (d) 45 and (e) 60 min.

The diffraction peaks obtained from composite processed at lower holding time 15 min shows the presence of Al_3Ti, AlB_2 and TiB_2 phases along with Al. From the difference in intensities of the peaks, it is evident that the particles phases present in the composite matrix were of different weight fractions. Although the presence of TiB_2 peaks confirm its presence in the matrix, presence of Al_3Ti and AlB_2 along with TiB_2 peaks confirm that the reaction is incomplete at this holding time. Hence, the holding time to process the composite was further increased to 30 min. The XRD

diffraction pattern obtained from composite processed with a holding time of 30 min is shown in Fig. 4.11c.

Analysis on the pattern acquired from composite indicates that there is a significant increase in peak intensity of TiB_2 when compared with the peaks of TiB_2 in composite processed at 15 min. It is also evident that, with the increase of TiB_2 peak intensity, AlB_2 and Al_3Ti intensities have decreased substantially. This indicates that, as the holding time was increased from 30 to 60 min, the dissociation of Al_3Ti and AlB_2 has occurred leading to the formation of TiB_2 particles. In other words, with longer melt holding time more of TiB_2 particles were formed due to dissociation of Al_3Ti and AlB_2 particles. Although the results indicate the formation of more TiB_2 particles in the composite matrix, from the obtained peak intensities, presence of Al_3Ti and AlB_2 peaks indicates holding time is not sufficient for the complete dissociation of these intermetallic particles. The holding time was further increased to 45 min.

The XRD results obtained from the composite processed with a holding time of 45 min is shown in Fig4.11d. Upon indexing the pattern, it is evident the only TiB_2 phase is present in the aluminium alloy matrix. Furthermore, the presence of only TiB_2 peaks and the absence of peaks corresponding to Al_3Ti and AlB_2 phase, indicates that the complete dissociation of Al_3Ti and AlB_2 has occurred at melt holding time of 45 min. The XRD pattern obtained from composite processed at a melt holding time of 60 min is shown in Fig. 4.11e. The XRD peaks indicated that the results were similar to the composite processed at 45 min except a small increase in intensities of TiB_2 peaks. Although the XRD is a wonderful tool used for the identification of an unknown material or phases present in the material, it still has its own limitations. One of the limitations includes the inability of XRD to identify the phases, which are present in less than 2wt%. Hence, the XRD pattern obtained from composite (45 min) shows the presence of only TiB_2 peaks and no Al_3Ti or AlB_2 peaks were detected.

The results indicates that, complete dissociation of Al_3Ti and AlB_2 particles occurs in melt leading to the formation of TiB_2 particles in composite processed with a melt holding time of 60 min at a 850°C. Moreover, complete dissociation of Al_3Ti and AlB_2 leading to formation of only TiB_2 particles in the melt occurs in between 45 and

60 min of holing time. Hence, a small increase in TiB_2 peak intensity is seen in composite processed with longer holding time of 60 min.

4.5.2 Scanning electron microscopy

The scanning electron photomicrographs acquired from composite processed at different holding times of 15 to 60 min in steps of 15 min is shown in Fig.4.12 (a-d). Fig.4.12a shows the photomicrograph acquired from the composite processed at a melt holding time of 15 min. From the EDS analysis (Fig. 4.13(b-d)) acquired from the particles it was confirmed that the blocky particles in dull grey colour belonged to AlTiSi phase and the smaller dull grey colour particles were identified as Al_3Ti phase. The large blocky particles with dark black contrast with different size and shape with smooth edges were found to be AlB_2 particles.

The size of AlB_2 particles present in the microstructure ranged from 6µm to 14µm. The fine particles with the size range of few microns to 2 µm belonged to the TiB_2 phases. From the micrograph, it is evident at lower holding time of 15 min; more of AlB_2, Al_3Ti and AlTiSi particles and fewer TiB_2 particles are present. These results corroborate well with the XRD results shown in Fig.4.11b. The SEM photomicrograph shown in Fig.4.12b corresponds to the composite processed with a holding time of 30 min. Compared to the composite processed at 45 min more of TiB_2 particles are seen. Moreover, the particles formed were fine with size not larger than 1µm. Presence of less number of AlB_2 and Al_3Ti particles confirm that at longer holding time the dissolution of the intermetallic particles has occurred leading to the formation of TiB_2.

Fig.4.12c shows the SEM micrographs obtained from the composite processed at a holding time of 45 min. Presence of TiB_2 particles with size ranging from few microns to a maximum size of 3 µm is evident. Although some uniform distribution of the TiB_2 particles is seen in the composite processed at 45 min, more of agglomerations are seen. These agglomerations of the TiB_2 particles could have occurred due to the presence of small amount of Al_3Ti on the surface of TiB_2 particles. Similar results were observed by I.G. Watson et al [Watson et al., 2005].
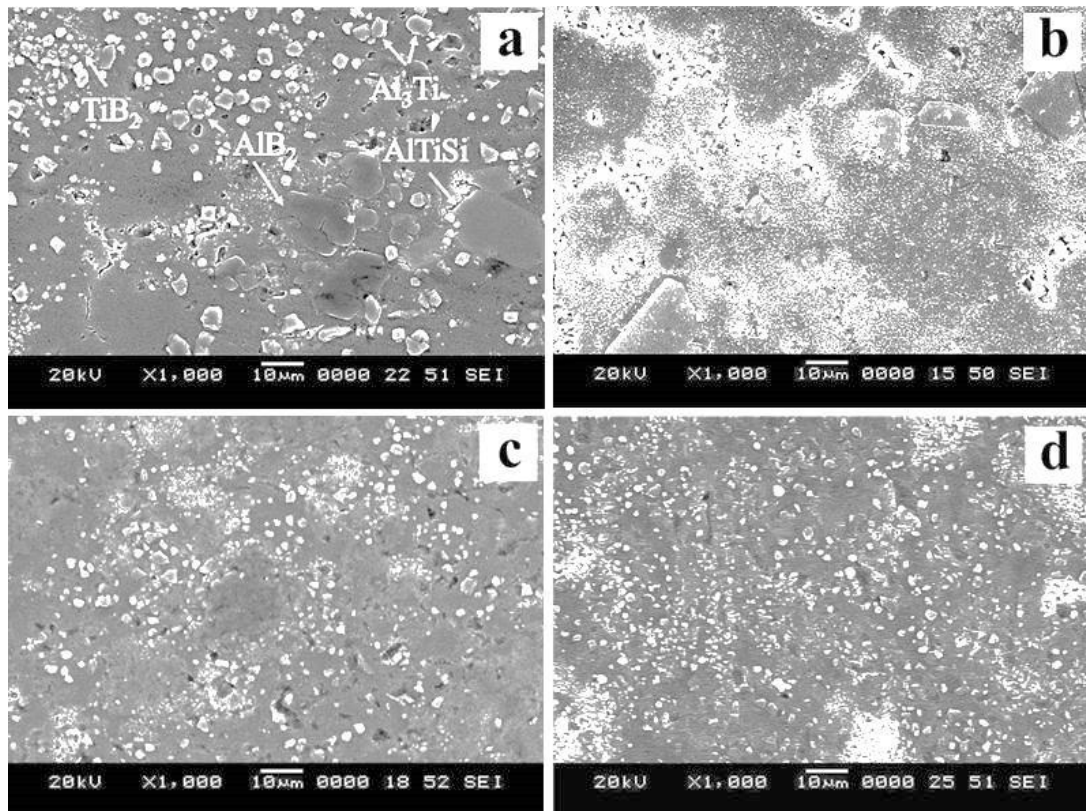
Fig. 4.12 (a-d) SEM photomicrographs showing the composite processed at different melt holding times; (a) 15, (b) 30, (c) 45 and (d) 60 min.

Along with the particles some pits are also evident, these pits have occurred due to particle pullout from the matrix when the processed composites were subjected to disk polishing at high rpms. In other words at high rpms the particle pullout has occurred, hence the pits are seen in those regions where the particle pullout has occurred. Fig.4.12d shows the SEM photomicrographs obtained from composite processed with a holding time of 60 min. The observations from the micrograph reveals that as the melt holding time was increased from 45 to 60 min the agglomerations seems to reduce. Homogeneous distribution of TiB_2 particles further indicates that absence of Al_3Ti phase in the matrix. Analysis on the particles present in composite (60 min) indicates that there is no significant change in particles size or morphology when compared with composite processed at 45 min.
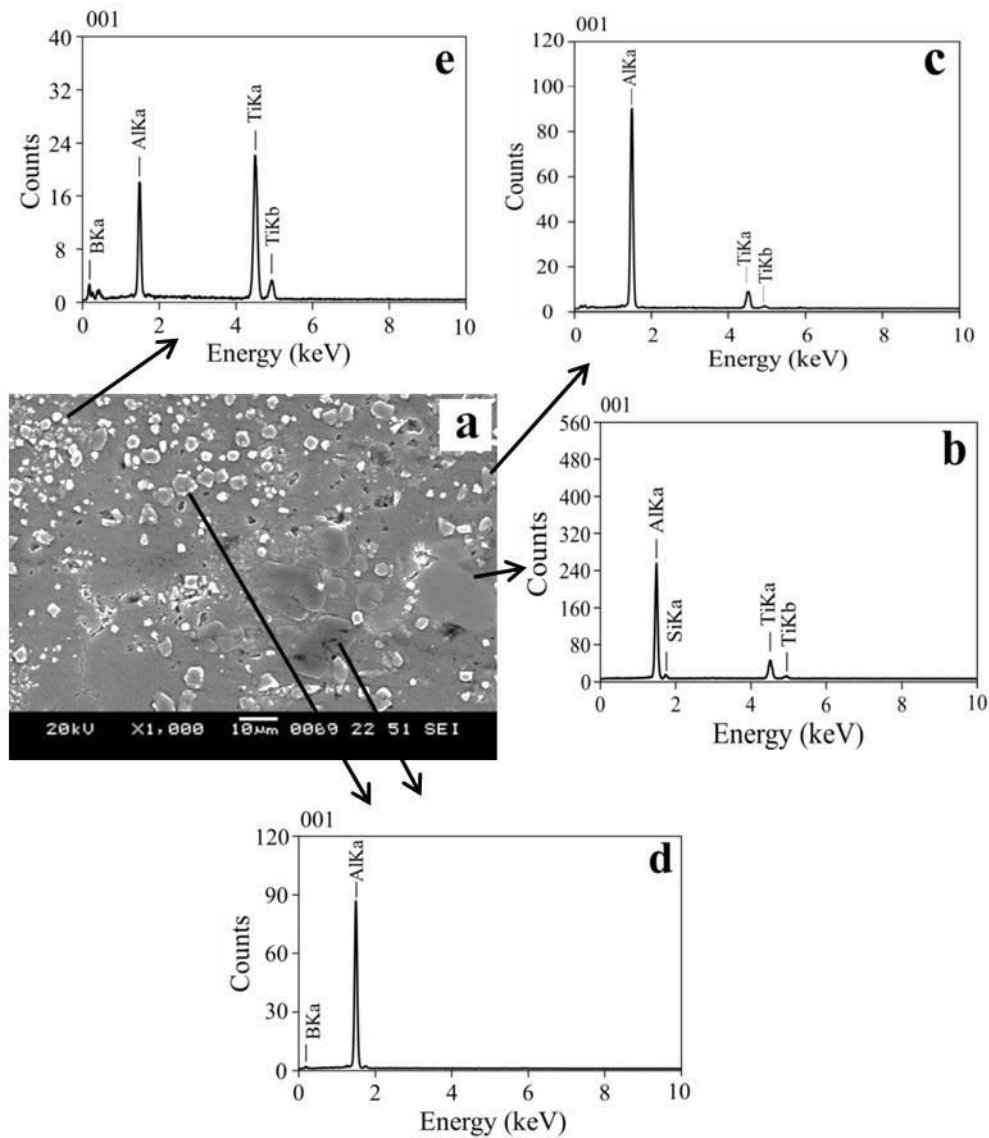
Fig. 4.13 (a-e) SEM micrograph and EDS spectrum obtained from the particles; (a) SEM micrograph of as cast composite 15min., EDS spectrum of (b) AlTiSi, (c) Al$_3$Ti, (d) AlB$_2$, and (e) TiB$_2$ particles

4.5.3 Optical microscopy

Optical micrographs of composite processed at different holding times of 15 to 60 min in steps of 15 min are presented in Fig. 4.14 (a-d). The corresponding bar diagrams presenting the mean and standard deviation of the grain size present in the unreinforced alloy and composite is shown in Fig.4.15. The micrograph shown in Fig.4.14a was obtained from the composite processed with a holding time of 15min. From the micrograph, it is evident that the grain structures formed in the composite

were of both globular and equiaxed. Image analysis on the optical micrograph confirmed that the average grain to be 45.62 ±11.24 µm.
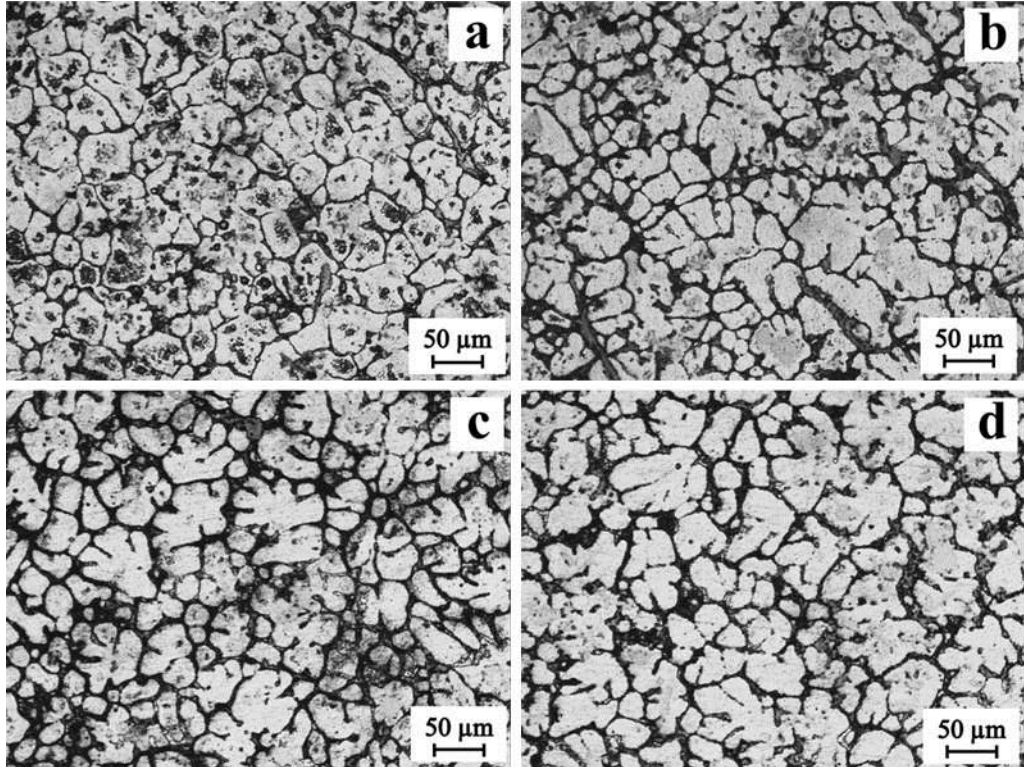
Fig. 4.14 (a-d) Optical micrograph of as-cast composite processed at different melt holding time: (a) 15, (b) 30, (c) 45 and (d) 60 min.
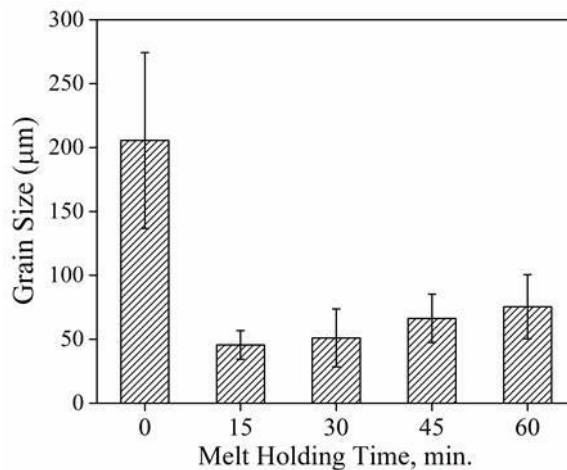
Fig. 4.15 Bar diagrams showing the mean grain size and standard deviation of the composite processed at different holding time.

Composite possessed more number of Al_3Ti and AlB_2 particles than TiB_2 particles and this has been confirmed from the results shown XRD (Fig.4.11) and SEM (Fig.4.12). When these particles are present in the melt, upon solidification of the melt these particles tends to act as effective nucleating centers. Moreover, from the literatures it is has been well established that the presence of Al_3Ti particles in aluminium alloys leads to better grain refinement than AlB_2 and TiB_2 [Lee. and Chen., 2002]. Hence, with the presence of these particles in large numbers has led to grain refinement, which has been found to be cause for the formation of fine globular and equiaxed grain in composite processed at 15 min.

Fig.4.14b shows the optical micrograph of composite processed with a holding time 30 min. From the image analysis on micrograph, the average size of grains and its standard deviation were found to be 51.11±22.62 μm. Although the composite (30 min) showed a marginal difference in grain size compared to the composite processed at 15 min, more change in grain morphology of composite processed at 30 min can be observed. The optical micrograph of composite processed at 30 min reveals a mixture of equiaxed and irregular rosette type grain morphology. As the melt holding time increased, more of Al_3Ti and AlB_2 particles present in the composite melt began to dissociate, leading to the formation of TiB_2 particles. Although the density of TiB_2 particles increased, the reduction of effective Al_3Ti nucleant particles has been the reason behind the increase in grain size and morphology of the grains in the composite.

Fig.4.14c shows the optical micrograph of composite processed at a holding time 45 min. The average grain size of composite was found to be 66.37±18.88 μm and the morphology of the grains was predominantly of rosette type. Observations reveal that there is no significant change in grain morphology of composite is observed compared to composite (30 min), whereas significant change in the size of the grain is evident. With the increase of longer holding time 45 min, the dissolution of more of Al_3Ti and AlB_2 particles has occurred. This has led to the reduction in number of effective nucleant particles in the melt which in turn has led to the growth of grains. The micrograph of composite processed at a holding time of 60 min is shown in Fig.4.14d. The grain size was found to be 75.39±25.12 μm. From the Fig.4.14d it is apparent that

90

longer holding time of 60 min had no effect on the grain morphology the composite. Overall, from the optical micrographs it is evident that change in grain morphology and increase in grain size occurred in the composites with increase in melt holding time.

4.5.4 Mechanical properties

4.5.4.1 Hardness
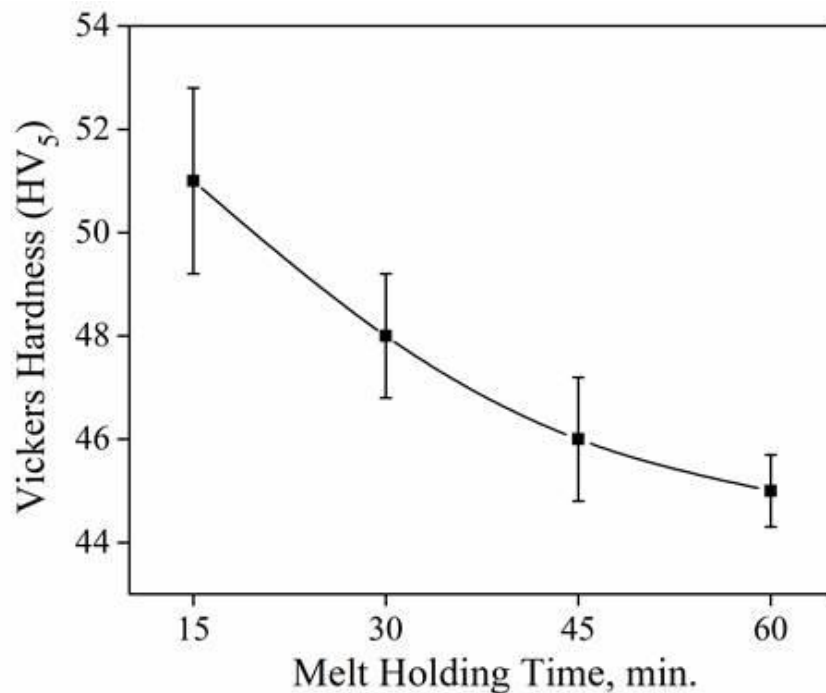
Fig.4.16 Plot showing the variation of hardness in composites processed at different melt holding time.

Fig.4.16 present the plot depicting the Vickers hardness values obtained from as cast unreinforced alloy and composite processed at different holding time. From the plot, it is evident that as the melt holding time increased, reduction of hardness in the composite occurred. The composite processed at 15 min of holding time showed a hardness of 51 VHN. Although the hardness value of composite seems to be lesser than unreinforced alloy, it was higher than the composite processed at 30 min. It is evident that at lower holding time the density of particles (Al_3Ti, AlB_2, AlTiSi and TiB_2) is higher. This high density of particles present in the composite could be the reason behind the composite hardness.

With further increase in holding time these particles have tend to dissociate leading to the formation of TiB$_2$ particles, which are less in density. Hence, from the plot it can be seen that as the holding time increases the hardness eventually reduced. It is well know that with the addition of hard reinforcing particles to unreinforced alloy, the hardness of the alloys tends to increase. In our case, the hardness of composite processed at different holding time in this section as well the hardness of composite processed during the section 4.4.3 shows a reduction in hardness values. In spite of completely achieving the TiB$_2$ hard phase in the matrix alloy (60 min) the hardness deteriorated.

4.5.4.2 Tensile properties

Table 4.4 Hardness and Tensile properties of as cast unreinforced alloy and AA6082-5TiB$_2$ composites at different holding time.

Melt holding Time (Min.)	Hardness (HV$_5$)	(0.2%) Y.S (MPa)	U.T.S (MPa)	% Elong.
0	55	128	172	8
15	51	139	183	14
30	48	135	177	15
45	46	125	159	17
60	45	121	154	18

Table 4.4 shows the tensile properties of composite synthesized at different melt holding time of 15-60 min in steps of 15 min at a constant temperature of 850°C. The composite processed at 15 min shows higher Y.S and U.T.S compared to the unreinforced alloy. The presence of more number of reinforcement particles and the fine globular grains in the composite has significantly contributed to the improvement in tensile properties of composite processed at 15 min. The presence of more particle density reinforcements with along with fine globular shaped grains lead to smaller mean free path for dislocation movement thereby increasing the dislocation density as well as work hardening. Hence, compared to the unreinforced alloy the U.T.S of the composite has improved. The % Elongation of the as cast composite (15 min)

compared with the unreinforced alloy is higher by 75%. This drastic increase in elongation has resulted from the grain morphology and grain size of the composite. Compared to composite processed at 15 min, composite processed at 30 min showed a reduction in U.T.S, Y.S and increase in % Elongation. However, the tensile property of composite (30 min) is still higher than unreinforced alloy. The decrease in density of reinforcement particles and the change in grain morphology could be reason behind the decrease in tensile properties of composite processed at 30 min. The increase in ductility of composite is caused by the presence of fine TiB_2 particles, which are present in matrix. With further increase in holding time, the tensile properties of composite processed at 45 and 60 min deteriorated. This decrease in tensile properties of the composite could also be attributed to decrease in density of secondary particles and grain morphology and size.

Compared to the unreinforced alloy ductility of the composite has increase by 125%. This increase in ductility is caused by the presence of fine TiB_2 particles which are well bonded with the matrix. Upon tensile loading the propagation of cracks is hindered by these hard TiB_2 particles. Moreover due to a strong bonding between the matrix and composites, when cracks propagate thorough the matrix they are surely hindered by the TiB_2 particles. Tensile fracture surfaces of the composites processed at different melt holding time is shown in SEM micrographs presented in Fig.4.17 (a-d). The SEM fractograph in Fig. 4.17a shows the evidence for the ductile fracture with numerous dimples.

Presence of both bigger and smaller dimples confirms that the dimples occurred during fracture were of bimodal in nature have suggest that large particles tends to crack because of the flaws present in them, whereas the presence of large AlTiSi particles inside the dimples shows that the particle cracking has not occurred. The presence of particles inside the dimples also suggests that there exist a good bonding between the particle and the matrix. Observations on the fracture surface of the composite processed at other holding time also indicate that the mode of fracture was ductile in nature. SEM photomicrographs on composite processed at 45 min (Fig.4.12c) indicates the presence of agglomerations. During tensile loading voids are formed as a result of decohesion of the clusters of fine particles and because of these

clusters fine voids are formed in the matrix and these voids coalesce leading to the failure of composite.
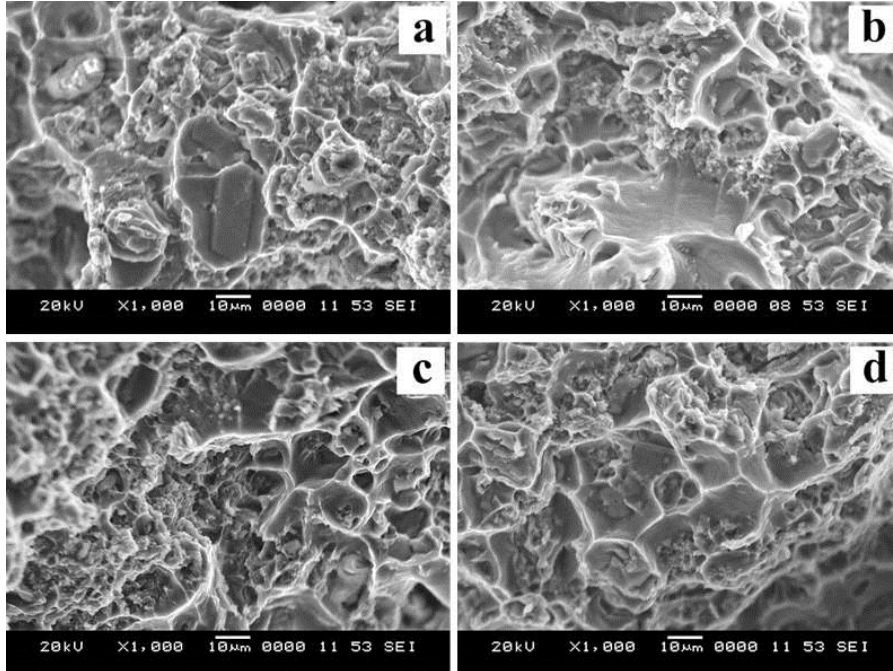
Fig.4.17 SEM (SE) images of tensile fracture surface of composite processed at different melt holding time; (a) 15, (b) 30, (c) 45 and (d) 60 min.

4.5.5 ICP-OES

Table 4.5 Elemental composition of unreinforced alloy and composites processed at different melt holding time.

Samples	Matrix Chemical Composition (Wt. %)					
Time (Min.)	Mg	Si	Mn	Cr	Fe	Al
Standard	0.6-1.2	0.7-1.3	0.4-1.0	0.25	0-0.5	Bal
0	1.026	1.300	0.475	0.147	0.174	Bal
15	0.108	1.082	0.397	0.139	0.164	Bal
30	0.021	1.144	0.418	0.141	0.167	Bal
45	0.017	1.264	0.447	0.142	0.171	Bal
60	0.011	1.287	0.459	0.144	0.172	Bal

The ICP-OES is a simple and an accurate technique for the determination of elemental concentration present in the composite matrix alloy. The acquired chemical composition of elements present in the composite matrix alloy processed at different holding time for a constant temperature of 850°C and the unreinforced alloy is presented in Table 4.5. Analysis on the composite processed at 15 min indicates that the Mg present in the alloy matrix is almost lost. It is also evident that the loss of Mg is huge such that almost 0.91% is lost from the matrix alloy. Moreover the loss of Mg in composite alloy matrix is far below the allowable standard composition of alloy.

Composites processed with longer holding time shows that almost all the Mg from the matrix alloy has depleted. The loss of Mg in the matrix alloy of the composite has probably occurred due to addition of the fluoride salts to matrix alloy. Apart from Mg, the results also indicate that a small reduction in Si, Mn and Cr is seen. This marginal decrease of these elements is attributed to its diffusion into the particles present in the composite. Although there seems to be a small decrease of Si, Mn and Cr elements in the matrix alloy, they are well under the allowable range of the standard composition of alloy. A detailed experimentation and analysis on the influence of Mg, Mn and Si elements, during the processing of *in-situ* AA6082-5TiB$_2$ composites has been discussed in chapter 5.

4.5.6 Inference

In section 4.4 the results obtained from the composite processed at 800°C for different holding time of 15 to 90 min were interpreted and discussed. The mechanical properties of the composites seem to deteriorate with increase in holding time. From the interpretation it was assumed that the presence of unwanted intermediate Al$_3$Ti particles could be cause for the deteriorating of mechanical properties. Hence, the experiments were repeated with small modification in the parameters, so that only TiB$_2$ particles are present in the final composite. The second set of experiments was carried out at a melt temperature of 850°C rather than 800°C.

In section 4.5 the results obtained from the composite processed at 850°C for different holding time of 15 to 60 min was interpreted and discussed. The characterization studies on the composite confirmed the formation on only TiB$_2$ particles in the composite processed at holding time of 60 min. However, the mechanical property

studies on processed composites shows deterioration in properties almost similar to that of processed composite discussed in section 4.4. Although the reinforcement phase plays an important role in the composite microstructure and its properties, property deterioration occurs in the processed composite in spite of the presence of hard TiB_2 particles. Hence, the realiasation gave us an insight to focus on matrix alloy along with reinforcements. The elemental composition present in the composite was determined by using ICP-OES.

The results indicated the loss of elements in the composite matrix has occurred during processing. With the loss of elements in the alloy, the properties of the matrix alloy deteriorated. In spite of the presence of hard TiB_2 reinforcements, the properties of the composite deteriorated because of the weakening of the matrix alloy. Henceforth, from the knowledge obtained from the previous sections (4.4 &4.5) it was decided to compensate the loss of alloying element by external addition. Therefore, to understand the effect of alloying elements, separate set of experiments were carried out and the influence of alloying elements on the properties of the composites was studied. This has been discussed briefly in chapter 5.

From the knowledge obtained from experiments in chapter 5, the amount of alloying elements need for the compensation of the loss of elements during processing was composite was understood. To further understand and to prepare AA6082-5TiB$_2$ composite with excellent properties, third set of experiments were carried out to understand the influence of processing time. It should be noted that the loss of alloying elements in the matrix alloy was compensated by externally adding the alloying elements to the alloy melt before pouring.

4.6 Influence of melt holding time with the addition of Mg

4.6.1 ICP-OES

ICP-OES analysis on composites processed at different holding time shown in Table 4.5 confirmed that during the processing of composites severe loss of alloying elements in the composite alloy matrix has occurred. Hence, from the knowledge gained during the experiments carried out in chapter 5, required amount of excess of Mg element was added to the alloy matrix to compensate the elemental loss. In order

compensate the loss of Mg and to attain 1% in the final matrix, 7gm of Mg strips were added the 500gm of composite melt.

Table 4.6 Elemental composition of matrix alloy and composites processed at different melt holding time.

Holding Time (Min.)	Matrix Chemical Composition (Wt. %)					
	Mg	Si	Mn	Cr	Fe	Al
Standard	0.6-1.2	0.7-1.3	0.4-1.0	0.25	0-0.5	Bal
0	1.026	1.300	0.471	0.151	0.174	Bal
15	1.063	1.201	0.439	0.143	0.159	Bal
30	0.984	1.232	0.446	0.152	0.152	Bal
45	0.996	1.278	0.458	0.155	0.161	Bal
60	1.038	1.296	0.463	0.149	0.172	Bal

The procedure carried out for the compensation of alloy element loss has been elucidated in section 3.3.1.3. Table 4.6 shows the ICP-OES results obtained from the composites processed at different holding times after compensation of alloying elements. The results shows that the alloying elements present in the matrix alloy were equivalent to the standard elemental composition, specified for the AA6082 alloy.

4.6.2 X-ray diffraction analysis

The XRD patterns from the as-cast composite processed at different holding time and the as-cast AA6082 alloy is presented in Fig. 4.18 (a-e). It is seen that in composite processed with holding time of 15 and 30 min, the peaks of Al_3Ti and AlB_2 are visible in addition to TiB_2 and Al. The identities of the phases indexed are shown against the XRD peaks. The presence of the Al_3Ti and AlB_2 peaks in the XRD pattern indicates the incomplete reaction between the fluoride salts and the aluminium alloy melt. Hence, rather than the expected presence of only TiB_2 peaks, Al_3Ti and AlB_2 peaks

are evident. Although the presences of Al_3Ti and AlB_2 peaks are evident in both the composites, significant change in intensities of the peaks can be seen in the pattern. Compared to composite processed at 15 min composite processed at 30 min shows a sharp decrease in intensities among the peaks of Al_3Ti and AlB_2. It should be also noted that with the decrease in the peak intensities of composite Al_3Ti and AlB_2, a sharp increase in peaks intensities of TiB_2 could be observed. This indicates that as the holding time was increased from 15 to 30 min, the dissolution of more intermediate intermetallic particles has occurred leading to the formation of more TiB_2 particles in the matrix. With further increase in melt holding time to 45 min, composite shows the presence of only TIB_2 peaks, indicating the complete dissolution of the Al_3Ti and AlB_2 particles has occurred.
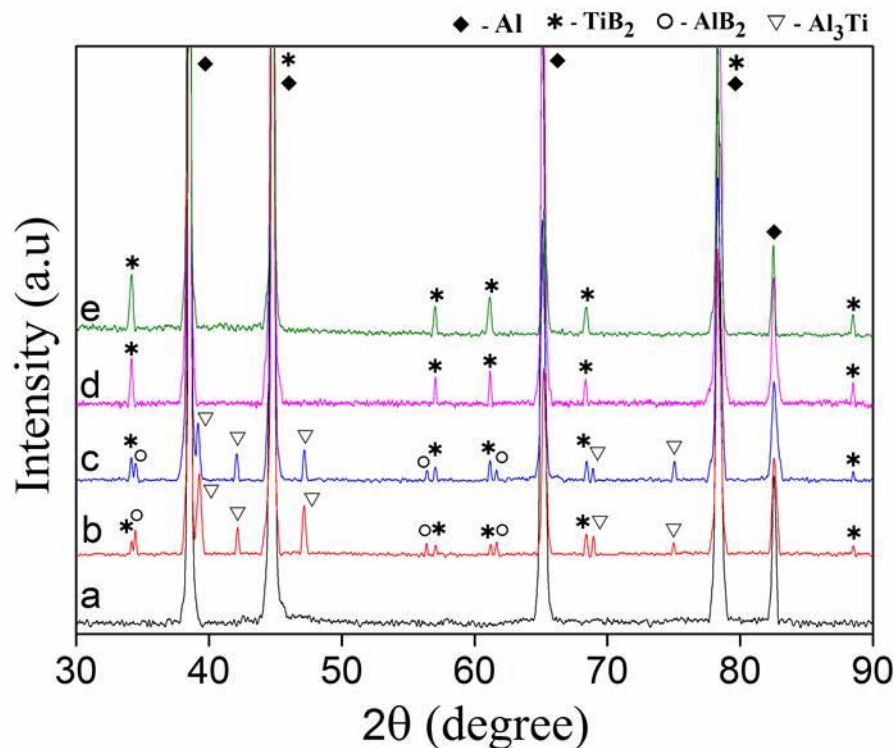
Fig. 4.18 X-ray diffraction pattern showing the peaks of Al, Al_3Ti, AlB_2 and TiB_2 from the processed composites with different holding time at a constant temperature of 850°C with the addition of alloying elements: (a) AA6082 alloy, (b) 15, (c) 30, (d) 45 and (e) 60 min.

XRD Pattern obtained from composite processed at melt holding time of 60 min also showed the presence of only TiB_2 peaks along with Al. The overall observations from the patterns obtained from composites processed with different holding times indicated that, processing of in-situ TiB_2 reinforced composites is possible only at longer holding times. The analysis also indicates that shorter holding time leads to the formation of unwanted Al_3Ti and AlB_2 intermetallic in the composite.

4.6.3 Scanning electron microscopy
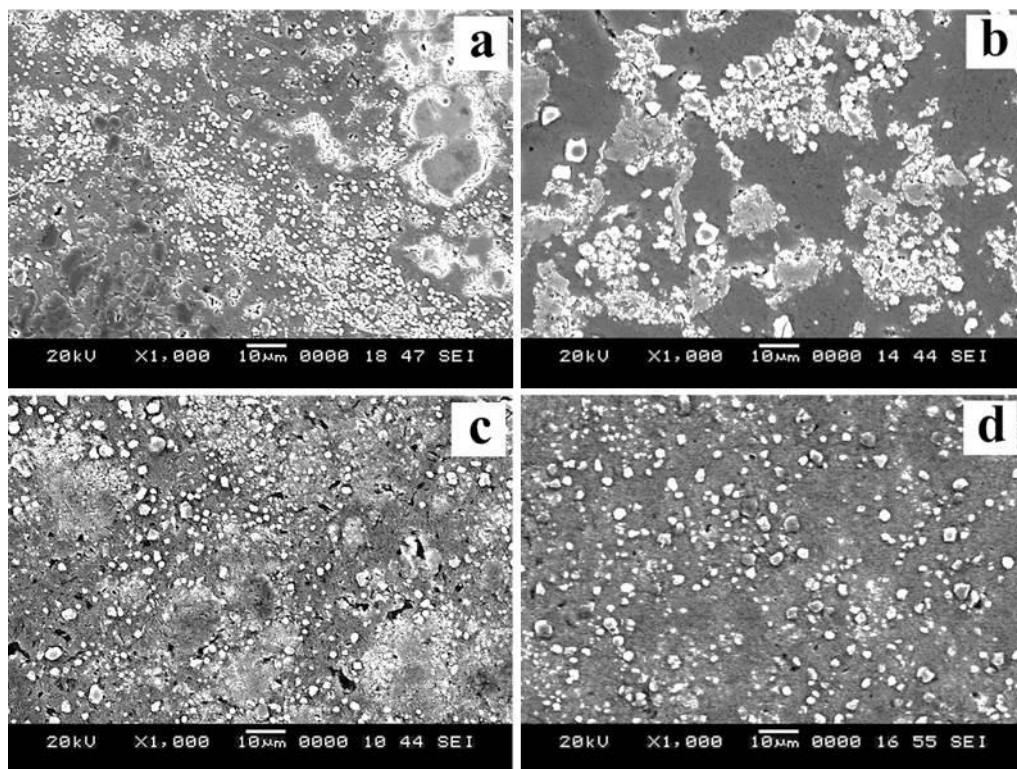
Fig. 4.19 (a-d) SEM photomicrographs showing the composite processed at different melt holding times with the addition of alloying elements; (a) 15, (b) 30, (c) 45 and (d) 60 min.

Representative SEM photomicrographs of composite processed at different melt holding time is shown in Fig. 4.19 (a-d). SEM photomicrographs of composite processed with a melt holding time of 15 min is shown in Fig.4.19a. Three types of particles with different morphology and colour can be seen. From the EDS analysis the large particles having greying colour with irregular morphology were found to be Al_3Ti particles. The Al_3Ti particles present in the matrix were not of same size, their

size ranged from a minimum of 1 to a maximum of 30 μm. Moreover small Al_3Ti particles were having a lot of cracks in them. This indicates the dissolution of Al_3Ti particles due to presence of Boron [Gowoski et al., 1987]. Similarly, the black contrasted particles with size ranging from 2 to 13 μm were found to be AlB_2 particles. Compared to Al_3Ti particles the reduction in size of AlB_2 particles confirms that the dissolution of AlB_2 is quicker than Al_3Ti. The white contrasted particles with irregular morphology and with size ranging from submicron size to 3.5 μm were found to be TiB_2 particles. These results were in agreement with the results of XRD shown in Fig.4.18b.
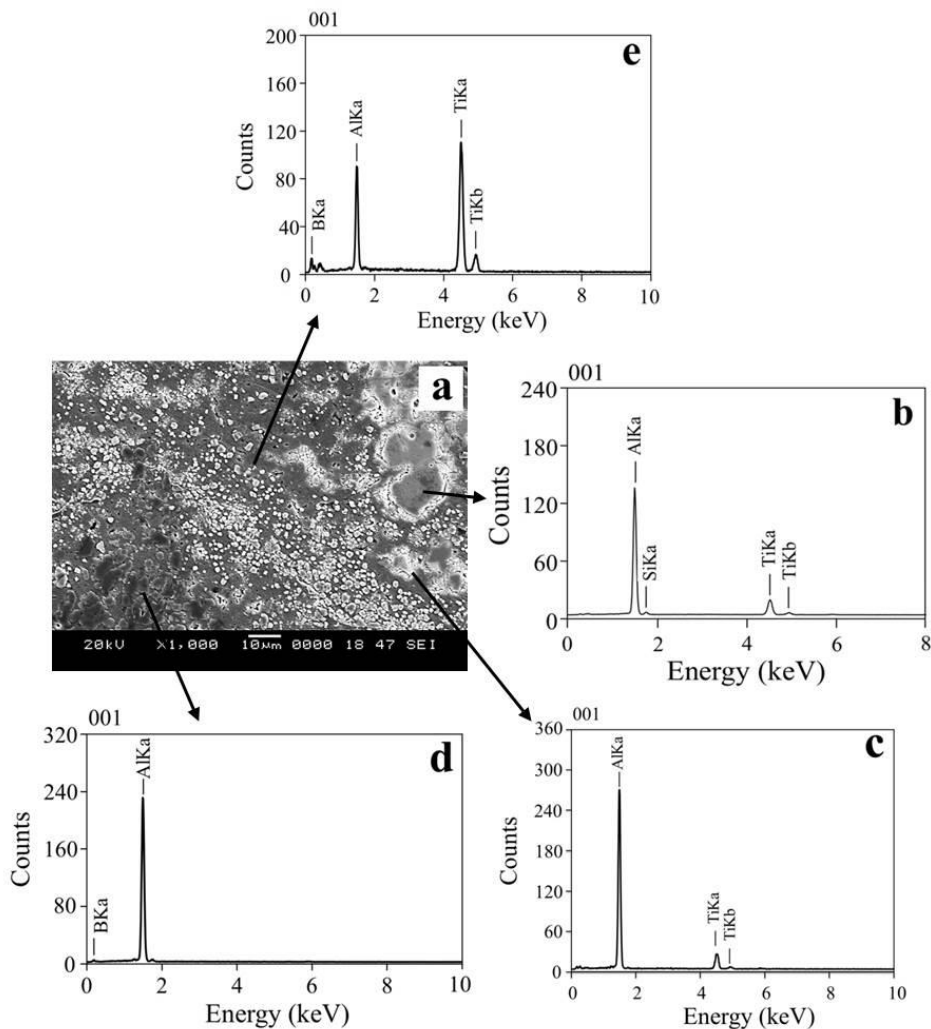
Fig. 4.20 (a-e) SEM micrograph and EDS spectrum obtained from the particles; (a) SEM micrograph of as cast composite 15min., EDS spectrum of (b) AlTiSi, (c) Al_3Ti, (d) AlB_2, and (e) TiB_2 particle.

SEM photomicrograph of composite processed with a holding time of 30 min is shown in Fig.4.19b. Al_3Ti, AlB_2 and TiB_2 were the found to be present in the matrix. Although the three types of particles present in the composite were similar to composite processed at 15 min, drastic change in morphology among the particles was observed. The maximum size of the Al_3Ti particles was found to be 13 μm, AlB_2 was around 6 μm and TiB_2 particles were of 3.5 μm.

The observations indicates that with increase in time more dissolution of the Al_3Ti and AlB_2 particles has occurred, there by transforming into TiB_2 particles. Hence compared to the average size of TiB_2 particles found in composite (1.7 μm) a small increase in size of TiB_2 particles composite processed at 30 min (2 μm), confirms that growth of TiB_2 particle occurs with the dissolution of Al_3Ti and AlB_2 particles. Fig. 4.19c&d shows the micrographs of composite processed with 45 and 60 min. The micrographs showed the presence of only TiB_2 particles in the alloy matrix. However, agglomerations of the particles were evident in composite (45 min). These agglomerations are caused by the presence of residual Al_3Ti phase. As the holding time was increase to 60 min, homogeneous distribution of TiB_2 particles with average size of 2.2 μm is evident. The observations indicates that at longer holding time composite with the presence of only TiB_2 particles with homogeneous distribution can be processed.

4.6.4 Optical microscopy

A relative comparison of grain structure present in the composite processed at different holding time, casted after the addition of Mg alloying elements is shown in Fig. 4.21 (a-d). The corresponding bar diagrams presenting the mean and standard deviation of the grain is presented in the in Fig. 4.22. Compared to the unreinforced alloy (Fig. 4.2), the processed composites show a drastic change in the size and morphology of grains. Fig. 4.22a shows the optical micrograph of composite processed with a holding time of 15 min. The average grain size of composite (15 min) was found to be 39±17.92 μm and possessed fine irregular, rosette type grain structure with dendritic character. The insufficient melt holding time of 15 min lead to the presence of Al_3Ti, AlB_2 and AlTiSi along with TiB_2 particles. Compared to the TiB_2 particles the fraction of Al_3Ti, AlB_2 and AlTiSi particles were found to be

higher. During grain refinement the size and morphology of the grains is dictated by the number of active potent nucleant particles. Hence, better gain refinement has taken place in composite (15 min) due to the presence more active Al_3Ti, AlTiSi particles along with TiB_2. As the melt holding time was increased to 30 min, grains with equiaxed morphology with an average size of 51 ± 18.79 μm are formed (Fig.4.21b).
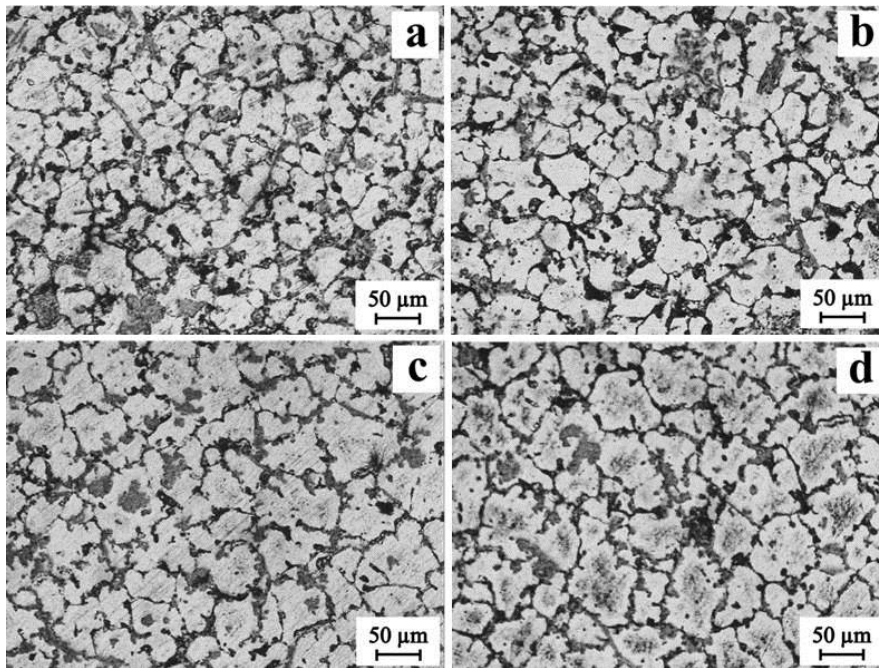
Fig. 4.21 (a-d) Optical micrograph of as-cast composite processed at different melt holding time: (a) 15, (b) 30, (c) 45 and (d) 60 min.
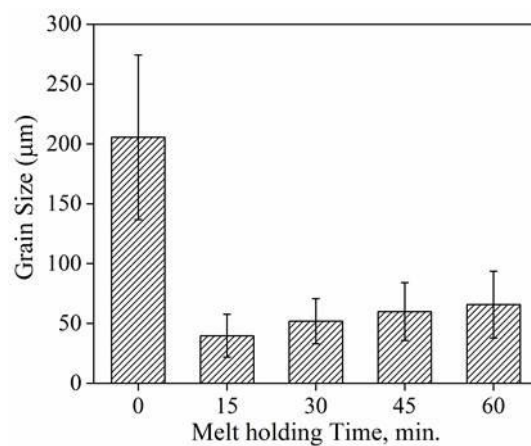
Fig. 4.22 Bar diagrams showing the mean grain size and standard deviation of the composite processed at different holding time.

As the holding time of the melt was increased, the dissolution of more Al_3Ti, AlTiSi and AlB_2 particles occurred thereby transforming into TiB_2 particles. Due to the dissolution of potent Al_3Ti and AlTiSi nucleant, number of effective nucleant particle reduced, leading to a small increase in the grain size of the composite. Although the grain size seems to increase due to the dissolution of Al_3Ti, AlTiSi and AlB_2 particles, there is no significant change in the grain size. This is due to the presence of more number of potent TiB_2 particles in the matrix. The grain size and morphology of composite processed at 45 and 60 min are shown in Fig 4.21c&d respectively. Although the composite processed at 45 and 60 min showed an average grain size of 59 ± 24.22 and 66 ± 27.85 μm, the morphology of both the composites seems to be similar showing the presence of equiaxed dendrites without the presence of secondary arms.

The growth of grains in both the composites is attributed to the reduction in number of active nucleants. However the increase in the fraction of TiB_2 particles which are found to be potent nucleants in the presence of alloying elements have contributed to the refinement of grains in both the composites. Compared to the unreinforced alloy, the processed composites show a significant reduction in the size of grain. The reduction in the size and morphology of the grains in composites has been caused by the presence of secondary particles like Al_3Ti, AlTiSi, AlB_2 and TiB_2. When Al_3Ti particles are present in the melt, during solidification the nucleation of aluminium requires little or no undercooling, indicating that Al_3Ti particles are better nucleant for aluminium [Marcantono and Mondolfo, 1971]. Davis et. al. have observed Al_3Ti particles with the grains, indicated that Al_3Ti as a good nucleant for aluminium [Davies et al., 1970].

In addition, Arnberg et al. and Kobyashi et al. have supported this view with evidence of existence of multiple orientation relationships between aluminium and Al_3Ti. The Al_3Ti phase is known to possess a greater number of planes having a good orientation relationship with aluminium. Kobyashinet al. revealed that, the most frequently measured orientation relationship was (1-1-1)Al//(11-2)Al_3Ti , [01-1]Al//[-110]Al_3Ti, which has a low disregistry between two lattices on the probable matching plane. This orientation relationship reduces the surface energy of the interface to

facilitate nucleation of α-aluminium [Arnberg et al., 1982]. When Ti is added to the Si based aluminium alloy, upon reaching the maximum solubility of 0.15% (Peritectic point) precipitation of Ti based particles occurs.

Observations in SEM micrographs confirmed the precipitation of AlTiSi particles along with Al_3Ti. The solubility of Si in Al_3Ti depends on the amount of Si present in the alloy. Kori et al. showed that the presence of AlTiSi particles in Al-Si alloys improved the grain refining efficiency upto 7wt.% of silicon and above the alloy showed poisoning effect [Kori et al., 2013]. Whilest Johnsson et al. observed that the growth of grains began to occur above 2-3wt.% of Si [Johnsson, 1994]. From the observations it is evident that AlTiSi based particles are potent nucleant for the refinement of grains. Hence with less than 1wt.% Si, the AlTiSi particles in the composite alloy were potent enough for the refinement of grains.

Other than Al_3Ti and AlTiSi particles, AlB_2 particles were also present in the alloy matrix (Fig.4.19). Studies indicate that AlB_2 is not an effective nucleant for the refinement of grains. Recently Zongning Chen et al. [Chen et al., 2016] showed that AlB_2 became potent nuclean agent under the presence of high Si. They also confirmed that, AlB_2 particles showed grain refining potency only when the Si present in the alloy was above 4wt.%. The present observation confirms that the grain refinement in composite processed at 15 and 30 min seems to occur due to the presence of both Al_3Ti and AlTiSi particles. Hence, the composite (15 min) with more number of these potent particles shows pronounced grain refinement than composite processed at 30 min.

With complete dissolution of Al_3Ti, AlB_2 and AlTiSi particles, composite processed at 45 & 60 min with the presence of only TiB_2 particles, also showed pounced reduction in grain size compared to the unreinforced alloy. In order to understand the grain refining efficiency in alloy systems, several mechanisms were proposed. In common, two mechanisms are widely accepted in grain refinement of aluminium alloys. The first mechanism states that grain refinement in aluminium alloys is caused by the presence of potent nucleating particles. The second mechanism that causes grain refinement results from the growth restriction factor (Q) instigated by

constitutional undercooling. Earlier studies suggested that TiB_2 is not an effective nucleant for aluminium [Iqbal et al., 2004].

Investigation on the influence of Si and Fe during the grain refinement of aluminium alloys, Johnsons found that besides the presence of nucleating particles, solutes present in the alloy showed substantial improvement in grain refinement. Furthermore the TiB_2 particles which was found to be an impotent nuclean particle in pure aluminium, showed good grain refining efficiency in aluminium alloys due to the presence of solute. Compared to the results shown in Fig. 4.14 (section 4.5.3) from the composite processed without the addition of alloying elements to that of the composites processed with the addition of alloying elements shown in Fig. 4.21 confirms that the reduction in size of grains is composite processed at 45 & 60 min is attributed to the potent TiB_2 present in the alloy matrix.

4.6.5 Mechanical properties

4.6.5.1 Hardness

Fig. 4.23 presents the plot of Vickers hardness results obtained from the composites processed at different melt holding time, casted after the addition of Mg to the composite melt. Compared to the unreinforced alloy, the composites processed at different holding times shows significant improvement in hardness values. The improvement in hardness of composites indicates that the addition of secondary particles enhances the hardness of unreinforced alloy.
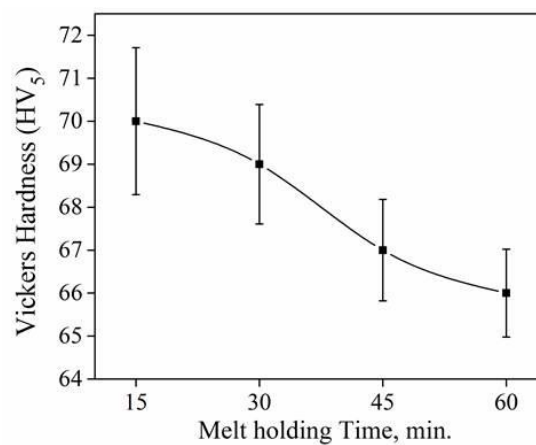
Fig. 4.23 Plot showing the variation of hardness in composites processed at different melt holding time after the addition of Mg.

The composite processed with a holding time of 15 min show a hardness value of 70 VHN. Compared to the unreinforced alloy the composite shows a 27% increase in hardness. Combined contribution of hardness values from individual Al_3Ti, $AlTiSi$, AlB_2 and TiB_2 particles present in the matrix alloy was responsible for the increase in hardness of composite. Composite processed with a holding time 30 min show a hardness value of 69 VHN. Although, no significant change in hardness value is seen between composites processed at 15 & 30 min, it is evident that the hardness of composite processed at 30 min has reduced compared to composite processed at 15 min.

At longer holding time the dissolution of Al_3Ti, AlB_2 and $AlTiSi$ particles occurs leading to the formation of TiB_2 particles. The dissolution of these particles has led to a minor decrease in the overall volume fraction of the particles in the matrix. Hence, the composite (30 min) showed a reduction in hardness. As the melt holding time was increased, composite processed at 45 & 60 min showed hardness values of 67 & 66 VHN respectively. The decrease in hardness of these composites is also attributed to the reduction in total volume fraction of the particles, which has occurred due to the complete dissolution of Al_3Ti, AlB_2 and $AlTiSi$ particles. Although it seems that, the dissolution of Al_3Ti, AlB_2 and $AlTiSi$ particles has led to the decrease in hardness of composites, no significant decrease in hardness is evident. Formation of hard TiB_2 particles in the alloy matrix, due to the dissolution of Al_3Ti, AlB_2 and $AlTiSi$, has compensated for the large reduction of hardness in composites processed at longer holding time of 45 and 60 min. Hence, no significant reduction in hardness is observed among composites. During Vickers hardness estimation, an indentation is created in the material by the application of known load with the use of an indenter. In order to obtain accurate results, during the indentation of particulate reinforced composites, the load must be large enough to create an indentation larger than the size and spacing between the particles.

Due to the indentation, the density of particles present under the indenter or in the area of indentation increases, compared to the area away from the indentation. Hence, in the area of indentation severe work hardening takes place. Compared to the unreinforced alloy, in composites severe work hardening occurs due to the presence

of particles. More work hardening tends to occur with more number of particles. Hence the composite (15 min) with more number of particles showed higher hardness. As the density of particles in composite reduced with increase in holding time, the hardness of the composite also deteriorated. The overall observation showed that, however, the composite showed variation in hardness, it is evident that change in hardness is not significant. Moreover the hardness of composites is much higher than the unreinforced alloy.

4.6.5.2 Tensile properties

Table 4.7 Tensile properties of as cast unreinforced alloy and composites processed at different melt holding time with the addition of Mg.

Melt holding Time (Min.)	Hardness (HV$_5$)	(0.2%)Y.S (MPa)	U.T.S (MPa)	% Elong.
0	55	128	172	8
15	70	158	214	9
30	69	160	217	9
45	67	163	222	10
60	66	167	225	12

The data (Youngs modulus, U.T.S and % Elongation) derived from the tensile curves obtained from the composite processed at different melt holding time, with the addition of alloying elements is shown in Table 4.7 and the corresponding SEM fractographs are shown in Fig. 4.19 (a-d). The values of Y.S and U.T.S of as cast composites are higher than the unreinforced alloy, implies that the increase in strength of alloy is achieved due to the addition of secondary particles.

Compared to unreinforced alloy, composite processed with a holding time of 15 min shows a 16% increase in Y.S and 24% in U.T.S values. As expected, the YS and UTS of the as cast composite processed at 15 min is found to be higher than the unreinforced alloy. Interestingly, %El. of the composite is also higher than the alloy. Composite processed with a holding time of 30 minutes shows a 17% increase in Y.S and 26% increase in U.T.S. Although the composites processed at were processed at

different holding times, no change in values of ductility is evident. As the melt holding time for the processing of the composites was increased to 45 and 60 min, the composite processed at 45 & 60 min show improvement in both Y.S and U.T.S values. It is interesting to note that the ductility of the composite also increased with holding time. The increase in ductility of composites is attributed to the absence of Al_3Ti particles at longer holding time.

Although the composites show a decrease in hardness with increase in melt holding time, increase in tensile strength of the composites is evident. The observation indicates that hardness and tensile properties of particulate reinforced composites are not interrelated. Yielding in composite depends on the interaction between reinforced particles and dislocations. Generally Orowan looping mechanism will be operate in composites having particles less than 1 μm, whereas in composites having particles larger than 1μm dislocation pile up mechanism will be operative [Lee et al., 1998]. Although the fraction of particles with size more than 3 μm are seen in composite processed with increase in holding time due to the dissolution of larger particles more of fine particles were formed in the matrix. Since the composite possessed both the sub-micron and micron size particles both the mechanism seems to operate. Hence, an increase in yield strength is seen in composites as the holding time was increased.

During tensile loading, the applied load is transferred from the matrix to the reinforcements. When the applied load on the particles becomes larger than the threshold limit of the particles, failure of composites occurs at particle/reinforcement interface due to poor bonding, or by the fracture of particles [Doel and Bowen, 1996]. Since the reinforced are processed by *in-situ* methods, the bonding between the particles and reinforcements is excellent. Hence, the processed composite would not have failed due to particle/reinforcement interface problems. The other possibility of failure of composite is by the fracture of particles.

Generally, presence of larger particles, which has more flaws than the smaller particles, will cause failure. Hence, due to the fracture of particles at lower applied stresses, the strength of material is reduced. The fracture of larger particles seen in the SEM fractographs (Fig. 4.21a&b) of composites (15 & 30 min) further supports the argument. Therefore, the composite (15 & 30 min) with the presence of larger

particles showed reduced strength compared to the composite processed at 60 min Addition to the reinforcements the matrix also plays an important role in strengthening of composites. Yielding of composite occurs with the yields of matrix material. From the experiments carried out in the previous section 4.5, it was understood that loss of alloying elements during the processing of composites has led to the deterioration of properties. During the processing of composites with the addition of alloying elements, thereby compensating the loss of alloying elements, the properties of the matrix has been restored. Hence, by improving the strength of the matrix alloy the overall strength of the composite has increased.
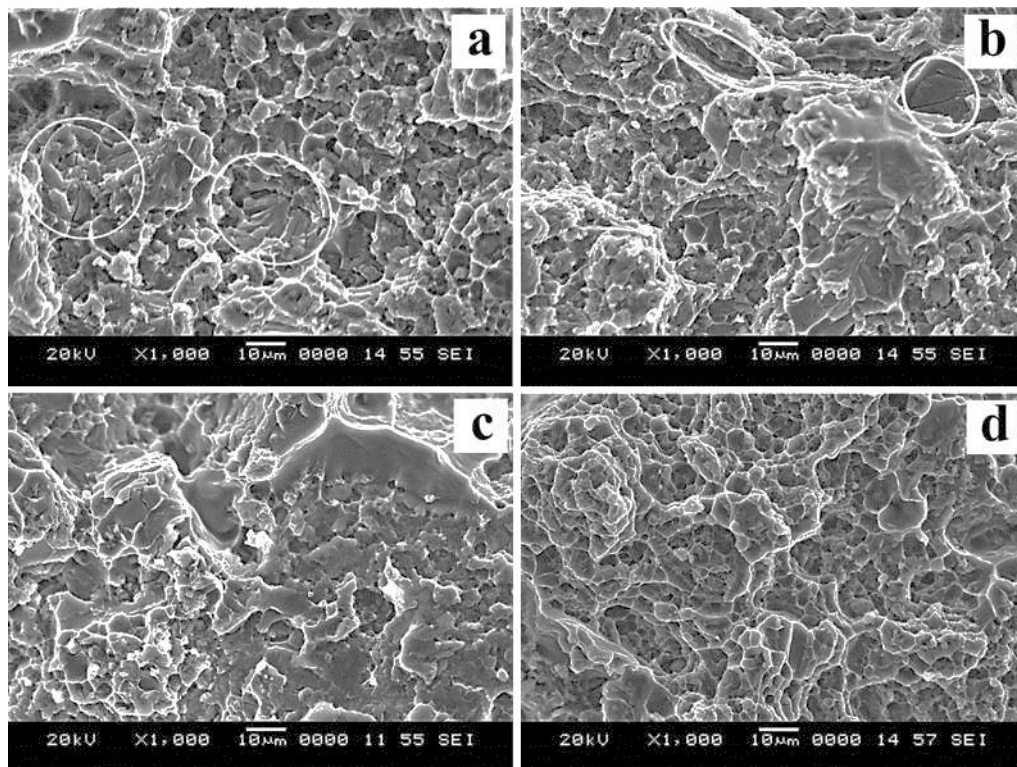
Fig.4.24 SEM (SE) images of tensile fracture surface of composite processed at different melt holding time with addition of Mg; (a) 15, (b) 30, (c) 45 and (d) 60 min.

The SEM (SE) photomicrographs of the tensile specimen fracture surface composite processed at different melt holding time casted after the addition of alloying elements is shown in Fig. 4.24 (a-d). The SEM fractographs of the composites bead distinctive evidence of ductile fracture with numerous dimples. Fracture of large AlTiSi and Al_3Ti particles that were present in composites is evident from the Fig.4.24a, whereas the smaller particles were found inside the dimples. Tensile values and the fracture

surface indicate that the composite has failed at lower stress due to the fracture of larger particles. Although the size of the larger particles in composite processed with 30 min is small compared to the particles in composite processed at 15 min, the presence of cracks in the particles indicate that the failure has occurred due to particle fracture. At longer holding time due to the increase in amount of TiB_2 particles drastic decrease in size of dimples is evident (Fig.4.24d).

4.6.6 Inference

Analysis of the results obtained from the composites processed at different melt holding time with the addition of alloying elements showed a substantial improvement in properties. During casting addition of alloying elements compensated its loss which occurred due to the addition of fluoride salts. Hence, during the development of *in-situ* Al-TiB_2 reinforced composites by FAS technique, especially when using alloys with Mg solutes as matrix, the loss of solute elements has to be compensated before casting. By compensating the properties of the matrix alloy is restored thereby improving the overall properties of the composites. Based on the above experience, the loss of alloying element in the matrix will be compensated before casting in all the fore-coming experiments.

4.7 Influence of melt holding temperature

4.7.1 DTA-TGA analysis

DTA and TG curve shown in Fig. 4.25 reveals the decomposition behavior of fluoride salts (K_2TiF_6 and KBF_4) with aluminium alloy, over the temperature range of 30 to 900ºC. From the obtained DTA curve it is evident that as the temperature increases, decomposition of salts with aluminium alloy has resulted in both endothermic and exothermic reactions. As the temperature increases the first endothermic peak was found to occur along the DTA curve at 286ºC. The formation of this peak is due to the endothermic reaction is caused by the polymorphic transformation of KBF_4 salts from orthorhombic to cubic crystal structure. The second endothermic peak observed at 397ºC indicates the removal of moisture from fluoride salts. The TG curve indicates that until the second endothermic reaction a weight loss of 1.2% in the sample was observed. This negligible weight loss in the sample has been caused by the

vaporization of volatile compound and moisture. Further heating leads to the formation of two exothermic peak at 480 and 533ºC respectively.
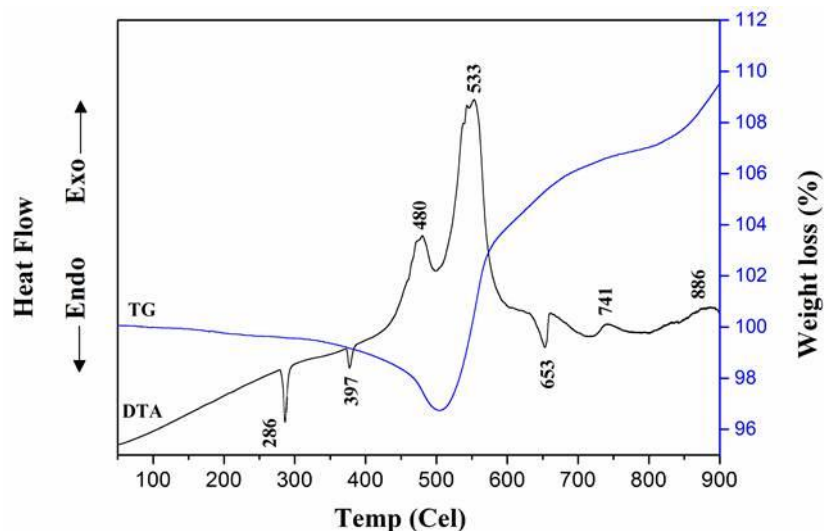
Fig.4.25 TG and DTA graph showing the thermal decomposition behavior of K_2TiF_6 and KBF_4 salts with aluminium alloy

The exothermic peak at 480ºC corresponds to the reaction of KBF_4 salt with aluminum alloy, whereas the peak present at 533ºC indicates the exothermic reaction caused between K_2TiF_6 salts and aluminium alloy. The exothermic reaction at these temperatures causes the dissociation of Ti and B from their respective salts. The exothermic peak at 480ºC confirms that the KBF_4 salts can react with aluminium below the melting point aluminium alloy, whereas the exothermic reaction of K_2TiF_6 with aluminium at 533ºC is an unexpected one. Both from Al-Ti phase diagram and experimental observations, it is evident that a minimum temperature of 728ºC is essential for the dissociation of Ti from K_2TiF_6 [Prasad, K.V.S. et al., 1996]. It should be noted that the minimum dissociation temperature that was found from the reaction of K_2TiF_6 with aluminium, where as in the present observations the dissociation temperature of K_2TiF_6 has reduced due to the presence of KBF_4 salts. Although the salts were added to aluminium alloy in the mixture form, the results indicate that they were found to react separately with aluminium alloy.

As the first exothermic reaction begins a weight loss of 2.5% in the sample is observed in the TG curve. At this temperature as, the salts begins to react with aluminium exothermically, gases such as BF_3 and TiF_4 formed during reduction of

111

salts could have caused the weight loss. But in real conditions this loss of BF_3 and TiF_4 gases is reduced by plunging the salts into the aluminium melt. Increase in weight of the sample can be seen as soon as the end of first exothermic reaction. This increase is weight has been caused by the nucleation of Al_3Ti and AlB_2 phases. Moreover, the K-Al-F slag formed during the reaction might be the cause for increase in weight of the sample. As the reaction between the salts and aluminium increases over the temperature range, the continuous increase in weight of the sample is observed. With further increase in temperature an endothermic peak is formed at 653°C. The formation of this endothermic peak corresponds to the melting of aluminium. Along the DTA curve a small exothermic peak is formed around 741ºC. This peak indicates the formation of Al_3Ti and AlB_2 phases in the aluminium alloy melt.

Although the dissociation of Ti and B were possible at 480°C and 533°C, the complete dissociation of salts seems to happen at 741°C in molten aluminium. At this temperature formation of TiB_2 occurs by the partial dissolution of Al_3Ti and AlB_2 phases. The presence of Al_3Ti, AlB_2 and TiB_2 peaks in the XRD pattern (Fig.4.26b) acquired from the composite prepared at 750°C confirms it. This interpretation is further confirmed by SEM micrographs shown in Fig.4.27a. The last exothermic peak at 886ºC in the DTA curve indicates the complete conversion of Al_3Ti and AlB_2 into TiB_2 according to the formula $Al_3Ti + AlB_2$ leads to the formation of TiB_2. The XRD pattern (Fig.4.26) and the SEM micrographs (Fig.4.27) obtained from the sample prepared at 850°C confirms that all the Al_3Ti and AlB_2 has completely transformed into TiB_2.

4.7.2 X-ray diffraction analysis

The phases present in the prepared composites at different holding temperatures was analysed using X-ray diffraction technique. The obtained XRD patterns from the unreinforced alloy and composites are shown in Fig.4.26 (a-e). From the Fig.4.26 (b-e), it can be seen that there is a significant change in the X-ray diffraction pattern over the different melt holding temperatures. The most important change observed among the diffractograms is the change in the peak intensities of different phases, which indicates the dissociation and formation of different phases in the matrix melt.

112

Indexing of the XRD pattern confirms the presence of Al_3Ti, AlB_2 and TiB_2 compound phases along with Al. The indexed patterns are in good agreement with the JCPDS card number for the phases Al_3Ti (65-4505), AlB_2 (89-3191) and TiB_2 (35-0741).
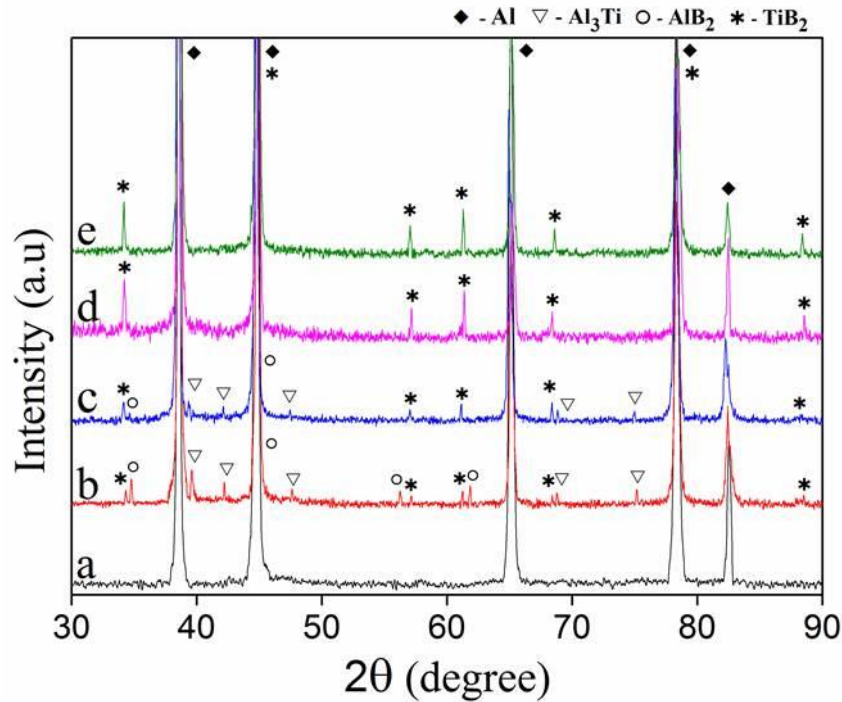
Fig. 4.26 (a-e) XRD patterns of in-situ $AA6082–5TiB_2$ composite produced at different holding temperatures: (a) AA6082, (b) 750, (c) 800, (d) 850 and (e) 900ºC

Fig.4.26b show the XRD pattern obtained from composite processed at a holding temperature of 750ºC. The phases present in the composite were found to be Al_3Ti, AlB_2, TiB_2 and Al. The relative intensities of Al_3Ti and AlB_2 are higher compared to TiB_2 phase, indicating that the presences of former particle phases in the composite matrix are higher. Indexing of the XRD pattern acquired from composite processed at 800°C also showed same phases as observed in composite processed at 750°C. However, the relative intensities of the Al_3Ti and AlB_2 phases on 800°C processed composite are found to be reduced compared to composite (750°C). Moreover, the intensity of TiB_2 peaks has increased. This suggests that at 800°C more reduction of Al_3Ti and AlB_2 phase has occurred leading to the formation of more TiB_2 particles in the matrix. Presence of Al_3Ti and AlB_2 peaks in composite (800°C) indicates that the

melt temperature is not sufficient to reduce these intermediate phases completely. Upon further increase of holding temperature, presence of only TiB_2 peaks in the XRD pattern of composite processed at 850 and 900°C (Fig.4.26 (d & e)) confirms the complete dissolution of Al_3Ti and AlB_2 leaving only TiB_2 particles in the matrix. From the diffractograms it is evident that increase in melt temperatures has induced vigorous exothermic reaction between the salts and the aluminium alloy melt which in turn caused the complete formation of TiB_2 particles in the melt by the dissociation of Ti and B from Al_3Ti and AlB_2 intermediate compounds.

4.7.3 Scanning electron microscopy
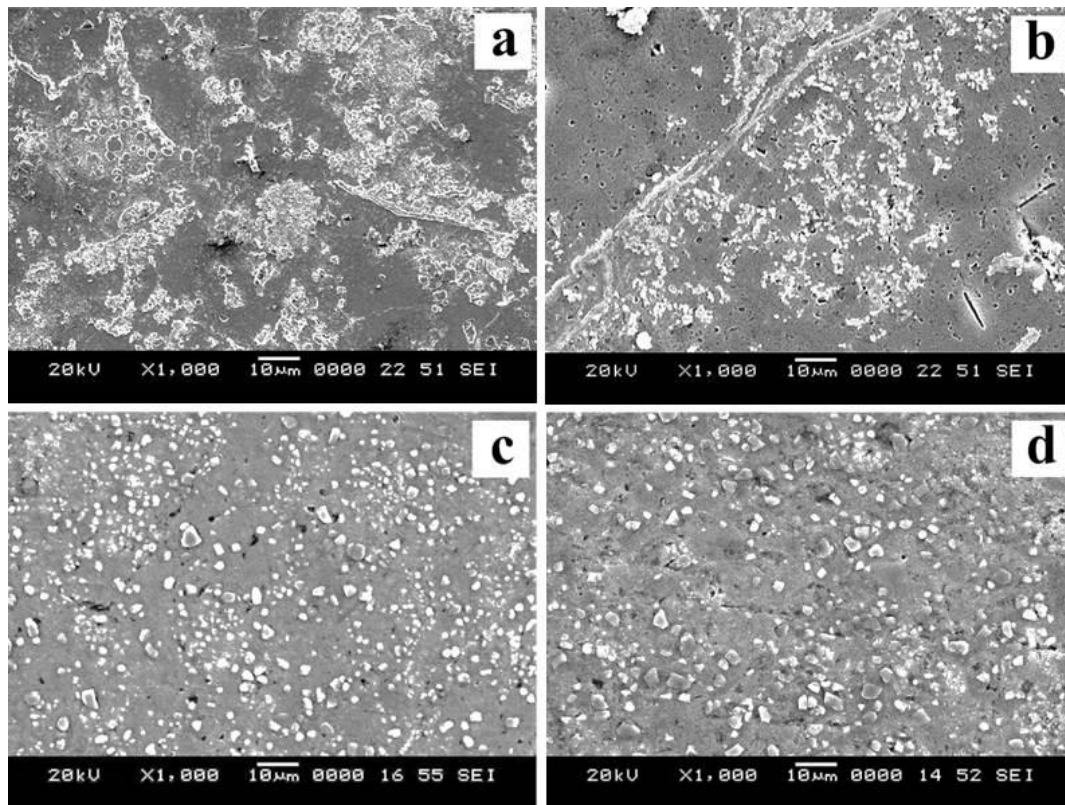
Fig. 4. 27 (a-d) SEM photomicrographs showing composites processed at different temperatures; (a) 750, (b) 800, (c) 850 and (d) 900°C.

SEM photomicrographs of composites prepared at different melt holding temperatures of 750, 800, 850 and 900ºC, at a constant time of 60 min is shown in Fig. 4.27. The SEM image (Fig.4.27a) acquired from sample prepared at 750ºC show the presence of particles with different morphology and size. The EDS spectrum (Fig.4.28b) obtained

from the elongated string like particles shows the presence of Si peak along with Al and Ti, confirming that they belonged to AlTiSi phase.

The fine blocky particles were found to be Al_3Ti particles (Fig.28c). The EDS spectrum obtained from other particles (Fig.4.28 d & e) confirms the presence of AlB_2 and TiB_2 particles in the matrix. The TiB_2 particles were seen to be very fine with sizes ranging from submicron to 1 μm. Moreover they were found to be agglomerated. It has been well established that when K_2TiF_6 and KBF_4 salts are added to aluminium melt, it is reduced to Ti and B. As the Ti and B exceed its solubility limit in aluminium, Al_3Ti and AlB_2 particle tends to precipitate. However, the formation of AlTiSi particle in the present investigation indicates that the Si present in aluminium alloy matrix has diffused into the binary Al_3Ti particle.

The diffusion of Si atoms into the Al_3Ti lattice has occurred by replacing some of the Al atoms with Si atoms, thereby changing the overall composition of the particle. Since the Si dissolution into the Al_3Ti lattice occurs over a wide range, hence it results in the formation of AlTiSi with different composition. Therefore, the particles are commonly referred to as AlTiSi intermetallic phase. Although it has been confirmed that the particles formed were AlTiSi from EDS microanalysis, it is interesting to note that the XRD spectrum obtained from 750°C processed composite (Fig.4.26b) did not reveal the presence of the AlTiSi phase. This indicates that the diffusion of Si into the Al_3Ti lattice is very less and it has not caused large enough distortion in the Al_3Ti lattice to be detected by XRD [Hoffmeyer and Perepezko, 1991].

Large AlTiSi and AlB_2 particles present in the matrix confirm the inadequacy of melt temperature needed for the complete transformation of these intermediate phases into TiB_2 particles. Fig.4.27b shows the SEM photomicrograph of composite prepared with a melt holding temperature of 800°C for 60 min. Particles present as long string were found to be Al_3Ti and the fine particles belong to TiB_2 phase. Unlike the AlTiSi particle observed in composite (750°C), presence of string like Al_3Ti particles in composite processed at 800°C indicates that the Si has diffused into the aluminium alloy matrix during the dissolution of Al_3Ti particles at this temperature range. Moreover, presence of more TiB_2 particles suggests that the dissolution of Al_3Ti particles at the temperature range of 800°C is higher compared to 750°C. Fine strings

of Al_3Ti phase in the matrix alloy indicate that, at this temperature range (800ºC) Al_3Ti phase has almost dissolved and transformed into fine TiB_2 particles.
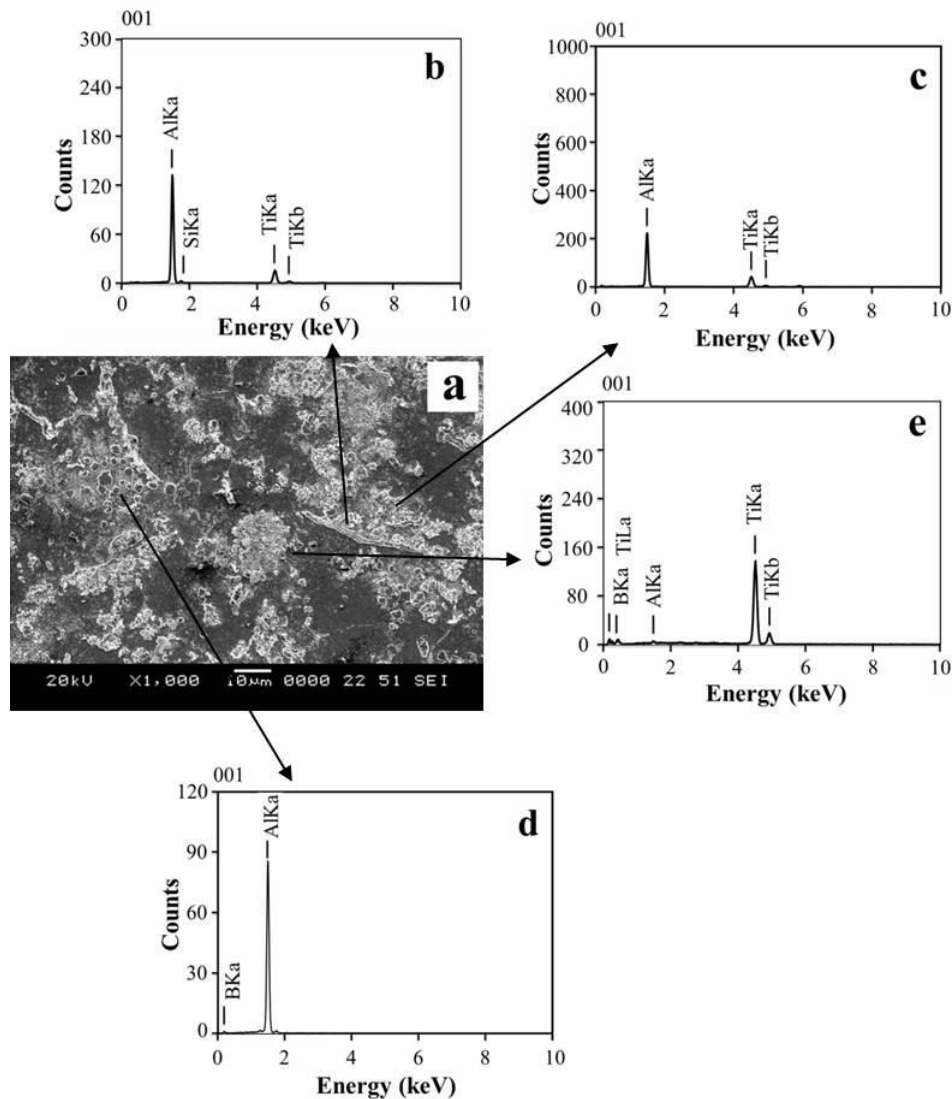
Fig. 4.28 (a-e) shows the SEM micrograph and EDS spectrum obtained from the particles; (a) SEM micrograph of as cast composite 15 min, EDS spectrum of (b) AlTiSi (c) Al_3Ti (d) AlB_2 and (e) TiB_2 particle

The results indicate that at higher temperatures Al_3Ti particles become much more unstable due to the movement of high amount of boron. Despite the higher amount of TiB_2 particles, presence of Al_3Ti particles in the matrix alloy indicates that the reaction is still incomplete at 800ºC.

Fig.4.27c show the presence of TiB_2 particles distributed homogeneously in the matrix of composite prepared at 850 and 900 ºC. Absence of Al_3Ti and AlB_2 particles indicates that the reaction between the Ti & B is complete, thereby leaving only TiB_2 particles in the matrix. The average size of the TiB_2 particles in the composite (850°C) was 2.5 and 2.7 μm in composite processed at 900°C. Although the fine particles in the composites showed hexagonal morphology, the larger particles were having irregular shape. This observation suggests that the change in temperature of melt does not have a big impact on the size of TiB_2 particles [Feng and Froyen, 2000].

4.7.4 Optical microscopy

Optical micrographs showing the microstructure of composites subjected to different melt holding temperatures of 750-900°C with increase in step of 50°C for a constant time of 60 min are presented in Fig.4.29 (a-d). The corresponding bar diagram showing the mean and standard deviation of the grains present in composite is shown in Fig.4.30. The composite processed at 750°C shows fine equiaxed grains having an average size of 34.69±17.22 μm. The fine size of grains is attributed to the presence of more number of aluminides (Fig.4.29a) in the alloy matrix. Incomplete reaction between the melt and the fluoride salts has led to the formation of Al_3Ti, AlTiSi particles in the matrix. During solidification presence of these potent nucleating particles induces high nucleation rate with leads to refinement of grains [Lu et al., 1997].

Increase in melt holding temperature results in the dissolution of more number of Al_3Ti, AlB_2 and AlTiSi particles, thereby reducing the grain refining efficiency. Hence, with increase in melt holding temperature from 750 to 800°C the grain size of composite increased to 38.62±15.15 μm. Although there is an increase in grain size of composite (800°C) compared to composite processed at 750°C is observed, the increase in grain size not significant because of the presence of potent aluminides. However as the holding temperature is further increased, complete dissolution of alumnides occur thereby leading to the presence of TiB_2 particles. When compared to Al_3Ti, the nucleating efficiency of TiB_2 particles is poorer. But with the presence of alloying elements or in the presence of excess Ti, TiB_2 particles were found to effective in grain refiners [Mohanty and Gruzesky, 1995]. Hence, even after the

complete dissolution of aluminides, significant change in the grain size (63.28±21.47 µm) is seen. However, the morphology of the grains has changed from equiaxed to rossetty. This change in morphology of the grains is due to the reduction in number of potent nucleants.
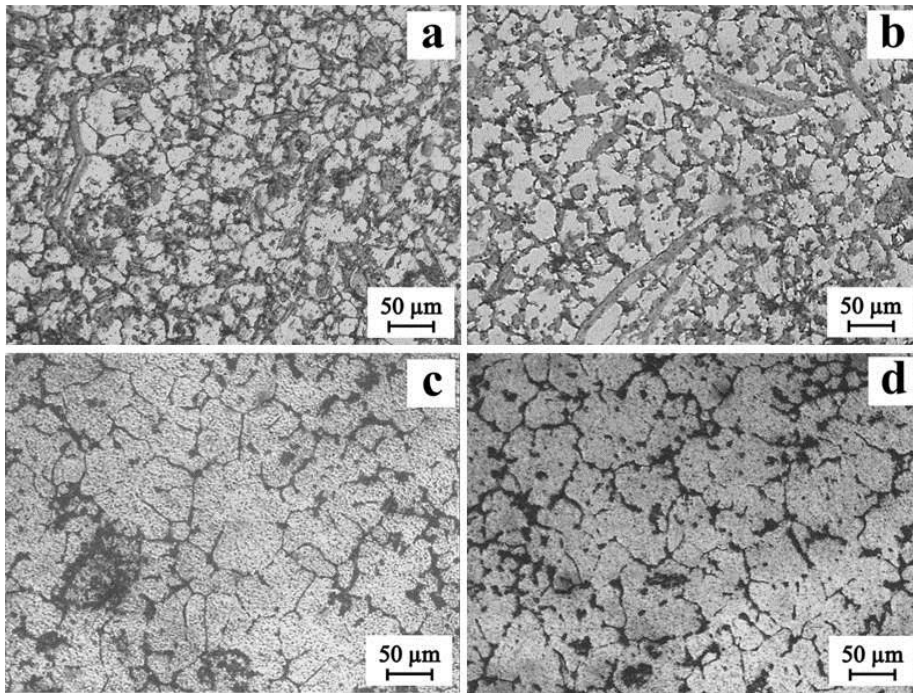
Fig.4.29 (a-d) Optical micrograph of as-cast composite processed at different melt holding temperatures ; (a) 750, (b) 800, (c) 850 and (d) 900°C.
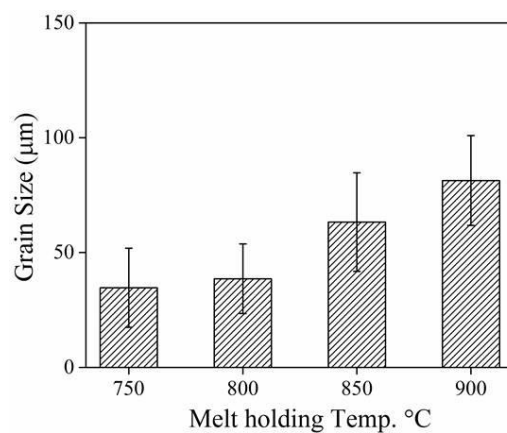
Fig. 4.30 Bar diagrams showing the mean grain size and standard deviation of the composite processed at different holding temperature.

As the holding temperature is further increased to 900°C the grain size of the composite was found to be 81.35±19.55 μm with rosette structure. Since both the composite processed at 850 and 900°C had almost equal weigh fraction (5wt.%) of TiB$_2$ particles no considerable change in grain size is observed in composite processed with 900°C.

4.7.5 Mechanical properties

4.7.5.1 Hardness
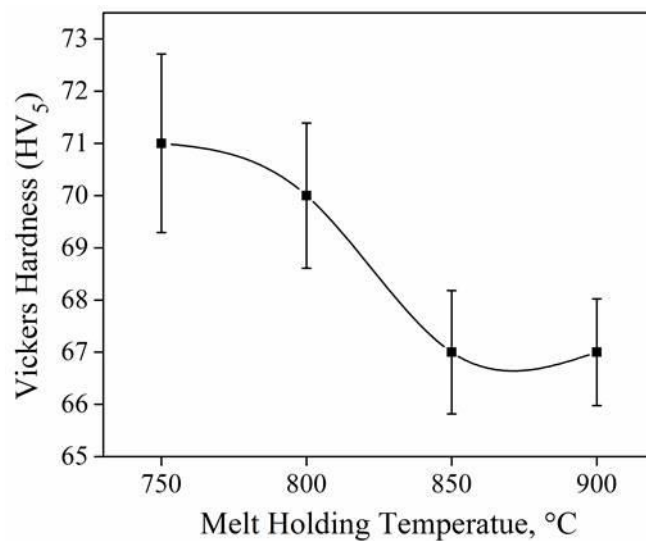
Fig.4.31 Plot showing the variation of hardness in composites processed at different melt holding temperature.

Fig.4.31 shows the plot of Vickers hardness results obtained from the composites processed at different melt holding temperature. The composites exhibits substantial improvement in hardness compared to the unreinforced alloys. Composite processed with 750°C show a hardness value of 73 VHN, with an increase of 33% in hardness compared to the unreinforced alloy. The increase in hardness is attributed to the presence of more weight fraction of particles (Al$_3$Ti, AlTiSi, AlB$_2$ and TiB$_2$) in the matrix. Composite processed with a holding temperature of 800°C show a hardness value of 70 VHN, which is 29% higher in hardness compared to the unreinforced alloy. The reduction in number of particle density had led to decrease in hardness of composite. Composite processed with 850 and 900°C showed a hardness value of 68 and 67 VHN respectively. Due to the presence of equal (5wt.%) fraction of TiB$_2$

119

particles in the composites no significant difference in hardness among these composite is seen. Decrease in density of particles has led to the significant decrease in hardness of composites. However, substantial decrease in hardness of composites is not evident among composite processed with 850 and 900°C, because of the formation of more TiB_2 particles in the matrix due to the dissolution of aluminides.

4.7.5.2 Tensile properties

Table 4.8 Tensile properties of as cast composites processed at different melt holding temperatures.

Melt holding Temp. (°C)	Hardness (HV_5)	(0.2%)Y.S (MPa)	U.T.S (MPa)	% Elong.
800	55	128	172	8
750	73	151	208	8
800	71	156	214	9
850	68	160	231	12
900	67	164	233	12

The data Yield streng (Y.S), Ultimate tensile strength (U.T.S) and % Elongation) derived from the tensile curves obtained from the composite processed at different melt holding temperature is shown in Table 4.8 and the corresponding SEM fractographs are shown in Fig. 4.27 (a-d). Compared to the unreinforced alloy the processed composite shows substantial improvements in tensile properties as a function of melt holding temperature. Composite processed with 750°C shows a 21% increase in U.T.S compared to the unreinforced alloy, whereas no improvements in ductility seen. The composite (800°C) shows a 24% increase in tensile strength and a 12.5% increase in ductility.

From Fig.4.27a it is evident that the more number of Al_3Ti particles in the form of string and blocks are present in both the 750 and 800°C processed composites. Moreover, the strength of secondary particles decides the strength of the composites. Generally, the presence of Al_3Ti particles will bring the strength of the composites [Tee et al., 1999]. Hence, due to the presence of more aluminides, the strength of the

composite has come down. With increase in temperature, composite (800°C) shows a significant strength in Y.S and U.T.S compared to composite processed at 750°C because of the reduction in number of aluminides and increase in number of TiB_2 particles. Moreover, with the increase of fine TiB_2 particles the ductility of the composite (800°C) is also improved 12.5%.
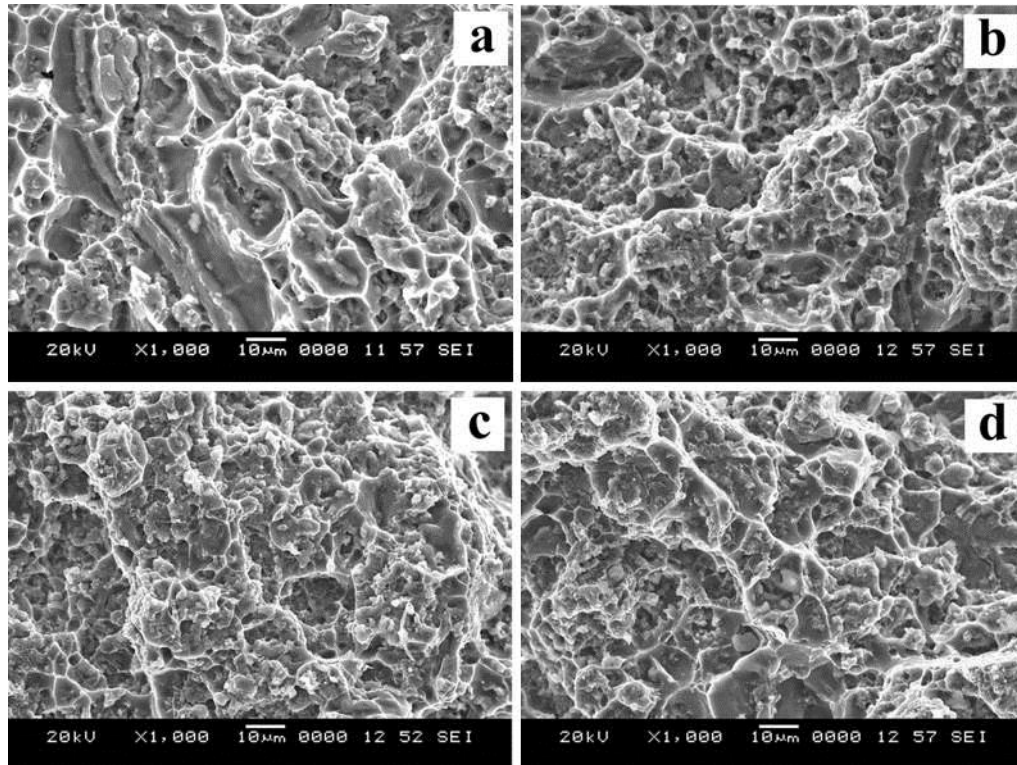
Fig.4.32 SEM (SE) images of tensile fracture surface of composite processed at different melt holding temperature; (a) 750, (b) 800, (c) 850 and (d) 900°C

Composite processed at 850 and 900°C shows a 34 and 35% increase in U.T.S and 50% increase in ductility. The increase in strength of composites processed at 850 and 900°C is attributed to the presence of fine TiB_2 particles. The absence of Al_3Ti particles has substantially improved the ductility of the composite.

The SEM (SE) photomicrographs of the tensile specimen fracture surface composite processed at different melt holding temperature is shown in Fig. 4.32(a-d). The SEM fractographs of the composites show distinctive evidence of ductile fracture with numerous dimples. Fracture surface of composite (750°C) shows the presence of large and fine dimples. The large dimples were caused by the AlTiSi particles, and the

small dimples were from the fine Al_3Ti and TiB_2 particles. This is in agreement with the SEM microstructure shown in Fig4.27a. With increase in melt holding temperature to 800°C, the size of Al_3Ti present in the fractograph has reduced indicating the dissolution of particles with time. Moreover, near to the long AlTiSi string like particle more fine dimples are present which indicates the presence of more TiB_2 particles. This fractograph is also in agreement with the SEM microstructure shown in Fig 4.27b. The fractograph obtained from composite (850°C) shows fine dimples, indicating the presence of only TiB_2 particles in the matrix. As the temperature was increase to 900°C composite showed a mixture of large and fine dimples. The presence of large dimples is caused due to the presence of large TiB_2 particles and the small dimples were due to the presence of fine TiB_2 particles. Overall observations on the fractographs confirm that the composites exhibit ductile mode of fracture.

4.7.6 Inference

From the obtained results it is evident that the melt holding temperature plays an important role during the development of *in-situ* composites. Inadequate (750ºC) and excess (900ºC) of melt temperatures seems to deteriorate the properties of the composites. The results indicate that 850ºC would be the apt melt temperature in order to prepare the *in-situ* AA6082-5TiB$_2$ composites.

4.8 Effect of (Ti:B) weight ratio during the processing of AA6082-5TiB$_2$ composites

For the processing of TiB_2 reinforced *in-situ* aluminium matrix composites, the most common method involves the addition of fluoride based K_2TiF_6 and KBF_4 salts salts to the aluminium melt. Upon the addition of the salts to the melt, TiB_2 reinforcements are formed in the melt depending on the control of processing parameters like melt holding time, melt holding temperature, melt stirring and stoichiometry of the fluoride salts. In spite of the control of these parameters, inadequate addition of these salt mixtures will lead to the formation of undesirable Al_3Ti and AlB_2 particles in the matrix along with TiB_2 particles. This is because, with the addition of excess of K_2TiF_6 salt to the stoichiometry mixture of K_2TiF_6 and KBF_4 salts more of Ti will be

introduced in the melt, resulting in the formation of Al_3Ti particle. When excess KBF_4 salts are added in excess to the melt, it will result in the formation of more AlB_2 particles in the melt. Results obtained from the experiments in previous section (4.4-4.7) indicate that there is always a deficiency of boron, in spite of adding the stoichimetrically weighed salts. Hence, a comprehensive understanding on the stoichiometric mixture of the fluoride salts added to the melt is very much essential for the processing of the TiB_2 reinforced aluminium matrix composites. Therefore in this section, experiments were carried out to understand the influence of adding excess B (different Ti:B ratio) to the AA6082 alloy melt, so as to prepare AA6082-5wt.%TiB_2 composites without the presence of the intermediate particles.

Table.4.9 Composition of starting mixtures with excess addition of KBF_4 salts to the stoichiometric mixtures of K_2TiF_6 and KBF_4 salts added to the alloy melt.

K_2TiF_6+KBF_4	Ti (wt.%)	B (wt.%)	Ti:B
Stoichiometry	35.54	64.45	0.551
10% KBF_4	33.46	66.53	0.503
20% KBF_4	31.48	68.51	0.459
30% KBF_4	29.78	70.21	0.424
40% KBF_4	28.40	71.59	0.396

The chemical composition of the K_2TiF_6 and KBF_4 salt mixtures added to the AA6082 alloy melt are shown in Table. 4.9. Composite processed with the addition of stochiometrically calculated and weighed K_2TiF_6 and KBF_4 salt mixture to the aluminium alloy melt is shown in table. With the addition of excess 10% KBF_4 salt to the stoichiometric salt mixture the second composite was prepared. Similarly, the third, fourth and fifth composite were prepared by the adding stoichiometrically weighed K_2TiF_6 and KBF_4 salt mixture with 20, 30 and 40% of excess KBF_4 salt to the alloy melt.

4.8.1 X-ray diffraction analysis

The XRD spectrum acquired from the composite processed with varying the quantity of B in Ti:B ratio by adding excess KBF_4 salt to the stoichiometric mixture of K_2TiF_6 and KBF_4 salts is shown in Fig. 4.33 (a-e). The XRD spectrum acquired from composite processed by the addition of calculated stoichiometric mixture of K_2TiF_6 and KBF_4 salt (Ti:B molar ratio of 0.551) is shown in Fig. 4.33a. The Ti:B ratio is greater than ½ indicating that more of Ti is added to the melt than B. Deficit of B in the melt led to the formation of more Al_3Ti particles in the matrix. Hence, Al_3Ti peaks with high intensities are observed in XRD spectrum of composite processed with stoichiometric ratio.
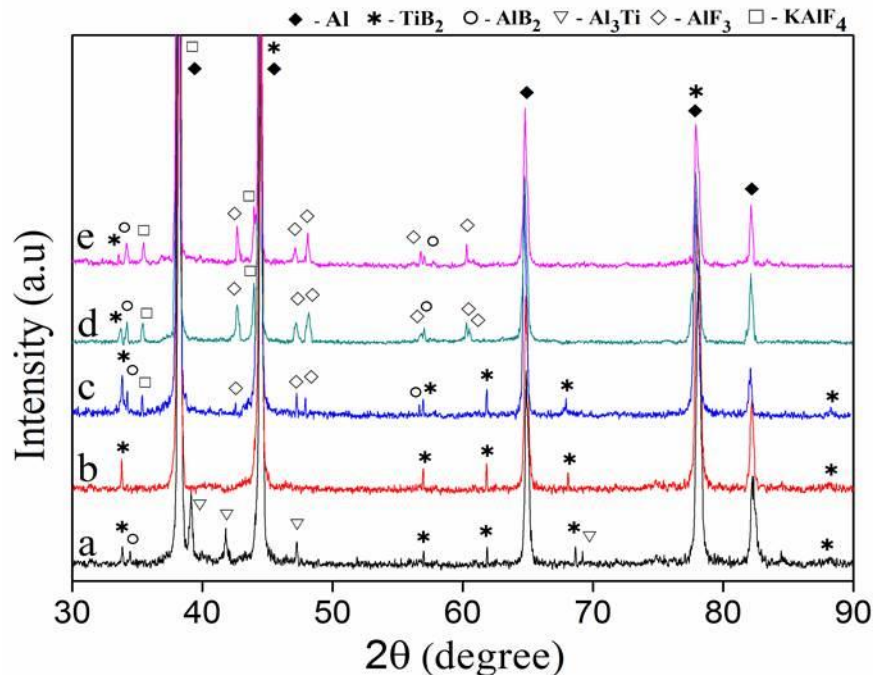
Fig. 4.33 (a-e) XRD patterns of composite processed by the addition of excess of KBF_4 salts to the stoichiometric mixture of K_2TiF_6 and KBF_4 salt: (a) stoichiometric, (b) 10, (c) 20, (d) 30 and (e) 40% KBF_4

The XRD spectrum obtained from second composite show the presence of only TiB_2 peaks, indicating the presence of only TiB_2 particles in the matrix. As the composition of B in the mixture of K_2TiF_6 and KBF_4 salts added to the melt was increased by adding 10wt.% of excess KBF_4 (Ti:B atomic ratio of 0.503, i.e when Ti:B ratio was equal to ½), the reaction between the salts and melt was complete leading to the

124

formation of only TiB_2 particles in the melt. The XRD pattern acquired from the composite processed by adding 20%KBF_4 salt to the stoichiometry mixture of K_2TiF_6 and KBF_4 salts (Ti:B atomic ratio of 0.459) is shown in Fig. 4.33c. Along with Al, peaks of TiB_2, AlB_2, AlF_3 and $KAlF_4$ are seen to be present in the spectrum. The presence of AlB_2 peaks indicates that due to the addition of more B, deprivation in Ti has occurred, thereby resulting AlB_2 particles.

The AlF_3 and $KAlF_4$ peaks in the spectrum were from the contamination caused by the slag present in melt. With further increase of B in the alloy melt by adding 30wt.% of excess KBF_4 salts (Ti:B atomic ratio 0.424) to the stoichiometric ration K_2TiF_6 and KBF_4 salts, the composite melt was contaminated with more slag inclusions. Hence, the XRD spectrum of composite with 20% excess KBF_4 shows the peaks of $KAlF_4$ and AlF_3 (Fig.4.33d) with higher intensities. Fig.4.33e shows the XRD spectrum acquired from composites processed by adding 40wt.% of excess KBF_4 salts (Ti:B atomic ratio 0.396) to the melt. Compared to the spectrum of composite processed with 20% excess KBF_4 noticeable increase in intensities of $KAlF_4$ and AlF_3 peaks observed in composite processed with 40% excess KBF_4 suggests that severe contamination of the composite melt has occurred due to the excess addition KBF_4 salts. This contamination of the melt has probably occurred due to the high viscosity of the melt cause by the excess addition of these fluoride salts.

4.8.2 Scanning electron microscopy

Fig.4.34 (a-e) shows the SEM photomicrographs obtained from the composites processed with the addition of excess KBF_4 salt to the stoichiometric mixture of K_2TiF_6 and KBF_4 salts. The SEM photomicrographs of composite processed with the calculated stoichiometric addition of K_2TiF_6 and KBF_4 salt is shown in Fig.4.34a. Three types of particles with different morphology is evident. The larger particles in light grey colour were found to belong to Al_3Ti (AlTiSi) phase. The smaller particles with size not more than 6 μm with blackish grey colour belonged to AlB_2 phase. The fine white contrasted particles with size not more than 2 μm were found to be TiB_2 particles. Although the fluoride salts were added according to the stoichiometry, calculations (Ti:B molar ration of 0.551) suggests that more of Ti was present in the melt. In other words, the Ti/B ratio was greater than ½, which has been found to be

cause for the formation of more Al$_3$Ti particles in the composite processed with stoichiometry salt mixture. With increase of boron content in the stoichiometric mixture by adding 10% excess of KBF$_4$, the SEM micrographs (Fig.4.34b) of composite shows the presence of TiB$_2$ particles in the matrix.
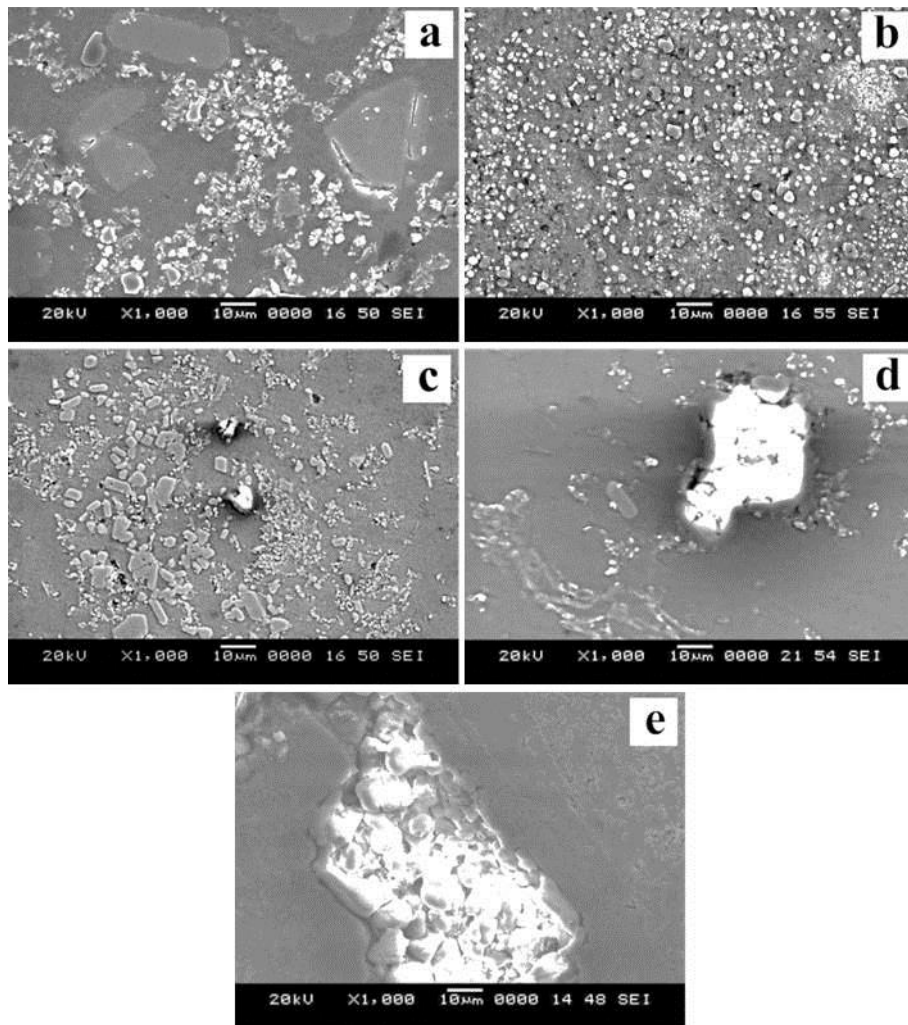
Fig. 4.34 SEM photomicrographs of composite processed by the addition of excess of KBF$_4$ salts to the stoichiometric mixture of K$_2$TiF$_6$ and KBF$_4$ salt: (a) Stoichiometric, (b) 10, (c) 20, (d) 30 and (e) 40 % KBF$_4$ salts

Addition of 10wt.% of excess KBF$_4$ salts introduces more of B into the melt to compensate the excess presence of Ti. Hence, by compensating the reduction of B in composite processed with 10% of excess KBF$_4$, the reaction between Ti and B is complete, leaving only TiB$_2$ particles in the matrix. Moreover, absence of Al$_3$Ti (AlTiSi) and AlB$_2$ particles in the matrix further confirms the above discussion.

126
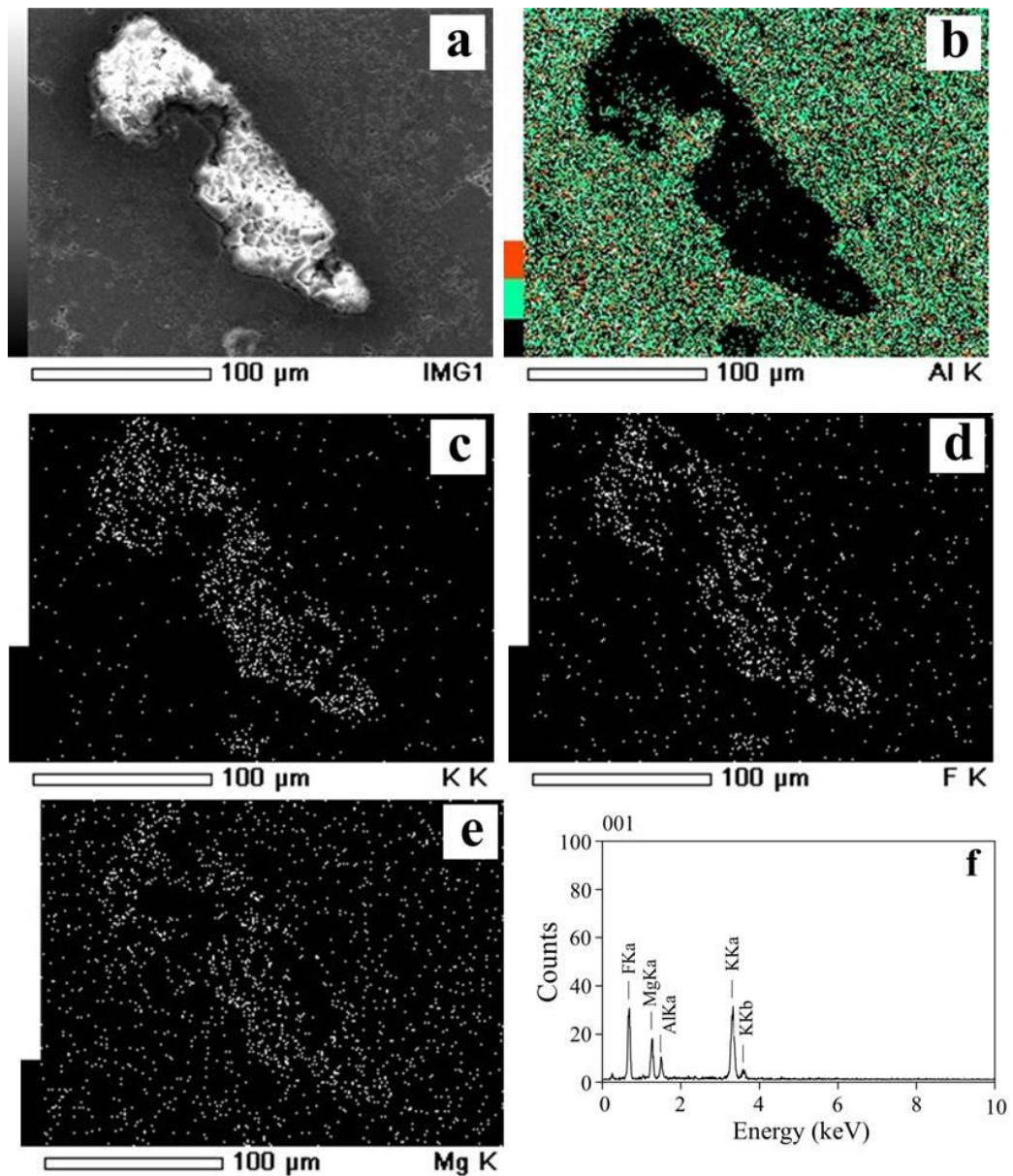
Fig.4.35 Composite processed by the addition of excess of KBF_4 salts to the stoichiometric mixture of K_2TiF_6 and KBF_4 salt: (a) SEM image, EDS map of (b) Al (c) K (d) F and (e) Mg and (f) EDS spectrum acquired from the slag.

Fig.4.34c shows the SEM photomicrographs of composite showing the presence of more AlB_2 along with TiB_2 particles. The average size of the TiB_2 particles were found to be less than 1μm, whereas the AlB_2 particles were present in size ranging from 3 to 9 μm. Addition of excess B to the melt than the stoichiometric proportions of Ti and B, has led formation of more AlB_2 particles. This is because, after the complete formation of TiB_2 particles, no Ti is left in the melt to further react with the

127

excess B. Hence, the boron will react with Al, thereby forming AlB_2 particles along with TiB_2 particles. From the SEM micrograph of composite processed with 30% excess KBF_4 salts, it is important to note the presence of slag in between the ceramic particles.

Addition of 30% excess KBF_4 not only resulted in formation of more AlB_2 particles, it also led to the rise of more AlF_3 and $KAlF_4$ slags in the matrix of composite processed with 30% excess KBF_4. Moreover, the AlB_2 and TiB_2 particles were present around the slag, which is evident from the SEM micrograph shown in Fig.4.34d. With an intention to further increase the B in the melt, addition of 40% excess KBF_4 salt to the stoichiometric mixture in the melt resulted in the formation of more AlF_3 and $KAlF_4$ slag. From the SEM micrograph (Fig.4.34e), the presence of AlB_2 particles around the slag indicates the formation of more AlB_2 particles in the melt due to excess addition of KBF_4 salts.

Observations on the micrograph indicate that addition of excess KBF_4 salts not only resulted in the formation of unwanted AlB_2 particles, it also caused the formation of more slag in the composite. SEM, EDS and elemental mapping on the slag present in the composite processed with 40% excess KBF_4 further confirms the presence K, Al, F and Mg elements in the slag. Absence of Ti and B in the slag further confirms that all the Ti present in the fluoride salts have been completely dissociated from the salts. With the addition of excess fluoride salts to the melt the viscosity of the melt is drastically increased, thereby trapping more of the slag. The increase in viscosity of the melt reduces its fluidity thus making pouring difficult.

The influence of Ti:B ratio on the grain of composites was analysed during the processing of composites by the adding excess KBF_4 salt to the stoichiometric K_2TIF_6 and KBF_4 mixture. Fig.4.36 (a-e) are optical micrographs showing the microstructure of composite processed by varying the boron in the melt by adding excess of KBF_4 salt to the stoichiometry mixture of K_2TiF_6 and KBF_4 mixture. It is obvious that an equiaxed grain structure has evolved in the composite (Fig.4.36a) from the dendritic structure of the unreinforced alloy. From the stoichiometric calculations shown in Table 4.8, it is evident that excess of Ti is fed into the melt than that of boron. Hence, Al_3Ti particles are also formed along with the TiB_2 particles. Due to the presence of

128

Al$_3$Ti particles nucleation of the aluminium grains is facilitated by peritectic reaction and hence grain refinement in the composite has occurred. Studies also confirm that this phenomenon can occur only under the presence of high Ti concentration in the melt. [Johnsson et al., 1993, Marcantonio and Monodolfo, 1971].

4.8.3 Optical microscopy
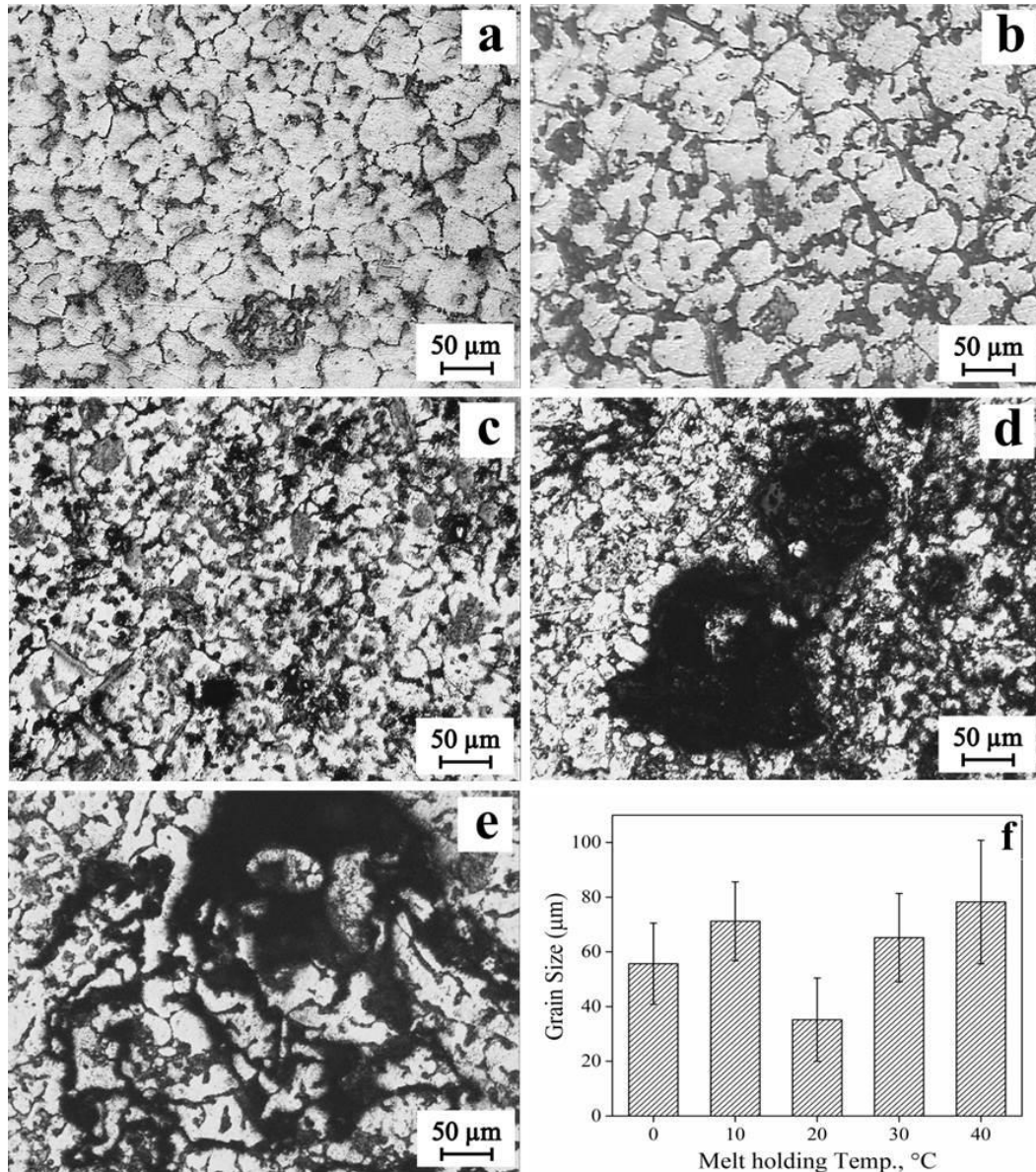
Fig.4.36 Optical micrograph and bar diagram of as cast composites processed with the addition of excess boron: (a) Stoichiometry, (b) 10, (c) 20, (d) 30 and (e) 40% KBF$_4$, (f) Bar diagram showing the average grain size of alloy and composite.

When 10% of excess KBF_4 was added to the melt along with the stoichiometric mixture, the excess boron reacted with the left out Al_3Ti and led to a complete formation of TiB_2 particles in the matrix. The morphology of the grains was found to be equiaxed with dendritic in nature. The absence of Al_3Ti particles has led to small increase in grain size (71.20± 16.42 µm) of composite processed with 10% excess KBF_4 compared to the grain size of composite with stoichiometric mixture (55.69± 14.82 µm). However, observations reveal that there is no significant increase in grain size of 10%KBF_4 as compared to that of stoichiometric mixture. Although, studies prove that TiB_2 is not an effective nucleant in pure aluminium [Iqbal et al., 2004] whereas, in alloys the potency of TiB_2 is improved by the presence of solute elements [Mohanty and Gurezleski, 1996]. Hence, even in the presence of TiB_2 particles the composite with 10% excess KBF_4 showed better grain refining efficiency.

The optical micrograph of composite processed by adding 20% of excess KBF_4 salt to the stoichiometry mixture is shown in Fig.4.36c. The average size of the grains was found to be 35.22± 15.22 µm. With the addition of excess KBF_4 salts more of boron is introduced into the melt which leads to the formation of AlB_2 along with TiB_2 particles. The fraction of particles in the matrix alloy becomes higher, moreover in the presence of solutes; the potency of AlB_2 particles is also improved[Lu et al., 1981]. Hence the composite with 20% excess KBF_4 show fine grains than 10% excess KBF_4. The dark black contrasted regions in the micrograph correspond to the slag, which has got entrapped between the dendrites.

Fig. 4.36d shows the optical micrograph of composite processed by adding 30% of excess KBF_4 to the stoichiometric mixture. With excess addition of KBF_4 salts more of slag is entrapped into the melt, thereby contaminating the melt. Although the average size of grains in composite was found to be 65.21±16.14 µm, very fine grains with size of 25 µm are present. The fine size of grain near the slag was due to the presence of large number of AlB_2 and TiB_2 particles near the slag and this is evident in Fig. 4.34d. As the KBF_4 added to the melt was increase to 40wt.% more of slag is seen to be entrapped in the matrix. Moreover the size of the grains in composite processed with 30% excess KBF_4 was found to be 78.24±22.57 µm. With the increase in addition of KBF_4 salt to the melt, the viscosity of the melt also increased.

As the viscosity of the composite melt increased pouring became difficult. From the micrographs of composite processed with 20-40%KBF$_4$, it is evident that as the slag in the melt increase, poisoning began to occur. The presence of slag reduces the potency of the boride particles, which leads to the reduction in number of nucleation sites thereby increasing the grain size. However, the in spite of the presence of slag, composites processed with 20-40%KBF$_4$ showed better grain refining efficiency because of the presence of more weight fraction of AlB$_2$ and TiB$_2$ particles.

4.8.4 Mechanical properties

4.8.4.1 Hardness

Plot showing the Vickers hardness results obtained from the composites processed with addition of excess KBF$_4$ salts to the stoichiometric K$_2$TiF$_6$ and KBF$_4$ salt mixture is presented in Fig.4.37. Among the processed composites, composite processed with the stoichiometric mixture showed a hardness of 65 VHN.
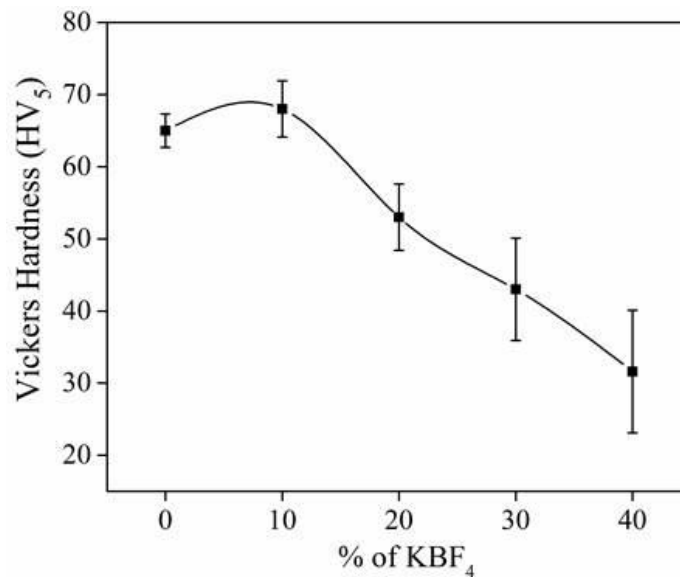
Fig.4.37 Plot showing the variation of hardness in composite processed with addition of excess KBF$_4$ salts to the stoichiometric K$_2$TiF$_6$ and KBF$_4$ salt mixture.

The addition of secondary particles has improved the hardness of the matrix. Although the composite showed increase in hardness when compared with unreinforced alloy, its hardness is inferior to the hardness of composite processed with 10% excess KBF$_4$. This is because of the presence of Al$_3$Ti particles in the

matrix, which indicates the reaction is incomplete. Complete transformation of Al_3Ti particles to TiB_2 particles has occurred in composite with 10% excess KBF_4, leaving only TiB_2 particles with size ranging from nanometre to 3 μm. With the presence of hard TiB_2 particles the composite with 10% excess of KBF_4 showed a hardness value of 68 VHN. During hardness testing, an indentation is created, which causes a high concentration of severe plastic flow in that region.

Due to indentation, the density of particles under the indentation increases thereby providing more resistance for further occurrence of indentation. Hence an increase in hardness is seen in composite with 10% excess KBF_4. Composite processed with 20% of excess KBF_4 showed a hardness of 53 VHN. The hardness of the composites was lesser than the unreinforced alloy. As the addition of KBF_4 was further increased to 30 and 40% in fourth and fifth castings, the hardness of the composites reduced drastically. The reduction in hardness is attributed to the entrainment of slag in the composites. From the SEM (Fig.4.34) and OM (4.36) it is evident that with increase in addition of KBF_4 salts, the entrapment of slag in the composite increases. The presence of slag in the matrix alloy has impaired the hardness of the composite. The increase in the dimension of indentation of composites during harness testing, further confirms that due to the addition of more KBF_4 salts, the melt is contaminated by slag due to which the hardness of the composite is reduced.

4.8.4.2 Tensile properties

The tensile properties of as-cast unreinforced alloy and composites processed by varying the stoichiometry of K_2TIF_6 and KBF_4 salt mixture by adding excess of KBF_4 salts is shown in Table.4.10. The composite processed with the stoichiometric ratio of K_2TiF_6 and KBF_4 salts shows a yield strength of 152 MPa, an ultimate tensile strength of 191 MPa and a 10% elongation respectively, which are 19%, 11% and 13% higher than the unreinforced alloy. The increase of tensile strength and elongation is seen in composite compared to the unreinforced alloy. The increase in tensile strength is attributed to the addition of secondary particles. However the strength of composite processed with stoichiometric salts addition is found to be inferior to composite processed with 10% excess KBF_4 salts. This is due to the presence of Al_3Ti particles

132

in the matrix. Moreover the ductility of the composite is also reduced by the presence of these intermediate Al_3Ti particles [Zongy et al., 1993].

Table 4.10 Tensile properties of as cast unreinforced alloy and composites processed with the excess addition of KBF_4 salt to stoichiometric mixture of K_2TiF_6 and KBF_4 salts.

% of KBF_4 added	Hardness (HV_5)	(0.2%)Y.S (MPa)	U.T.S (MPa)	% Elong.
AA6082	55	128	172	8
Stoichiometry (0)	65	152	191	10
10	68	161	219	11
20	53	132	158	7
30	43	-	-	-
40	32	-	-	-

Composite processed with 10% excess KBF_4 salts shows a 26% increase in yield stress and 27% increase in ultimate tensile strength. The % elongation of the composites is also increases by 38%. The increase in tensile properties of composite is attributed to the decrease in grain size and presence of fine TiB_2 particles in the matrix. Moreover due to the *in-situ* processing method, the wetting between the matrix and reinforcements is excellent, leading to better strength and elongation of composite.

The composite processed with 20% excess KBF_4 shows a decrease in tensile properties. Compared to the unreinforced alloy, the composite processed with 20% excess KBF_4 salts showed a 3% increase in yield, -8% decreases in UTS and -13% decrease in elongation. During the addition excess KBF_4 salts to the melt, the slag is trapped between the interdendritic regions as evident from the corresponding optical micrograph shown in Fig. 4.36c. Hence when load is applied cracks are formed in the region where inclusions are present. Although the composite was able to withstand a minimum load, showing a 3% increase in yield, the material failed abruptly at lower loads. With further increase in addition of KBF_4 to 30 and 40% to the stoichiometric mixture, the composite failed before yielding, due to the presence of more slag.

Fig. 4.38 (a-e) shows the fracture surface of the tensile specimen from the processed composites with varying % of KBF_4 salts. Fig.4.38a shows the typical fracture surface of composite processed with stroichiometric ration of K_2TiF_6 and KBF_4 salts. The presence of both fine and large dimples suggests that the fracture is ductile in nature. Large AlTiSi particles are seen in the cleavage indicating that during the tensile loading the cracks have propagated through these brittle particles leading to a decrease in strength.
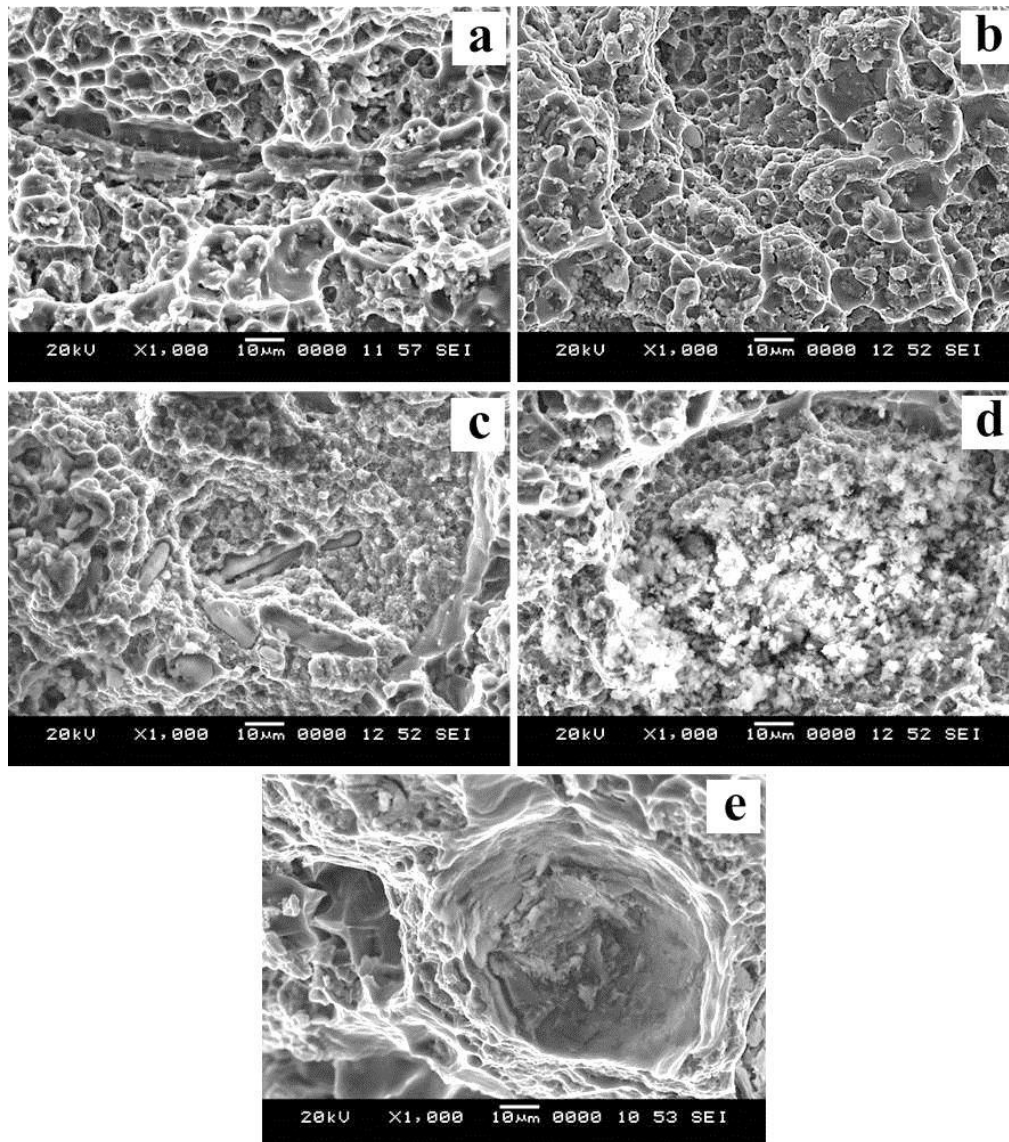
Fig.4.38. SEM fractographs showing the tensile fracture surfaces of composite processed with addition of excess KBF_4 salts to the stoichiometric K_2TiF_6 and KBF_4 salt mixture: (a) stoichiometric, (b) 10, (c) 20, (d) 30 and (e) 40% KBF_4

134

Absence of these AlTiSi particles is evident in the fracture surface of composite processed with 10% excess KBF$_4$ salts. Hence only fine dimples indicating that the mode of fracture was ductile in nature. Since the interfacial strength between the matrix and reinforcements are strong, because of the in-situ processing, the applied load is easily transferred to the strong reinforcements. Hence the tensile strength is substantially improved in composite processed with 10% excess KBF$_4$.

The presence of particles inside the dimples present in the fracture surface further supports it. The fracture surface of composite processed with 20% excess KBF$_4$ salts shows that the fracture has occurred around the agglomerations of TiB$_2$ particles. From the micrograph the presence of slag is also evident in between the agglomerations. This is support with the SEM micrographs shown in Fig. 4.34c. It is very much evident that the reduction in strength of composites is due to the presence of slag and agglomeration in the matrix.

The composite processed with 30% excess KBF$_4$ salts shows the presence of more slag clustered in the fracture surface. The presence of these clusters of slags causes poor wetting and are found to be source for crack nucleation and growth thereby reducing the strength of composite. Composite processed with 40% excess KBF$_4$ salts show deep craters with the presence of slag in it. The hollow region indicates the place where the slag were presence, and once after the test, due to the poor wetting nature it seems most of them has fallen out.

4.8.5 Inference

The Experiments indicate that the composite processed with the exact stoichiometric proportions, had both Al$_3$Ti and AlB$_2$ particles. Investigations revealed the deficiency of boron caused the formation of Al$_3$Ti particles. Hence the boron content in the melt was increased by adding excess of KBF$_4$ salts to the melt. The presence of Al$_3$Ti particles in the matrix reduced the overall properties of the composite. Adding 10% of excess KBF$_4$ to the mixture of K$_2$TiF$_6$ and KBF$_4$ mixture showed fruitful results. Due to the excess addition of boron, the composite was reinforced with only TiB$_2$ particles. The formation of TiB$_2$ particles and the absence of Al$_3$Ti particles in matrix improved the properties of the composites processed with 10% excess of KBF$_4$. Addition of 20, 30 and 40% of not only contaminated the melt with slag; it also

caused the deterioration in properties of the composites. Hence from the investigations it is clear that 10% of excess KBF_4 salts should be added to the stoichiometric mixture of K_2TiF_6 and KBF_4 salts to avoid the formation of the unwanted Al_3Ti particles in the composites, thereby resulting in the complete formation of TiB_2 particles in the matrix.

4.9 Influence of intermittent stirring time interval

Since the development of composites by liquid metallurgy technique, stirring of the melt has been an inherent processing parameter. During the ex-situ composite processing, stirring was employed to reduce the agglomeration of particles thereby improving its dispersion and to avoid the settling of reinforcement particles. Generally high speed of stirring using motor is carried out during the processing of composite. In the recently developed in-situ processing methods also stirring is employed. Unlike the ex-situ processing technique where a motor is used for the stirring of melt, in the in-situ techniques manual stirring is used. Since a strong exothermic reaction occurs between the melt and the added salts, severe stirring is unnecessary. Hence during the processing of in-situ composites, the composite melt is stirred intermittently at regular intervals in order to facilitate the exothermic reaction and to avoid the settling of reinforcement. Although stirring is important processing parameter for the development of composites, less emphasis has been given to it. Therefore, investigation on the influence of intermittent stirring at different time interval is carried out.

4.9.1 X-ray diffraction analysis

The XRD diffractograms acquired from the composites prepared at different intermittent stirring time interval is shown in Fig.4.39. The XRD spectrum obtained from composite processed at 5 min of stirring interval is shown in Fig.4.39a. Upon indexing the spectrum, it is confirmed that, three types of particles Al_3Ti (AlTiSi), AlB_2 and TiB_2 existed in the matrix alloy. This indicates that during the processing of composite, 5 min of intermittent stirring hindered the reaction occurring between the salts and melt.
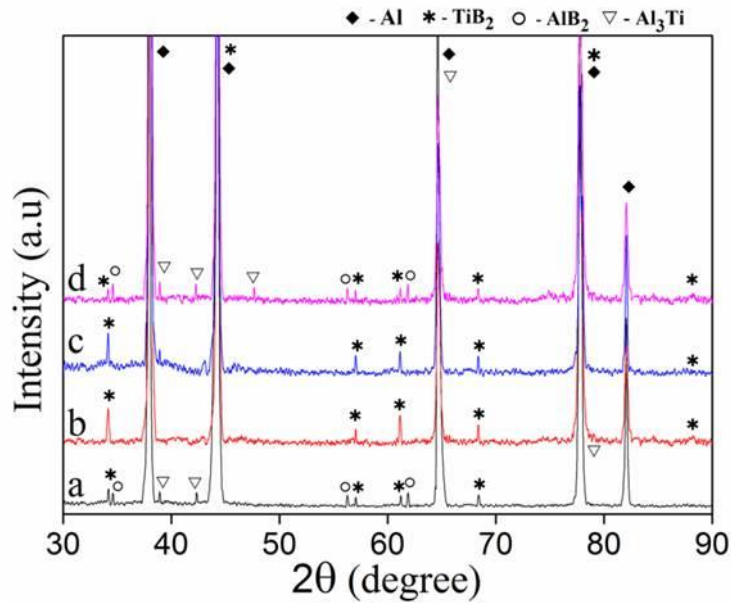
Fig.4.39 XRD spectrum acquired from composite processed at different time intervals of intermittent stirring; (a) 5, (b) 8, (c) 10 and (d) 15 min.

The incomplete reaction between the salts and melt led to the presence of these intermetallic particles. As the intermittent stirring time interval was increased to 8 min., the reaction between the salts seems to be complete, thereby leaving only TiB_2 particles in the melt. Hence the XRD spectrum of composite processed at 8 min (Fig.4.39b) shows the presence of only TiB_2 peaks. The spectrum acquired from composite processed with a stirring time interval of 10 min is shown in Fig.4.39c. The presence of TiB_2 peaks along with Al is evident. From the results it is evident that even 10 min of intermittent stirring interval is good enough for the processing of composites.

Formation of TiB_2 particles in the composite processed at 8 and 10 min, suggests that this stirring time interval, was sufficient enough for the reaction to be complete, leaving only TiB_2 particles in the matrix alloy. The XRD spectrum showing the composite processed with a stirring time interval of 15 min is shown in Fig. 4.39d. The presence of Al_3Ti (AlTiSi) and AlB_2 peaks along with TiB_2 peaks confirm the reaction is incomplete. During intermittent stirring, the reaction between the salt and melt is initiated which causes dissociation of intermetallic particles and leads to the formation of TiB_2 particles. Hence when the melt is stirred at longer stirring time

intervals, reduction in exothermic reaction occurs which is the cause for the formation of intermetallic particles along with TiB_2.

4.9.2 Scanning electron microscopy

Fig. 4.40 (a-d) SEM micrographs showing the composite processed at different intermittent stirring time interval: (a) 5, (b) 8, (c) 10 and (d) 15 min.

Fig. 4.40 (a-d) shows the scanning electron micrographs acquired from composites processed at different intervals of intermittent melt stirring. The micrograph of composite processed with a 5 min of stirring at regular intervals shows the presence of blocky and flaky particles with different sizes.

The EDS spectrum obtained on these particles confirm that the particles with blocky morphology were found to be AlB_2 and with flaky morphology were found to be AlTiSi. The fine particles with the size less than 3µm were found to be TiB_2 particles. When the melt is stirred at regular intervals of 5 min, sufficient time for the dissociation of the intermetallic particles to form into TiB_2 is hindered. This therefore leads to the existence of intermetallic AlTiSi and AlB_2 particles in the matrix alloy,

than the intended TiB_2 particles. Larger cracks seen on the Al_3Ti particles suggest that the diffusion of boron has occurred. This is in accordance with the results obtained by emamy et. al. [Emamy et al., 2006]. Quantative analysis on the flaky particles reveals that along with Al and Ti small amount of Si was also present. This is due to the diffusion of Si into the Al_3Ti lattice thereby occupying some of the Al lattice.

SEM photomicrograph of composite processed with an interval of 8 min stirring is shown in Fig. 4.40b. The composite showed homogeneous distribution of TiB_2 particles in the alloy matrix. The TiB_2 particles present in the matrix were of size ranging from few nanometers to 5 μm. It seems that stirring of the melt at regular intervals of 8 min gave sufficient time for the reaction to complete. This led to the dissociation of AlTiSi and AlB_2 particles thereby leaving only TiB_2 particles in the matrix. As the stirring time interval was increased to 10 min, the composite also showed the complete formation of TiB_2 particles (Fig.4.40c). Absence of AlTiSi and AlB_2 particles indicate that the even with stirring time of 10 min, complete formation of TiB_2 particles in the matrix can be achieved. However, mild agglomerations of TiB_2 seen in the micrograph of composite suggest that 10 min of stirring interval may not be suitable enough for the processing of composites.

When the melt stirring time interval was increased to 15 min, presence of AlTiSi, AlB_2 and TiB_2 particles in the matrix suggest the occurrence of incomplete reaction in composite processed at 15 min (Fig.4.40d). The AlTiSi phase was present as strings; AlB_2 and TiB_2 were seen to be agglomerated together. Although it was assumed that longer stirring time interval would yield the formation of only TiB_2 particles, the obtained results were found to be contrary. Experience indicates that intermittent stirring not only helps in dispersing the particles, it also aids in the acceleration of the reaction kinetics. Hence at longer stirring time interval the acceleration of the reaction kinetics caused by stirring is reduced thereby yielding the formation of AlTiSi and AlB_2 particles along with the TiB_2 particles. Moreover due to the longer stirring duration agglomeration of particles tends to occur, which is evident in Fig.4.40d. The overall results indicate that an interval of 8 min of intermittent stirring is the most suitable for the processing of *in-situ* TiB_2 reinforced composites using FAS technique.

4.9.3 Optical microscopy

Optical micrograph showing the grain structure obtained from as-cast composite processed at different interval of melt stirring is shown in Fig. 4.41 (a-d). It is well known that the addition of secondary particles aids in the refinement of grains in alloys. Fig.4.41a shows the bar diagram representing the mean and standard deviation of grains as measured from the composites. The composite processed with an intermittent melt stirring interval of 5 min shows fine equiaxed grain structure with an average grain size of 38.69±14.82 μm.

The drastic change in morphology and in size of grains compared to the unreinforced alloy is attributed to the combined effect of potent nucleating particles (AlTiSi, AlB$_2$ and TiB$_2$) present in the matrix. Short intermittent stirring interval was found to be the cause for the existence of both intermediate intermetallic and TiB$_2$ particles in the matrix. The intermetallic particles seem to disappear from the matrix due to the complete formation TiB$_2$ in the matrix and hence a small increment in size of grains (64.53±10.15 μm) as seen in the optical micrograph of composite processed at 8 min. which is shown in Fig. 4.41b. No drastic change in size of grains is evident; this is because the potency of TiB$_2$ particles is improved in the presence of solute elements present in the matrix alloy [Birol, 2013].

Fig. 4.41c shows the optical micrograph obtained from the composite processed with an intermittent melt stirring interval of 10 min. The size of the grains was found to be 67.22±18.22 μm with equiaxed morphology. No significant difference in size of grains and morphology is seen in composite processed at 8 and 10 min. As the stirring interval was further increased to 15 min during the processing of composite, reduction in size of grains seems to occur in composite compared to the composite processed at 8 and 10 min. The presences of potent nucleating particles such as AlTiSi and AlB$_2$ along with TiB$_2$ particles were found to be the cause for the grain refinement in composite processed at 15 min. Stirring at long time interval of 15 min caused the formation of the intermediate particles which led to pronounced grain refinement composite processed at 15 min. The pronounced standard deviation (Fig.4.42) indicates that the grain size of the composite was scattered.

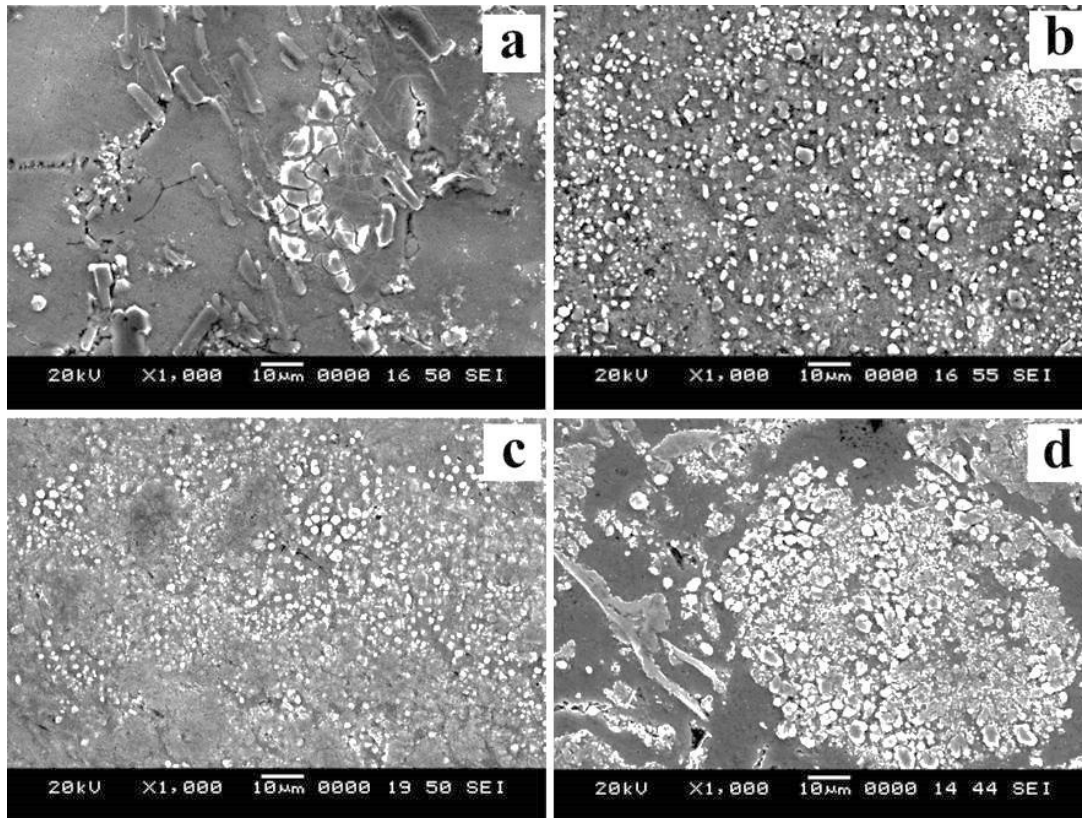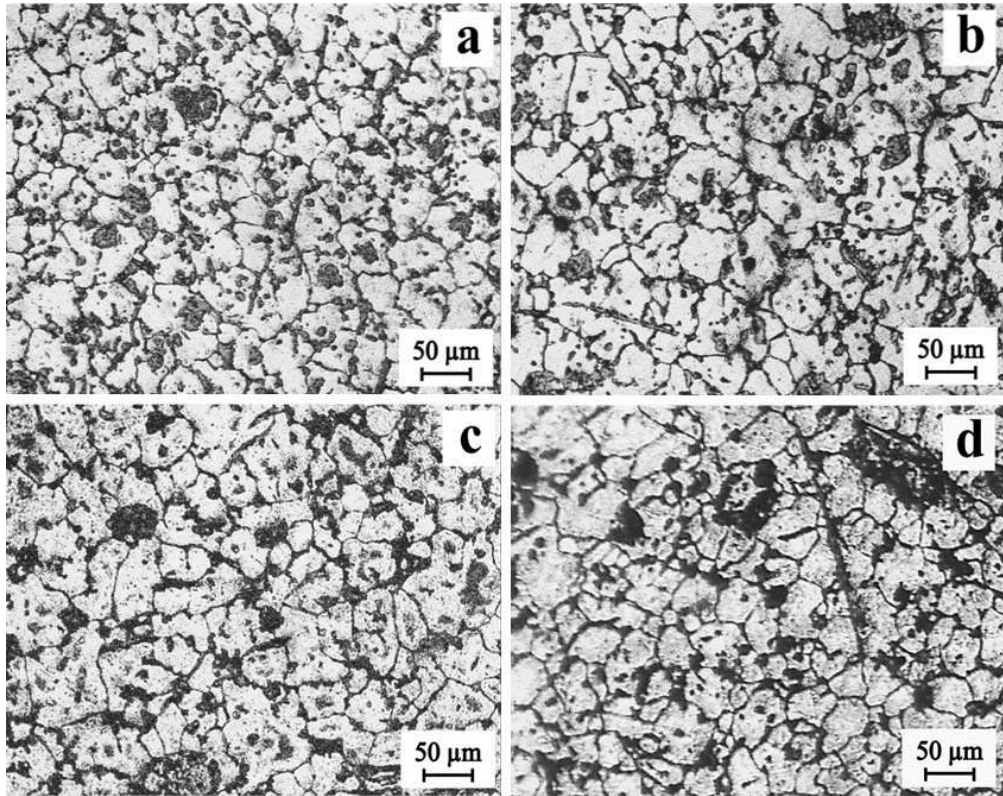Fig. 4.41 (a-d) Optical micrographs showing the grain morphology of composite processed at different intermittent stirring time interval: (a) 5, (b) 8, (c) 10 and (d) 15 min.
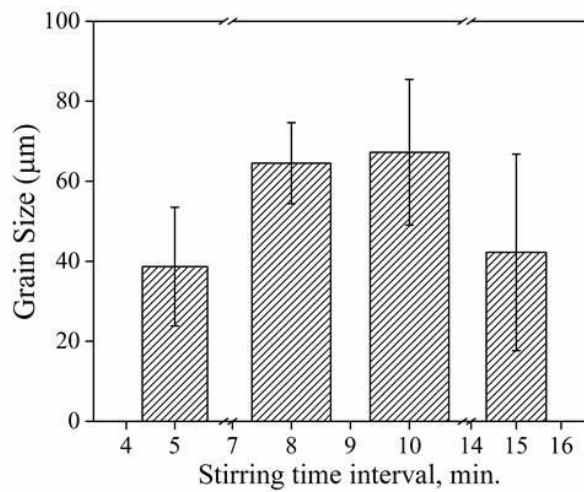
Fig. 4.42 Bar diagram showing the mean grain size and standard deviation for the composite processed at different stirring time interval.

4.9.4 Mechanical properties

4.9.4.1 Hardness
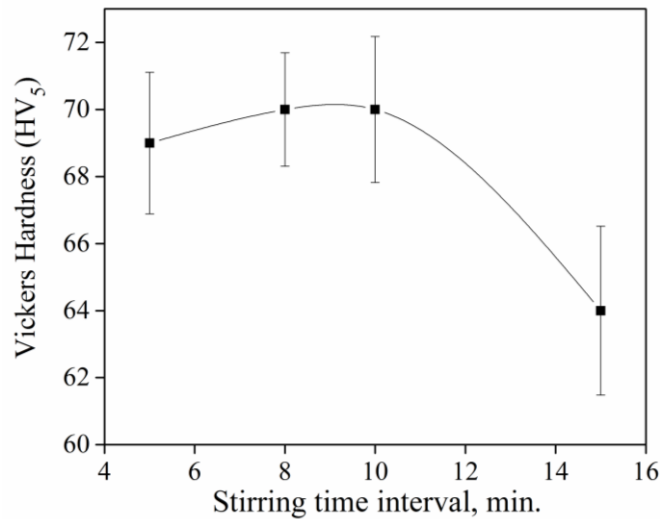
Fig. 4.43 Plot showing the variation of hardness in composites processed at different intervals of intermittent stirring time.

Fig.4.43 shows the plot depicting the Vickers hardness values obtained from as cast unreinforced alloy and composites processed at different intervals of intermittent stirring time. The composite processed with an intermittent stirring time interval of 5 min shows an increase in hardness of 69 VHN compared to the 55 VHN of unreinforced alloy. The increase in hardness of the composite is attributed to the presence of more fraction of particle in the matrix. With further increase in stirring time interval to 8 min, the composite showed a hardness value of 70 VHN. Compare to the unreinforced alloy the composite showed a 27% increase in hardness. This increase in hardness is attributed to the presence homogeneously distributed hard TiB_2 particles.

Composite processed with a stirring time interval of 10 min showed a hardness value of 70 VHN. The composite processed with a stirring time interval of 15 min showed a hardness of 64 VHN, which is 16% improvement when compared with the unreinforced alloy. Severe agglomerations of particles have impaired the hardness of composites processed at 15 min. Although the composite processed at stirring time intervals of 5, 8 and 10 min seem to show a variation in hardness, the variation in not

significant enough. Hence it can be concluded that, composites having good hardness can be prepared by using any of the 5, 8 or 10 min of intermittent stirring time interval.

4.9.4.2 Tensile properties

Table 4.11 Tensile properties of composites processed at different interval of intermittent stirring time.

Stirring time interval (Min.)	Hardness (HV$_5$)	(0.2%)Y.S (MPa)	U.T.S (MPa)	% Elong.
5	69	165	201	10
8	70	172	221	12
10	70	170	220	12
15	64	157	195	9

Table. 4.11 shows the tensile properties of composites processed at different time interval of intermittent stirring time of 5, 8, 10 and 15 min. It is obvious that the composites will show a higher Y.S and U.T.S compared to unreinforced alloy. The composite processed at 5 min of stirring time interval shows 165 MPa of yield stress and 201 MPa of U.T.S which is a 29% increase in yield and 34% increase in U.T.S. compared to the unreinforced alloy. As the interval for intermittent stirring of melt was increased to 8 min, composite showed an increase in yield and U.T.S values. The yield strength and U.T.S of composite processed at 8 min of stirring time interval was found to be 172 MPa and 221 MPa respectively.

The increase in tensile strength of composites processed at 8 min of stirring time interval is due the presence homogeneously distributed fine TiB$_2$ particles. With further increase in the interval of intermittent stirring to 10 min. the composite show an Y.S of 170 MPa and U.T.S 220 MPa compared to the composite processed at 8 min of stirring time interval. However, comparing the tensile strength of composite processed at 8 and 10 min it is very much evident that no significant change in the tensile strength of composites processed at 10 min has occurred. At stirring time intervals of 8 and 10 min, complete formation of TiB$_2$ particles has occurred in the matrix alloy, hence both the composites exhibits almost similar tensile properties. The

composite processed with further increase in the interval of intermittent stirring time of 15 min showed an Y.S and U.T.S of 157 and 195 MPa respectively. Compared to the composite processed at 8 min of stirring time interval the composite processed at 15 min showed a 9.5% and 13% decrease in Y.S and U.T.S. The decrease in strength of composite is attributed to the presence of brittle AlTiSi particles in the matrix. This brittle phase tends to act as crack initiations during tensile loading, leading to the early failure of composite. It should be noted that with increase in tensile strength the ductility of composites also increases. This is contrary to the observed results seen in composites [Lakshmi et al., 1998]. The increase in ductility on in-situ processed composites is attributed to the presence of fine TiB_2 reinforcements in the matrix alloy. Moreover due to in-situ processing a strong bonding between the particles and matrix exist, which leads to improvement in ductility. The overall observations from the tensile tests on composites processed at different intervals of intermittent stirring time suggest that an interval of 8 min intermittent stirring would be apt for the processing of *in-situ* TiB_2 reinforced composites.
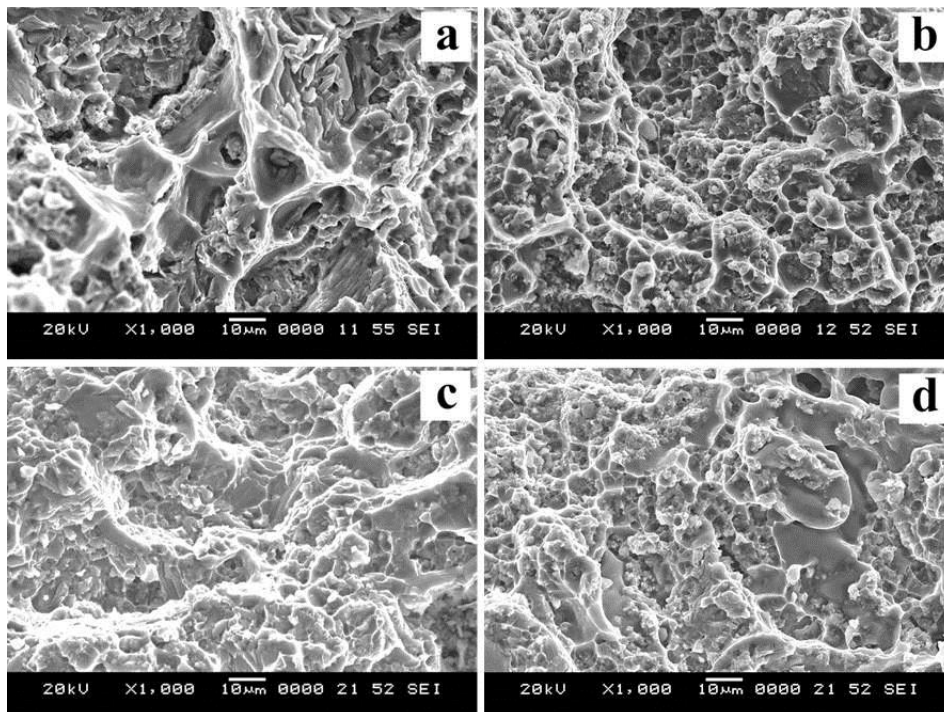
Fig.4.44 SEM fractographs showing the tensile fracture surface of composite processed at different time intervals of intermittent stirring

Fig. 4.44 (a-d) shows the SEM fractographs acquired from the tensile fracture surface of composites processed at different time intervals of melt stirring. Fig.4.44a showing the fracture surface of composite processed at 5 min of stirring time interval, shows tear ridges and larger dimples with the presence of particles can be seen inside the dimples.

The fracture surface was found show quasi-cleavage behaviour. On increasing the interval of intermittent stirring time to 8 min, the fracture surface of composite processed at 8 min of stirring time interval shows fine dimples. It can be noted that as the interval of stirring time was increased the fracture behaviour of composite changed from larger dimples to fine dimples indicating the formation of fine particles in the matrix. The composite processed at 10 min of stirring time interval and composite processed at 10 min also showed ductile fracture behaviour similar to that of the composite processed with 8 min of stirring interval. An examination on the fracture surface indicates that no particle fracture has occurred.

4.9.5 Inference

Investigations indicate that the interval of intermittent stirring time has an influence during the processing of composites. The composite processed with a stirring time interval of 5, 8 and 10 min showed similar properties, in spite of its microstructural differences. The composites processed with 15 min of intermittent stirring showed deterioration in properties. Although the composite processed at 5, 8 and 10 min of stirring time interval showed similar properties; among them the composite processed at 8 min of stirring time interval was found to be better. Hence, an interval of 8 min of intermittent stirring time has been found to be more apt for the processing of composites.

CHAPTER 5

Influence of Mg, Mn and Si in AA6082-5TiB$_2$ composites. Effect of AA6082-TiB$_2$ composites with different weight fractions and its ageing behaviour

5.1 Introduction

The alloys were developed in order to overcome the low strength exhibited by pure aluminium. With the addition of desired solute elements to pure aluminium, several alloy systems were developed. The microstructural and mechanical properties of aluminium alloys were dictated by these alloying elements present in them. However, the strength of the alloys was not improving beyond a limit. Hence to overcome this problem, composites were developed. Since the development of composites, people have developed different composite using various alloys as matrix. The properties of composites are decided by the matrix alloy and the reinforcements added to it. If the reinforcements are added to poor matrix alloy then the composite will have poor properties. Hence, during the development of composites the properties of the matrix alloy are equally important as that of the reinforcement. The properties are matrix alloy depends on the solute elements.

In ex-situ processed composites, as prior prepared reinforcements are added to the alloy melt during the composites preparation, the matrix alloy composition is not much disturbed. The reaction between the matrix and reinforcements is decided by the type of reinforcements added. Moreover in ex-situ composites the reaction leading to property deterioration occurs at the interface between the matrix and reinforcements, the whole of the matrix is not affected. In *in-situ* composites the reaction between the matrix and the reinforcements is avoided by nucleating the reinforcements in the melt by series of chemical reactions between the melt and the added salts. Although the reaction between the reinforcements and the matrix is avoided, the exothermic chemical reaction between the salts and alloy melt may alter the matrix alloy composition to a larger extent thereby affecting the properties of the composite.

147

Moreover the results obtained during the processing of *in-situ* AA6082-5TiB$_2$ composites, in section 4.3 and 4.5 suggest that the deterioration in property of composite could have been caused by solute elements. Hence to understand and to overcome the problems caused by the solutes present in the AA6082 matrix alloy, a thorough investigation has been carried out in this chapter. Since Mg, Mn and Si are the major alloying elements in the AA6082 alloy, the investigations were mainly focused on these elements. With the obtained knowledge on influence of process parameters and solute during the processing of AA6082-5TiB$_2$ composites, AA6082-TiB$_2$ composites with different weight fractions were processed and its microstructural and mechanical behavior with the addition and without the addition of Mg was investigated. Further the ageing kinetics on the composites was studied.

5.2 Influence of Mg on the AA6082-5TiB$_2$ composites

Among the principal alloying elements added to the aluminium alloys, magnesium (Mg) addition enhances the strength and corrosion resistance of the alloys. Mg when added as a sole element to aluminium, the strength of alloy is improved by solid solution strengthening [Pai et al., 1995, Wen et al., 2005], whereas when added with other alloying elements especially with silicon the alloy is strengthened by precipitation hardening [Salleh et al., 2015, Tao et al., 2015]. Apart from the aluminium alloy systems, Mg additions was found to have greater impact on the properties of exsitu processed aluminium based Metal matrix composites [Pai et al., 1995]. Over the addition of Mg to the matrix alloy, firstly the wetting between the reinforcement and the matrix is improved by scavenging the oxygen present on the surface of reinforcement by forming stable MgO or MgAl$_2$O$_4$ compounds depending on the thermodynamic feasibility [Do-Suck et al., 1993, Mogilevsky et al., 1995, Sreekumar et al., 2008], secondly the compounds formed on the surface of the reinforcements protects the reinforcements from further reacting with the matrix and thirdly the interfacial bonding between the reinforcement and the matrix alloy is improved due to better wetting which in turn enhances the load bearing capacity of the composite by transmitting the load from a ductile matrix to the strong reinforcement [Kaptay, 1997].

Since the development of *in-situ* Al-TiB$_2$ composites several reports have been published on the successful development of *in-situ* formed TiB$_2$ reinforcements in different aluminium alloy systems. Most of the aluminium alloy systems used as matrix were either pure aluminium or binary aluminum alloys [Lakshmi et al., 1998, Lu et al., 1997] and very few investigations were carried on Ternary alloy systems. Being relatively a new technique, review on the available literatures confirms that most of the investigations on the processing of TiB$_2$ reinforced aluminium matrix composites was carried out to either understand the reaction kinetics between the alloy and the added salts or to understand the influence of processing parameters like Holding time, temperature, stoichiometry of the fluoride salts, stirring conditions, ageing behaviour and mechanical properties [Beffort et al., 2007]. The principal objective of this current investigation is to analyse the influence of Mg on microstructural and mechanical properties during processing of Al-TiB$_2$ composite using flux assisted synthesis in AA6082 alloy.

5.2.1 ICP-OES

Table 5.1 Chemical composition of the as-cast alloy and composites processed with the addition of different wt.% of Mg.

Castings	Mg wt.%	Matrix Chemical Composition (Wt. %)					
		Mg	Si	Mn	Cr	Fe	Al
Standard		0.6-1.2	0.7-1.3	0.4-1.0	0.25	0-0.5	Bal
AA6082	-	1.026	1.300	0.471	0.146	0.174	Bal
AA6082-5wt.%TiB$_2$	0	0.011	1.287	0.414	0.144	0.172	Bal
AA6082-5wt.%TiB$_2$	0.6	0.631	1.280	0.434	0.151	0.151	Bal
AA6082-5wt.%TiB$_2$	0.8	0.864	1.271	0.415	0.149	0.162	Bal
AA6082-5wt.%TiB$_2$	1.0	1.056	1.281	0.418	0.154	0.171	Bal
AA6082-5wt.%TiB$_2$	1.2	1.276	1.294	0.451	0.157	0.164	Bal

Chemical composition of as-cast alloy and composite processed with the addition of different wt.% of Mg is shown in Table. 5.1. The analysis on the as-cast alloy confirms that the solute elements present in the alloy is equivalent to the standard composition of AA6082 alloy.

Analysis on the composite processed without the addition of solute elements, shows that there is a complete loss of Mg from the matrix alloy. However, no significant change is evident among the other alloying elements present in the matrix alloy. Thermodynamic calculations by Tongxiang Fan et al. [Fan, T. et al., 2005]] on the reaction of the fluoride salts with the Al melt may proceed by

$$3K_2TiF_6 + 6KBF_4 + 10Al \rightarrow 3TiB_2 + 10AlF_3 + 12KF \qquad (1)$$

The reaction between Mg and fluoride salts is given by

$$K_2TiF_6 + 2KBF_4 + 5Mg \rightarrow TiB_2 + 5MgF_2 + 4KF \qquad (2)$$
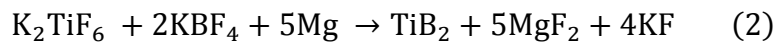
Both Mg and Al tend to react independently with the fluoride fluxes to form TiB_2 reinforcements. Reaction of Mg with the fluoride salts is crucial, after the reaction Mg gets converted to MgF_2 slag and hence the depletion of Mg has occurred in the alloy matrix. Moreover the AlF_3 flux formed from the reaction sequence of equation (1) reacts with Mg and thereby removes it from the aluminium alloy matrix very effectively compared to other available fluxes, the reaction of AlF_3 with Mg generally proceeds by [Augustzn et al., 1986].

$$3Mg + 2AlF_3 \rightarrow 3MgF_2 + 2Al \qquad (3)$$

Moreover, the $KAlF_4$ slag which is formed during the exothermic reaction of K_2TiF_6 and KBF_4 salts with the alloy melt, also reacts with Mg thereby depleting the Mg from the alloy matrix. The reaction of $KAlF_4$ with Mg proceeds by [Garcia et al., 2001]

$$Mg + KAlF_4 \rightarrow KAlF_4 + KMgF_3 \qquad (4)$$

The above reaction which occurs during the processing of *in-situ* AA6082-5TiB$_2$ composites confirms that, the loss of Mg from the matrix alloy is inevitable. Hence the composite shows a complete loss of Mg from its matrix. Furthermore the loss of Mg from the matrix alloy is also confirmed from the EDS spectrum acquired on the

150

slag Fig. 5.1. The presence of Mg along with K, F and Al is evident. Absence of Ti in the EDS spectrum further indicates the reaction between aluminium and fluoride salts is complete. However, no significant change in the composition of other alloying elements in the matrix alloy confirms that they are not affected by the reaction sequence. More importantly, the major alloying elements such as Si and Mn are not influenced by the fluoride fluxes. Since all the composites are prepared using fluoride salts, depletion of Mg from the matrix is certain. Hence, all the composites were prepared by externally adding Mg to the melt, so as to compensate for its loss. Moreover, in the present study, the influence of Mg on the composite was investigated by adding different weight percent of Mg. The chemical composition of the composite processed with the addition of 0.6% Mg is shown in Table 5.1. Considering the loss of Mg during its addition to the melt an excess of 0.1% was added to the 0.6% Mg. Hence the chemical analysis results from composite shows 0.631% of Mg in the matrix alloy. Similarly the other composites with 0.8, 1 and 1.2% of Mg were prepared and its chemical composition is shown in Table 5.1.
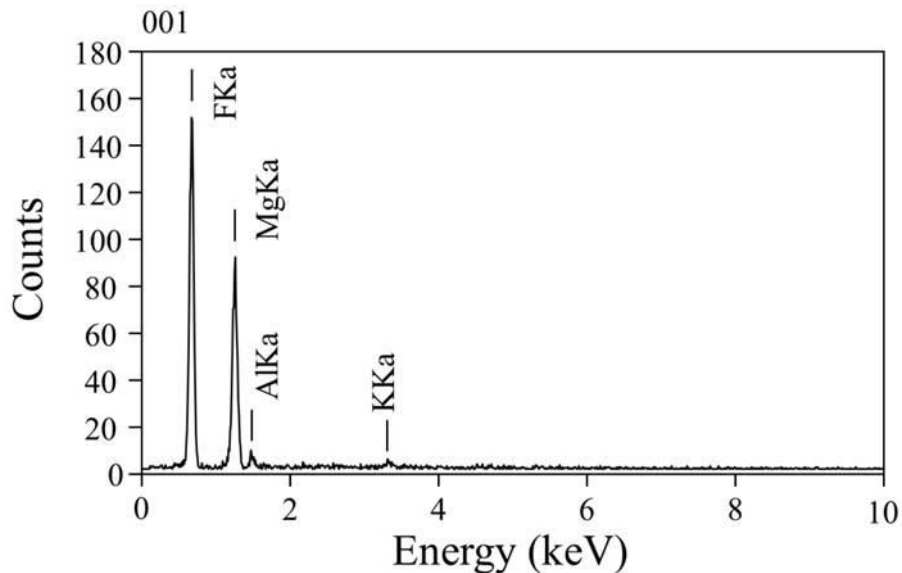
Fig. 5.1 EDS spectrum obtained from the slag.

5.2.2 Scanning electron microscopy

Fig. 5.2 (a-e) shows the AA6082-5TiB$_2$ composites processed without and with the addition of different weight fractions of Mg. The complete formation of TiB$_2$ particles

and the absence of Al_3Ti and AlB_2 particles indicate that the reaction between the Ti and B bearing fluoride salts and the melt is complete. All the composites show a homogeneous distribution of TiB_2 particles. The fine black spots seen on the micrograph are the places where the particles pull out has taken place during disc polishing. The sizes of TiB_2 particles present in composite processed without the addition of Mg ranged from few nanometres to a maximum of 2.3 µm.
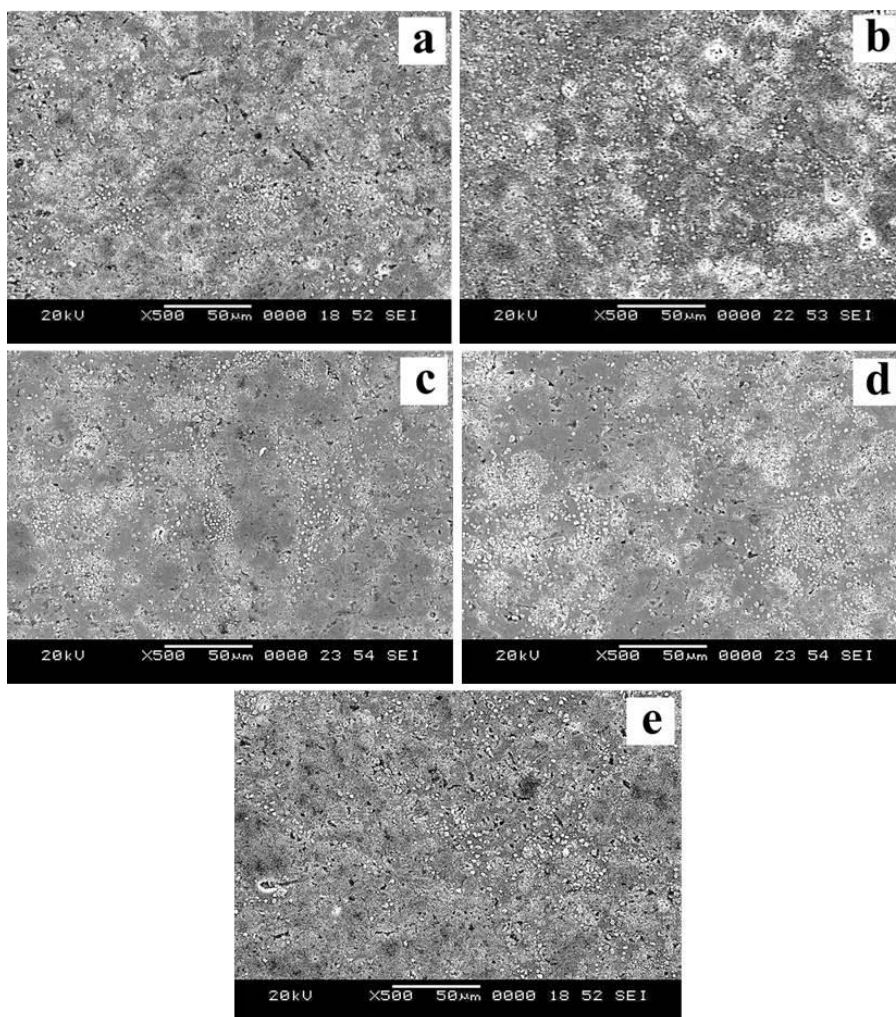
Fig. 5.2 (a-e) SEM photomicrographs of AA6082-5TiB$_2$ composites processed without and with varying addition of Mg: (a) 0, (b) 0.6, (c) 0.8, (d) 1 and (e) 1.2%.(Etchant:Keller's)

Similarly the maximum size of particles in composite with 0.6, 0.8, 1, and 1.2% of Mg was found to be 2.7, 3.1, 3.5 and 2.9 µm respectively. The analysis on the size of TiB_2 particles present in composites indicates that addition or change in the

composition of Mg content neither have a role in changing the component activity nor on the size of TiB_2 particles. These results are in agreement with the results obtained by Emilia-Maria UŞURELU et al. [Usurelu et al., 2011]. The acid dissolutions tests confirmed that all the composites were having TiB_2 particles equivalent to 5wt.%.

5.2.3 Optical microscopy
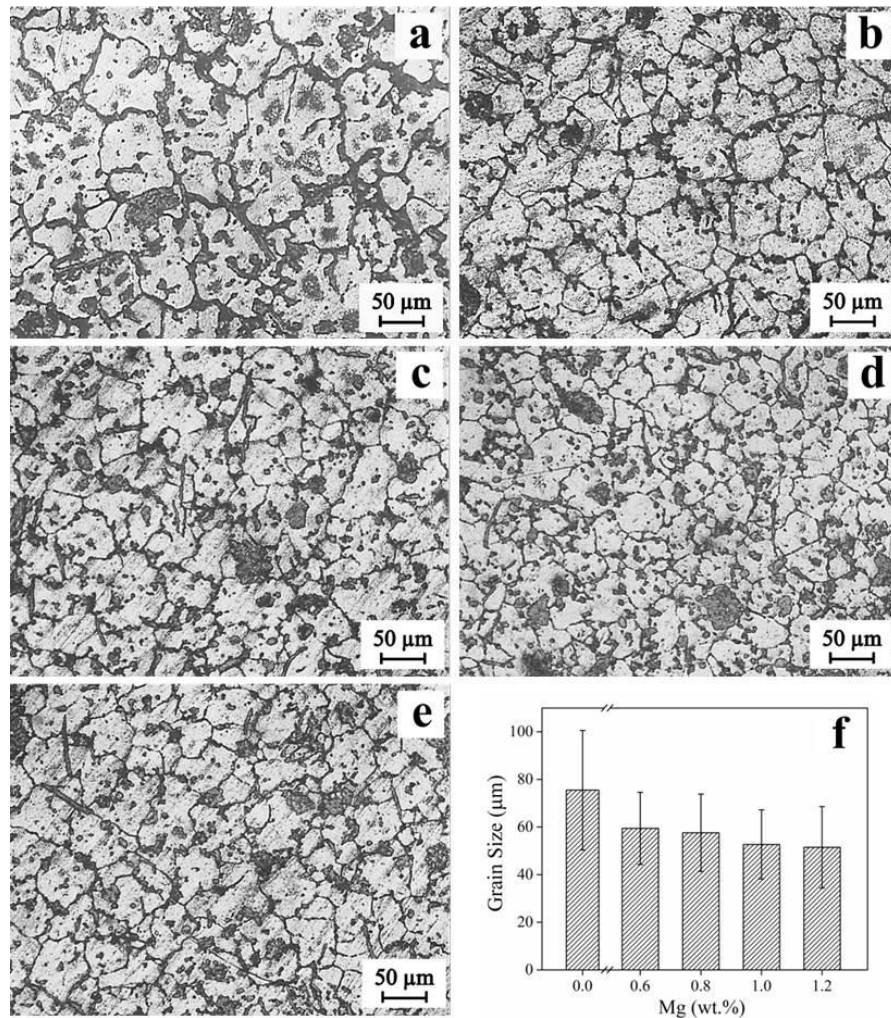
Fig. 5.3 (a-f) Optical micrograph and bar diagram of AA6082-5TiB_2 composites processed without and with varying addition of Mg: (a) 0, (b) 0.6, (c) 0.8, (d) 1, (e) 1.2 % and (f) Bar diagram showing the mean and standard deviation of composite shown in Fig.5.3 (a-e).(Etchant:Poulton's)

Fig. 5.3 (a-e) shows the optical micrograph of AA6082-5TiB_2 composites samples processed with and without the addition of Mg. The bar diagram showing the mean

and standard deviation of AA6082-5TiB$_2$ composites processed with and without the addition of Mg is shown in Fig.5.3f.

The optical micrograph of composite processed without addition of Mg is shown in Fig.5.3a. The grains exhibited both dendritic and rosette structures. This indicates that with the addition of TiB$_2$ particles to the matrix alloy, the coarse dendritic structure of unreinforced alloy (Fig.4.2) has been refined to a fine rosette structure. Addition of TiB$_2$ particles to the alloy has reduced its grain size from 206 to 77 µm. With the addition of 0.6% of Mg to the matrix alloy, composite showed a grain size of 59µm, with an equiaxed dendritic morphology. On adding 0.8% Mg to the matrix alloy, the average grain size of composite (Fig.5.3c) was found to be 57 µm with equiaxed morphology. Composite with 0.8 Mg did not show significant change in the size and morphology of grains compared to composite with 0.6% Mg.

Optical micrograph of composite processed with the addition of 1% to AA6082-5TiB$_2$ composite is shown in Fig.5.3d. The average grain size of composite was found to be 53µm with fine equiaxed morphology. No evidence of dendritic nature is seen in the composite. On adding 1.2% Mg to the AA6082-5TiB$_2$ composites, the composite with 1.2 Mg (Fig.5.3e) shows an average grain size of 51 µm, with equiaxed morphology. No change is seen in the size and morphology among the composites with 1 and 1.2 Mg. Due to the absence of constitution supercooling, pure aluminium exhibits grains with columnar structure. Hence additions of solute were employed to improve the properties of pure aluminium. In aluminium alloys, during solidification solute segregation occurs resulting in the formation of constitutional supercooled zone ahead of the growing solid/liquid interface there by restricting the growth of grains. Hence even under the absence of potent nucleants, the solute in the aluminium alloys has a considerable impact on the grain size. However when the solutes such as Mg and Si are present below their maximum solubility limit, they show very limited grain refining efficiency in aluminium alloys without inoculation [Tao et al., 2015].

When the solutes are present in the TiB$_2$ reinforced aluminium alloy composites, the refining of the grains in the alloy is not only from the solutes present in the alloy, it is also from the potent particles in the melt. During the preparation of Al-TiB$_2$ composites by the addition of Ti and B based slats. The Ti tends to segregate out of

the melt once it reaches it maximum solubility of 0.15. Hence, by default 0.15% of Ti is retained in the melt. Hence these peritectic forming solutes along with the TiB_2 particles and other solutes in the melt produce a better grain refinement of the matrix alloy. Hence there is drastic change in grain refinement in composite without the addition of Mg is seen compared to the unreinforced alloy. However depletion of Mg from the matrix alloy during processing of composite has reduced its ability to show better grain refinement. The composite with the addition of 0.6% Mg show better grain refinement. This suggests that addition of Mg has considerably contributed to the grain refinement of composite. However the addition of 0.8, 1 and 1.2% of Mg addition do not show significant change in size of grain in composites.

5.2.4 Density and porosity

Table 5.2 Density and porosity of unreinforced alloy and composite processed with and without the addition of Mg.

Castings	Mg wt.%	Matrix Porosity (%)		
		Theoretical Density (g/cm^3)	Actual Density (g/cm^3)	Porosity (%)
AA6082		2.70	2.647	1.962
AA6082-5TiB$_2$	0	2.756	2.681	2.721
AA6082-5TiB$_2$	0.6	2.756	2.668	3.193
AA6082-5TiB$_2$	0.8	2.756	2.676	2.902
AA6082-5TiB$_2$	1.0	2.756	2.671	3.084
AA6082-5TiB$_2$	1.2	2.756	2.663	3.374

Variation in measured densities and porosities present in unreinforced AA6082 alloy and composites processed with the varying addition of Mg is presented in Table.5.2. Since all the composites were having a constant 5wt.% of TiB_2 particles, the theoretical densities calculated from the rule of mixtures showed a constant 2.756 g/cm^3. Although the composite showed minor variation in actual densities, no

significant change among the density values is evident. This further indicates that all the composites were having equal amount of TiB$_2$ particles.

The porosity present in the unreinforced alloy was estimated to be 1.962%. Since the unreinforced alloy was protected by a thick coat of coverall, the oxidation and porosity in the cast alloy was reduced. In composites the minor increase in porosity is observed. This is due to the extensive melt handling of the melt during composite processing. In spite of the extensive melt handling the composites did not exhibit much porosity; this is because of thick coat of slag which protected the melt from contamination. However, the minor increase in porosity observed among the composites could have occurred during the Mg addition. The overall observation indicates that the porosity in the composites tends to increase with increase in addition of Mg.

5.2.5 Mechanical properties

5.2.5.1 Hardness
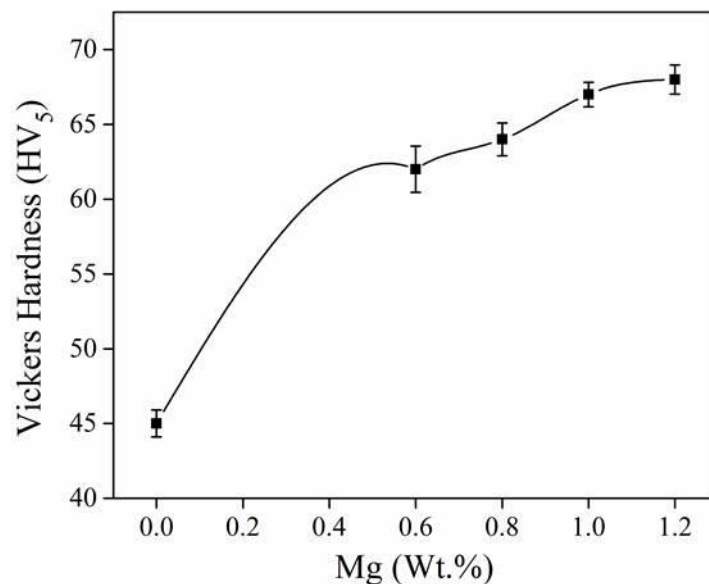
Fig. 5.4 Plot showing the variation of hardness obtained from the composites processed without and with varying addition of Mg.

The plot depicting the Vickers hardness values obtained from the unreinforced alloy and composite processed with different Mg concentration and the composite without the addition of Mg is presented in Fig.5.4. In order to have a clear understanding on

the influence of Mg during composites processing the hardness of composites processed without the addition of Mg was compared with the hardness of composites processed by different fraction of Mg. From the plot it is evident that the composite processed without the addition of Mg showed a hardness of 45 VHN. In spite of the presence of TiB_2 reinforcement in the matrix, the hardness of the composite is found to be inferior to the hardness of unreinforced alloy (55 VHN). The decrease in hardness is attributed to the depletion of Mg, which occurred during the processing of composites using fluoride salts. Due to the depletion of Mg from the matrix alloy, the matrix becomes softer. When the load is applied during hardness testing, in spite of the presence of reinforcements, more deformation occurs due to the poor strength of matrix alloy. Hence the composite shows a reduction in hardness. From the plot it is evident that the hardness of composite with 0.6% Mg is restored as soon as the Mg is added to the matrix alloy. Moreover addition of Mg not only restores the matrix hardness, it also increases the overall hardness of the composites due to the presence of TiB_2 particles the composites. Hence the composite with the addition of 0.6% Mg shows a hardness of 62 VHN, which is 13% increase in hardness compared to the unreinforced alloy. As the Mg content in the matrix alloy was increased to 0.8% the composite shows a hardness of 64 VHN. With further increase of Mg content in the matrix alloy to 1 and 1.2%, the composite shows a hardness of 67 and 68 VHN respectively. Addition of 1 and 1.2% of Mg to the matrix alloy do not show significant increase hardness of composite. The overall observation from the hardness test suggests that the harness of composite increase with increase in weight percent of Mg content.

5.2.5.2 Tensile properties

The tensile properties of unreinforced alloy and composites processed with different Mg concentration and composite without the addition of Mg is presented in Table.5.3. The composite processed without the addition of Mg shows Y.S of 121 MPa, U.T.S of 154 MPa and 18% of elongation. Compared to the unreinforced alloy, composite processed without Mg shows a 3.2 and 7.2 % of decrease in Y.S and U.T.S, whereas the composite show 18% increases in ductility. In spite of possessing fine grains and homogeneous distribution of TiB_2 particles in the matrix alloy, the decrease in

strength of composite without Mg is attributed to the loss of Mg solutes from the matrix alloy. Loss of solute reduces the dislocation density in the matrix alloy. Strength in composites results from the high dislocation density, which is caused by the difference in coefficient of thermal expansion between the matrix and reinforcements.

Table 5.3 Tensile properties acquired from the unreinforced alloy and composite processed without and with varying addition of Mg.

Samples	Mg. wt.%	Hardness (HV$_5$)	0.2% Y.S (MPa)	U.T.S (MPa)	%El.
AA6082		55	128	172	8
AA6082-5TiB$_2$	0	45	121	154	18
AA6082-5TiB$_2$	0.6	62	162	198	13
AA6082-5TiB$_2$	0.8	64	166	206	13
AA6082-5TiB$_2$	1.0	67	171	219	12
AA6082-5TiB$_2$	1.2	68	173	224	10

The loss of Mg solutes leads to reduction in matrix strength, thereby reduction in dislocations. Hence the main strengthening mechanism such as dislocation pile up and Orowans strengthening mechanism becomes inoperative, leading to the low strength of composites. With the addition of 0.6% Mg, the loss of Mg is compensated in the composite alloy matrix. By restoring the composition of the matrix alloy, the overall strength of the composite is seen to improve. Hence the composite shows a 26.5 and 19.2% increase in Y.S and U.T.S compared to the unreinforced alloy. As the Mg concentration of the matrix alloy is increased to 0.8, 1 and 1.2%, increase in Y.S and U.T.S strength of the composite also occurs. With more solute atoms more of dislocations are formed in the matrix alloy thereby leading to high strength of composites. No significant increase in Y.S is seen among the composite with 1 and 1.2% Mg. This may be attributed to the presence of porosity in the matrix alloy. It's obvious that increase in strength will bring down the ductility of composites. In the

present investigation also the increase in strength of composites has reduced the strength of the composites considerably. However, the minimum ductility (10% elongation) exhibited by composite with 1.2% Mg is better than the ductility of unreinforced alloy. In spite of adding reinforcement particles, the ductility of the composite is improved by the presence of well bonded, homogenously distributed fine TiB_2 particles in the matrix.
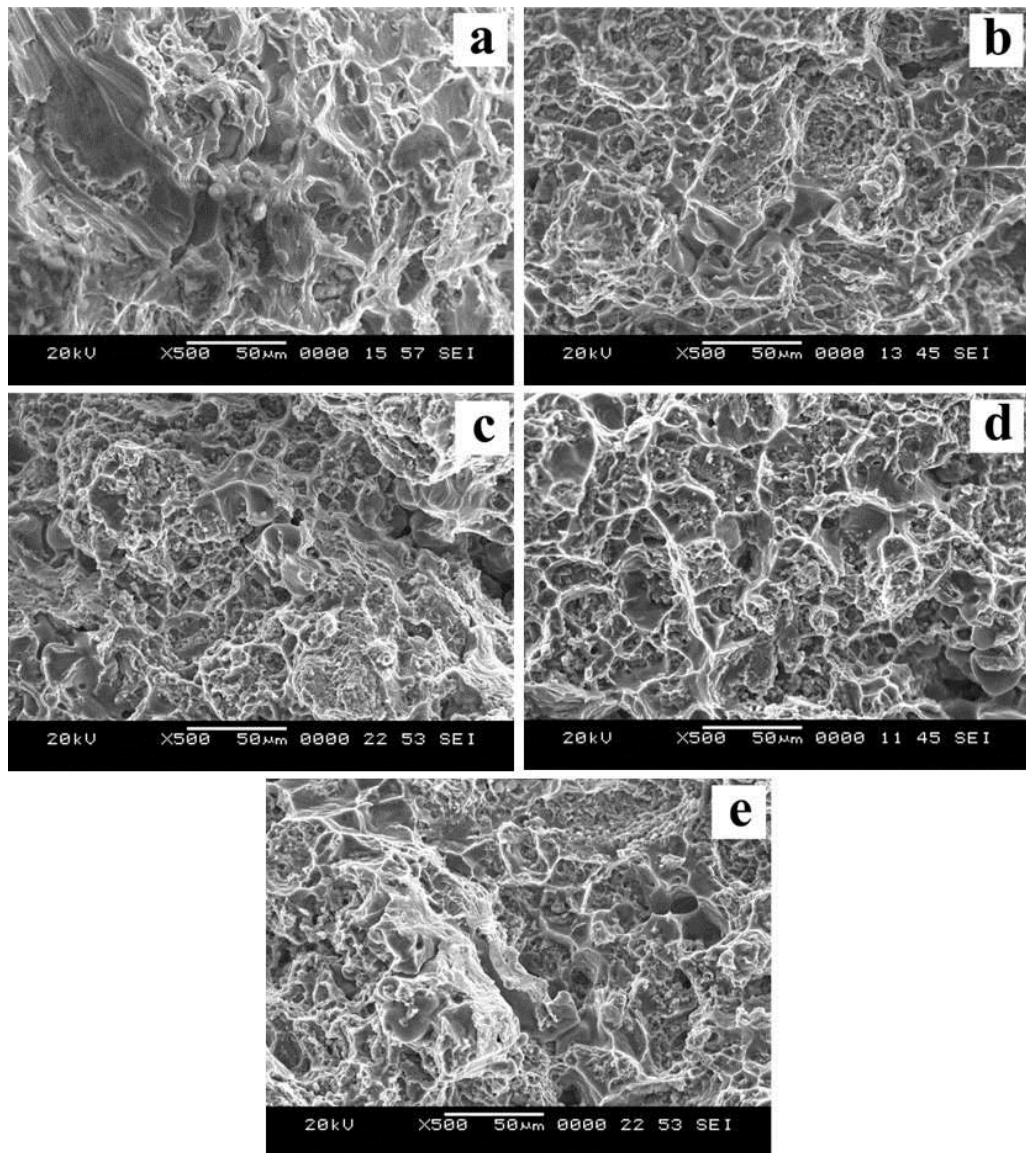
Fig. 5.5 (a-e) SEM images of tensile fracture surface of composite processed AA6082-5TiB$_2$ composites processed without and with varying addition of Mg: (a) 0, (b) 0.6, (c) 0.8, (d) 1 and (e) 1.2 %.

Tensile fracture surface of AA6082-5TiB$_2$ composite processed without and with varying addition of Mg is shown in SEM micrographs presented in Fig. 5.5. The SEM fractograph in Fig.5.5a shows the fracture surface of composite without Mg with dimples. Fig.5.5b shows the fracture surface of composite with 0.6% Mg, compared to the size of dimples in composite (0% Mg), the composite with 0.6% shows fine dimples. The fine dimples present on the fracture surface confirm that the nature of the agglomeration of TiB$_2$ particles. It further suggests that the cracks do not propagate thorough the agglomeration. The composite with 0.8% Mg (Fig.5.5c) shows the fracture surface with shrinkage cavity, which usually aid in failure initiation during the tension test, and whose presence is expected to reduce the strength and elongation. Uniform distribution of dimples is seen in composite processed with the addition 1% of Mg indicating a ductile failure. The intergranular mode of failure is evident from the fracture surface. The particles were seen to be intact inside the dimples and no particle fracture is evident. Fig. 5.5e shows the fracture surface of composite with 1.2% Mg, where the surface indicates the presence of dimples and cleavage. It seems that the cleavage is caused by the shearing of particles during tensile loading. However presence of dimples indicates its ductile nature of failure.

5.2.6 Inference

The observations reveals that the solute present in the matrix alloy plays an important role in the deciding the overall properties of the composites. In spite of adding high strength TiB$_2$ particle reinforcements, loss of Mg solute showed poor properties. Upon compensating the loss of Mg in the matrix alloy, improvements in properties of composites is observed. From the investigation, it was understood that during the processing of TiB$_2$ reinforced composites using magnesium based aluminium alloy by adding fluoride fluxes, loss of Mg solute in the melt is inevitable. The loss should be compensating by adding Mg to the matrix alloy after removing the fluxes. Hence the properties of the overall composites can be improved. Varying the Mg content in the matrix alloy of AA6082-5TiB$_2$ composites showed improvement in properties. As the Mg content in the matrix alloy was increased, minor increase in viscosity of the melt was observed causing difficulty during pouring. In order to compensate the Mg loss, it

was decided to add 0.8wt.% of Mg to AA6082-5TiB$_2$ composites melt soon after the removal of slag.

5.3 Influence of Mn on the AA6082-5TiB$_2$ composites

Among aluminium alloys, iron is one of the most common impurities present in it. When the presence of iron in aluminium is more than 0.052wt.%, it reacts with aluminium and Si and form AlFeSi based intermetallic, which are brittle and tends to affect the properties of the alloy. Hence to overcome the problems formed due to iron, Mn is intentionally added to the alloy system. Addition of Mn will reduce the brittle nature of AlFeSi alloy by forming Al(FeMn)Si based intermetallics. When such Mn alloy systems are used as matrix for the processing of composites, its effect on the composite has not been explored, hence in an attempt to understand the influence of Mn the experiments were carried out and the results obtained were discussed in this section.

5.3.1 ICP-OES

Table 5.4 Chemical composition of the as-cast alloy and composites processed with the addition of different wt.% of Mn.

Samples	Mn. Added Wt.%	Matrix Chemical Composition (Wt. %)					
		Mg	Si	Mn	Cr	Fe	Al
Standard		0.6-1.2	0.7-1.3	0.4-1.0	0.25	0-0.5	Bal
AA6082		1.026	1.300	0.471	0.146	0.174	Bal
AA6082-5wt.%TiB$_2$	-	0.864	1.271	0.415	0.149	0.162	Bal
AA6082-5wt.%TiB$_2$	0.2	0.842	1.280	0.612	0.143	0.109	Bal
AA6082-5wt.%TiB$_2$	0.4	0.837	1.271	0.808	0.149	0.102	Bal
AA6082-5wt.%TiB$_2$	0.6	0.845	1.281	1.068	0.142	0.103	Bal

Table. 5.4 shows the chemical composition of the as-cast unreinforced alloy and AA6082-5TiB$_2$ composites processed with different weight percent of Mn. The first composites casting was processed without any addition of excess Mn, hence it

showed the retained 0.415% Mn present in the alloy. In the second casting with the addition of 0.2% excess Mn, the overall composition of Mn in the alloy was made to 0.6%, which is evident in the from the chemical compositional analysis shown in Table. 5.4. Simillarly the third and fourth casting added with excess addition of 0.4 and 0.6% of Mn, showed the presence of 0.8 and 1% in the composite.

5.3.2 Scanning electron microscopy
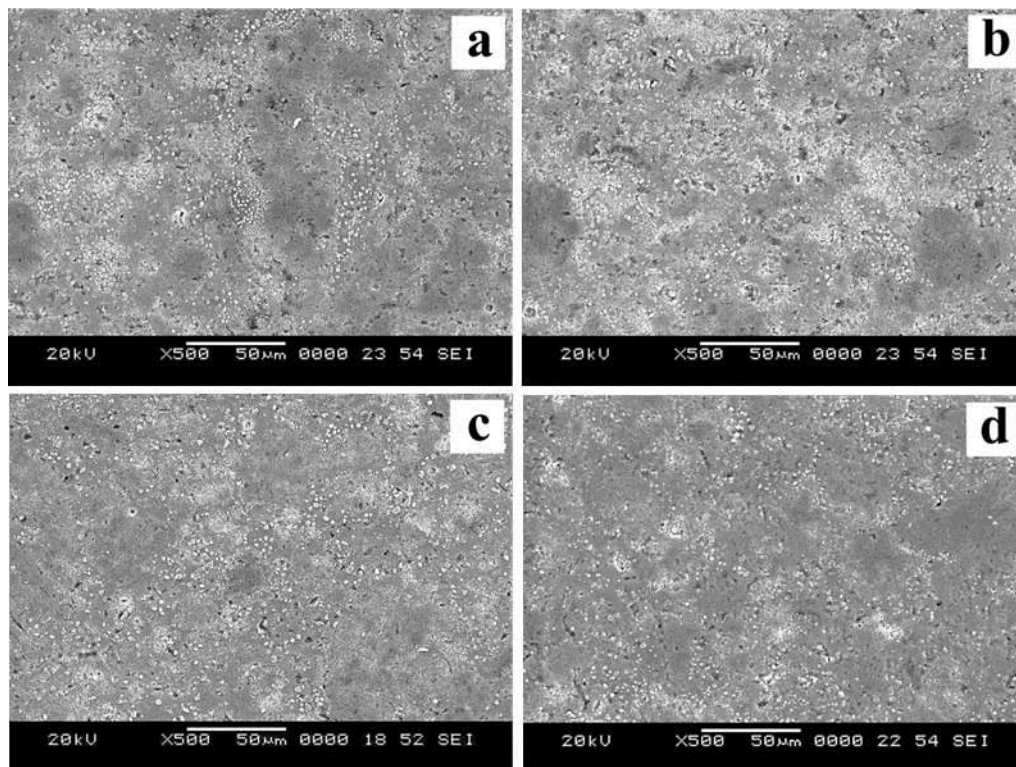
Fig. 5.6 (a-d) SEM photomicrographs of AA6082-5TiB$_2$ composites processed with varying addition of Mn: (a) 0.4, (b) 0.6, (c) 0.8 and 1%.(Etchant:Keller's)

Fig. 5.6 (a-d) shows the SEM micrographs obtained from the composite processed with varying addition of Mn. From the micrographs it is evident that all the particles are distributed homogeneously in the matrix alloy. The absence of Al$_3$Ti and AlB$_2$ particles in the matrix alloy indicates that the reaction between the melt and added fluoride salts is complete leading to the complete formation of TiB$_2$ particles in the matrix. The formed TiB$_2$ particles were seen to be distributed along the matrix grain boundaries. Particle size measurements confirmed the average size of TiB$_2$ particles was found to be 3 μm. This further confirms that addition of Mn did not have any

influence on the growth of TiB_2 particles. However EDS spectrum and mapping on some of the particles in the composite with 1% Mn showed the diffusion of Mn into the TiB_2 lattice (Fig5.7(a-b)) and 5.8(a-d).

From the Xray mapping it is also evident the fine particles do not possesses Mn in them. The EDS spectrum obtained from the intermetallic particle present along the grain boundaries after deep etching shows the presence of Ti in it which indicates that the diffusion of Ti into the particles has occurred during solidification. Dendritic plate like intermetallic phase was observer in the composite matrix. Area analysis was done on the intermetallic phase using EDS attached to SEM.
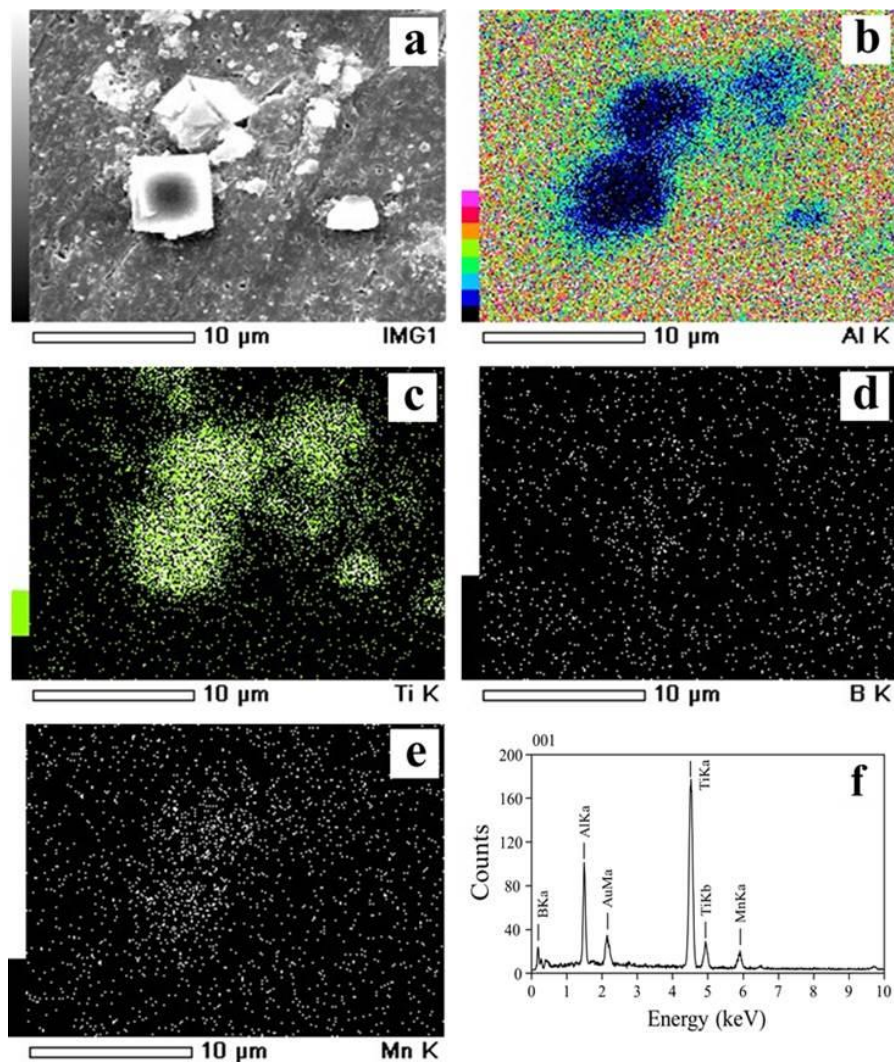
Fig. 5.7 Composite processed by the addition of Mn: (a) SEM image, EDS mapping of (b) Al, (c) Ti, (d) B, (e) Mn, and (f) EDS spectrum acquired from the particle.
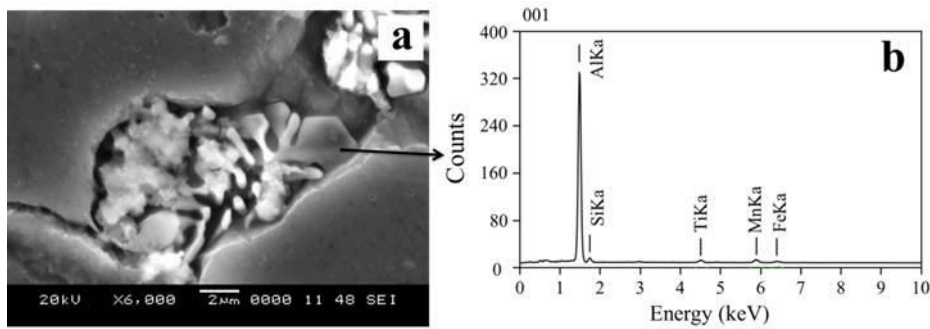
Fig. 5.8 (a,b) shows the SEM micrograph and EDS spectrum obtained from the Al (TiFeSi) Mn; (a) Deep etched SEM micrograph (b) Al(TiFeSi)Mn intermetallic.

EDS analysis confirm the presence of α-Al(FeMn)Si intermetallic shown in Fig. 5b. α-Al$_x$(Fe,Ti,Mn)$_y$Si$_z$ intermetallics phase is formed when Mn combine with Al, Si, Ti and Fe elements. These intermetallics formed have found to segregate along the grain boundaries in the matrix.

5.3.3 Optical microscopy

Fig. 5.9 (a-d) shows the optical micrograph of AA6082-5TiB$_2$ composites processed with varying Mn: (a) 0.4 (b) 0.6 (c) 0.8 and (d) 1 wt.% of manganese. The bar diagram showing the mean and standard deviation of the grains is shown in Fig.5.9e. The composite processed with 0.4% Mn is shown in Fig.5.9a. From the micrograph it is evident that the composite possess equiaxed grains. The average size of grains was found to be 58μm. With increase of manganese to 0.6% in composite alloy matrix, the composite showed an average grain size of 59 μm. No change in size of grains is observed. This indicates that excess addition of 0.2% Mn do not have influence on the size of grains.

As the Mn in the matrix alloy was further increased to 0.8 and 1%, the size of the grains of these composites was found to be 70 and 78 μm respectively. Although it seems that there is a minor growth of grains with the addition of more Mn, the growth is not significant enough. However the morphology of the grains in 0.8 and 1% Mn added composite showed rosette and dendritic structure. This indicates that the potency of particles is reduced by addition of more manganese. Moreover the EDS analysis shown in Fig.5.8 confirms the diffusion of Ti into the Al(FeMn)Si indicating the loss of Ti from matrix alloy. Since the Ti which is need for improving the potency

164

of the TiB_2 the potency effect of TiB_2 particles may have reduced thereby showing a negligible increase in size of grains and morphology.
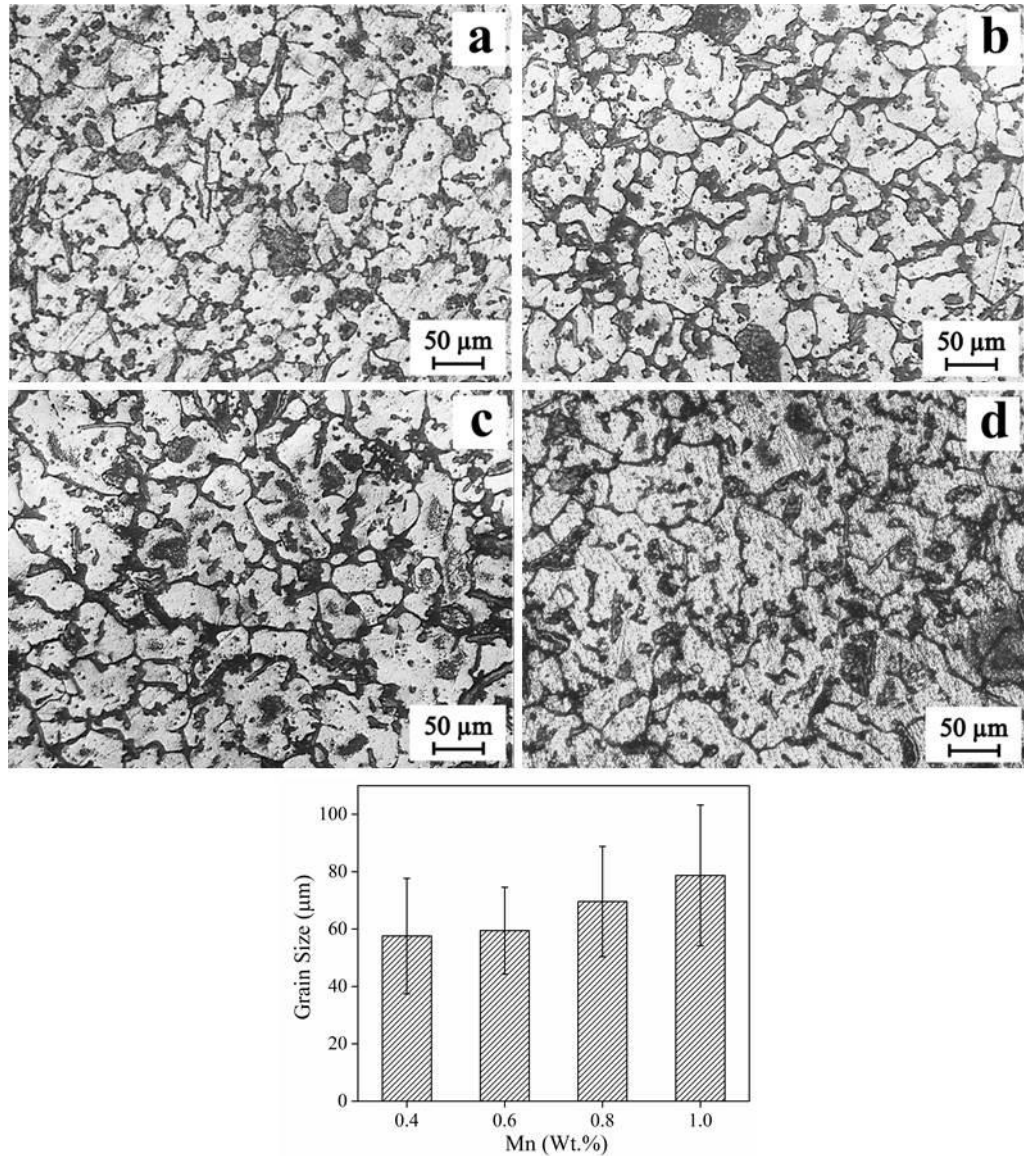
Fig. 5.9 (a-e) Optical micrograph and bar diagram of AA6082-5TiB_2 composites processed with varying Mn: (a) 0.4, (b) 0.6, (c) 0.8 and (d) 1%, (e) Bar diagram showing the mean and standard deviation of composite shown in Fig. 5.9 (a-d) .(Etchant:Poulton's)

5.3.4 Density and porosity

The density of processed composites and the percentage of porosity present them is shown in Table. 5.5. The theoretical density found by rule of mixtures shows the

density of composite was 2.756 g/cm^3. The actual densities of composites seem show minor difference. The porosity calculations shows that the porosity level in the processed composites are well below the specified porosity of 4%.

Table 5.5 Density and porosity of unreinforced alloy and composite processed with the addition of Mn.

Castings	Mn wt.%	Matrix Porosity (%)		
		Theoretical Density (g/cm^3)	Actual Density (g/cm^3)	Porosity (%)
AA6082		2.70	2.647	1.962
AA6082-5TiB$_2$	0.4	2.756	2.671	3.084
AA6082-5TiB$_2$	0.6	2.756	2.676	2.902
AA6082-5TiB$_2$	0.8	2.756	2.696	2.141
AA6082-5TiB$_2$	1.0	2.756	2.668	2.418

.3.5 Mechanical properties

5.3.5.1 Hardness
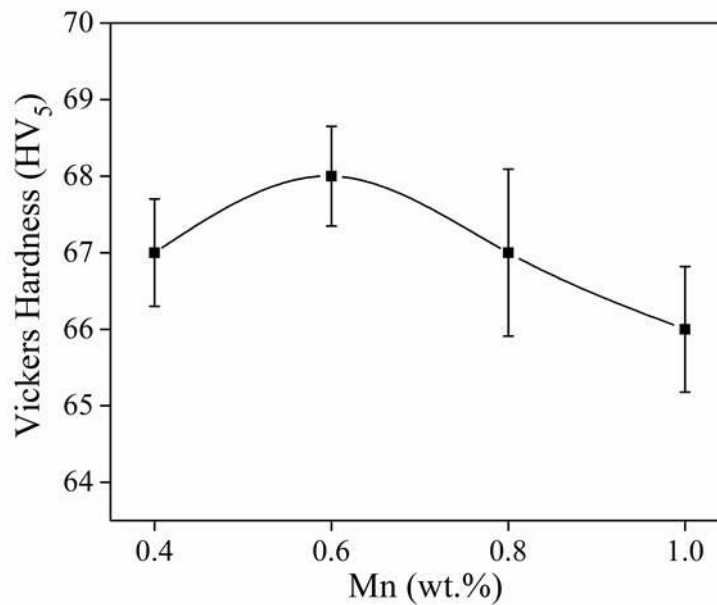
Fig. 5.10 Plot showing the variation of hardness obtained from the composite processed with varying addition of Mn.

The hardness plot obtained from the composites processed by varying the weight percent of Mn. is shown in Fig. 5.10. Compared to the unreinforced alloy, composites processed with 0.4% of Mn showed 22% increase in hardness. Since 0.4% of Mn was already present in the matrix alloy, the increment in hardness of composite was due to the addition of TiB_2 particles. When excess of 0.2% of Mn was added to the matrix alloy, the composite showed a 24% increment in hardness compared to the unreinforced alloy. The composite with 0.8% Mn showed a 22% increase in hardness, whereas the composite with 1% showed a 20% increase in hardness compared to the unreinforced alloy. Upon increase the Mn to 0.8 and 1%, the composite showed decrease in hardness. However the decrease in hardness of the composite is not significant. The overall observation indicates that there is no change in hardness of composites with increase in Mn content of the matrix alloy.

5.3.5.2 Tensile properties

Table 5.6. Tensile properties acquired from the unreinforced alloy and composite processed with varying addition of Mn.

Samples	Mn (wt.%)	Hardness (HV$_5$)	0.2%Y.S (MPa)	UTS (MPa)	%Elong
AA6082		55	128	172	8
AA6082-5TiB$_2$	0.4	67	171	219	12
AA6082-5TiB$_2$	0.6	68	171	223	11
AA6082-5TiB$_2$	0.8	67	173	229	9
AA6082-5TiB$_2$	1.0	66	175	234	9

Table 5.6 shows the tensile properties, namely the Y.S, U.T.S and % Elongation of the unreinforced alloy and the composites with different weight percent of Mn. The mechanical property of as-cast alloy is shown in Table 4.2. The values of Y.S and U.T.S of the as cast alloy, shown in Table 5.8, are much higher than that of as cast pure Al, implying that strengthening occurs due to present of solutes. In addition

strengthening is also achieved due to dispersion of Al(FeMn)Si precipitates present at the interdendritic locations. The strength of the alloy is improved by the presence of Mn dispersoids, which are incoherent with the matrix. This incoherent Mn hinders the motion of dislocations thereby increasing the strength of alloy. The composite with 0.4% of manganese shows an Y.S and U.T.S of 171 and 219 MPa respectively. Compared to the unreinforced alloy a 34% increase in Y.S and 27% increase in U.T.S was observed. This increase in strength was mainly due to the addition of TiB_2 particles. The ductility of the composite was found to be 12% which is higher than the unreinforced alloy. The presence of hard and fine TiB_2 particles improved the ductility of composite.
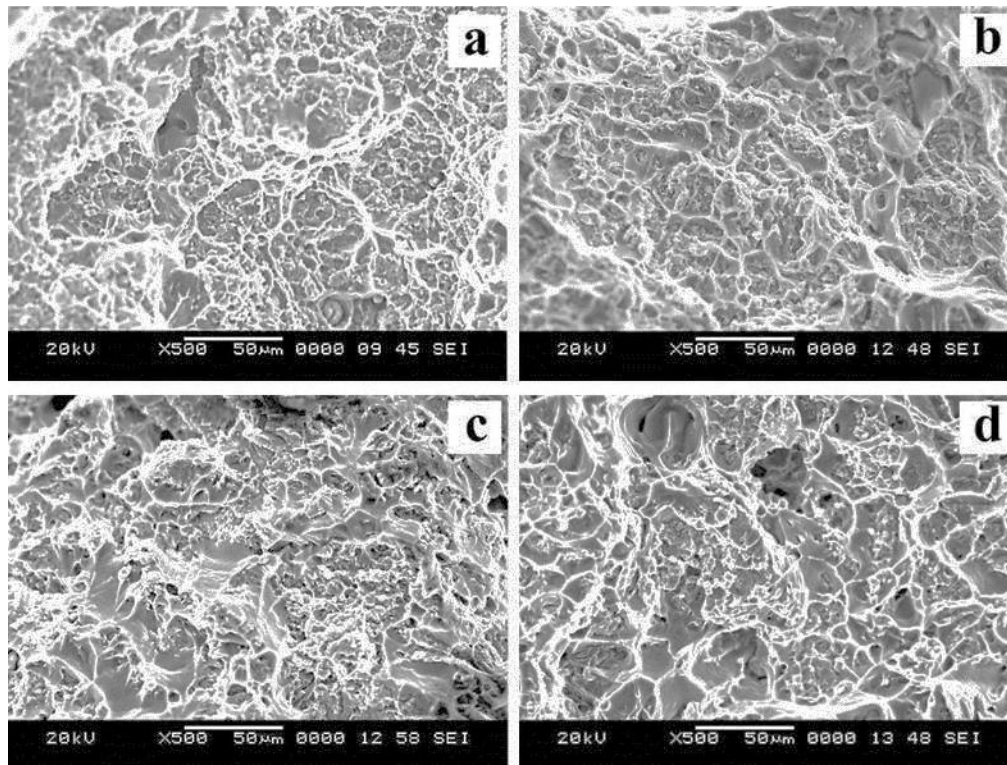
Fig. 5.11 SEM (SE) images of tensile fracture surface of composite processed with different weight percent of Mn.; (a) 0.4, (b) 0.6, (c) 0.8 and (d) 1% Mn.

Composite prepared with 0.6% Mn did not show any improvements in the yield strength, whereas a marginal increase in U.T.S is seen. Similarly, the composite with 0.8 and 1% also did not show improvements in yield strength. From the table it is evident that the ductility is retained even with excess addition of Mn. The data in Table 5.6 indicate that both Y.S and U.T.S are higher than higher in the composite.

The increase in tensile properties is due to the addition of TiB_2 particles. Since TiB_2 are more effective in strengthening than solutes the strength of the composites has improved considerably. From the tensile data it is evident, that along with the TiB_2 particles, addition of Mn solute also show some marginal improvements of the composites. Hence it can be concluded that the composite processed with excess addition of Mn did not show significant improvements.

Fig.5.11 shows the SEM (SE) photomicrographs of the tensile specimen fracture surfaces of the composite processed with different weight percent of Mn is shown in Fig.5.11. The fractographs show evidence of complete ductile fracture with the presence of dimples and tear ridges. The presence of TiB_2 particle is seen inside the dimples, which indicates its strong bonding with the matrix. In the composite larger voids with short cracks perpendicular to the tensile loading direction are observed. The fracture study indicates that the mode of fracture was ductile in nature.

5.3.6 Inference

The investigation reveals that, varying the Mn content in the matrix alloy from 0.4 to 1% did not show any change in particle morphology, grain size or mechanical properties of the AA6082-5TiB$_2$ composites. Hence adding excess Mn to the composite alloy matrix is not necessary.

5.4 Influence of Si

5.4.1 ICP-OES

Table 5.7 show the chemical composition of the as-cast AA6082 composites processed at different holding time. It should be noted that the composite was prepared with the stoichiometry ratio of K_2TiF_6 and KBF_4 salts. Since the silicon present in the alloy matrix was equivalent to the standard composition of AA6082 alloy, no excess of Si was added to the composite matrix. From the table it is evident that the matrix composition of the alloy was maintained equivalent to the standard composition for the processing time of 60 min.

Table 5.7 Chemical composition of the as-cast alloy and composites processed at different holding time.

Samples	Time, Min.	Matrix Chemical Composition (Wt. %)					
		Mg	Si	Mn	Cr	Fe	Al
Standard		0.6-1.2	0.7-1.3	0.4-1.0	0.25	0-0.5	Bal
AA6082		1.026	1.300	0.471	0.146	0.174	Bal
AA6082-5wt.%TiB$_2$	15	0.864	1.271	0.415	0.149	0.162	Bal
AA6082-5wt.%TiB$_2$	30	0.842	1.279	0.422	0.141	0.159	Bal
AA6082-5wt.%TiB$_2$	45	0.837	1.281	0.429	0.147	0.162	Bal
AA6082-5wt.%TiB$_2$	60	0.845	1.282	0.438	0.140	0.153	Bal

5.4.2 Scanning electron microscopy
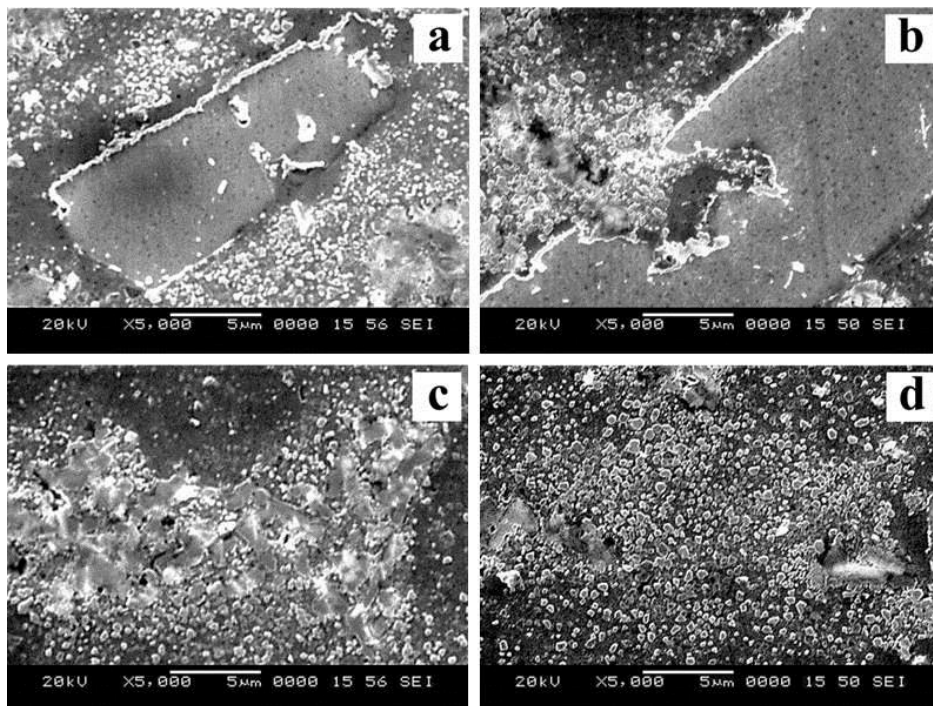
Fig. 5.12 SEM micrographs of composite processed at different holding time; (a) 15 (b) 30 (c) 45 and (d) 60 min.(Etchant:Keller's)

Fig. 5.12 (a-d) shows the SEM photomicrographs of composite processed at time different time intervals. Fig.5.12a shows the composite processed at 15 min. Fine bright contrasted particles along with large blocky particles are seen in the micrograph. EDS spectrum obtained from the particles confirmed that they belong to AlTiSi particles and the fine particles were TiB_2 and Al_3Ti.

The SEM micrograph obtained from composite processed at 30 min of time shows that dissolution of blocky particles. On the edges of the blocky particles a thin bright contrasted coating region is seen. The EDS spectrum obtained from the bright contrasted region belonged to TiB_2 phase. This indicates the diffusion of boron onto to the AlTiSi particles. The EDS mapping shown in Fig. 5.13 confirmed that particles belonged of AlTiSi phase. More of Si is seen on the area where the dissolution has occurred. This indicates that with the dissolution of AlTiSi particles, the Si present in the particles is diffused out. The EDS spectrum (Fig.5.14d) obtained from the fine particles confirmed that the particles were Al_3Ti. Along with Al_3Ti particles AlB_2 particles were also present indicating that the diffusion of B not only results in TiB_2 particles, it also forms into AlB_2. With increase in time to 45 minutes the particles began to dissolve completely (Fig.5.12c).
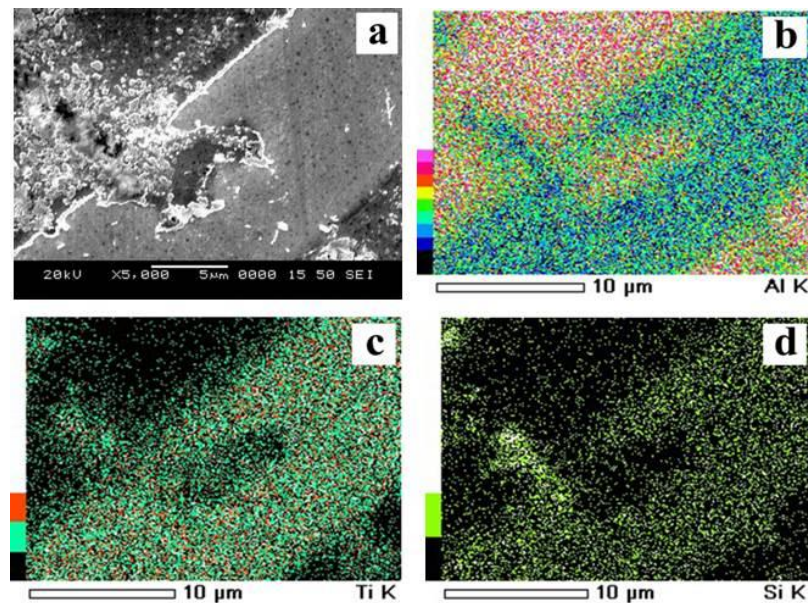
Fig. 5.13 X-ray mapping obtained on the particle (a) SEM image (b) Al (c) Ti and (d) Si.
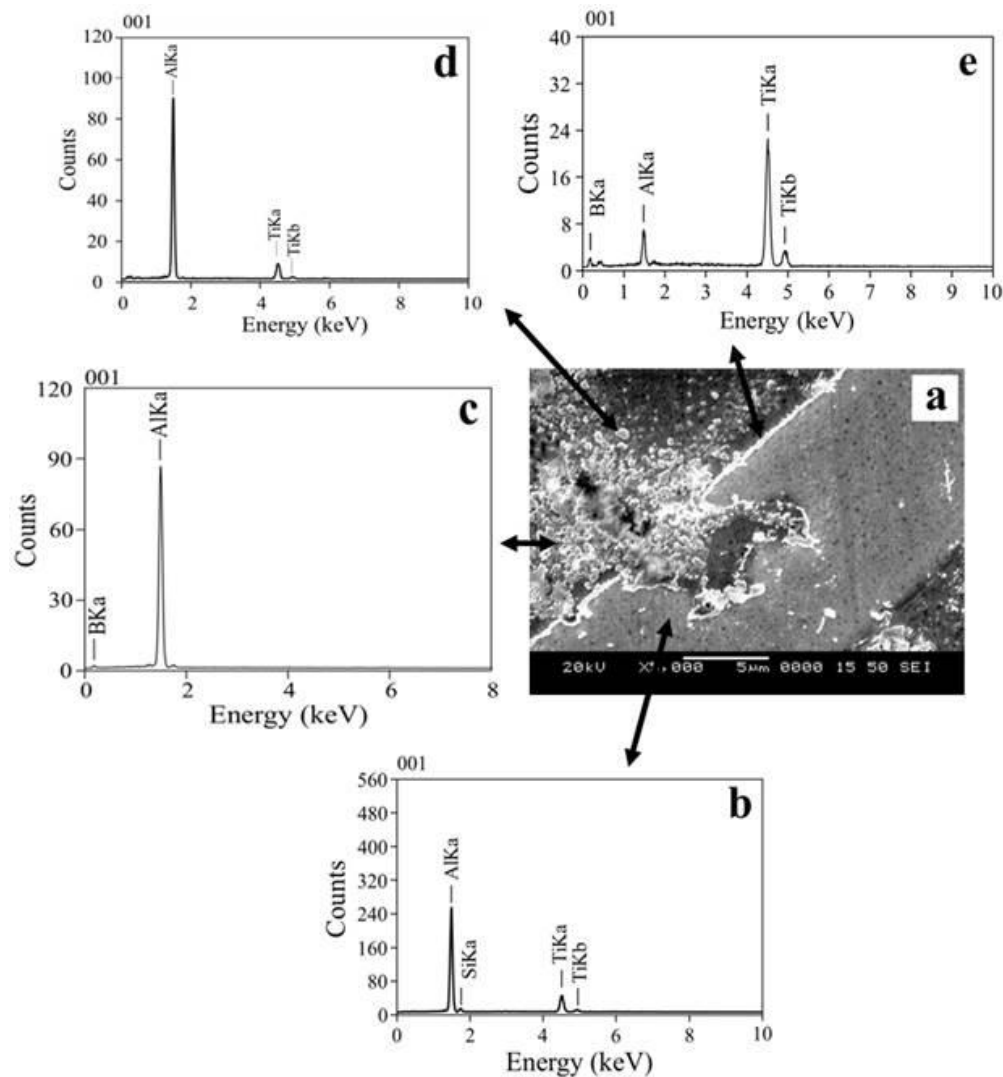
Fig. 5.14 EDS spectrum acquired from particle (a) SEM image (b) AlTiSi (c) AlB$_2$ (d) Al$_3$Ti and (e) TiB$_2$.

As the melt holding time was further increase to 60 min the blocky particles have dissolved completely leading to the formation of mixture of Al$_3$Ti, AlB$_2$ and TiB$_2$. The EDS analysis confirmed that no Si was present in the particles, indicating that the particles have completely diffused out during dissolution. The investigation indicates that Si which is present in the aluminium alloy matrix diffuses into the Al$_3$Ti lattice and forms AlTiSi based particles. During the dissolution of the AlTiSi particles the Si diffused out of the particles leaving Al$_3$Ti particles in the matrix. There observation shows that there is no direct transformation of AlTiSi particles into TiB$_2$.

172

5.4.3 Inference

The investigations indicate that the diffusion of Si into the Al_3Ti lattice occurs during its precipitation. AlTiSi particles with different Si concentration are evident from the EDS analysis. During the dissolution of AlTiSi particles the Si diffuses out thereby forming Al_3Ti particles.

5.5 Processing of AA6082-TiB_2 composites with different weight fractions

Investigation on optimising the process parameters and the effect of alloying elements for the processing of AA6082-5TiB_2 composites revealed that the following conditions. To prepare a composite with good properties, the alloy melt should be held at a temperature of 850°C and the processing time needed for the preparation of the composite should be 60 min with an intermittent melt stirring time interval of 8 min. To completely form TiB_2 particles in the matrix alloy, an excess of 10% KBF_4 salts should added to the stoichiometric mixture of K_2TiF_6 and KBF_4 salts. Before pouring the Mg loss should be compensated by adding 0.8% of Mg to the composite melt. Having gained some knowledge on the processing of AA6082-TiB_2 composites, the same processing conditions was extended to prepare *in-situ* AA6082-TiB_2 composites with different weight fractions of TiB_2 particles. In order to analyse the effect of Mg, two sets of composites with different weight fraction was prepared using the optimised process parameters. By keeping all the process conditions identical, the first set of AA6082-TiB_2 was prepared without the addition of Mg, and the second set was prepared with the addition of Mg and their mechanical properties were compared.

5.6 AA6082-TiB_2 composites with different weight fractions with and without the addition of Mg

5.6.1 X-ray diffraction analysis

The XRD pattern of AA6082-TiB_2 composites with different weight fractions of TiB_2 particles is shown in Fig. 5.15 (a-e). The XRD pattern (Fig.5.15b) obtained from composite processed with 2.5wt.% TiB_2 particles showed no distinct peaks. This is due to the lower weight fraction of the particles present in the composite. The composite processed with 5wt.% TiB_2 particle shows the prominent peaks of TiB_2

indicating its presence in the matrix (Fig.5.15c). The XRD pattern in Fig.5.15c shows the composite processed with 7.5wt.% of TiB$_2$ particles. An increase in intensity of the TiB$_2$ particles is seen the pattern. With further increase of TiB$_2$ particles to 10wt.% the intensities of peaks were still higher indicating more of TiB$_2$ particles are present in the matrix.
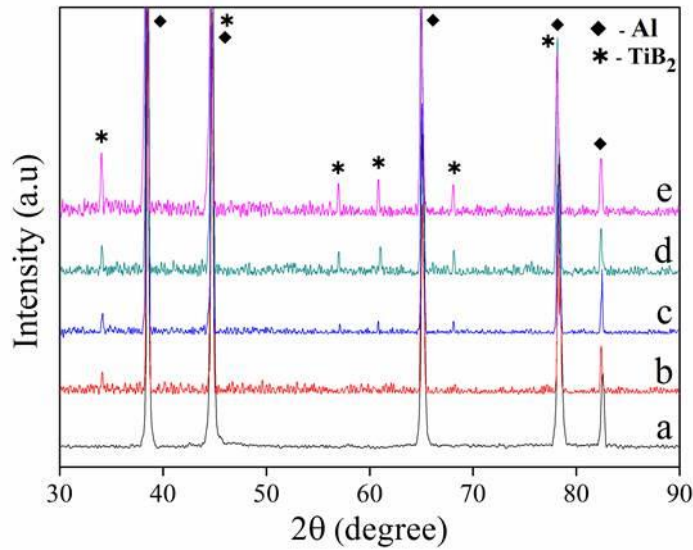
Fig. 5.15 (a-e) XRD patterns of composite processed with different weight fractions of TiB$_2$ particles (a) 0, (b) 2.5, (c) 5, (d) 7.5 and (e) 10%TiB$_2$.

(a)   (b)
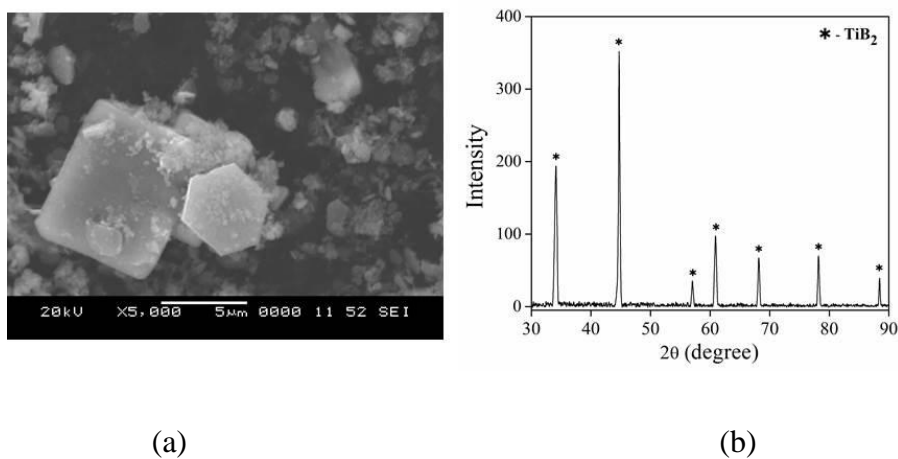
Fig. 5.16 SEM and XRD spectrum acquired from the extracted particles (a) SEM photomicrograph. (b) XRD pattern acquired from TiB$_2$ particles.

The particles present in the composite with 2.5wt.% extracted by acid dissolution method is shown in Fig.5.16a. The XRD pattern obtained from the corresponding

particles show the presence of TiB_2 peaks, which confirms the presence of TiB_2 particle in the matrix. The analysis on the extracted particles shown in Table 5.8 further confirms that the particles in the processed composites were almost equal to the estimated value quantity of TiB_2 particles.

Table 5.8 Estimated and actual wt.% of TiB_2 particles present in the matrix alloy

Composite	Estimated (wt.% TiB_2)	Actual (wt.% TiB_2) (from extraction)
AA6082-2.5TiB$_2$	2.5	2.3
AA6082-5TiB$_2$	5	5.2
AA6082-7.5TiB$_2$	7.5	7.2
AA6082-10TiB$_2$	10	9.7

5.6.2 Scanning electron microscopy
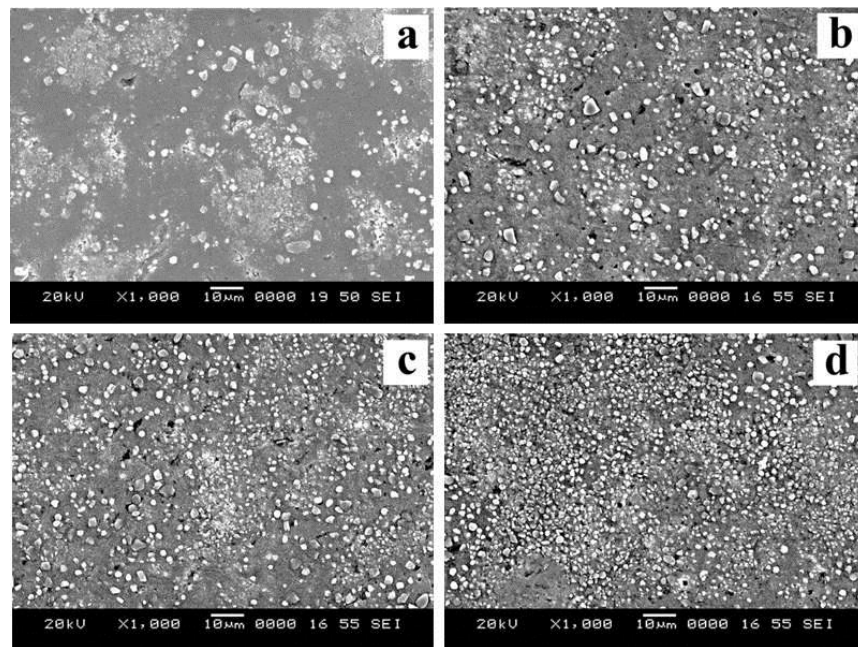
Fig. 5.17 (a-d) SEM photomicrographs of composites with different wt.% of TiB_2 particles (a) 2.5, (b) 5, (c) 7.5 and (d) 10%TiB_2.(Etchant:Keller's)
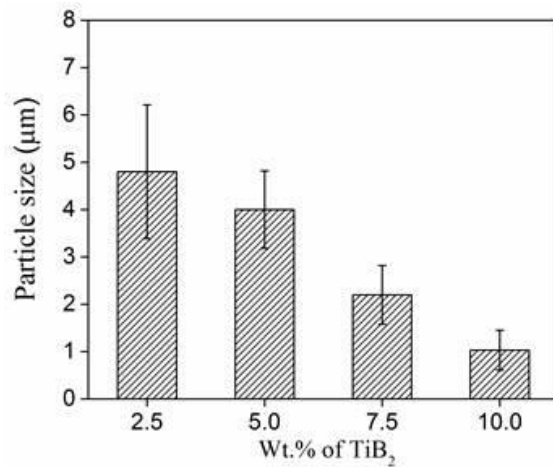
Fig. 5.18 Plot showing the average size of particle present in the composites

Fig. 5.17 (a-d) shows the SEM photomicrographs obtained from composites processed with different weight fraction of the TiB_2 particles. The brighter phase indicates the TiB_2 particles. The large particles were irregular in shape, whereas the smaller particles clearly reveal the hexagonal morphology. The increase in weight fractions is evident from the micrographs. The increase in density of the particle is also evident from the micrograph which is shown in Fig. 5.17. It is very much evident that as the weight fractions in the composite increased the size of the particles reduced. The reduction in size of TiB_2 particles is attributed to the high nucleation rate which reduces the growth of TiB_2 particles. Hence composite processed with higher weight fractions of TiB_2 particles show fine size. The higher magnification SEM image further confirms the present of fine TiB_2 particles with hexagonal and cubic morphology. The size of the TiB_2 particle ranged from submicron to a maximum of 3μm in size. Fig.5.81 shows the plot between the average size of the particle present in the composites with respect to the composites processed with different weight fractions of TiB_2 particles. It is well evident that with increase in weight fractions of TiB_2 particles, the size of the TiB2 particle decreases. This is attributed to the high nucleation rate than the growth phenomenon.

Fig.5.19 shows the higher magnification SEM micrographs of AA6082-10TiB$_2$ composites. The micrograph shows the presence of fine TiB_2 particles. The morphology of the TiB_2 particles is hexagonal. The absence of Al3Ti particles indicated that the reaction between the salts and matrix alloy is complete.

176
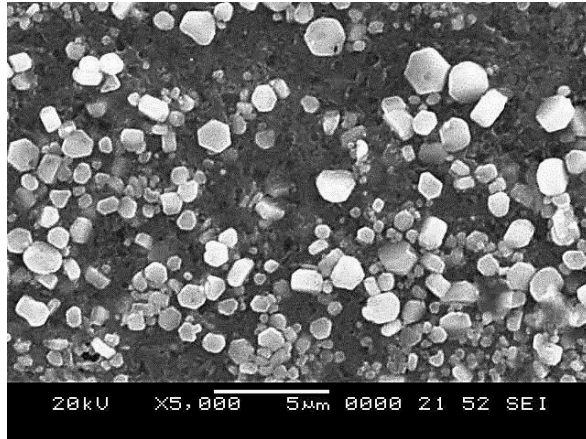
Fig. 5.19 SEM photomicrographs showing the TiB$_2$ particles at higher magnification. (Etchant:Keller's)
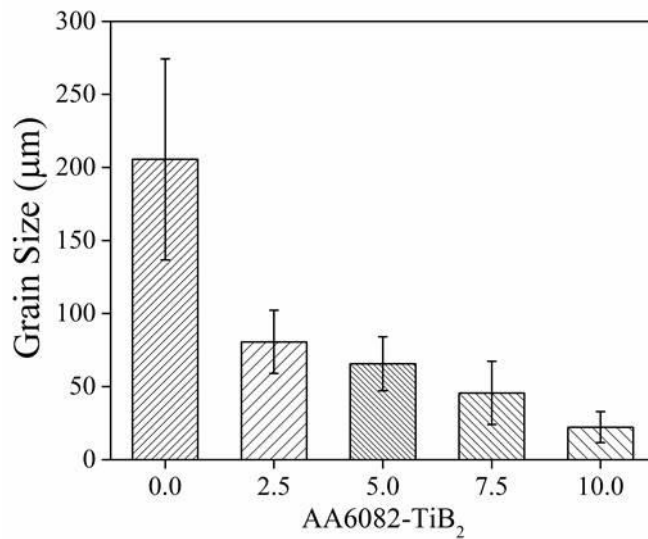
Fig. 5.20 Plot showing the average grain size of composites by varying TiB$_2$ weight fraction

The grain size of composite processed with different weight fractions is shown in Plot 5.20. From the plot it is evident that with increase in TiB$_2$ weight fraction the size of the grains reduced indicating that the TiB$_2$ particles are efficient grain refiners[Naess and Ronningen, 1975]. The composite with 2.5% showed an average grain size of 80.64±21.71 µm. Similarly the grain size of composite with 5, 7.5 and 10% showed 65.62±18.52 µm, 45.62±21.62 µm, 22.21±10.62 µm respectively. When these numerous potent TiB$_2$ particles are introduced into the melt, the particles act as

nucleation sites for the growth of grains. Hence with increase in TiB_2 particle, reduction in size of grains occurs.

5.6.3 Mechanical properties

Since both the composite with different weight fractions processed with and without the addition of Mg show similar microstructure and weight fractions, the characterisation of composite processed with the addition of Mg is not shown. Although the composite processed with the same process conditions had similar microstructural features, the composite showed distinct mechanical behaviour. Hence in this section both the composite processed with and without the addition of Mg has been compared.

5.6.3.1 Hardness

Table 5.9 Hardness of composite with different weight fractions processed with and without addition of Mg.

Castings	Hardness (HV_5) Without the addition of Mg	Hardness (HV_5) With the addition of Mg
AA6082 (0)	55	55
AA6082-2.5% TiB_2	39	61
AA6082-5% TiB_2	46	69
AA6082-7.5% TiB_2	59	75
AA6082-10% TiB_2	64	83

The hardness values obtained from the composite with different weight percent of TiB_2 particles processed with and without the addition of TiB_2 particles is shown in Table. 5.9. Compared to the unreinforced alloy hardness of composite decreases with the addition of 2.5 and 5TiB_2 particles. The decrease in hardness is attributed to the loss of Mg from the matrix alloy. Since the matrix strength deteriorated addition of secondary particles were not effective in improving the strength of composite. However an increase in hardness is seen to improve slightly in composite with 7.5 and

10%TiB_2 particles. When the weight fraction of TiB_2 particles was increased in the matrix, the particle present in the matrix took most of the load in-spite of the loss of Mg from the matrix. The composite with 10% TiB_2 showed a 16% increase in hardness. The hardness of composite processed with addition of Mg increases progressively as the function of TiB_2 content. There is a 51% increment in hardness of composite reinforced with 10%TiB_2 as compared to the unreinforced alloy.

5.6.3.2 Tensile Properties

Table 5.10 Comparison of Tensile properties of unreinforced alloy and composites processed by varying weight fraction of TiB_2 particles, with and without addition of Mg.

Casting	(0.2%) Y.S (MPa)		U.T.S (MPa)		%Elong.	
	Without Mg	With Mg	Without Mg	With Mg	Without Mg	With Mg
0	-	128	-	172	-	8
2.5%TiB_2	111	153	166	201	8	14
5% TiB_2	124	178	123	229	22	12
7.5%TiB_2	174	202	146	263	17	9
10% TiB_2	196	229	219	295	12	9

Table 5.10 shows the tensile properties of AA6082-TiB_2 alloy with varying weight fraction of TiB_2 particles processed with and without the addition of Mg. It can be seen that the yield strength and ultimate tensile strength of the composite without the addition of Mg decreases with increase in weight fraction of TiB_2 particles. However the strength begins to improve in composites having 10% of TiB_2 particles. Due to the loss of Mg from the matrix the alloy strength is reduced. Hence even after the addition of TiB_2 particles, no improvement in strength is seen among the composites.

Moreover due to the loss of Mg the matrix becomes softer, hence with the presence of well bonded TiB_2 particles composites show better ductility. Among the composite with the addition of Mg the U.T.S and Y.S values show a steady increase in strength, the ductility of the composites decreases as the amount of TiB_2 particles increases. The improvements in properties can be attributed to the increase in strength of matrix by compensating it with Mg and complete suppression of Al_3Ti particles in the composite by optimisation of process parameters.

Fig. 5.21a shows the presence of deep and equiaxed dimples in the fracture surface of composite with 2.5%TiB_2 particles indicating a completely ductile fracture corresponding to 75% elongation compared to the unreinforced alloy. The intact TiB_2 particles are evident inside the dimples, indicating its good bonding between the particle and the matrix. The fracture surfaces also show the presence of dimple of varying size. With increase in TiB_2 particle weight fraction the dimples become decrease in size and progressively shallower. The decrease in size of dimples is very prominent in case of the composite with 10wt.%TiB_2 reinforced composite.
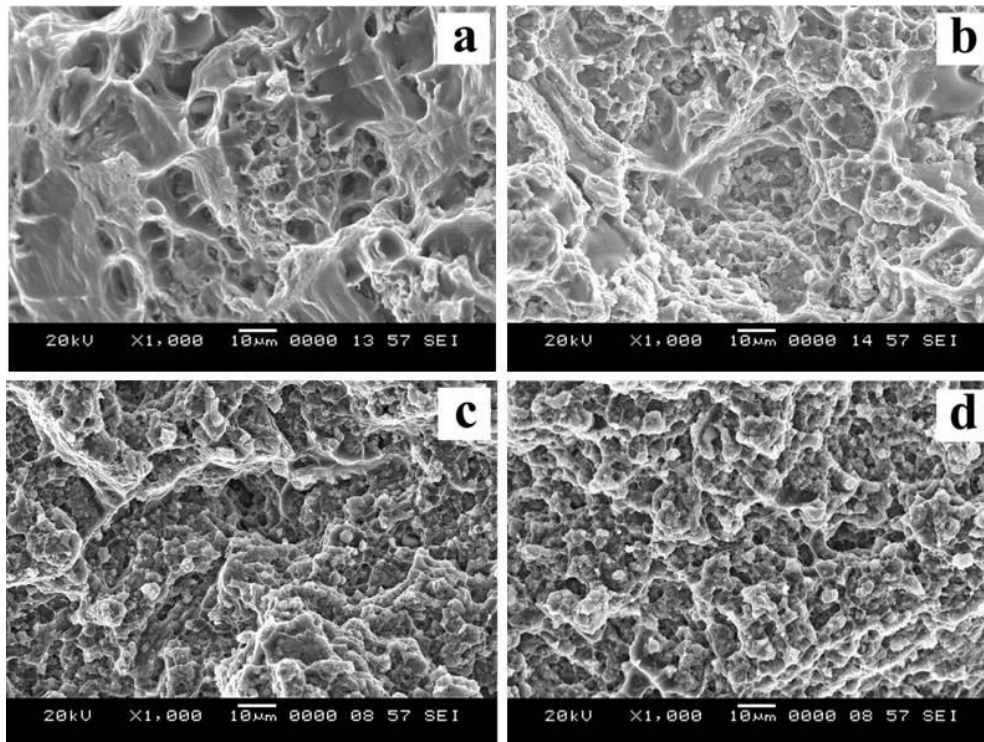
Fig. 5.21 (a-d) SEM fractographs of AA6082-TiB_2 composites with different weight fractions of TiB_2 (a) 2.5, (b) 5, (c) 7.5 and (d) 10% TiB_2

5.6.4 Inference

The investigations indicate that even after the addition of high weigh fractions of TiB_2 particles (10% TiB_2), the strength of composite decreased due to the loss of Mg. On compensating the loss of magnesium in the alloy matrix, even small addition of TiB_2 particles (2.5% TiB_2) showed substantial improvements over the unreinforced alloys.

5.7 Ageing studies of as-cast unreinforced alloy and AA6082-TiB$_2$ composites

The ageing behaviour of as-cast ureinforced AA6082 alloy and the AA6082-5TiB$_2$ composites with different weight fractions has been studied in the following section.

5.7.1 Hardness and ageing studies of AA6082-TiB$_2$ composites

Table 5.11 Hardness of AA6082 alloy and AA6082-TiB$_2$ composites

TiB$_2$ (Wt. %)	Vickers Hardness (HV$_5$)		
	As-cast	Solutionised	Peak Aged
0	55	59	78
2.5	61	66	110
5	66	70	122
7.5	70	76	125
10	78	80	129

Table 5.11 shows the hardness of unreinforced alloy and AA6082-TiB$_2$ composites processed under different conditions. Fig.5.22 shows the isothermal ageing curve of the base alloy and composites was derived from the Vickers hardness measurments carried out on a number of samples taken out of the furnace at regular time intervals. The hardness of the unreiforce alloy and composites with different weight fractions represented by zero hours corresponds to the as-cast conditions. The details of the heat treatment procedures are given in section 3.6. Fig. 5.22 shows the hardness of unreiforced alloy and composite with different weight fractions of TiB$_2$ as a function of ageing time at 180°C.

The age hardening curves of the base alloy and composite was compared with the composites to have an idea on the effect of TiB$_2$ particles. In the absence of TiB$_2$

particles, the age hardening curve is very broad and the peak hardness of 78VHN is reached after 8 hrs of ageing. The age hardening curves do not show shap peak for the alloy. The age hardeneing curves of composites show sharp curves during peak ageing. It is intersting to note that with the increase in weight fraction of TiB_2 particles not only the peak hardness value increases but also the time to attain the peak hardness decreases. The peak hardness value increases from 78 VHN in the unreiforced alloy to 129 VHN in the AA6082-10wt.%TiB_2 composites (Fig.5.23). An 65% of increase in hardness is attained by the heat treatment conditions. The time required to reach the peak hardness also decreased from 8 hrs. in unreinforced alloy to 2 hrs. in composite with 10wt.% of TiB_2 particles. Such reports of enhaced ageing kinetics is in agreeement with some of the earlier reports [Nandam, S. H. et al., 2011]. The increase in ageing kinetics in the presence of TiB_2 particles could be attributed to the the possible nucleation of AlFeMnSi based precipitates. In addition due to the difference in coefficient of thermal expansion between Al(23.5×10^{-6}/K) and TiB_2(7×10^{-6})/K strian fields are developed in the interface between the reinforcement and the matrix, which leads to an increase in dislocation density. This nucleation can also act as nucleting sites during precipitation and enhace the dislocation density in the matrix of composites with TiB_2 particles.
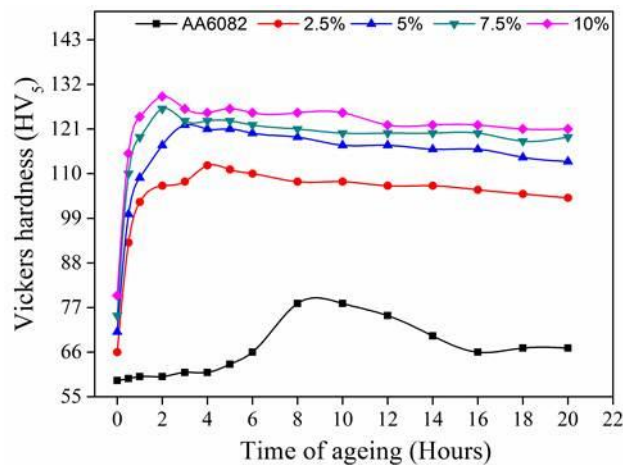
Fig. 5.22 Hardness of unreinforced alloy and AA6082-TiB_2 composites as a function of ageing time
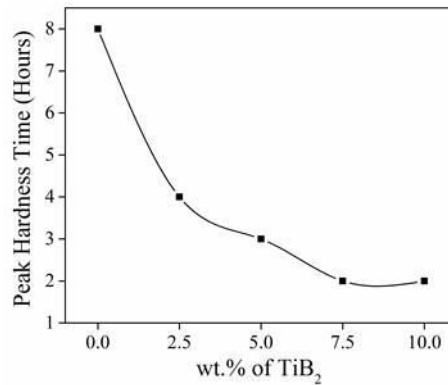
Fig. 5.23 Time to reach peak hardness in AA6082-TiB$_2$ composites

5.7.2 Transmission electron microscopy

The peak aged specimen of AA6082-5TiB$_2$ composite was examined in the TEM. Fine precipitates with rod like structures are evident from the TEM images. From the EDS analysis obtained from the particle its was evident that precipitates were α-Al(FeMn)Si.
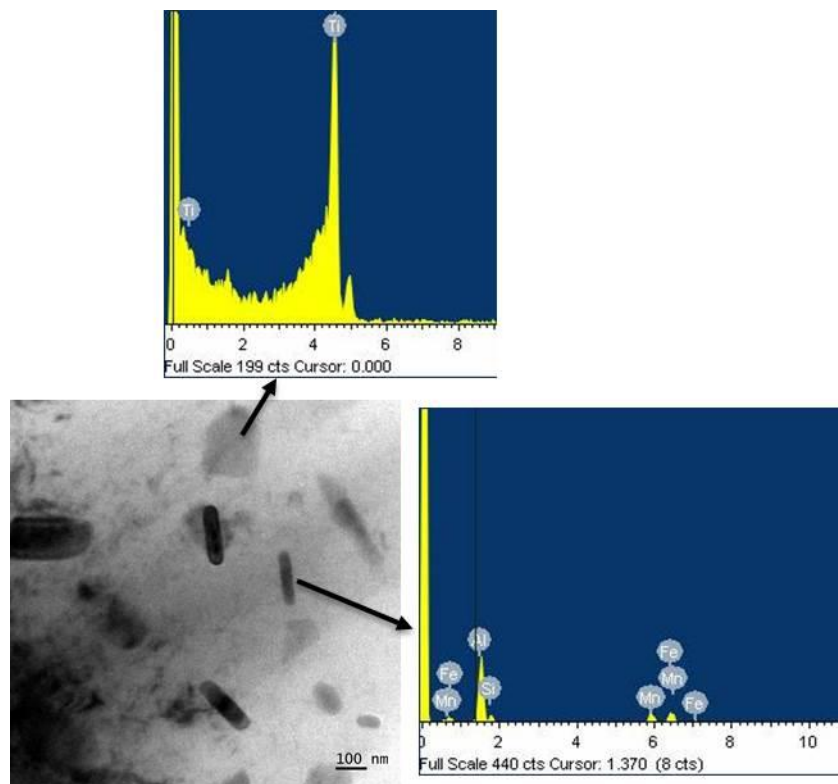
Fig. 5.24 Bright field TEM image and EDS spectrum obtained from the peak aged AA6082-TiB$_2$ composite.

Since the solubility of the Mn, Si and Fe in the matrix alloy is very less, the precipitates were having different concentration are present in the matrix alloy. Hence the precipitates are designated as α-Al(FeMn)Si. The EDS microanalysis also confirmed the present of fine TiB_2 particles in the matrix.

5.7.3 Tensile properties of AA6082-TiB$_2$ composites

Tensile properties of AA6082-TiB$_2$ composites, the their as cast and peak aged conditions are given in Table. 5.12. The Y.S and U.T.S values are seen to increase with progressive increament of TiB_2 particles. It is peculiar to see the improvements in ductile values with the addition of TiB_2 particles. The increase in ductility is attributed to the decrease in grain size, which occurred due to the addition of TiB_2 particles. The grain refinement is caused by Ti solute atoms which go into the solid solution during the addition of Ti to the melt in order to prepare TiB_2 reinforcments. The Ti in the matrix alloy makes the TiB_2 particles more potent thereby aiding in the grain refinement of the matrix alloy.

Table 5.12 Tensile properties of AA6082-TiB$_2$ composites in as cast and peak aged condition

Casting	As Cast condition			Peak Aged condition		
	(0.2%)Y.S (MPa)	U.T.S (MPa)	%Elong.	(0.2%)Y.S (MPa)	U.T.S (MPa)	%Elong.
0	128	172	8	288	317	9
2.5%TiB$_2$	153	201	14	318	349	12
5% TiB$_2$	178	229	12	336	351	10
7.5%TiB$_2$	202	263	9	353	373	8
10% TiB$_2$	229	295	9	371	392	7

A considerable improvement in the tensile properties of peak aged composite is evident. Comparision of as cast and peak aged unreinfroced alloy showed the the Y.S and U.T.S increased by 125% and 84% respectively. In composite with 10%TiB$_2$ particles the increase in Y.S and U.T.S was found to be 142% and 97% respectively. The ductilty of the composite is seen to reduce with ageing. However, the ductily in both the as cast and aged composites were considerablly better. The improvements in ductility is due to the presence of coherent and semicoherent precipitates present throughout the matrix along with TiB$_2$ particles.

5.7.4 Inference

Improvements in the properteies of unreinforced alloy and composites were evient during its ageing. The improvments in strength is attributed to the strengthening of the matrix alloy from both the TiB$_2$ particles as well as fine α-Al(FeMn)Si precipitates formed during ageing.

CHAPTER 6
CONCLUSIONS

In-situ AA6082-TiB$_2$ composites with different weight percent of TiB$_2$ particles were successfully prepared using flux assisted synthesis technique. The process parameters such as melt holding time, melt holding temperature, salt stoichiometry and interval of intermittent stirring was investigated and a suitable condition for the processing of AA6082-5TiB$_2$ composite was found. The influence of Mg, Mn and Si solutes during the processing of AA6082-5TiB$_2$ composite was analysed. AA6082-TiB$_2$ composites having different weight percent (2.5, 5, 7.5 and 10wt.%) of TiB$_2$ particle was processed, with and without the addition of Mg. Finally the ageing kinetics of as cast unreinforced AA6082 alloy and AA6082-TiB$_2$ composites was studied. Having discussed the results of the experiments the following conclusions are recorded:

➢ The investigation on the influence of melt holding time indicates that 60 min of holding time would be appropriate enough for the processing of AA6082-5TiB$_2$ composites without the incidence of AlTiSi, Al$_3$Ti and AlB$_2$ intermetallic particles. The mechanical property of the composites improved with the addition of Mg.

➢ Examinations on the influence of melt holding temperature indicates that a minimum melt temperature of 850°C is essential for the complete formation of TiB$_2$ particles.

➢ Addition of 10% excess KBF$_4$ salts to the stoichiometric mixture of K$_2$TiF$_6$ and KBF$_4$ salts would result in complete formation of TiB$_2$ particles in the matrix.

➢ Investigations on the influence of intermittent stirring time interval of melt confirmed that 8 min. of stirring time interval would be suitable for the processing of TiB$_2$ reinforced composites.

➢ In spite of adding high strength TiB$_2$ particle reinforcements, AA6082-5TiB$_2$ composites showed poor properties due to the loss of Mg. Upon compensating for the loss of Mg in the matrix alloy significant improvement in properties of composites was observed. Varying the Mg content in matrix alloy of AA6082-

5TiB$_2$ composites showed minor improvement in hardness and tensile properties.

- Addition of excess Mn thereby varying the concentration of Mn solute in AA6082-5TiB$_2$ composites showed minor improvements in the overall properties of the composites. Observations on TiB$_2$ particles indicated the diffusion of Mn into the TiB$_2$ lattice. Excess addition of Mn did not show significant improvements in hardness and tensile properties of composites.

- Investigations on the influence of Si indicated the diffusion of Si into the Al$_3$Ti lattice thereby forming AlTiSi particles. The analysis also showed that the concentration of Si in AlTiSi particles changed from particle to particles. With increase in melt holding time, Si tends to diffuse out of AlTiSi particles resulting in the formation of fine Al$_3$Ti particles in the matrix.

- Analysis on the AA6082-xTiB$_2$ (x=2.5, 5, 7.5 and 10wt.%) composites processed without the addition Mg showed deterioration in properties. Compared to the unreinforced AA6082 alloy, composites with 2.5 and 5% showed lesser hardness and tensile strength whereas increments in hardness and strength was in composites with 7.5 and 10%TiB$_2$ particles.

- AA6082-xTiB$_2$(x=2.5, 5, 7.5 and 10wt.%) composites processed with compensation for loss of Mg showed excellent improvement in properties.

- Studies on ageing at 180ºC after solution treatment at 560ºC has shown significant reduction in the time for peak ageing, and increase in the peak age hardness for the as cast AA6082-TiB$_2$ composites, with respect to those of the as cast unreinforced AA6082 alloy. The ageing kinetics is enhanced and the peak age hardness rises with increase in weight percent of TiB$_2$ particles.

Scope for future work

The following suggestions could be made for carrying out the investigative work in the future in this field:

- The entrapment of unwanted slag into the aluminium alloy matrix along with TiB$_2$ particles is a major concern. This deteriorates the excellent properties exhibited by the composite. It is necessary to establish a suitable method for the complete removal of slag from the melt.

- Theoretical study to understand the influence of alloying elements during the processing of composites can be carried out.

- Most of the alloy based products are made by secondary processing techniques. Hence the as cast composites can be further finished by secondary processing methods and its behaviour during the secondary processing can be studied.

- Tribological studies can be carried out by preparation of AA6082 with different weight fractions of TiB_2 particles and to correlate the wear behaviour with the microstructural characteristics.

- Studies on machinability of the alloy using conventional and laser machining can be carried out.

- The components with complicated shapes can be fabricated for specific applications.

- Due to the cost effectiveness of the process, preparation of the composites can be upgraded from lab scale to industrial scale.

REFERENCES

Abdel Hamid, A. and Durand, F. (1985). "Liquid-Solid equilibria of Al-rich Al-Ti-B alloys, liquid-Solid Equilibria of Al-Rich Al-Ti-B Alloys, Part 2: Crystallization sequence leading to TiB_2 crystals." *Z. Metallkd.*, 76, 739-746.

Arnberg, L., Backerud, L. and Klang, H. (1982). "Production and properties of master alloys of AI-Ti-B type and their ability to grain refine aluminium." *Metals Technology*, 1-6.

Arsenault, R. J. (1984). "The strengthening of aluminum alloy 6061 by fiber and platelet silicon carbide." *Mater. Sci. Eng.,* 64, 171-181.

Augustzn, C. O., Dandapanz, K. S. and Srznivasan, K. S. (1986). "Removal of magnesium from aluminium scrap." *Bull. Electrochem.,* 26, 619-620.

Backerud, L. (1971). "On the grain refining mechanism in Al–Ti–B Alloys." *Jernkontorets Ann.*, 155, 422-424.

Beffort, O., Long, S., Cayron, C., Kuebler, J. and Buffat, P.-A. (2007). "Alloying effects on microstructure and mechanical properties of high volume fraction SiC-particle reinforced Al-MMCs made by squeeze casting infiltration." *Compos. Sci. Technol.*, 67(3-4), 737-745.

Birol, Y. (2006). "The effect of processing and Mn content on the T5 and T6 properties of AA6082 profiles." *J. Mater. Process. Technol.*, 173(1), 84-91.

Birol, Y. (2013). "Effect of solute Mg on grain size of aluminium alloys." *J. Mater. Sci. Technol.*, 28(8), 924-927.

Briyol, Y. (2013)"Effect of silicon content in grain refining hypoeutectic Al–Si foundry alloys with boron and titanium additions." *Matal. Sci. Technology.,* 28(4), 385-389.

Brinkman, H. J., Duszczyk, J. and Katgerman, L. (1997). "In-situ formation of TiB_2 in a P/M aluminium matrix." *Scripta Mater.*, 37(3), 293-297.

Calka, A. and Oleszak, D. (2007). "Synthesis of TiB_2 by electric discharge assisted mechanical milling." *J. Alloys Compd.*, 440(1-2), 346-348.

Chen, F., Chen, Z., Mao, F., Wang, T. and Cao, Z. (2015). "TiB_2 reinforced aluminum based in situ composites fabricated by stir casting." *Mater. Sci. Eng., A*, 625, 357-368.

Chen, Z., Kang, H., Fan, G., Li, J., Lu, Y., Jie, J., Zhang, Y., Li, T., Jian, X. and Wang, T. (2016). "Grain refinement of hypoeutectic Al-Si alloys with B." *Acta Mater.*, 120, 168-178.

Chen, Z., Wang, T., Zheng, Y., Zhao, Y., Kang, H. and Gao, L. (2014). "Development of TiB_2 reinforced aluminum foundry alloy based in situ composites-Part I: An improved halide salt route to fabricate Al–5wt%TiB_2 master composite." *Mater. Sci. Eng., A,* 605, 301-309.

Chen, Z. Y., Chen, Y. Y., Shu, Q., An, G. Y., Li, D. and Liu, Y. Y. (2000). "Microstructure and properties of in situ Al-TiB_2 composite fabricated by in-melt reaction method " *Metall. Mater. Trans. A,* 31A, 1959-1964.

Chen., Y. and Chung, D. D. L. (1996). "In situ Al-TiB composite obtained by stir casting " *J. Mater. Sci.,* 31, 311-316.

Christy, T. V., Murugan, N. and Kumar, S. (2010). "A comparative study on the microstructures and mechanical properties of al 6061 alloy and the MMC al 6061/TiB_2/12P." *Journal of minerals & Materials Characterization & Engineering.*, 9(1), 57-65.

Cibula, A. (1951). "The grain refinement of aluminuim alloy castings by additions of Titannium and Boron." *Journal of the Institute of Metals.,* 80, 1-16.

Cibula, A. (1972). "Discussion of the mechanisms of grain refinement in dilute Al alloy " *Metall. Trans. A,* 3, 751-753.

Clough., R. B., Biancaniello., F. S., Wadley., H. N. G. and Kattner., U. R. (1990). "Fiber and interface fracture in single crystal aluminum/SiC fiber composites." *Metall. Trans. A*, 21A, 2747-2757.

Cornish, A. J. (1975). "The influence of boron on the mechanism of grain refinement in dilute Aluminium-Titanium alloys."*Metal Science*, 8, 477-484.

Davies, I. G., Dennis, J. M. and Hellawell, A. (1970). "The nucleation of aluminum grains in alloys of aluminum with Titanium and Boron." *Metall. Trans. A*, 1, 275-280.

Davies, P., Kellie, J. L. F. and Wood, J. V. (1992). "Development of cast aluminium metal matrix composites." *Key Eng. Mater.*, 77-78, 357-362.

Davis, I. G., Dennis, J. M. and Hellawell, A. (1970). "The nucleation of aluminum grains in alloys of aluminum with Titanium and Boron." *Metall. Trans. A.*, 1, 270-280.

Ding, H., Liu, X. and Nie, J. (2012). "Study of preparation of TiB_2 by TiC in Al melts." *Mater. Charact.,* 63, 56-62.

Do-Suck, H., Jones, H. and Atkinson, H. V. (1993). "The wettability of silicon carbide by liquid aluminium: the effect of free silicon in the carbide and of magnesium, silicon and copper alloy additions to the aluminium." *J. Mater. Sci.,* 28, 2654-2658.

Doel, T. J. A. and Bowen, P. (1996). "Tensile properties of particulate-reinforced metal matrix composites." *Composites Part A., 27A*, 655-665.

El-Mahallawy., N., Taha., M. A., Jarfors., A. E. W. and Fredriksson., H. (1999). "On the reaction between aluminium, K_2TiF_6 and KBF_4." *J. Alloys Compd.,* 292, 221-229.

Emamy, M., Mahta, M. and Rasizadeh, J. (2006). "Formation of TiB_2 particles during dissolution of $TiAl_3$ in Al–TiB_2 metal matrix composite using an in situ technique." *Compos. Sci. Technol.,* 66(7-8), 1063-1066.

Fan, T., Yang, G. and Zhang, D. L. (2005). "Thermodynamic effect of alloying addition on in-situ reinforced TiB_2/Al composites." *Metall. Mater. Trans. A.,* 36A, 226-233.

Feng, C. F. and Froyen, L. (1997). "Incorporation of Al into TIB_2 in Al matrix composites and Al-Ti-B master alloys." *Mater. Lett.,* 32, 275-279.

Feng, C. F. and Froyen, L. (1998). "On the reaction mechanism of an Al-TiO$_2$-B system for producing in-situ (Al$_2$O$_3$+TiB$_2$) /Al composites." *Scripta Mater.*, 39(1), 109-118.

Feng, C. F. and Froyen, L. (2000). "Microstructures of in situ Al-TiB$_2$ MMCs prepared by a casting route." *J. Mater. Sci.,* 35, 835-850.

Feufel, H., Gödecke, T., Lukas, H.L., Sommer, F. (1997). "Investigation of the Al-Mg-Si System by Experiments and Thermodynamic Calculations", *J. Alloys Compd*., 247, 31-42.

Fjellstedt, J. and Jarfors, A. E. W. (2005). "On the precipitation of TiB$_2$ in aluminum melts from the reaction with KBF$_4$ and K$_2$TiF$_6$." *Mater. Sci. Eng., A,* 413-414, 527-532.

Gao, Q., Wu, S., LÜ, S., Duan, X. and An, P. (2016). "Preparation of in-situ 5vol% TiB$_2$ particulate reinforced Al–4.5 Cu alloy matrix composites assisted by improved mechanical stirring process." *Mater. Des.,* 94, 79-86.

Gao, T., Li, P., Li, Y. and Liu, X. (2011). "Influence of Si and Ti contents on the microstructure, microhardness and performance of TiAlSi intermetallics in Al–Si–Ti alloys." *J. Alloys Compd.*, 509(31), 8013-8017.

Garcia, J., Massoulier, C. and Faille, P. (2001). "Brazeability of aluminum alloys containing magnesium by cab process using cesium flux." *Society for automotive engineers*.

Ghomashchi, R. (2012). "The evolution of AlTiSi intermetallic phases in Ti-added A356 Al–Si alloy." *J. Alloys Compd.*, 537, 255-260.

Gonzalez, G., Salvo, L., Seury, M. and Eserance, G. L. (1995). "Interfacial reactions in Al-Mg metal matrix composites reinforced with (SnSb) oxide coated SiC particles." *Scripta Metall.*, 33, 1969.

Gotman, I. and Koczak, M. J. (1994). "Fabrication of Al matrix in situ composites via Self Propogating Synthesis " *Mater. Sci. Eng. A*, 187, 189-199.

Grard, C.,(1921). "*Aluminium and its Alloys*, "The Mayflower Press, Plymouth, Great Britain.

Greer, A. L., Bunn, A. M., Tronche, A., Evance, P. V. and Bristow, D. J. (2000). "Modellig of innoculation of metallic melts application to grain reifinement of aluminium by Al-Ti-B." *Acta mater.*, 48, 2823-2835.

Gu, Y., Qian, Y., Chen, L. and Zhou, F. (2003). "A mild solvo-thermal route to nanocrystalline titanium diboride." *J. Alloys Compd.,* 352(1-2), 325-327.

Guinier, A. (1996). "On the birth of GP Zones." *Mater. Sci. Forum.*, 217-222, 3-6.

Guzowski, M. M., Sigworth, G. K. and Sentner, D. A. (1987). "The role of boron in the grain refinement of Aluminum with Titanium." *Metall. Trans. A*, 18A, 603-619.

Han, G., Zhang, W., Zhang, G., Feng, Z. and Wang, Y. (2015). "High-temperature mechanical properties and fracture mechanisms of Al–Si piston alloy reinforced with in situ TiB_2 particles." *Mater. Sci. Eng., A* , 633, 161-168.

Han, Y., Liu, X. and Bian, X. (2002). "In situ TiB_2 particulate reinforced near eutectic Al-Si alloy composites." *Composites Part A.*, 33, 439-444.

Hashim, J., Looney, L. and Hashmi, M. S. J. (2002). "Particle distribution in cast metal matrix composites-Part I." *J. Mater. Process. Technol.*, 123, 251-257.

Higashi, I. and Atoda, T. (1970). "Growth of Titanium Diboride single crystals in molten aluminium." *J. Cryst. Growth.,* 7, 251-230.

Higashi, I., Takashashi, Y. and Atoda, T. (1976). "Crystal growth of Borides and Carbides of transition metals from molten aluminium solutions." *J. Cryst. Growth.,* 33, 207-211.

Hoffmeyer, M. K. and Perepezko, H.,(1991). "*Light Metals* Warrendale, PA.,1105.

Holt, J. B. and Munir, Z. A. (1986). "Combustion synthesis of titanium carbide theory and experiment " *J. Mater. Sci.,* 21, 251-259.

Hong, T., Li, X., Wang, H., Chen, D. and Wang, K. (2015). "Effects of TiB_2 particles on aging behavior of in-situ TiB_2/Al–Cu–Mg composites." *Mater. Sci. Eng., A*, 624, 110-117.

Hwanga., Y. and Lee., J. K. (2002). "Preparation of TiB_2 powders by mechanical alloying." *Mater. Lett.,* 54, 1-7.

Iqbal, N., Dijk, N. H. v., Hansen, T., Katgerman, L. and Kearley, G. J. (2004). "The role of solute titanium and TiB_2 particles in the liquid–solid phase transformation of aluminum alloys." *Mater. Sci. Eng., A,* 386(1-2), 20-26.

Iwahashi, Y., Horita, Z., Nemoto, M. and Langdon, T. G. (1998). "Factors Influencing the Equilibrium Grain Size in Equal Channel Angular Pressing: Role of Mg Additions to Aluminum." *Metall. Mater. Trans. A*, 29A, 2503-2510.

Jha, A. and Dometakis, C. (1997). "The dispersion mechanism of TiB_2 ceramic phase in molten aluminium and its alloys." *Mater. Des.*, 18(4), 297-301.

Johnsson, M. (1994). "Influence of Si and Fe on the grain refinement of aluminium." *Z. MetaIlkd.,* 85(11), 781-785.

Johnsson, M., Backerud, L. and Sigworth, G. K. (1993). "Study of the mechanism of grain refinement of aluminum after additions of Ti and B containing master alloys." *Metall. Mater. Trans. A.,* 24A, 481-491.

Jonas, F., Anders, E. W. J. and Lena, S. (1999). "Experimental analysis of the intermediary phases AlB , AlB and TiB_2 in the Al–B and Al–Ti–B systems." *J. Alloys Compd.,* 283, 192-197.

Jones, G. P. and Pearson, J. (1976). "Factors affecting the grain-refinement of aluminum using Titanium and Boron Additives." *Metall. Trans. B,* 7B, 223-234.

Kang, S. H. and Kim, D. J. (2007). "*Synthesis* of nano-titanium diboride powders by carbothermal reduction." *J. Eur. Ceram. Soc.,* 27(2-3), 715-718.

Kaptay, G. (2003). "Interfacial criteria for producing metal matrix composites and ceramic particle stabilized metallic foams." *3rd Hungarian Conference on Materials Science, Testing and Informatics.,* 419-424.

Karbalaei Akbari, M., Baharvandi, H. R. and Shirvanimoghaddam, K. (2015). "Tensile and fracture behavior of nano/micro TiB_2 particle reinforced casting A356 aluminum alloy composites." *Mater. Des.,* 66, 150-161.

Kellie, J. and Wood, J. V. (1995). "Reaction processing in the metals industry." *Mater. World.*, 3(1), 10-12.

Koczak, M. J. and Premkumar, M. K. (1993). "Emerging technologies for the In-Situ production of MMCs." *Journal of Materials.,* 45(1), 44-48.

Kori, S. A., Murty, B. S. and Chakaraborty, M. (2000). "Development of an efficient grain refiner for Al-7Si alloy." *Mater. Sci. Eng. A*, 280, 58-61.

Kori, S. A., Murty, B. S. and Chakraborty, M. (2013). "Influence of silicon and magnesium on grain refinement in aluminium alloys." *J. Mater. Sci. Technol.,* 15(9), 986-992.

Kumar, N., Gautam, R. K. and Mohan, S. (2015). "In-situ development of ZrB_2 particles and their effect on microstructure and mechanical properties of AA5052 metal-matrix composites." *Mater. Des.*, 80, 129-136.

Kunnam, P. and Limmaneevichitr, C. (2008). "Effect of process parameters on morphology and grain refinemen efficiency of $TiAl_3$ and TiB_2 in aluminium casting." *J. Mater. Sci. Technol.*, 24(1), 54-56.

Kuruvilla, A. K., Prasad, K. S., Bhanuprasad, V. V. and Mahajan, Y. R. (1990). "Microstructure property correlation in Al-TiB_2 (XD) composites." *Scr. Metall. Mater.*, 24, 873-878.

Lakshmi, S., Lu, L. and Gupta, M. (1998). "In situ preparation of TiB_2 reinforced Al based composites." *J. Mater. Process. Technol.,* 73, 160-166.

Lee, J., Kim, J. N., Jung, J. Y., Lee, E. S. and Ahn, S. (1998). "The influence of reinforced particle fractur on strengthening of spray formed Cu-TiB_2 composite." *Scripta Mater.,* 39(8), 1063-1069.

Lee., C.T. and Chen., S.W. (2002). "Quantities of grains of aluminum and those of TiB_2 and Al_3Ti particle added in the grain-refining process." *Mater. Sci. Eng., A,* 325, 242-248.

Li, H., Sritharan, T., Lam, Y. M. and Leng, N. Y. (1997). "Effects of processing paramaters on the performance of Al grain refined master alloy Al-Ti and Al-B in small ingots." *J. Mater. Process. Technol.*, 66, 253-257.

Peng-ting LI, Yun-guo LI, Jin-feng NIE, Xiang-fa LIU. (2012). "Influence of forming process on three-dimensional morphology of TiB$_2$ particles in Al-Ti-B alloys." *Trans. Nonferrous Met. Soc. China.*, 22(3), 564-570.

Liu, Z., Rakita, M., Xu, W., Wang, X. and Han, Q. (2015). "Ultrasound assisted salts–metal reaction for synthesizing TiB$_2$ particles at low temperature." *Chem. Eng. J.*, 263, 317-324.

Lloyd, D. J. and Jin, I. (1988). "A method of assessing the reactivity between SiC and molten Al." *Metall. Trans. A*, 19, 3107-3109.

Lloyd, D. J., Lagace, H., Mcleod, A. and Morris, P. L. (1989). "Microstructural aspects of aiuminium-silicon carbide particulate composites produced by a Casting Method." *Mater. Sci. Eng. A*, 107, 73-80.

Lu, H. T., Wang, L. C. and Kung, S. K. (1981). "Grain refining in A356 alloys."*J.Chinese Foundrymen's Association.*, 29, 10-18.

Lu, L., Lai, M. O. and Chen, F. L. (1997). "Al-4 wt% Cu composite reinforced with in-situ TiB$_2$ particles." *Acta mater.*, 45(10), 4297-4309.

Lu, L., Lai, M. O., Niu, X. P. and Ho, H. N. (1998). "In situ formation of TiB$_2$ reinforced aluminium via mechanical alloying." *Metallkd*, 89, 567.

Lu, L., Lai, M. O., Sua, Y., Teo, H. L. and Feng, C. F. (2001). "In situ TiB$_2$ reinforced Al alloy composites." *Scripta Mater.,* 45, 1017-1023.

Ma, Z. Y., Bi, J., Lu, X., Lou, M. and Gao, Y. X. (1993). "Quench strengthening mechanism of Al-SiC composites." *Scr. Metall. Mater.*, 29, 225-229.

Ma, Z. Y., Bi, J., Luc, Y. X., Shend, H. W. and Gao, Y. X. (1993). "Microstructure and interface of the in situ forming TiB$_2$-reinforced aluminum composite." *Compos Interfaces.*, 1, 287-291.

Ma, Z. Y., Li, J. H., Luo, M., Ning, X. G., Ln, Y. X. and Bi, J. (1994). "In-Situ formed Al_2O_3 and TiB_2 particulate mixture-reinforced aluminium composite." *Scr. Metall. Mater.*, 31(5), 635-639.

Ma, Z. Y. and Tjong, S. C. (1997). "In Situ ceramic particle-reinforced aluminum matrix composites fabricated by reaction pressing in the TiO_2 (Ti)-Al-B (B_2O_3) systems." *Metall. Mater. Trans. A*, 28A, 1931-1942.

Mallikarjuna, C., Shashidhara, S. M., Mallik, U. S. and Parashivamurthy, K. I. (2011). "Grain refinement and wear properties evaluation of aluminum alloy 2014 matrix-TiB_2 in-situ composites." *Mater. Des.*, 32(6), 3554-3559.

Mandal, A., Chakraborty, M. and Murty, B. S. (2008). "Ageing behaviour of A356 alloy reinforced with in-situ formed TiB_2 particles." *Mater. Sci. Eng., A*, 489(1-2), 220-226.

Mandal, A., Maiti, R., Chakraborty, M. and Murty, B. S. (2004). "Effect of TiB_2 particles on aging response of Al–4Cu alloy." *Mater. Sci. Eng., A* , 386(1-2), 296-300.

Marcantonio, J. A. and Monodolfo, L. F. (1971). "Grain Refinement in Aluminum Alloyed with Titanium and Boron" *Metall. Trans. A*, 2, 465-471.

Mathan Kumar, N., Senthil Kumaran, S. and Kumaraswamidhas, L. A. (2016). "Aerospace application on Al 2618 with reinforced - Si_3N_4, AlN and ZrB_2 in-situ composites." *J. Alloys Compd.*, 672, 238-250.

Matin, M. A., Lu, L. and Gupta, M. (2001). "Investigation of reactions between boron and titanium compounds with magnesium." *Scripta Mater.*, 45, 479-486.

Maxwell, I. and Hellawell, A. (1972). "Processing Al-Ti-B-The constitution of the system AI-Ti-B with reference to aluminum-base alloys." *Metall. Trans. A,* 3, 1487-1493.

Mayes, C. D., McCartney, D. G. and Tatlock, G. J. (1993). "Influence of microstructure on grain refining performance of AI-Ti-B master alloys." *J. Mater. Sci. Technol.,* 9, 97-103.

McCartney, D. G. (1989). "Grain refining of aluminium and its alloy using inoculants" *Int. Mater. Rev.,* 34(5), 247-260.

Michael Rajan, H. B., Ramabalan, S., Dinaharan, I. and Vijay, S. J. (2013). "Synthesis and characterization of in situ formed titanium diboride particulate reinforced AA7075 aluminum alloy cast composites." *Mater. Des.*, 44, 438-445.

Milman, V. and Warren, M. C. (2001). "Elastic properties of TiB_2 and MgB_2." *J. Phys.: Condens. Matter.*, 13(24), 5585-5595.

Mitra, R., Chiou, W. A., Weertman, J. R. and Fine, M. E. (1991). "Relaxation mechanism at the interfaces in XD Al-TiC metal matrix composites." *Scr. Metall. Mater*, 25(4), 2689-269.

Mitra, R., Fine, M. E. and Weertman, I. R. (1993). "Chemical reaction strengthening of Al-TiC matrix composites by isothermal heat treatment at 913 K." *J. Mater. Res.*, 8(9), 2370-790.

Mogilevsky, R., Bryanb, S. R., Wolbach, W. S., Krucekb, T. W., Maierb, R. D., Shoemakerb, G. L., Chabala, J. M., Soni, K. K. and Levi-Setti, R. (1995). "Reactions at the matrix/reinforcement interface in aluminum alloy matrix composites." *Mater. Sci. Eng., A,* 191,209-222.

Mohanty , P. S. and Gruzesky, J. E. (1995). "Mechanism of grain refinement in aluminium." *Acta metall. mater.*, 43(5), 2001-2012.

Mohanty, P. S. and Gurezleski, J. E. (1996). "Grain refinement mechanism of Hypoeutectic Al-Si alloys." *Acta mater* 44(9), 3749-3760.

Mordike, B. L. and Ebert, B. L. (2001). "Magnesium properties applications potential." *Mater. Sci. Eng. A*, 302, 37-45.

Mrówka-Nowotnik, G., Sieniawski, J. and Werzbinska, M. (2007). "Intermetallic phase particles in 6082 aluminium alloy." *Archives of Materials Science and Engineering*, 28(2), 69-76.

Mukhopadhyay, P. (2012). "Alloy Designation, Processing, and Use of AA6XXX Series Aluminium Alloys." *ISRN Metallurgy*, 1-15.

Munir, Z. A. (1988). "Synthesis of high-temperature materials by self propagating combustion methods." *Am. Ceram. Soc. Bull.*, 67, 342-349.

Munir, Z. A. (1992). "Reaction synthesis processes mechanisms and characteristics." *Metall. Trans. A*, 23A, 7-13.

Munir., Z. A. and Holt, J. B. (1989). "Combustion and plasma synthesis of high temperature materials." first international symposium on combustion and plasma synthesis of high temperature materials., 771.

Munro, R. G. (2000). "Material Properties of Titanium Diboride." *J. Res. Natl. Inst. Stand. Technol.*, 105, 709-720.

Murray, J. L., Liao, P. K. and Spear, K. E. (1986). "The B-Ti (Boron - Titanium) System." *Bull. Alloy Phase Diagrams,*, 7, 550-555.

Murthy, B. S., Maiti, R. and Chakaraborty, M. (2001). "Development of in-situ Al-TiB$_2$ metal matrix composites " *Journal of Metallurgy and Materials Science.*, 43(2), 93-101.

Murty, B. S., Kori, S. A., Venkateswarlu, B., Bhat, R. R. and Chakaraborty, M. (1999). "Manufacture of Al–Ti–B master alloys by the reaction of complex halide salts with molten aluminium." *J. Mater. Process. Technol.,* 89-90, 152-158.

Naess, S. E. and Ronningen, J. A. (1975). "TiB$_2$ particles as nucleants for aluminum." *Metallography.*, 8, 391-400.

Naka, S. (1996). "Advanced titanium based alloys. "Current opinion in solid state & materials science, 1, 333-339.

Nam, S. W. and Lee, D. H. (2000). "The Effect of Mn on the mechanical behavior of Al alloys." *Metals and Materials.*, 6(1), 13-16.

Nampoothiri, J., Harini, R. S., Nayak, S. K., Raj, B. and Ravi, K. R. (2016). "Post in-situ reaction ultrasonic treatment for generation of Al–4.4Cu/TiB$_2$ nanocomposite: A route to enhance the strength of metal matrix nanocomposites." *J. Alloys Compd.,* 683, 370-378.

Nandam, S. H., Sankaran, S. and Murty, B. S. (2011). "Precipitation kinetics in Al-Si-Mg/TiB$_2$ in-situ composites." *Trans. Indian Inst. Metals.*, 64 (1&2), 123-126.

Nimbalkar, V. M., Rao, B. R. K., Deshmukha, V. P., Shah, A. K. and Marathe, K. V. (2011). "Development reaction synthesis process of novel Al-alloys-TiB$_2$ metal matrix composites by in-situ."*Journal of Metallurgy and Materials Science*, 53(2), 197-203.

Pai, B. C., Ramani, G., Pillai, R. M. and Satyanarayana, K. G. (1995). "Role of magnesium in cast aluminiurn alloy matrix composites." *J. Mater. Sci.,* 30, 1903-1911.

Pattnaik, A. B., Das, S., Jha, B. B. and Prasanth, N. (2015). "Effect of Al–5Ti–1B grain refiner on the microstructure, mechanical properties and acoustic emission characteristics of Al5052 aluminium alloy." *J. Mater. Res. Technol.*, 4(2), 171-179.

Philpot, K. A., Munir, Z. A. and Holt, J. B. (1987). "An investigation of the synthesis of nickel aluminides through gasless combustion " *J. Mater. Sci.,* 22, 159-169.

Polmear, I. J.,(1995). "*Light alloys metallurgy of the light metals*, "Arnold Press., 384.

Pramod, S. L., Prasada Rao, A. K., Murty, B. S. and Bakshi, S. R. (2015). "Effect of Sc addition on the microstructure and wear properties of A356 alloy and A356-TiB$_2$ in situ composite." *Mater. Des.*, 78, 85-94.

Prasad, K. V. S., Murty, B. S., Pramanik, P., Mukunda, P. G. and Chakaraborty, M. (1996). "Reaction of fluoride salts with alulminium " *Mater. Sci. Technol.,* 12, 766-770.

Peijie, Li., Kandalova, E.G., Nikitin, V.I., Luts, A.R., Makarenko, A.G., and Yanfei, Z. (2003). "Effect of fluxes on structure formation of SHS Al–Ti–B grain refiner." *Mater. Lett.,* 57, 3694–3698.

Rahul, M. and Mahajan, Y. R. (1993). "Interfaces in discontinuously reinforced metal-matrix composites interface " *Defen. Sci. Jour.*, 43(4), 397-418.

Rajesekaran, N. R. and Sampath, V. (2011). "Effect of In-Situ TiB$_2$ particle addition on the mechanical properties of AA 2219 Al alloy composite." *Journal of Minerals & Materials Characterization & Engineering.*, 10(6), 527-534.

Rengasamy, N. V., Rajkumar, M. and Senthil Kumaran, S. (2016). "Mining environment applications on Al 4032 – ZrB$_2$ and TiB$_2$ in-situ composites." *J. Alloys Compd.*, 658, 757-773.

Rohatgi, P. K., Kim, J. K., Guo, R. Q., Robertson, D. P. and Gadjdardziska Josifovska, M. (2001). "Age-Hardening Characteristics of Aluminum Alloy–Hollow Fly Ash Composites." *Metall. Mater. Trans. A.*, 33A, 1541-1547.

Romanova, V. A., Balokhonov, R. R. and Schmauder, S. (2009). "The influence of the reinforcing particle shape and interface strength on the fracture behavior of a metal matrix composite." *Acta Mater.*, 57(1), 97-107.

Salleh, M. S., Omar, M. Z. and Syarif, J. (2015). "The effects of Mg addition on the microstructure and mechanical properties of thixoformed Al–5%Si–Cu alloys." *J. Alloys Compd.*, 621, 121-130.

Satyaprasad, K., Hehajan, Y. R. and Bhanuprasad, V. U. (1992). "Strengthening of Al$_2$0$_3$ v/o TiC composites by isothermal heat treatment." *Scr. Metall. Mater.*, 26, 711-716.

Schumacher, P., Greer, A. L., Worth, J., Evans, P. V., Kearns, M. A., Fisher, P. and Green, A. H. (2013). "New studies of nucleation mechanisms in aluminium alloys: implications for grain refinement practice." *J. Mater. Sci. Technol.,* 14(5), 394-404.

Seifeddine, S. and Svensson, I. L. (2009). "The influence of Fe and Mn content and cooling rate on the microstructure and mechanical properties of A380-die casting alloys." *Metal. Sci. Technol.*, 27, 11-20.

Shebestari, S. G., Mahmudi, T., Emamy, M. and Campbell, T. (2002). "Effect of Mn and Sr on intermetallics in Fe rich eutectic Al-Si alloys." *Int. J. Cast Met. Res.,* 15(1), 17-24.

Shen, Y., Li, X., Hong, T., Geng, J. and Wang, H. (2016). "Effects of TiB_2 particles on microstructure and mechanical properties of an in-situ TiB_2-Al–Cu–Li matrix composite." *Mater. Sci. Eng., A*, 655, 265-268.

Sokolowski, J. H., Kierkus, C.A. and Evans, W. (2001). "The formation of insoluble $Ti(Al,Si)3$ crystals in 356 alloy castings and their sedimentation in foundry equipment: Causes, Effects and solutions." *Mater.Sci.Eng.,* A, 541, 234-241.

Shorowordi, K. M., Laoui, T., Haseeb, A. S. M. A., Celis, J. P. and Froyen, L. (2003). "Microstructure and interface characteristics of B_4C, SiC and Al_2O_3 reinforced Al matrix composites: a comparative study." *J. Mater. Process. Technol.,* 142(3), 738-743.

Sreekumar, V. M., Ravi, K. R., Pillai, R. M., Pai, B. C. and Chakraborty, M. (2008). "Thermodynamics and Kinetics of the formation of Al_2O_3/ $MgAl_2O_4$/MgO in Al-Silica Metal Matrix Composite." *Metall. Mater. Trans. A*, 39(4), 919-933.

Sun, J., Zhang, X., Zhang, Y., Ma, N. and Wang, H. (2015). "Effect of alloy elements on the morphology transformation of TiB_2 particles in Al matrix." *Micron*, 70, 21-5.

Tao, G. H., Liu, C. H., Chen, J. H., Lai, Y. X., Ma, P. P. and Liu, L. M. (2015). "The influence of Mg/Si ratio on the negative natural aging effect in Al–Mg–Si–Cu alloys." *Mater. Sci. Eng., A,* 642, 241-248.

Tayeh, T., Douin, J., Jouannigot, S., Zakhour, M., Nakhl, M., Silvain, J.F. and Bobet, J.L. (2014). "Hardness and Young's modulus behavior of Al composites reinforced by nanometric TiB_2 elaborated by mechanosynthesis." *Mater. Sci. Eng., A*, 591, 1-8.

Tee, K. L., Lu, L. and Lai, M. O. (1999). "Synthesis of in situ Al-TiB_2 using stir casting route." *Compos. Struct.,* 47, 589-593.

Tjong, S. C. and Ma, Z. Y. (2000). "Microstructural and mechanical characteristics of insitu MMCs " *Mater. Sci. Eng., R*, 29, 49-113.

Usurelu, E. M., Moldovan, P., Cicua, I. and Dragut, V. (2011). "On the mechanism and thermodynamics of the precipitation of TiB_2 particles in 6063 matrix aluminium alloy." *U.P.B. Sci. Bull., Series B.*, 73(3),

Wang, M., Chen, D., Chen, Z., Wu, Y., Wang, F., Ma, N. and Wang, H. (2014). "Mechanical properties of in-situ TiB$_2$/A356 composites." *Mater. Sci. Eng., A,* 590, 246-254.

Wang, N., Wang, Z. and Weatherly, G. C. (1992). "Formation of Magnesium Aluminate (Spinel) in cast SiC Particulate-Reinforced Al (A356) Metal Matrix Composites." *Metall. Trans. A*, 23A, 1423-1430.

Wang, T., Chen, Z., Zheng, Y., Zhao, Y., Kang, H. and Gao, L. (2014). "Development of TiB$_2$ reinforced aluminum foundry alloy based in situ composites – Part II: Enhancing the practical aluminum foundry alloys using the improved Al–5wt%TiB$_2$ master composite upon dilution." *Mater. Sci. Eng., A,* 605, 22-32.

Wang, T., Zheng, Y., Chen, Z., Zhao, Y. and Kang, H. (2014). "Effects of Sr on the microstructure and mechanical properties of in situ TiB$_2$ reinforced A356 composite." *Mater. Des.*, 64, 185-193.

Wang., Z. and Zhang, R. J. (1994). "Microscopic characteristics of fatigue crack propagation in aluminium alloy based particulate reinforced metal matrix composites." *Acta metall. mater.*, 42(4), 1433-1445.

Watson, I. G., Forster, M. F., Lee, P. D., Dashwood, R. J., Hamilton, R. W. and Chirazi, A. (2005). "Investigation of the clustering behaviour of titanium diboride particles in aluminium." *Composites Part A.*, 36(9), 1177-1187.

Wen, W., Zhao, Y. and Morris, J. G. (2005). "The effect of Mg precipitation on the mechanical properties of 5xxx aluminum alloys." *Mater. Sci. Eng., A,* 392(1-2), 136-144.

Westwood, A. R. C. (1988). "Materials for advanced studies and devices." *Metall. Trans. A,* 19(4), 749-758.

Wood, J. V., Davies, P. and Kellie, J. L. F. (1993). "Properties of reactively cast aluminium- TiB$_2$ alloys." *Mater. Sci. Technol.,* 9, 833-840.

Xiuqing, Z., Haowei, W., Lihua, L., Xinying, T. and Naiheng, M. (2005). "The mechanical properties of magnesium matrix composites reinforced with (TiB$_2$+TiC) ceramic particulates." *Mater. Lett.*, 59(17), 2105-2109.

Yao, J. P., Zhong, S., Zhang, L. and Zhao, H. P. (2010). "Mechanical Properties of Al-Si Alloy-Based Composites Reinforced by in-situ TiB$_2$ Particulates." *Adv. Mater. Res.*, 105-106, 126-129.

Yi, H., Ma, N., Li, X., Zhang, Y. and Wang, H. (2006). "High-temperature mechanics properties of in situ TiB$_2$p reinforced Al–Si alloy composites." *Mater. Sci. Eng., A*, 419(1-2), 12-17.

Yongdong, H., Xinming, Z. and Zhiqiang, C. (2010). "Effect of Minor Cr, Mn, Zr, Ti and B on Grain Refinement of As-Cast Al-Zn-Mg-Cu Alloys." *Rare metal materials and Engineering*, 39(7), 1135-1140.

Yue, N. L., Lu, L. and Lai, M. O. (1999). "Application of thermodynamic calculation in the in-situ process of Al/TiB$_2$." *Compos. Struct.,* 47, 691-694.

Zhang, M. X., Kelly, P. M., Qian, M. and Taylor, J. A. (2005). "Crystallography of grain refinement in Mg–Al based alloys." *Acta Materialia*, 53(11), 3261-3270.

Zhang, S. L., Yang, J., Zhang, B. R., Zhao, Y. T., Chen, G., Shi, X. X. and Liang, Z. P. (2015). "A novel fabrication technology of in situ TiB$_2$/6063Al composites: High energy ball milling and melt in situ reaction." *J. Alloys Compd.,* 639, 215-223.

Zhang, X., Liao, L., Ma, N. and Wang, H. (2006). "In-situ synthesis method of magnesium matrix composites reinforced with TiC particulates." *J. Mater. Res.,* 9(4), 357-360.

Zhao, D., Liu, X., Liu, Y. and Bian, Z. (2005). "In-situ preparation of Al matrix composites reinforced by TiB$_2$ particles and sub-micron ZrB$_2$" *J. Mater. Sci.,* 40, 4365-4368.

Zhu, H.G., Wang, H.Z., Ge, L.Q., Chen, S. and Wu, S.Q. (2007). "Formation of composites fabricated by exothermic dispersion reaction in Al-TiO$_2$-B$_2$O$_3$ system." *Trans. Nonferrous Met. Soc. China,* 17(3), 590-594.

Zongy, M. A., Jing, B. A., Yuxiong, L. U., Hongwei, S. and Yinxuan, G. (1993). "On the in-situ forming TiB$_2$ reinforced Al Composites " *Acta metallurgica sinica*, 6(2), 122-125.

LIST OF PUBLICATIONS

In Refereed International Journals

1. **Hemanthkumar V.** and Ravishankar K.S., (2016). "Evolution of microstructure during the preparation of TiB_2 reinforced in-situ aluminium matrix composites". *International Advanced Research Journal in Science, Engineering and Technology,* 3(6), 89-92.

2. **Hemanthkumar V.** and Ravishankar K.S., (2016). "Melt holding temperature and its effect on the microstructure of *in-situ* TiB_2 Aluminium matrix composite". *International Journal of Engineering Trends and Technology,* 42(5), 230-234

International Conference Proceedings

1. **Hemanthkumar V.** and Ravishankar K.S., (February-2016). "The effect of stirring medium on the microstructural evolution of in-situ AA6082-5wt.% TiB_2 Composites". *Advances in materials and manufacturing-INTCOMM, 2016,* Department of Mechanical Engineering, Hindusthan College of Engineering and Technology, Coimbatore, India.

2. **Hemanthkumar V.** and Ravishankar K.S., (February-2016). "Effect of melt holding temperatures on the microstructure of AA6082-5wt,% TiB_2 composites by in-situ process". *Advances in materials and manufacturing-INTCOMM, 2016,* Department of Mechanical Engineering, Hindusthan College of Engineering and Technology, Coimbatore, India.

3. **Hemanthkumar V.** and Ravishankar K.S., (December-2014). "Influence of Manganese on the microstructure and mechanical properties on in-situ AA6082-TiB_2 metal matrix composites". *International symposium for research scholars-ISRS, 2014,* Department of Metallurgical and materials Engineering, Indian Institute of Technology Madras, India.

4. **Hemanthkumar V.** and Ravishankar K.S., (December-2012). "Microstructure evolution of in-situ AA6351-TiB$_2$ metal matrix composites". *International symposium for research scholars-ISRS, 2012,* Department of Metallurgical and materials Engineering, Indian Institute of Technology Madras, India.

BIO-DATA

Name : HEMANTHKUMAR V.

Date of Birth : 20-02-1978

Permanent address : No.230, Periyar Nagar, Nellikuppam Road,

Nandhivaram, Guduvancheri -603202

Tamilnadu, India.

E-mail : hemmatsci@gmail.com

Contact number : +91-9611979850

Academic Qualification

♦ **Bachelor of Science (B.Sc.)**: Physics, South Indian Vaniyar Education Trust (S.I.V.E.T), Madras University, Tamilnadu,

.

♦ **Master of Science (M.Sc.)**: Materials Science, College of Engineering, Guindy (CEG), Anna University, Tamilnadu,

♦ **Master of Technology (M.Tech.)**: Materials Engineering, National Institute of Technology Karnataka, Surathkal.